Electronic Supplementary Material (ESI) for ChemComm.

Electronic Supplementary Information

Fine-tuning thio-pyridazinediones as SMDC scaffolds (with intracellular thiol release *via* a novel self-immolative linker)

Marcos Fernández[a], André Shamsabadi[a] and Vijay Chudasama[a]

a. Department of Chemistry, University College London, 20 Gordon Street, WC1H 0AJ, London, UK.

General Experimental

All reagents were purchased from Sigma Aldrich, Alfa Aesar, Thermo Fisher and Acros. Compounds and solvents were used as received. Petrol refers to petroleum ether (40–60 ˚C). All reactions were monitored using thin-layer chromatography (TLC) on pre-coated SIL G/UV254 silica gel plates (254 μm). Detection was by UV (254 nm and 365 nm) or chemical stain ($KMnO_4$). The term *in vacuo* refers to solvent removal using Büchi rotary evaporation between 15–60 ˚C, at approximately 10 mmHg. Flash column chromatography was carried out with pre-loaded FlashPure flash cartridges on a Biotage Isolera Spektra One flash chromatography system. ^{1}H NMR spectra were obtained at 600 or 700 MHz and ^{13}C NMR spectra were obtained at 150 MHz on Bruker NMR instrument Avance III 600 or Bruker NMR instrument Avane Neo 700. All samples were run at the default number of scans and at 21 ˚C. Chemical shifts (δ) for ^{1}H NMR and ^{13}C NMR are quoted relative to residual signals of the solvent on a parts per million (ppm) scale. Coupling constants (*J* values) are reported in Hertz (Hz) and are reported as $J_{H–H}$ couplings. The multiplicity of each signal is indicated as s-singlet, d-doublet, t-triplet, q-quartet and m-multiplet (*i.e.* complex peak obtained due to overlap). App. implies apparent. Infrared spectra were obtained on a Perkin Elmer Spectrum 100 FTIR Spectrometer operating in ATR mode with frequencies given in reciprocal centimetres (cm^{-1}). Optical rotations were determined from an average of five measurements at 21 ˚C using a 1 mL, 1 dm cell and were measured using a Perkin-Elmer 343 polarimeter. $[\alpha]_D$ values are reported in 10^{-1} deg cm^2 g^{-1}, *c* is concentration (g/100 mL). Mass spectra were obtained for synthetic products, from the UCL mass spectroscopy service on either a Thermo Finnigan MAT900Xp (EI and CI) or Waters LCT Premier XE (ES) mass spectrometer. Melting points and decomposition temperatures (d.t.) were measured with a Gallenkamp apparatus and are uncorrected. All bioconjugation reactions were carried out in duplicate.

Bioconjugation General Remarks

Conjugation experiments were carried out in standard polypropylene Eppendorf® safe-lock tubes (2.0 mL) at atmospheric pressure. All buffer solutions were prepared with doubly deionised water and filter-sterilised. Phosphate-buffered saline (PBS) was 10 mM phosphates, 137 mM NaCl and 2.7 mM KCl at pH 7.4. Ultrafiltration was carried out in Amicon® Ultra-4 Centrifugal Filter Units with a molecular weight cut-off (MWCO) of 5 kDa or in Vivaspin® 500 centrifugal concentrators (5 kDa MWCO). Centrifugation was carried out on an Eppendorf 5415R fixed

angle rotor centrifuge operating at 14000 rcf at 21 ˚C or in an Eppendorf 5810 swing-bucket rotor centrifuge operating at 3220 rcf at 21 ˚C. FPLC system (GE Healthcare), equilibrated in PBS. Detection was by absorption at 280 nm.

Protein LC-MS

After the 4 h incubations, the samples were diluted to 3 µM (0.2 mg/mL) in ammonium acetate buffer (20 mM, pH 7.4) and submitted to the Chemistry Mass Spectrometry Facility at the Chemistry Department, UCL for analysis of unmodified protein on the Agilent 6510 QTOF LC-MS system (Agilent, UK). 10 µL of each sample were injected onto a PLRP-S, 1000A, 8 µM, 150 mm × 2.1 mm column, which was maintained at 60 ˚C. The separation was achieved using mobile phase A (95% H_2O, 5% MeCN, 0.1% formic acid) and B (95% MeCN, 5% H_2O, 0.1% formic acid) using a gradient elution. Agilent 6510 QTOF mass spectrometer was operated in a positive polarity mode, coupled with an ESI ion source. The ion source parameters were set up with a VCap of 3500 V, a gas temperature at 350 ˚C, a dry gas flow rate at 10 L/min and a nebulizer of 30 psig. MS TOF was acquired under conditions of a fragmentor at 350 V, a skimmer at 65 V and an acquisition rate at 0.5 spectra/s in a profile mode, within a scan range between 40,000 and 100,000 *m/z* in profile mode. The raw data was converted to zero charge mass spectra using maximum entropy deconvolution algorithm over the *ca.* region 18.5–22.8 min with MassHunter software (version B.07.00).

Small Molecule LC-MS

After 0.05, 1, 2, 4 and 24 h incubations, the samples were analysed on a Waters Acquity uPLC connected to Waters Acquity Single Quad Detector (SQD) and a photodiode array. Flow rate was set at 0.600 mL/min. LC-MS was performed on a ThermoScientific MSQ Plus connected to an Accela 1250 pump and Accela UV-Vis detector, with 10 µL of each sample being injected onto an Acquity UPLC BEH C18 (50 × 21 mm) maintained at 50 ˚C. The separation was achieved using mobile phase A (H_2O, 0.1% formic acid) and B (MeCN, 0.1% formic acid) using a gradient elution. Mobile phase: 95:5 A:B; gradient over 5 minutes to 5:95 A:B. MS mode ES+; scan range: m/z 100–1000; scan time: 0.25 s. The electrospray source of the MS was operated with a capillary voltage of 3.5 kV and a cone voltage of 20 V were employed. All deconvoluted mass spectra were produced using the software provided by the manufacturer.

UV–Vis Spectroscopy

UV-Vis spectroscopy was used to determine the maximum UV absorption of a given reaction mixture. Measurements were obtained using a Varian Cary 100 Bio UV-Visible spectrophotometer operating at 21 ˚C. Sample buffer was used as a blank for baseline correction.

Fluorescence Emission Spectroscopy

Fluorescence emission spectroscopy was used to determine the maximum fluorescence emission of a given reaction mixture. Measurements were obtained using a Varian Cary Eclipse Fluorescence spectrophotometer operating at 21 ˚C. Sample buffer was used as a blank for baseline correction.

Synthesis of compounds

Di-*tert*-butyl 1,2-diethylhydrazine-1,2-dicarboxylate[1]

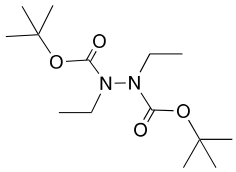

To a solution of di-*tert*-butyl hydrazine-1,2-dicarboxylate (3.10 g, 13.4 mmol) and bromoethane (2.34 mL, 31.4 mmol) in DMF (60 mL) was added cesium carbonate (17.4 g, 47.4 mmol), and the reaction mixture was stirred at 21 ˚C for 21 h. Following this, the reaction mixture was diluted with water (60 mL) and extracted with EtOAc (3 × 35 mL). The organic extracts were combined and subsequently washed with sat. aq. LiCl solution (35 mL). The organic phase was dried over $MgSO_4$, concentrated *in vacuo* and the crude residue was purified by flash column chromatography (0–20% EtOAc/Pet.). The appropriate fractions were then combined and concentrated *in vacuo* to afford di-*tert*-butyl 1,2-diethylhydrazine-1,2-dicarboxylate (3.70 g, 12.8 mmol, 96%) as a colourless oil. ^{1}H NMR (600 MHz, $CDCl_3$, rotamers) δ 3.54–3.38 (m, 4H), 1.50–1.43 (m, 18H), 1.18–1.14 (m, 6H); ^{13}C NMR (150 MHz, $CDCl_3$, rotamers) δ 155.8 (C), 155.1 (C), 154.9 (C), 80.7 (C), 80.6 (C), 80.5 (C), 46.4 (CH_2), 44.4 (CH_2), 28.4 (CH_3), 28.1 (CH_3), 13.6 (CH_3), 13.1 (CH_3), 13.0 (CH_3); IR (thin film) 2976, 1703 cm^{-1}.

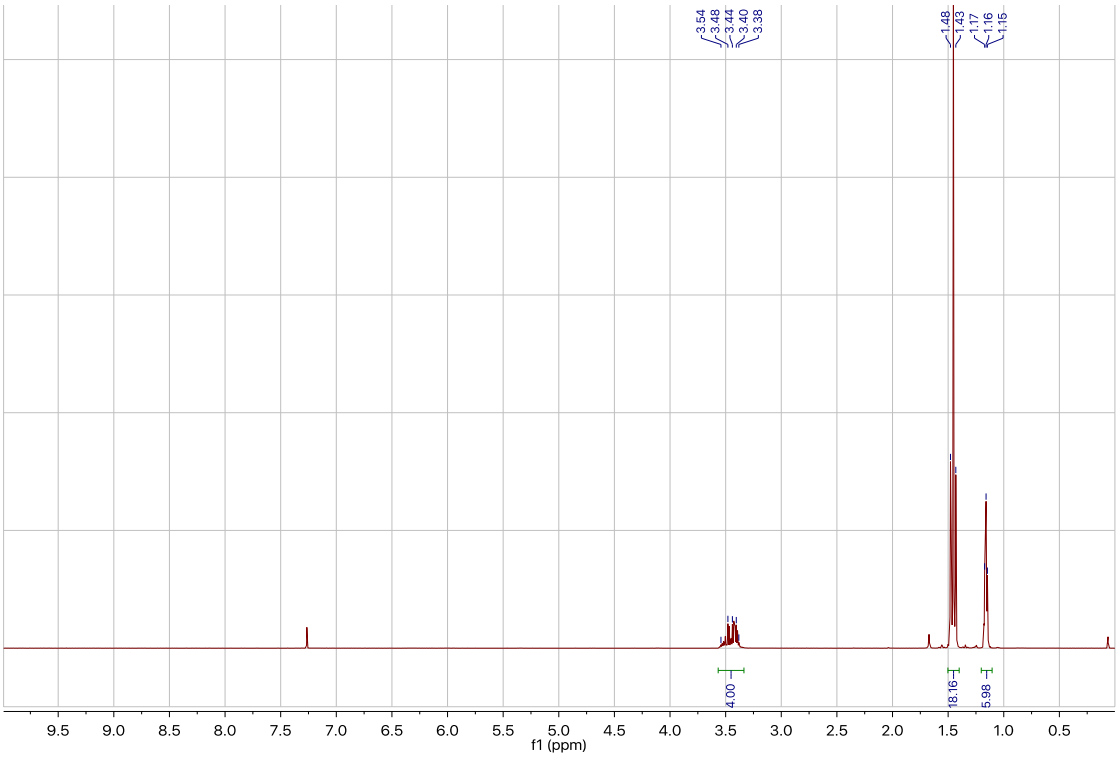

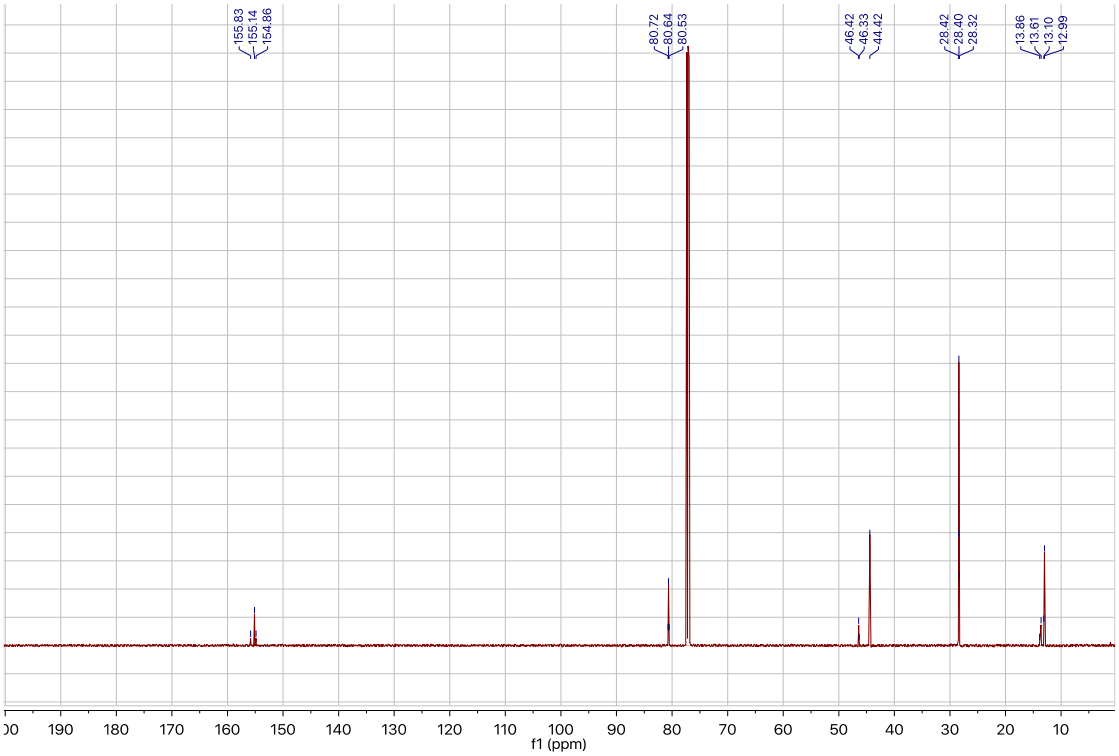

Figure **S1**. ^{1}H and ^{13}CNMR data for di-*tert*-butyl 1,2-diethylhydrazine-1,2-dicarboxylate.

4-Bromo-1,2-diethyl-1,2-dihydropyridazine-3,6-dione[2]

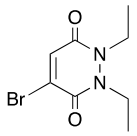

To a solution of bromomaleic anhydride (0.16 mL, 1.7 mmol) in AcOH (5 mL) was added di-*tert*-butyl 1,2-diethylhydrazine-1,2-dicarboxylate (0.50 g, 1.7 mmol), and the reaction mixture was stirred under reflux for 17 h. Following this, the reaction mixture was concentrated *in vacuo* and the crude residue was purified by flash column chromatography (15–85% EtOAc/Pet.). The appropriate fractions were then combined and concentrated *in vacuo* to afford 4-bromo-1,2-diethyl-1,2-dihydropyridazine-3,6-dione (0.40 g, 1.6 mmol, 94%) as a brown solid. m.p 73–76 ˚C; ^{1}H NMR (600 MHz, $CDCl_3$) δ 7.39 (s, 1H), 4.18 (q, *J* = 7.1 Hz, 2H), 4.11 (q, *J* = 7.1 Hz, 2H), 1.29 (t, *J* = 7.1 Hz, 3H), 1.26 (t, *J* = 7.1 Hz, 3H); ^{13}C NMR (150 MHz, $CDCl_3$) δ 156.4 (C), 154.3 (C), 135.9 (CH), 134.0 (C), 42.1 (CH_2), 41.0 (CH_2), 13.3 (CH_3), 13.2 (CH_3); IR (solid) 3047, 2982, 1712, 1615, 1591 cm^{-1}.

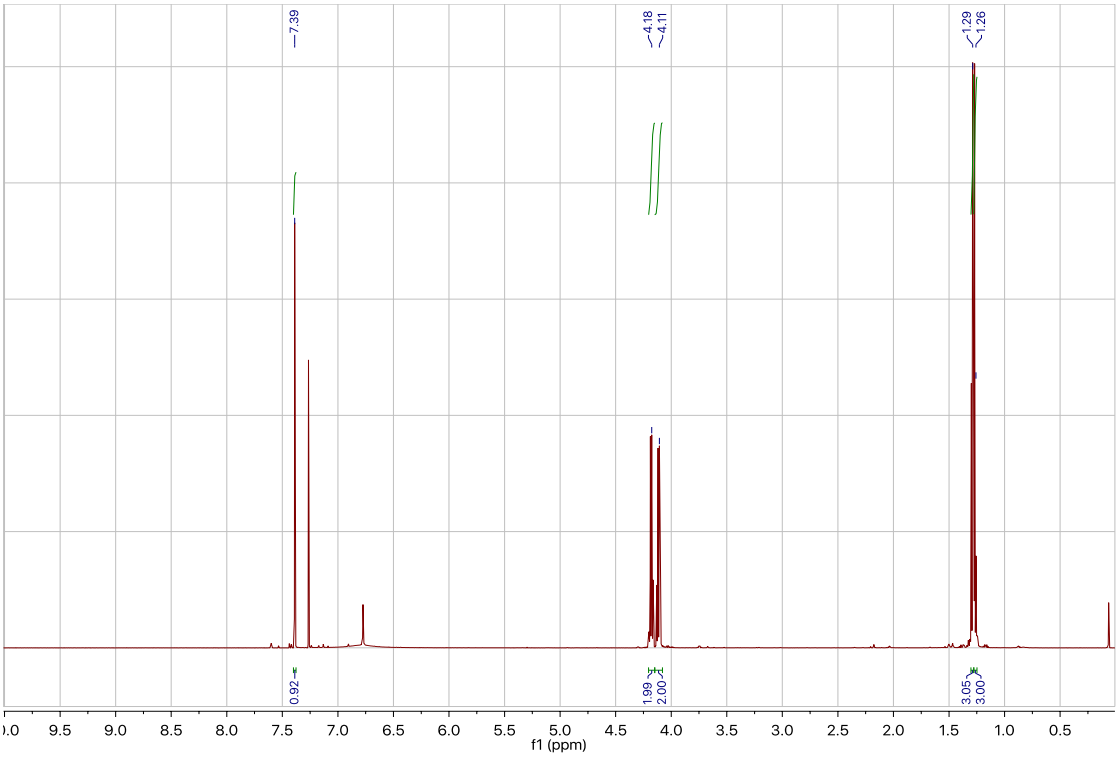

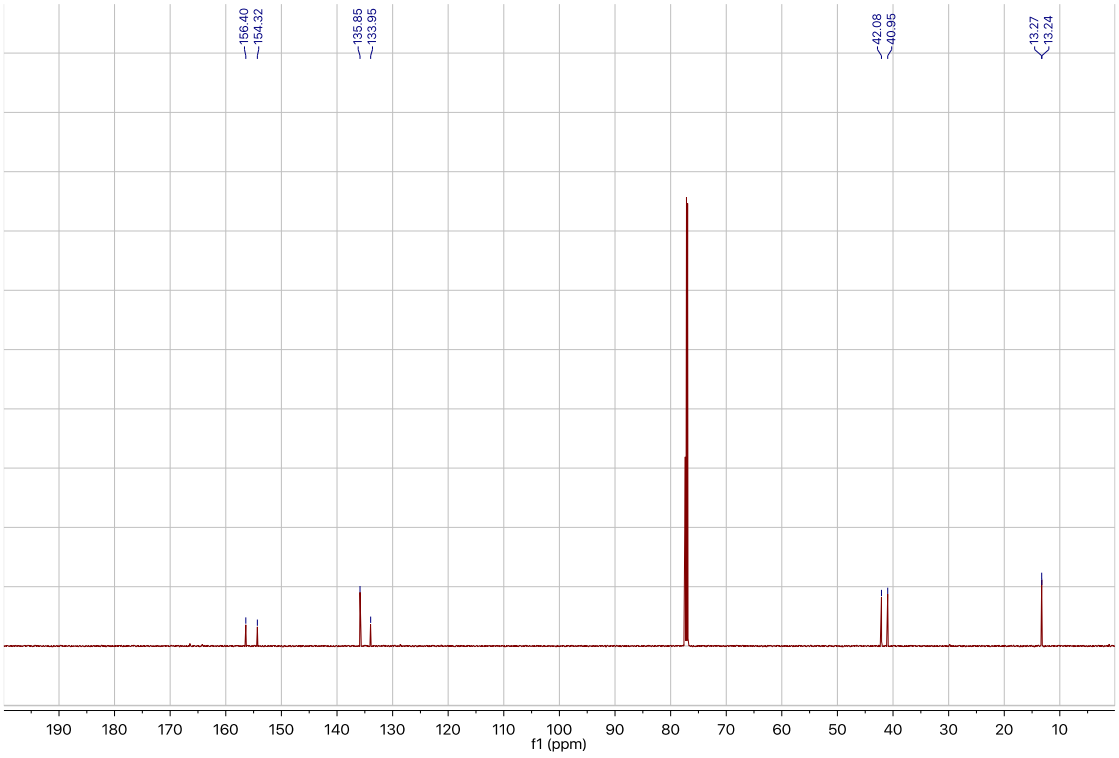

Figure **S2**. ^{1}H and ^{13}C NMR data for 4-bromo-1,2-diethyl-1,2-dihydropyridazine-3,6-dione.

4,5-Dibromo-1,2-diethyl-1,2-dihydropyridazine-3,6-dione[1]

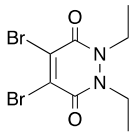

To a solution of dibromomaleic acid **19** (1.27 g, 4.64 mmol) in AcOH (6 mL) was added di-*tert*-butyl 1,2-diethylhydrazine-1,2-dicarboxylate (1.10 g, 3.81 mmol), and the reaction mixture was stirred under reflux for 20 h. Following this, the reaction mixture was concentrated *in vacuo* and the crude residue was purified by flash column chromatography (15–60% EtOAc/Pet.). The appropriate fractions were then combined and concentrated *in vacuo* to afford 4,5-dibromo-1,2-diethyl-1,2-dihydropyridazine-3,6-dione (1.00 g, 3.07 mmol, 81%) as an orange solid. m.p. 115–117 ˚C; ^{1}H NMR (600 MHz, $CDCl_3$) δ 4.18 (q, *J* = 7.1 Hz, 4H), 1.29 (t, *J* = 7.1 Hz, 6H); ^{13}C NMR (150 MHz, $CDCl_3$) δ 153.3 (C), 136.1 (C), 42.5 (CH_2), 13.2 (CH_3); IR (solid) 2978, 2937, 1655, 1567 cm^{-1}.

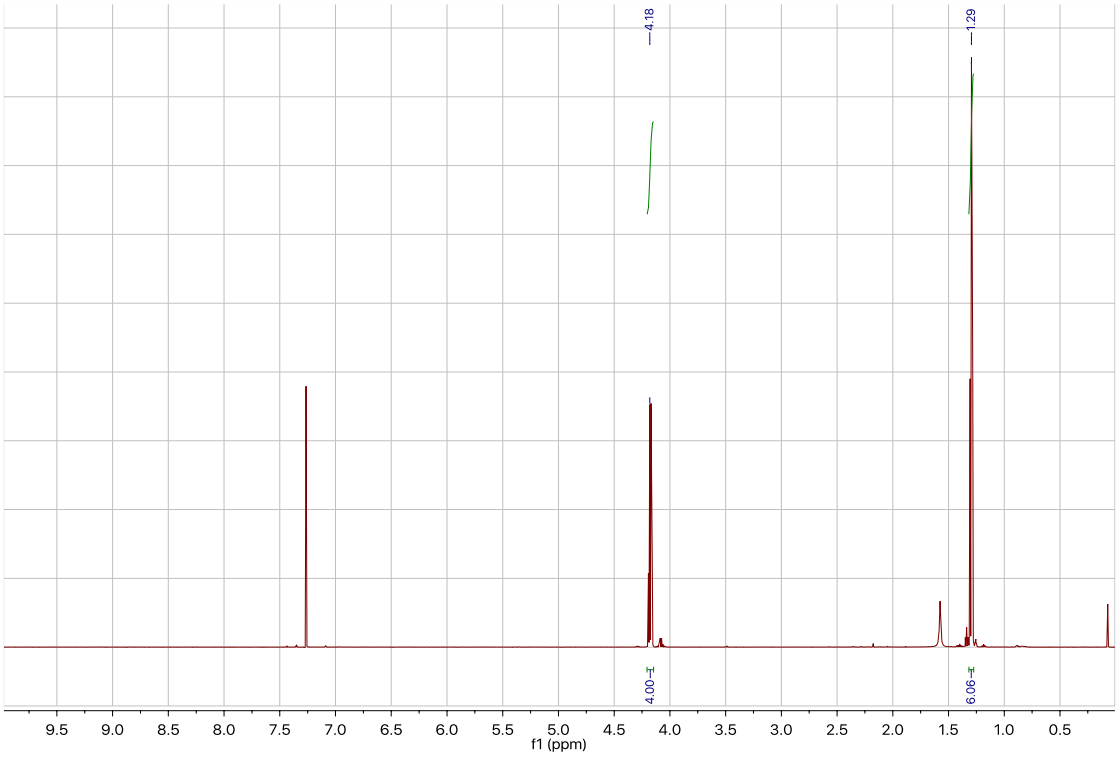

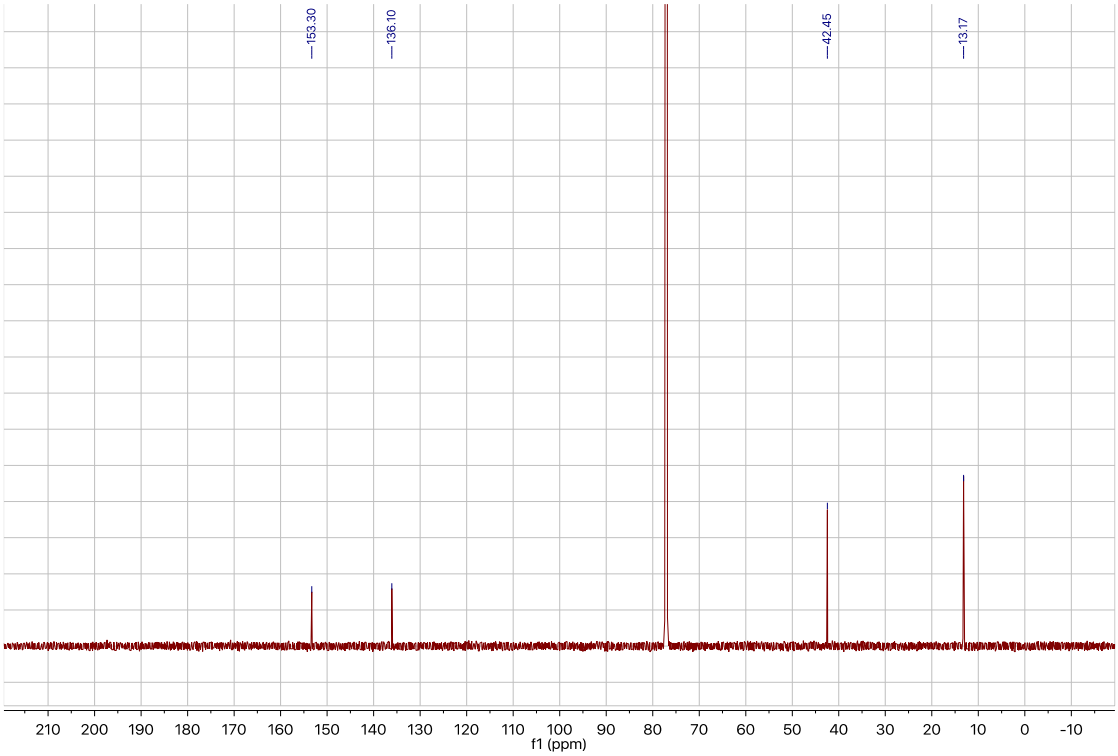

Figure **S3**. ^{1}H and ^{13}C NMR data for 4,5-dibromo-1,2-diethyl-1,2-dihydropyridazine-3,6-dione.

1,2-Diethyl-4-(phenylthio)-1,2-dihydropyridazine-3,6-dione 2

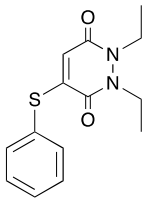

To a solution of thiophenol (0.05 mL, 0.5 mmol) and triethylamine (0.18 mL, 1.3 mmol) in CH_2Cl_2 (6 mL) at 21 ˚C, was added a solution of 4-bromo-1,2-diethyl-1,2-dihydropyridazine-3,6-dione (0.11 g, 0.45 mmol) in CH_2Cl_2 (6 mL), and the reaction mixture was stirred for 10 mins. Following this, the reaction mixture was diluted with CH_2Cl_2 (20 mL) and washed with water (3 × 15 mL) and brine (15 mL). The organic phase was dried over $MgSO_4$, concentrated *in vacuo* and the crude residue was purified by flash column chromatography (15–85% EtOAc/Pet.). The appropriate fractions were then combined and concentrated *in vacuo* to afford 1,2-diethyl-4-(phenylthio)-1,2-dihydropyridazine-3,6-dione (0.11 g, 0.40 mmol, 89%) as a green solid. m.p. 104–105 ˚C; ^{1}H NMR (600 MHz, $CDCl_3$) δ 7.53–7.46 (m, 5H), 5.96 (s, 1H), 4.17 (q, *J* = 7.0 Hz, 2H), 4.07 (q, *J* = 7.0 Hz, 2H), 1.29 (t, *J* = 7.0 Hz, 3H), 1.21 (t, *J* = 7.0 Hz, 3H); ^{13}C NMR (150 MHz, $CDCl_3$) δ 157.3 (C), 155.7 (C), 151.9 (C), 135.8 (C), 130.7 (CH), 130.5 (CH), 127.5 (CH), 123.0 (CH), 40.8 (CH_2), 40.1 (CH_2), 13.2 (CH_3), 13.2 (CH_3); IR (solid) 2967, 2926, 2854, 1654, 1616, 1573 cm^{-1}; LRMS (ES+) 277 (100, $[M+H]^+$); HRMS (ES+) calcd for $C_{14}H_{17}N_2O_2S$ $[M+H]^+$ 277.1011, observed 277.1011.

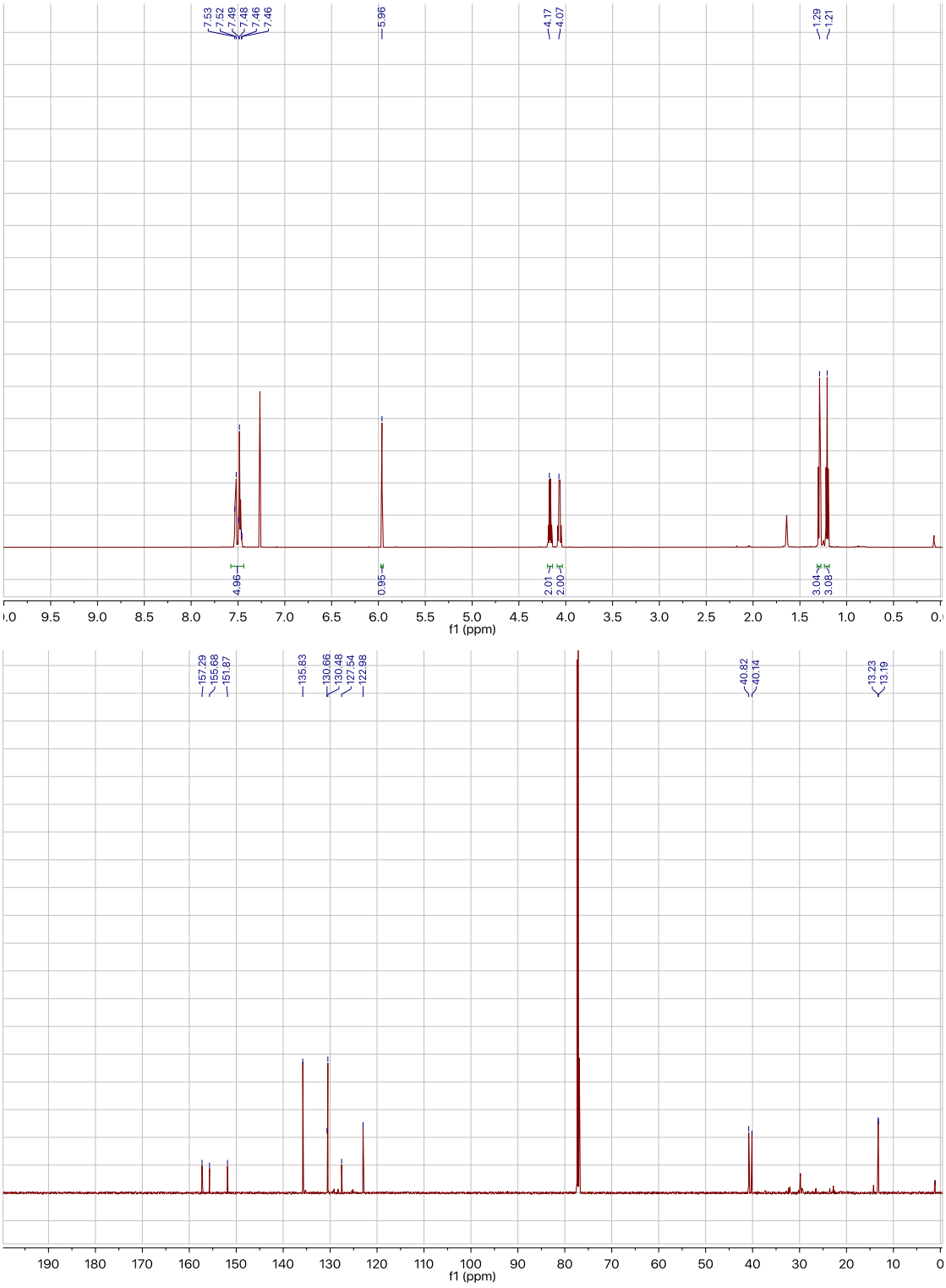

Figure **S4**. ^{1}H and ^{13}C NMR data for 1,2-diethyl-4-(phenylthio)-1,2-dihydropyridazine-3,6-dione **2**.

Methyl *N*-(*tert*-butoxycarbonyl)-*S*-(1,2-diethyl-3,6-dioxo-1,2,3,6-tetrahydropyridazin-4-yl)cysteinate 3

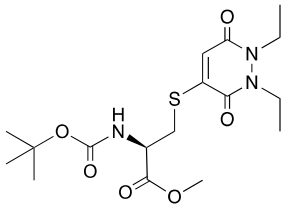

To a solution of *N*-(*tert*-butoxycarbonyl)-L-cysteine methyl ester (0.24 g, 1.02 mmol) and triethylamine (0.40 mL, 2.9 mmol) in CH_2Cl_2 (8 mL) at 21 ˚C, was added a solution of 4-bromo-1,2-diethyl-1,2-dihydropyridazine-3,6-dione (0.24 g, 0.97 mmol) in CH_2Cl_2 (8 mL), and the reaction mixture was stirred for 10 mins. Following this, the reaction mixture was diluted with CH_2Cl_2 (20 mL) and washed with water (3 × 15 mL) and brine (15 mL). The organic phase was dried over $MgSO_4$, concentrated *in vacuo* and the crude residue was purified by flash column chromatography (20–85% EtOAc/Pet.). The appropriate fractions were then combined and concentrated *in vacuo* to afford methyl *N*-(*tert*-butoxycarbonyl)-*S*-(1,2-diethyl-3,6-dioxo-1,2,3,6-tetrahydropyridazin-4-yl)cysteinate (0.31 g, 0.77 mmol, 80%) as a white solid. $[\alpha]_D^{20.0}$ +3.0 (*c* 1, $CHCl_3$); m.p. 86–90 ˚C; ^{1}H NMR (600 MHz, $CDCl_3$) δ 6.56 (s, 1H), 5.37 (d, *J* = 7.6 Hz, 1H), 4.68–4.65 (m, 1H), 4.17–4.07 (m, 4H), 3.79 (s, 3H), 3.31 (dd, *J* = 13.2, 5.0 Hz, 1H), 3.20 (dd, *J* = 13.2, 5.0 Hz, 1H), 1.44 (s, 9H), 1.26 (t, *J* = 7.1 Hz, 3H), 1.22 (t, *J* = 7.1 Hz, 3H); ^{13}C NMR (150 MHz, $CDCl_3$) δ 170.5 (C), 156.9 (C), 155.6 (C), 155.1 (C), 148.7 (C), 122.6 (CH), 80.7 (C), 53.1 (CH_3), 52.2 (CH), 40.9 (CH_2), 40.2 (CH_2), 33.0 (CH_2), 28.4 (CH_3), 13.2 (CH_3), 13.1 (CH_3); IR (solid) 2979, 1746, 1709, 1615 cm^{-1}; LRMS (ES+) 402 (100, $[M+H]^+$); HRMS (ES+) calcd for $C_{17}H_{28}N_3O_6S$ $[M+H]^+$ 402.1693, observed 402.1694.

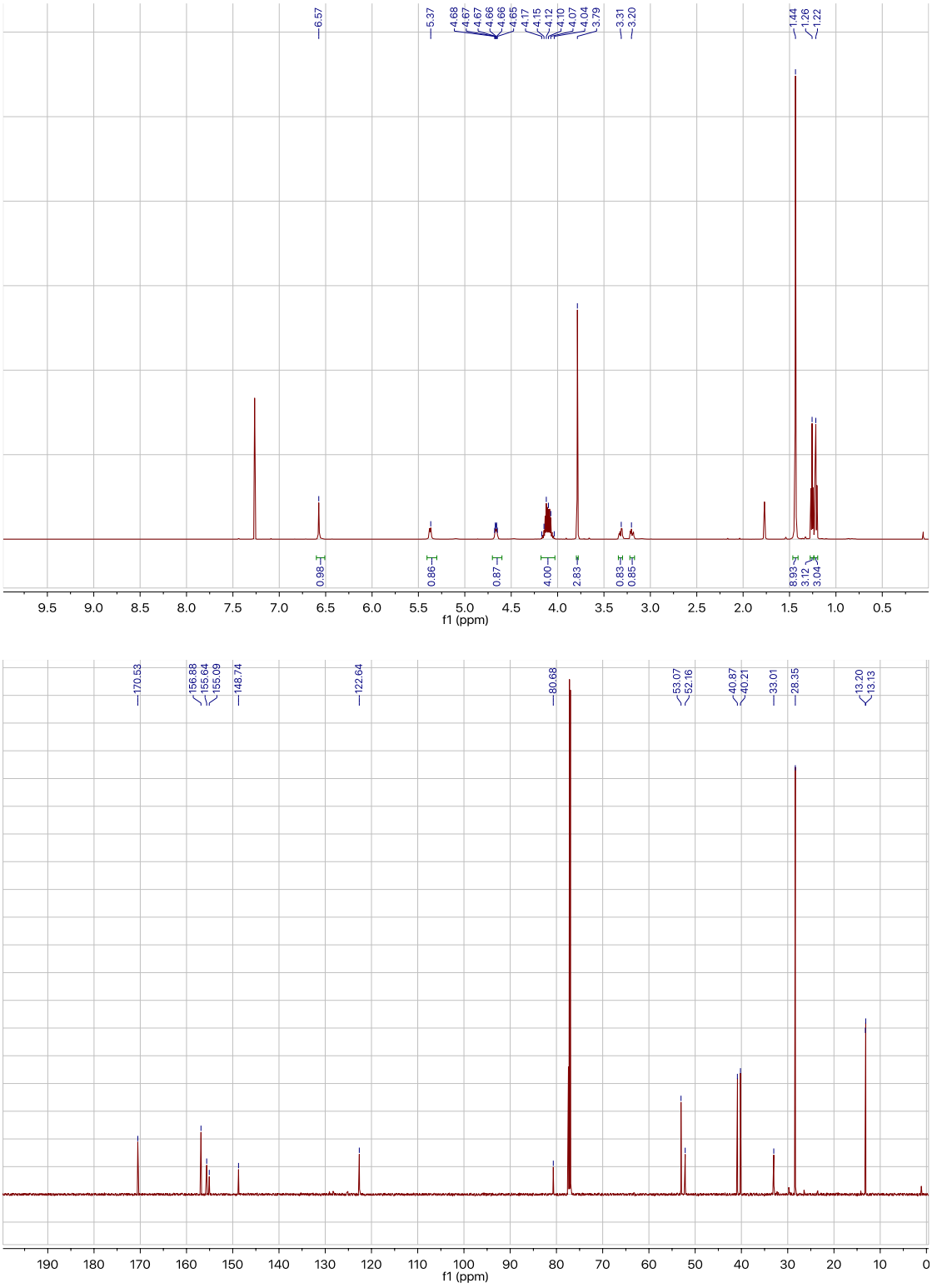

Figure **S5**. ^{1}H and ^{13}C NMR data for methyl *N*-(*tert*-butoxycarbonyl)-*S*-(1,2-diethyl-3,6-dioxo-1,2,3,6-tetrahydropyridazin-4-yl)cysteinate **3**.

1,2-Diethyl-4,5-bis(phenylthio)-1,2-dihydropyridazine-3,6-dione 4

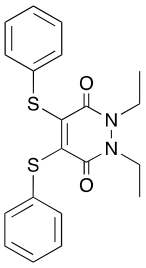

To a solution of thiophenol (0.10 mL, 0.97 mmol) and triethylamine (0.39 mL, 2.80 mmol) in CH_2Cl_2 (6 mL) at 21 ˚C, was added a solution of 4,5-dibromo-1,2-diethyl-1,2-dihydropyridazine-3,6-dione (0.10 g, 0.31 mmol) in CH_2Cl_2 (6 mL), and the reaction mixture was stirred for 10 mins. Following this, the reaction mixture was diluted with CH_2Cl_2 (20 mL) and washed with water (3 × 15 mL) and brine (15 mL). The organic phase was dried over $MgSO_4$, concentrated *in vacuo* and the crude residue was purified by flash column chromatography (15–80% EtOAc/Pet.). The appropriate fractions were then combined to afford 1,2-diethyl-4,5-bis(phenylthio)-1,2-dihydropyridazine-3,6-dione (0.09g, 0.23 mmol, 76%) as a yellow solid. m.p. 126–130 ˚C; ^{1}H NMR (600 MHz, $CDCl_3$) δ 7.28–7.25 (m, 7H), 7.22–7.20 (m, 3H), 4.05 (q, *J* = 7.1 Hz, 4H), 1.23 (t, *J* = 7.1 Hz, 6H); ^{13}C NMR (150 MHz, $CDCl_3$) δ 156.0 (C), 141.9 (C), 132.6 (C), 131.0 (CH), 129.1 (CH), 127.9 (CH), 41.2 (CH_2), 12.8 (CH_3); IR (solid) 3058, 2967, 2928, 1657, 1574 cm^{-1}; LRMS (ES+) 385 (100, $[M+H]^+$); HRMS (ES+) calcd for $C_{20}H_{21}N_2O_2S_2$ $[M+H]^+$ 385.1039, observed 385.1040.

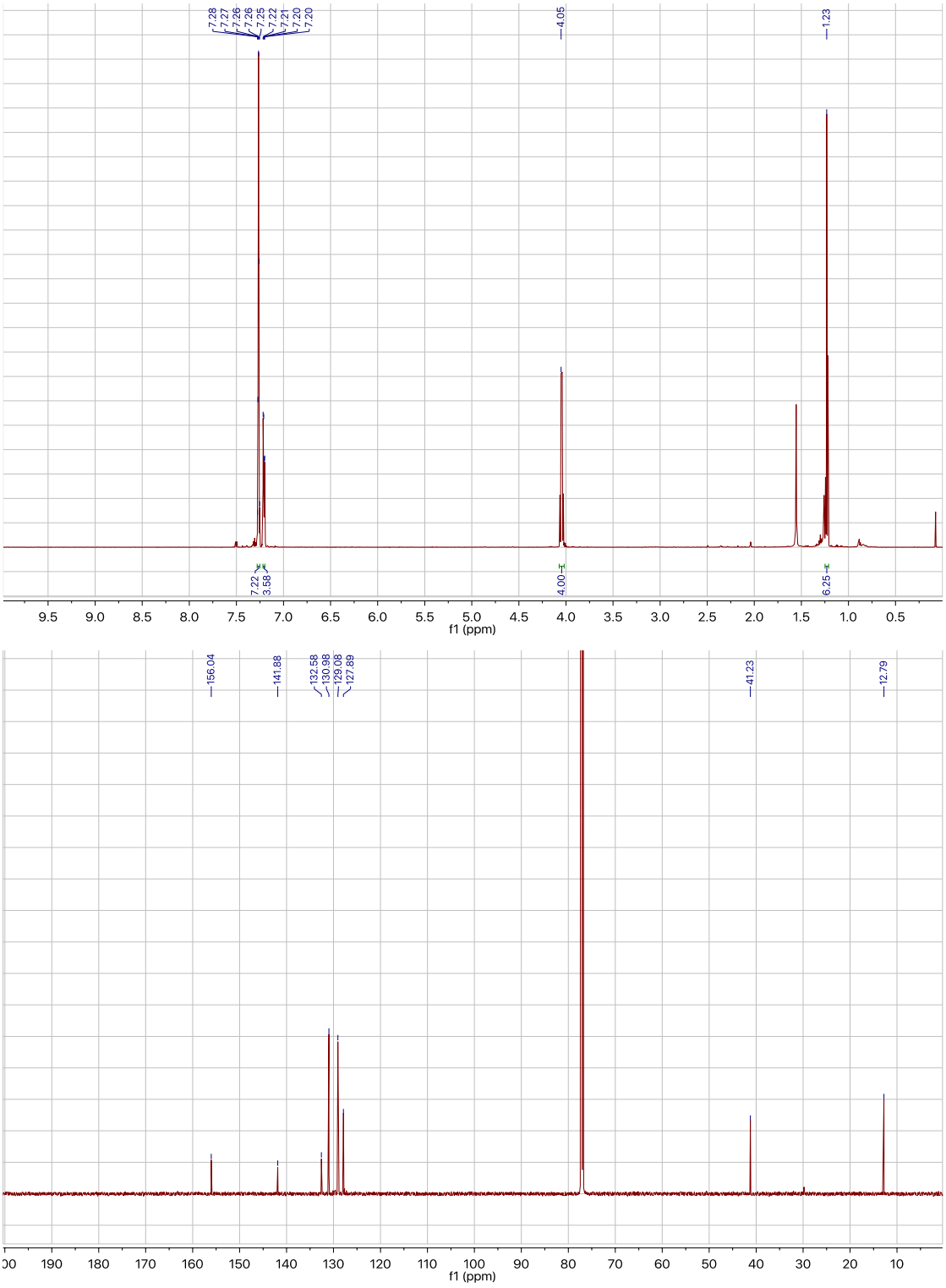

Figure **S6**. ^{1}H and ^{13}C NMR data for 1,2-diethyl-4,5-bis(phenylthio)-1,2-dihydropyridazine-3,6-dione **4**.

Dimethyl 3,3'-((1,2-diethyl-3,6-dioxo-1,2,3,6-tetrahydropyridazine-4,5-diyl)bis(sulfanediyl))bis(2-((*tert*-butoxycarbonyl)amino)propanoate) 5

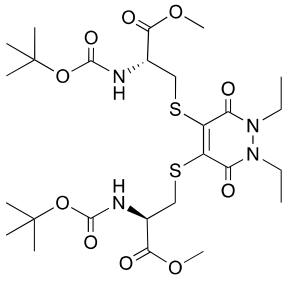

To a solution of 4,5-dibromo-1,2-diethyl-1,2-dihydropyridazine-3,6-dione (0.13 g, 0.40 mmol) and *N*-(*tert*-butoxycarbonyl)-L-cysteine methyl ester (0.47 g, 2.0 mmol) in CH_2Cl_2 (10 mL) was added triethylamine (0.07 mL, 0.5 mmol), and the reaction mixture was stirred at 21 ˚C for 65 h. Following this, the reaction mixture was diluted with CH_2Cl_2 (20 mL) and washed with water (3 × 20 mL) and brine (15 mL). The organic phase was dried over $MgSO_4$, concentrated *in vacuo* and the crude residue was purified by flash column chromatography (15–60% EtOAc/Pet.). The appropriate fractions were then combined and concentrated *in vacuo* to afford dimethyl 3,3'-((1,2-diethyl-3,6-dioxo-1,2,3,6-tetrahydropyridazine-4,5-diyl)bis(sulfanediyl))bis(2-((*tert*-butoxycarbonyl)amino)propanoate) (0.15 g, 0.24 mmol, 59%) as a yellow oil. $[\alpha]_D^{20.0}$ +60.6 (*c* 1, $CHCl_3$); ^{1}H NMR (600 MHz, $CDCl_3$) δ 5.76 (d, *J* = 7.8 Hz, 2H), 4.55–4.53 (m, 2H), 4.09–3.98 (m, 4H), 3.74–3.68 (m, 3H), 3.68 (s, 6H), 3.65–3.60 (m, 1H) 1.38 (s, 18H), 1.21 (t, *J* = 7.2 Hz, 6H); ^{13}C NMR (150 MHz, $CDCl_3$) δ 171.2 (C), 155.3 (C), 155.3 (C), 141.9 (C), 80.1 (C), 53.9 (CH), 52.6 (CH_3), 41.3 (CH_2), 35.7 (CH_2), 28.4 (CH_3), 13.0 (CH_3); IR (thin film) 2978, 1707, 1617 cm^{-1}; LRMS (ES+) 635 (100, $[M+H]^+$); HRMS (ES+) calcd for $C_{26}H_{43}N_4O_{10}S_2$ $[M+H]^+$ 635.2415, observed 635.2411.

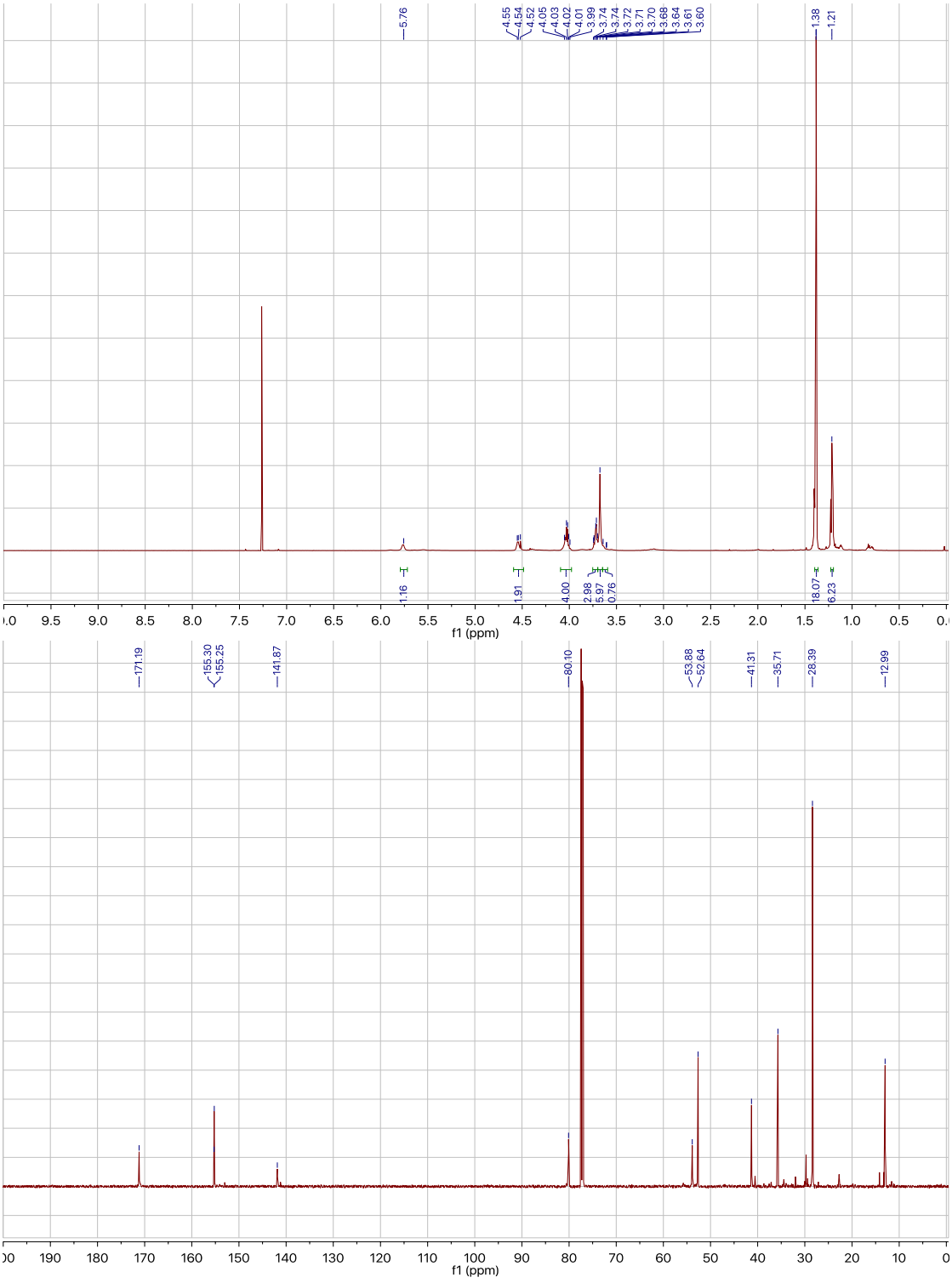

Figure **S7**. ^{1}H and ^{13}C NMR data for dimethyl 3,3'-((1,2-diethyl-3,6-dioxo-1,2,3,6-tetrahydropyridazine-4,5-diyl)bis(sulfanediyl))bis(2-((*tert*-butoxycarbonyl)amino)propanoate) **5**.

Methyl *S*-(5-bromo-1,2-diethyl-3,6-dioxo-1,2,3,6-tetrahydropyridazin-4-yl)-*N*-(*tert*-butoxycarbonyl)cysteinate

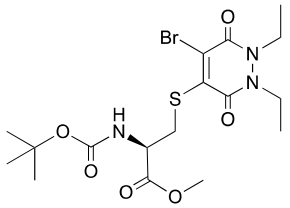

To a solution of 4,5-dibromo-1,2-diethyl-1,2-dihydropyridazine-3,6-dione (0.20 g, 0.61 mmol) in CH_2Cl_2 (6 mL) at 21 ˚C, was added dropwise over 10 mins a solution of N-(*tert*-butoxycarbonyl)-L-cysteine methyl ester (0.14 g, 0.59 mmol) and triethylamine (0.13 mL, 0.93 mmol) in CH_2Cl_2 (6 mL). Following this, the reaction mixture was diluted with CH_2Cl_2 (12 mL) and washed with water (3 × 15 mL) and brine (15 mL). The organic phase was dried over $MgSO_4$, concentrated *in vacuo* and the crude residue was purified by flash column chromatography (0–30% EtOAc/$CHCl_3$). The appropriate fractions were then combined and concentrated *in vacuo* to afford methyl *S*-(5-bromo-1,2-diethyl-3,6-dioxo-1,2,3,6-tetrahydropyridazin-4-yl)-*N*-(*tert*-butoxycarbonyl)cysteinate (0.17 g, 0.35 mmol, 60%) as a yellow oil. $[\alpha]_D^{20.0}$ +17.7 (*c* 1, $CHCl_3$); ^{1}H NMR (600 MHz, $CDCl_3$) δ 5.42 (d, *J* = 8.1 Hz, 1H), 4.63–4.59 (m, 1H), 4.22–4.03 (m, 4H), 3.85–3.82 (m, 1H), 3.75 (d, *J* = 7.0 Hz, 1H), 3.73 (s, 3H), 1.42 (s, 9H), 1.30–1.25 (m, 6H); ^{13}C NMR (150 MHz, $CDCl_3$) δ 171.1 (C), 155.2 (C), 154.6 (C), 153.7 (C), 145.3 (C), 130.9 (C), 80.4 (C), 53.9 (CH), 52.8 (CH_3), 42.2 (CH_2), 41.1 (CH_2), 35.9 (CH_2), 28.4 (CH_3), 13.2 (CH_3), 12.9 (CH_3); IR (thin film) 2977, 2934, 1743, 1708, 1622 cm^{-1}; LRMS (ES+) 482 (100, $[M^{81}Br+H]^+$), 480 (96, $[M^{79}Br+H]^+$); HRMS (ES+) calcd for $C_{17}H_{27}N_3O_6SBr$ $[M^{81}Br+H]^+$ 482.0779, observed 482.0770.

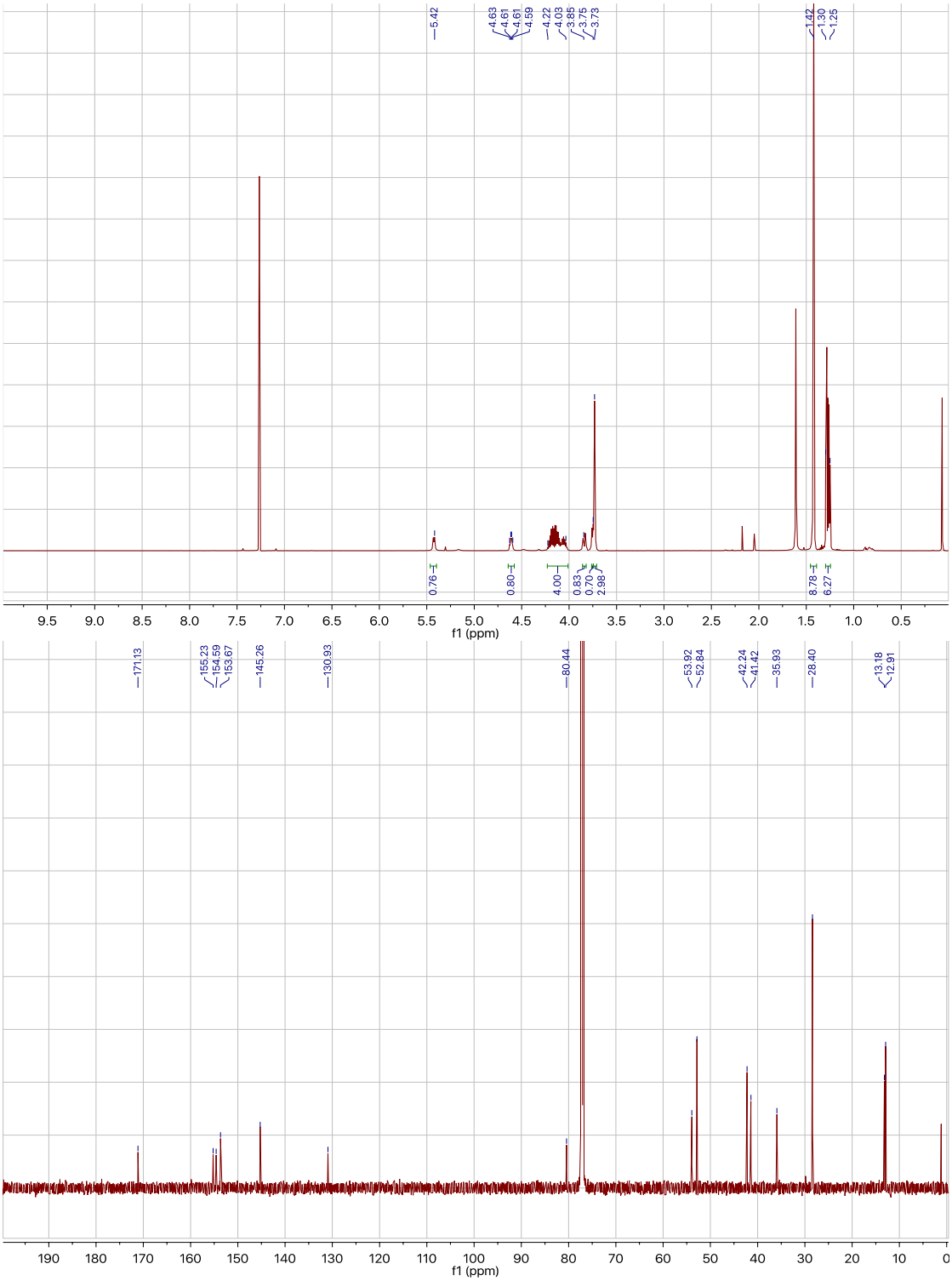

Figure **S8**. ^{1}H and ^{13}C NMR spectra for methyl *S*-(5-bromo-1,2-diethyl-3,6-dioxo-1,2,3,6-tetrahydropyridazin-4-yl)-*N*-(*tert*-butoxycarbonyl)cysteinate.

Methyl *N*-(*tert*-butoxycarbonyl)-*S*-(1,2-diethyl-3,6-dioxo-5-(phenylthio)-1,2,3,6-tetrahydropyridazin-4-yl)cysteinate 6

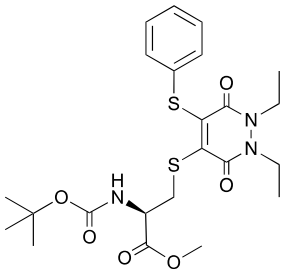

To a solution of methyl *S*-(5-bromo-1,2-diethyl-3,6-dioxo-1,2,3,6-tetrahydropyridazin-4-yl)-*N*-(*tert*-butoxycarbonyl)cysteinate (0.45 g, 0.94 mmol) in CH_2Cl_2 (8 mL) at 21 ˚C, was added a solution of thiophenol (0.10 mL, 0.98 mmol) and triethylamine (0.20 mL, 1.4 mmol) in CH_2Cl_2 (8 mL), and the reaction was stirred for 10 mins. Following this, the reaction mixture was diluted with CH_2Cl_2 (16 mL) and washed with water (3 × 15 mL) and brine (15 mL). The organic phase was dried over $MgSO_4$, concentrated *in vacuo* and the crude residue was purified by flash column chromatography (0–40% EtOAc/$CHCl_3$). The appropriate fractions were then combined and concentrated *in vacuo* to afford methyl *N*-(*tert*-butoxycarbonyl)-*S*-(1,2-diethyl-3,6-dioxo-5-(phenylthio)-1,2,3,6-tetrahydropyridazin-4-yl)cysteinate (0.24 g, 0.47 mmol, 50%) as a yellow oil. $[\alpha]_D^{20.0}$ +26.9 (*c* 1, $CHCl_3$); ^{1}H NMR (600 MHz, $CDCl_3$) δ 7.37–7.27 (m, 5H), 5.48 (d, *J* = 8.1 Hz, 1H), 4.52 (m, 1H), 4.15–3.98 (m, 4H), 3.70 (s, 3H), 3.68 (d, *J* = 6.3 Hz, 1H), 3.58 (dd, *J* = 14.0, 6.3 Hz, 1H), 1.41 (s, 9H), 1.27 (t, *J* = 7.1 Hz, 3H), 1.22 (t, *J* = 7.1 Hz, 3H); ^{13}C NMR (150 MHz, $CDCl_3$) δ 171.3 (C), 155.8 (C), 155.3 (C), 155.3 (C), 142.6 (C), 142.1 (C), 132.8 (C), 131.1 (CH), 129.3 (CH), 128.0 (CH), 80.3 (C), 53.8 (CH), 52.7 (CH_3), 41.3 (CH_2), 41.3 (CH_2), 35.7 (CH_2), 28.4 (CH_3), 13.0 (CH_3), 12.9 (CH_3); IR (thin film) 2975, 2932, 1743, 1708, 1614 cm^{-1}; LRMS (ES+) 510 (100, $[M+H]^+$); HRMS (ES+) calcd for $C_{23}H_{32}N_3O_6S_2$ $[M+H]^+$ 510.1727, observed 510.1718.

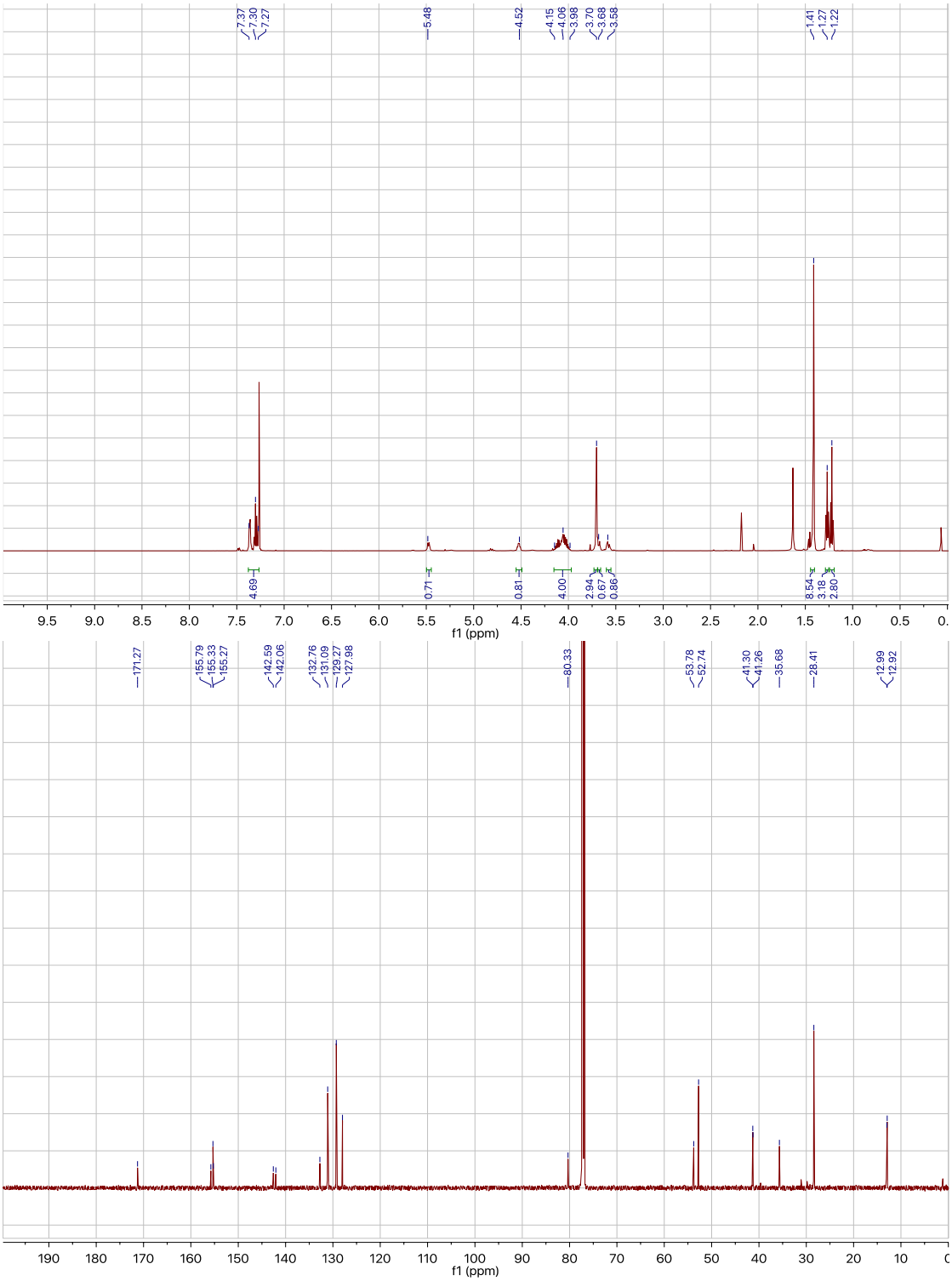

Figure **S9**. ^{1}H and ^{13}C NMR spectra for methyl *N*-(*tert*-butoxycarbonyl)-*S*-(1,2-diethyl-3,6-dioxo-5-(phenylthio)-1,2,3,6-tetrahydropyridazin-4-yl)cysteinate **6**.

1,2-Diethyl-4,5-bis(*p*-tolylthio)-1,2-dihydropyridazine-3,6-dione 8

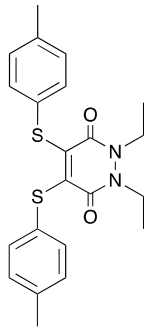

To a solution of 4,5-dibromo-1,2-diethyl-1,2-dihydropyridazine-3,6-dione (1.63 g, 5.00 mmol) in CH_2Cl_2 (10 mL) at 21 ˚C, was added a solution of 4-methylbenzenethiol **23** (1.55 g, 12.5 mmol) and triethylamine (2.27 mL, 16.3 mmol) in CH_2Cl_2 (10 mL), and the reaction mixture was stirred for 10 mins. Following this, the reaction mixture was diluted with CH_2Cl_2 (20 mL) and washed with water (3 × 30 mL) and brine (30 mL). The organic phase was dried over $MgSO_4$, concentrated *in vacuo* and the crude residue was purified by flash column chromatography (10–60% EtOAc/Pet.). The appropriate fractions were then combined and concentrated *in vacuo* to afford 1,2-diethyl-4,5-bis(*p*-tolylthio)-1,2-dihydropyridazine-3,6-dione (1.85 g, 4.49 mmol, 90%) as a yellow solid. m.p. 114–116 ˚C; ^{1}H NMR (600 MHz, $CDCl_3$) δ 7.15 (d, *J* = 8.2 Hz, 4H), 7.09 (d, *J* = 8.2 Hz, 4H), 4.02 (q, *J* = 7.1 Hz, 4H), 2.33 (s, 6H), 1.21 (t, *J* = 7.1 Hz, 6H); ^{13}C NMR (150 MHz, $CDCl_3$) δ 156.1 (C), 142.3 (C), 138.1 (C), 131.3 (CH), 129.9 (CH), 129.3 (C), 41.1 (CH_2), 21.4 (CH_3), 12.8 (CH_3); IR (solid) 2980, 2956, 2923, 2868, 1617, 1567 cm^{-1}; LRMS (ES+) 413 (100, $[M+H]^+$); HRMS (ES+) calcd for $C_{22}H_{25}N_2O_2S_2$ $[M+H]^+$ 413.1352, observed 413.1346.

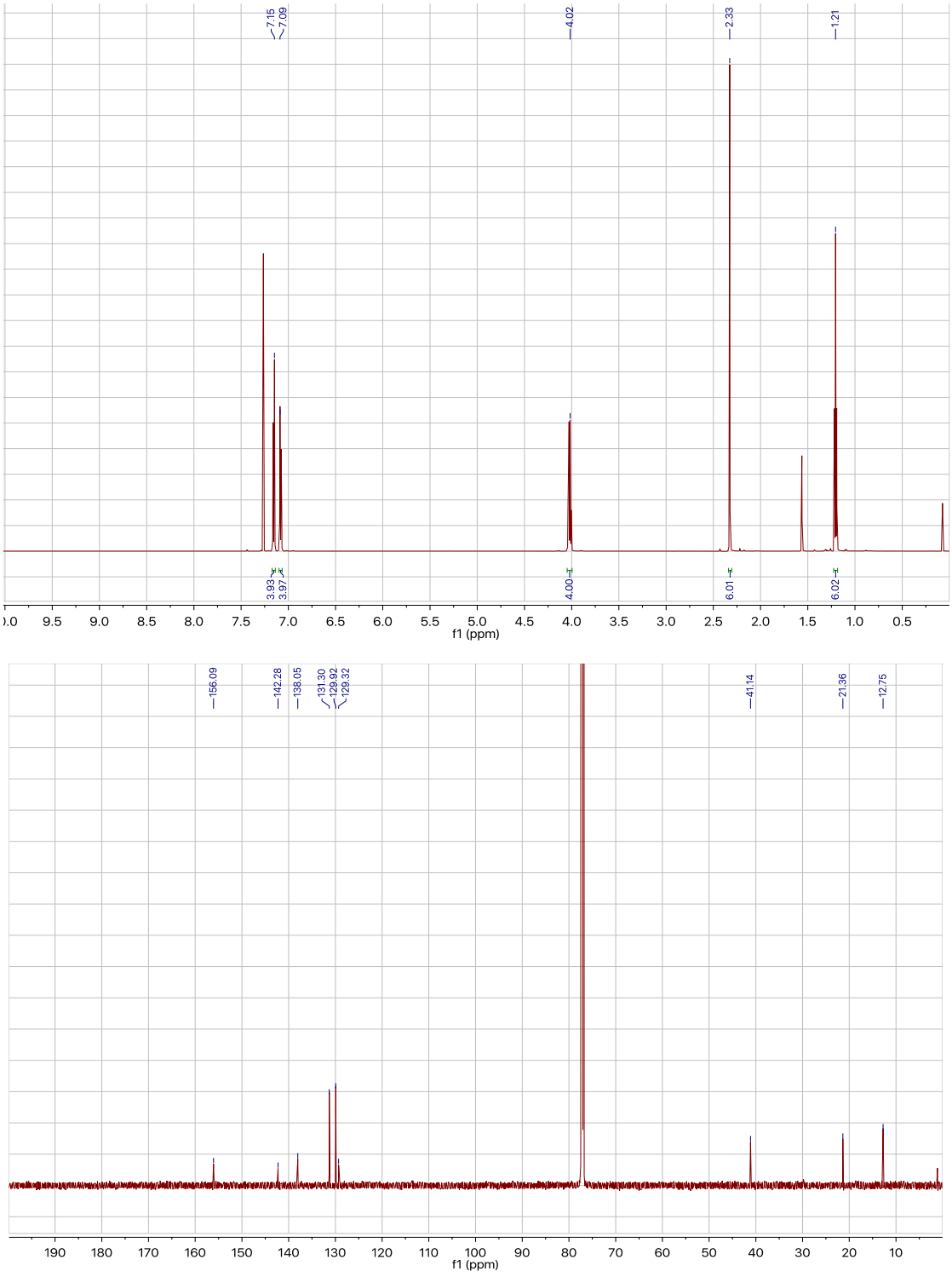

Figure **S10**. ^{1}H and ^{13}C NMR spectra for 1,2-diethyl-4,5-bis(*p*-tolylthio)-1,2-dihydropyridazine-3,6-dione **8**.

1,2-Diethyl-4,5-bis((4-(((2-oxo-2*H*-chromen-7-yl)oxy)methyl)phenyl)thio)-1,2-dihydropyridazine-3,6-dione 13

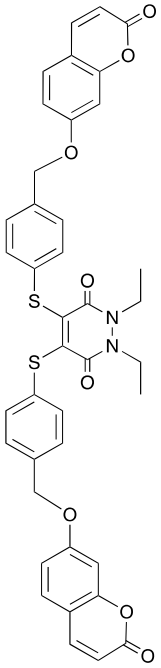

To a solution of 1,2-diethyl-4,5-bis(*p*-tolylthio)-1,2-dihydropyridazine-3,6-dione **8** (0.11 g, 0.27 mmol) in fluorobenzene (6 mL) was added NBS **9** (0.13 g, 0.73 mmol) and AIBN **10** (0.03 g, 0.2 mmol), and the reaction mixture was stirred under reflux for 7 h. Following this, the reaction mixture was diluted with EtOAc (20 mL) and washed with water (3 × 20 mL). The organic phase was dried over $MgSO_4$ and concentrated *in vacuo* to afford the crude 4,5-bis((4-(bromomethyl)phenyl)thio)-1,2-diethyl-1,2-dihydropyridazine-3,6-dione **11** (0.11 g total). The crude mixture was dissolved in dry THF (4 mL) along with cesium carbonate (0.22 g, 0.68 mmol) and umbelliferone **12** (0.08 g, 0.5 mmol), and the reaction mixture was stirred under reflux for 21 h. Following this, the reaction mixture was diluted with water (10 mL) and extracted with EtOAc (3 × 15 mL). The organic phase was dried over $MgSO_4$, concentrated *in vacuo* and the crude residue was purified by preparative TLC (50% EtOAc/$CHCl_3$) to afford 1,2-diethyl-4,5-bis((4-(((2-oxo-2*H*-chromen-7-yl)oxy)methyl)phenyl)thio)-1,2-dihydropyridazine-3,6-dione (0.02 g, 0.03 mmol, 9%) as a yellow solid. m.p. 179–183 ˚C; ^{1}H NMR (600 MHz, $CDCl_3$) δ 7.62 (d, *J* = 9.5 Hz, 2H), 7.37 (d, *J* = 8.6 Hz, 2H), 7.32 (d, *J* = 8.2 Hz, 4H), 7.22 (d, *J* = 8.2 Hz, 4H), 6.89 (dd, *J* = 8.6, 2.5 Hz, 2H), 6.86 (d,*J* = 2.5 Hz, 2H), 6.26 (d, *J* = 9.5 Hz, 2H), 5.10 (s, 4H), 4.05 (q, *J* = 7.0 Hz, 4H), 1.23 (t, *J* = 7.0 Hz, 6H); ^{13}C NMR (150 MHz, $CDCl_3$)* δ 161.8 (C), 161.2 (C), 156.0 (C), 155.8 (C), 143.5 (CH), 141.9 (C), 135.7 (C), 132.7 (C), 131.3 (CH), 129.0 (CH), 128.2 (CH), 113.5 (CH), 113.3 (CH), 113.0 (C), 102.1 (CH), 70.0 (CH_2), 41.4 (CH_2), 12.9

(CH_3); IR (solid) 2919, 2851, 1726, 1608 cm^{-1}; LRMS (ES+) 733 (100, $[M+H]^+$); HRMS (ES+) calcd for $C_{40}H_{33}N_2O_8S_2$ $[M+H]^+$ 733.1678, observed 733.1674.

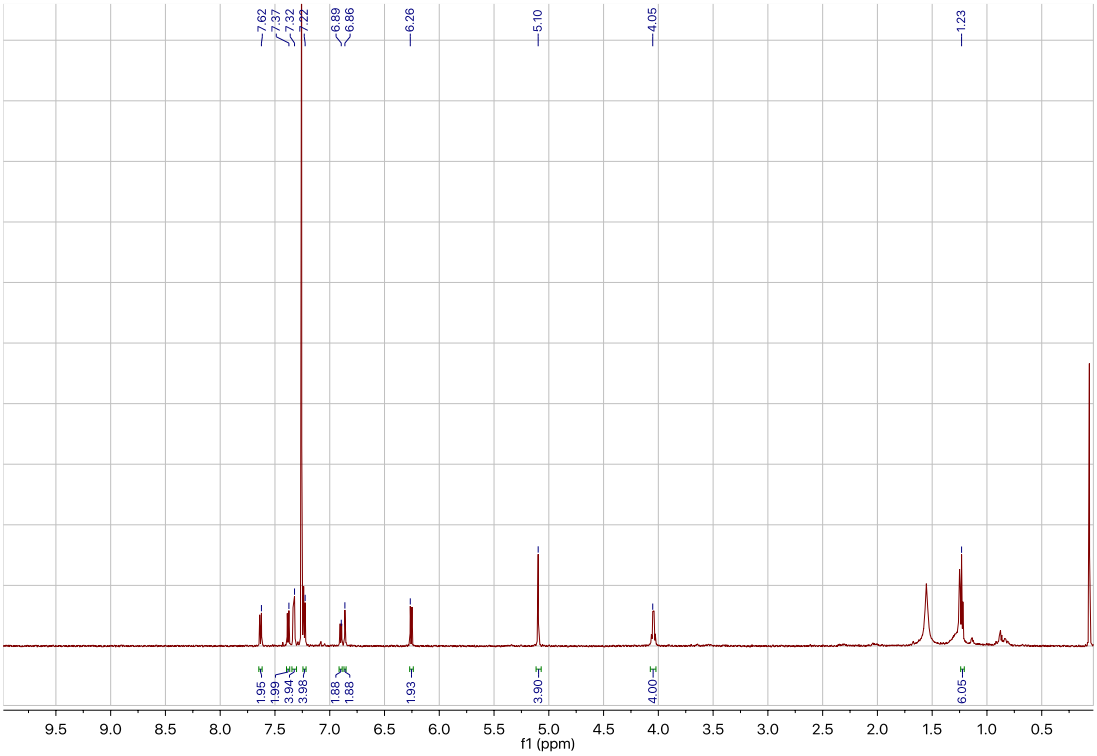

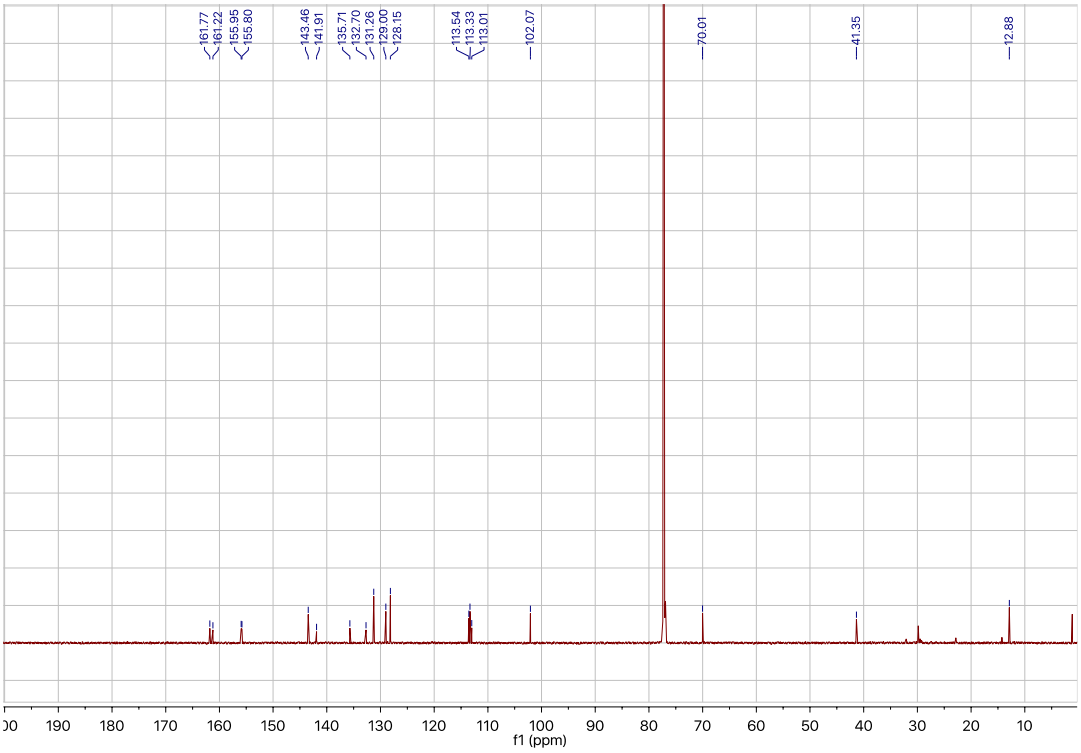

Figure **S11**. ^{1}H and ^{13}C NMR spectra for 1,2-diethyl-4,5-bis((4-(((2-oxo-2*H*-chromen-7-yl)oxy)methyl)phenyl)thio)-1,2-dihydropyridazine-3,6-dione **13**. *29.8 (H grease), 1.15 (silicon grease).

***Tert*-butyl 7-hydroxy-2-oxo-2*H*-chromene-3-carboxylate**[3]

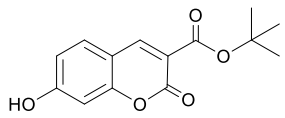

To a solution of di-*tert*-butyl malonate (0.69 g, 3.2 mmol) and potassium carbonate (1.11 g, 8.03 mmol) in DMF (16 mL), was added 2,4-dihydroxybenzaldehyde (0.22 g, 1.6 mmol), and the reaction mixture was stirred at 80 ˚C for 19 h. Following this, the reaction mixture was diluted with water (16 mL), 0.1 M citric acid (16 mL), and extracted with EtOAc (3 × 40 mL). The organic extracts were combined and subsequently washed with sat. aq. LiCl solution (40 mL). The organic phase was dried over $MgSO_4$, concentrated *in vacuo* and the crude residue was purified by flash column chromatography (10–60% EtOAc/Pet.). The appropriate fractions were then combined and concentrated *in vacuo* to afford *tert*-butyl 7-hydroxy-2-oxo-2*H*-chromene-3-carboxylate (0.05 g, 0.2 mmol, 12%) as a beige solid. m.p. 249–251 ˚C; ^{1}H NMR (700 MHz, $CDCl_3$) δ 8.39 (s, 1H), 7.47 (d, *J* = 8.5 Hz, 1H), 6.91 (d, *J* = 2.2 Hz, 1H), 6.87 (dd, *J* = 8.5, 2.2 Hz, 1H), 1.59 (s, 9H); ^{13}C NMR (150 MHz, $CDCl_3$) δ 162.5 (C), 162.3 (C), 158.0 (C), 157.3 (C), 148.5 (CH), 131.2 (CH), 115.1 (C) 114.3 (CH), 111.8 (C), 103.2 (CH), 82.6 (C), 28.3 (CH_3); IR (solid) 3314, 2920, 2851, 1743, 1615, 1558 cm^{-1}.

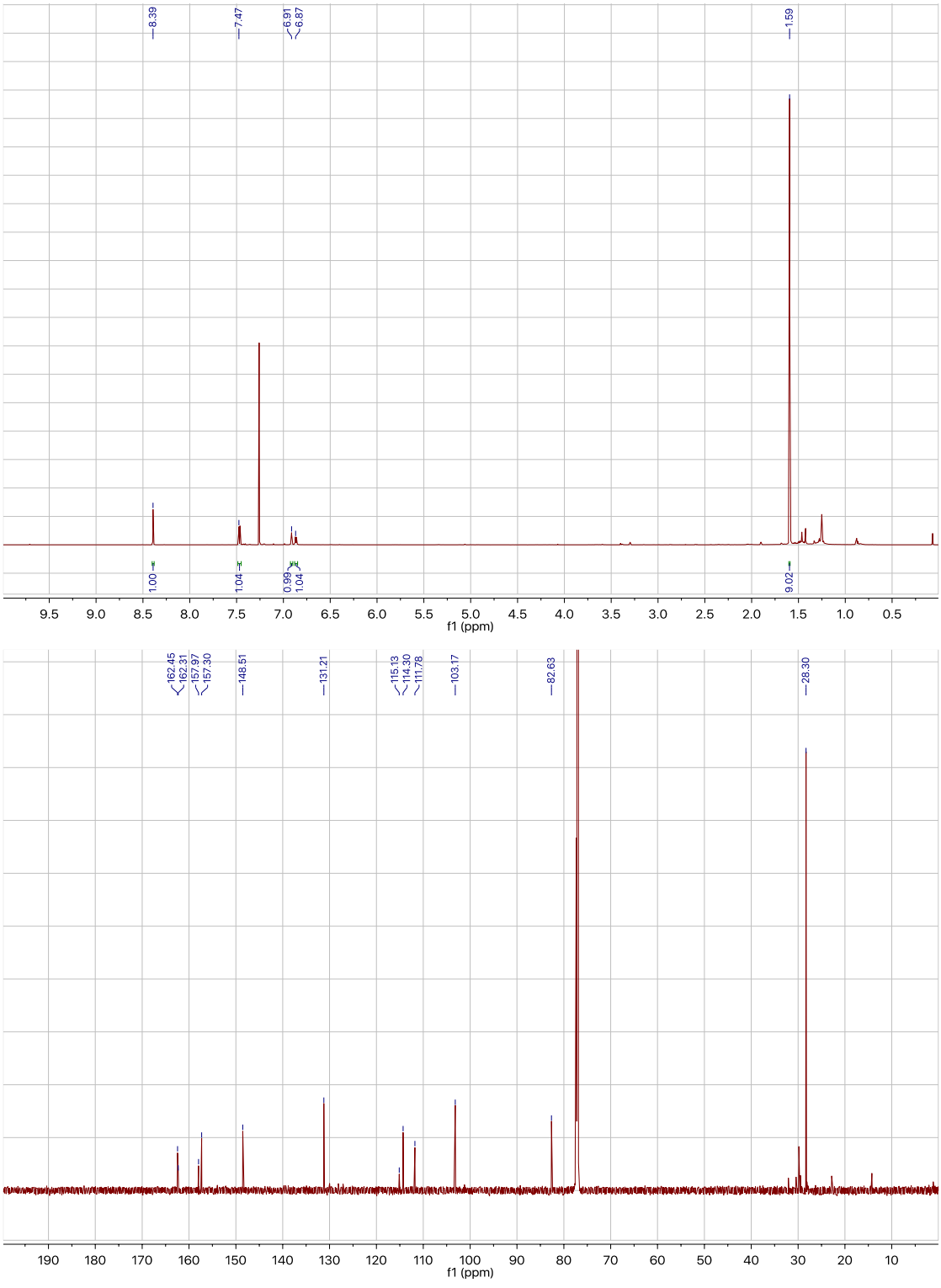

Figure **S12**. ^{1}H and ^{13}C NMR spectra for *tert*-butyl 7-hydroxy-2-oxo-2*H*-chromene-3-carboxylate.

Di-*tert*-butyl 7,7'-(((((1,2-diethyl-3,6-dioxo-1,2,3,6-tetrahydropyridazine-4,5-diyl)bis(sulfanediyl))bis(4,1-phenylene))bis(methylene))bis(oxy))bis(2-oxo-2*H*-chromene-3-carboxylate)

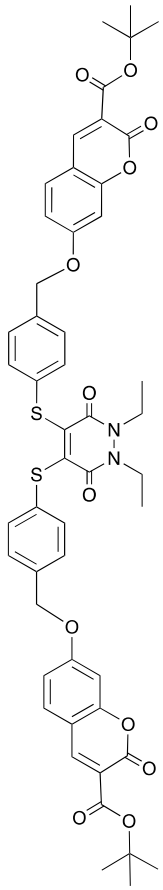

To a solution of 1,2-diethyl-4,5-bis(*p*-tolylthio)-1,2-dihydropyridazine-3,6-dione **8** (0.10 g, 0.24 mmol) in fluorobenzene (7 mL) was added NBS **9** (0.09 g, 0.5 mmol) and AIBN **10** (0.02 g, 0.1 mmol), and the reaction mixture was stirred at 60 ˚C for 21 h. Following this, the reaction mixture was diluted with fluorobenzene (7 mL) and washed with water (3 × 6 mL) and brine (7 mL). The organic phase was dried over $MgSO_4$ and concentrated *in vacuo* to afford the crude 4,5-bis((4-(bromomethyl)phenyl)thio)-1,2-diethyl-1,2-dihydropyridazine-3,6-dione **11** (0.11 g total). The crude mixture (0.04 g) was dissolved in dry THF (3 mL) along with cesium carbonate (0.03 g, 0.09 mmol) and *tert*-butyl 7-hydroxy-2-oxo-2*H*-chromene-3-carboxylate (0.02 g, 0.08 mmol), and the reaction mixture was stirred under reflux for 21 h. Following this, the reaction mixture was diluted with water (7 mL) and extracted with EtOAc (3 × 8 mL). The organic extracts were combined and subsequently washed with brine (8 mL). The organic phase was dried over $MgSO_4$, concentrated *in vacuo* and the crude residue was purified by flash column

chromatography (20–80% EtOAc/Pet.). The appropriate fractions were then combined and concentrated *in vacuo* to afford di-*tert*-butyl 7,7'-(((((1,2-diethyl-3,6-dioxo-1,2,3,6-tetrahydropyridazine-4,5-diyl)bis(sulfanediyl))bis(4,1-phenylene))bis(methylene))bis(oxy))bis(2-oxo-2*H*-chromene-3-carboxylate) (0.02 g, 0.02 mmol, 23%) as a yellow solid. m.p. 83–86 ˚C; ^{1}H NMR (700 MHz, $CDCl_3$) δ 8.37 (s, 2H), 7.49 (d, *J* = 8.7 Hz, 2H), 7.33 (d, *J* = 8.4 Hz, 4H), 7.24 (d, *J* = 8.4 Hz, 4H), 6.93 (dd, *J* = 8.7, 2.4 Hz, 2H), 6.84 (d, *J* = 2.4 Hz, 2H), 5.12 (s, 4H), 4.05 (q, *J* = 7.0 Hz, 4H), 1.59 (s, 18H), 1.23 (t, *J* = 7.0 Hz, 6H); ^{13}C NMR (150 MHz, $CDCl_3$)* δ 163.7 (C), 162.3 (C), 157.4 (C), 157.3 (C), 155.7 (C), 148.0 (CH), 141.9 (C), 135.3 (C), 132.9 (C), 131.3 (CH), 130.7 (CH), 128.2 (CH), 116.0 (C), 114.1 (CH), 112.1 (C), 101.5 (CH), 82.6 (C), 70.2 (CH_2), 41.4 (CH_2), 28.3 (CH_3), 12.9 (CH_3); IR (solid) 2924, 2854, 1748, 1606 cm^{-1}; LRMS (ES+) 933 (100, $[M+H]^+$); HRMS (ES+) calcd for $C_{50}H_{49}N_2O_{12}S_2$ $[M+H]^+$ 933.2727, observed 933.2778.

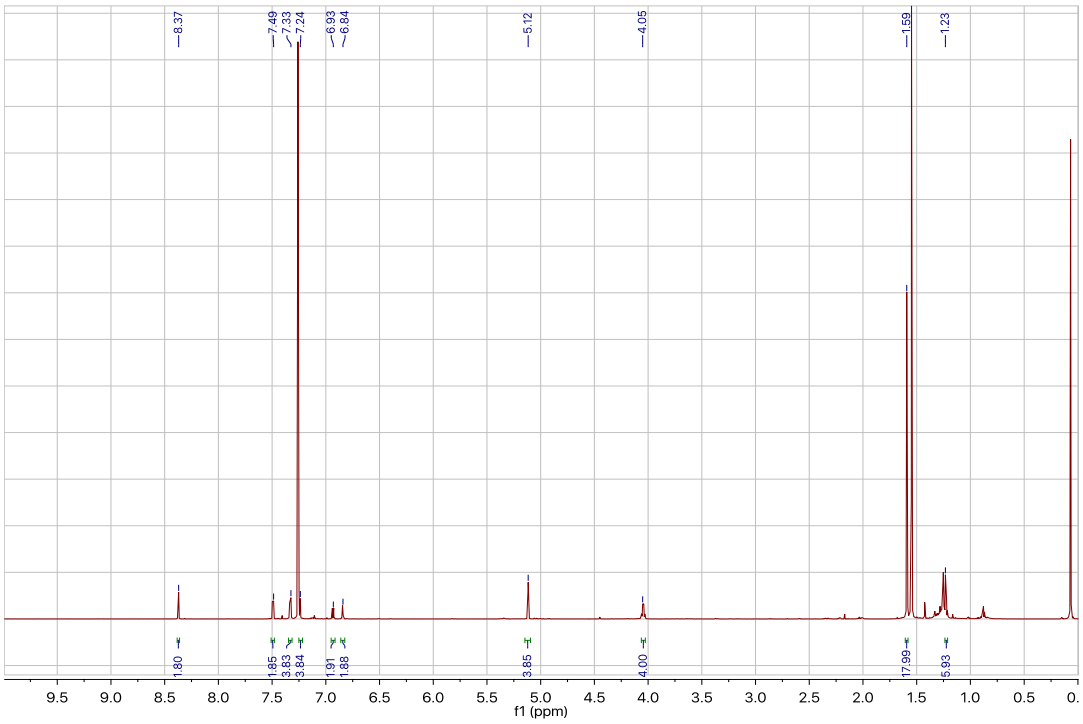

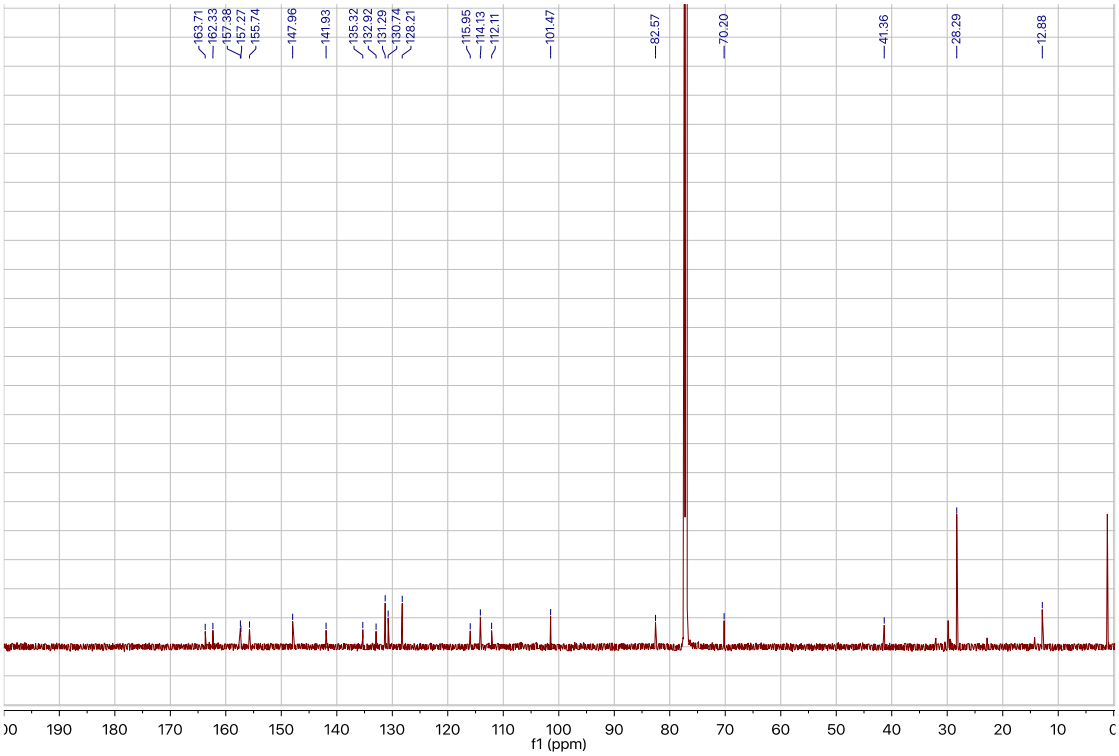

Figure **S13**. ^{1}H and ^{13}C NMR spectra for di-*tert*-butyl 7,7'-(((((1,2-diethyl-3,6-dioxo-1,2,3,6-tetrahydropyridazine-4,5-diyl)bis(sulfanediyl))bis(4,1-phenylene))bis(methylene))bis(oxy))bis(2-oxo-2*H*-chromene-3-carboxylate). *29.8 (H grease), 1.15 (silicon grease).

7,7'-(((((1,2-Diethyl-3,6-dioxo-1,2,3,6-tetrahydropyridazine-4,5-diyl)bis(sulfanediyl))bis(4,1-phenylene))bis(methylene))bis(oxy))bis(2-oxo-2*H*-chromene-3-carboxylic acid) 16

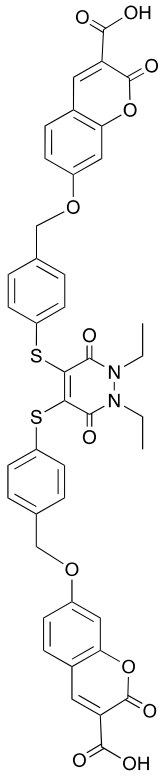

Di-*tert*-butyl 7,7'-(((((1,2-diethyl-3,6-dioxo-1,2,3,6-tetrahydropyridazine-4,5-diyl)bis(sulfanediyl))bis(4,1-phenylene))bis(methylene))bis(oxy))bis(2-oxo-2*H*-chromene-3-carboxylate) (11 mg, 0.010 mmol) was dissolved in TFA (0.25 mL) and CH_2Cl_2 (0.75 mL), and stirred at 21 ˚C for 4 h. Following this, the reaction mixture was concentrated *in vacuo* to afford 7,7'-(((((1,2-diethyl-3,6-dioxo-1,2,3,6-tetrahydropyridazine-4,5-diyl)bis(sulfanediyl))bis(4,1-phenylene))bis(methylene))bis(oxy))bis(2-oxo-2*H*-chromene-3-carboxylic acid) (10 mg, 0.010 mmol, quant.) as a yellow solid. d.t. 195–198 ˚C; ^{1}H NMR (700 MHz, $CDCl_3$) δ 8.86 (s, 2H), 7.66 (d, *J* = 8.8 Hz, 2H), 7.35 (d, *J* = 8.5 Hz, 4H), 7.28 (d, *J* = 8.5 Hz, 4H), 7.08 (dd, *J* = 8.8, 2.4 Hz, 2H), 6.97 (d, *J* = 2.4 Hz, 2H), 5.18 (s, 4H), 4.05 (q, *J* = 7.0 Hz, 4H), 1.24 (t, *J* = 7.0 Hz, 6H); ^{13}C NMR (150 MHz, $CDCl_3$) δ 165.1 (C), 164.6 (C), 163.1 (C), 157.0 (C), 155.7 (C), 151.3 (CH), 142.1 (C), 134.8 (C), 133.4 (C), 131.9 (CH), 131.4 (CH), 128.2 (CH), 115.8 (CH), 112.7 (C), 111.4 (C), 102.0 (CH), 70.6 (CH_2), 41.4 (CH_2), 12.9 (CH_3); IR (solid) 3056, 2926, 2853, 1787, 1717, 1596 cm^{-1}; LRMS (ES+) 821 (100, $[M+H]^+$); HRMS (ES+) calcd for $C_{42}H_{33}N_2O_{12}S_2$ $[M+H]^+$ 821.1450, observed 821.1475.

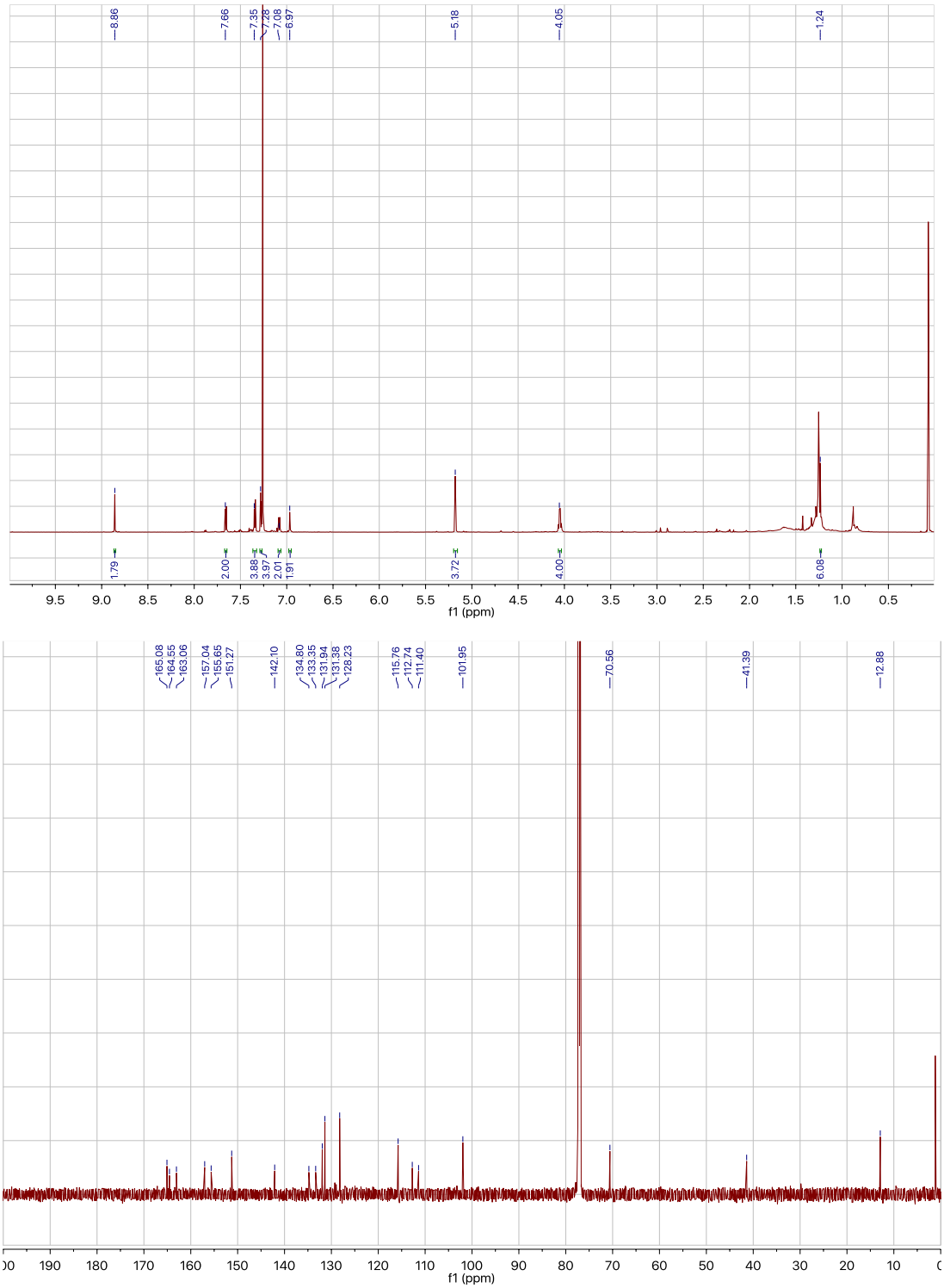

Figure **S14**. ^{1}H and ^{13}C NMR spectra for 7,7'-(((((1,2-diethyl-3,6-dioxo-1,2,3,6-tetrahydropyridazine-4,5-diyl)bis(sulfanediyl))bis(4,1-phenylene))bis(methylene))bis(oxy))bis(2-oxo-2*H*-chromene-3-carboxylic acid) **16**.

Di-*tert*-butyl 1-(3-(*tert*-butoxy)-3-oxopropyl)hydrazine-1,2-dicarboxylate

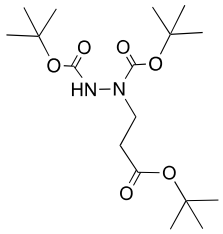

To a solution of di-*tert*-butyl hydrazine-1,2-dicarboxylate (1.22 g, 5.25 mmol) in EtOH (10 mL), was added fifteen drops of 2 M NaOH, and the reaction mixture was stirred at 21 ˚C for 10 mins. Following this, *tert*-butyl acrylate (0.91 mL, 6.3 mmol) was added to the solution and the reaction mixture was stirred under reflux for 48 h. Following this, the reaction mixture was concentrated *in vacuo* and the crude residue was purified by flash column chromatography (0–20% EtOAc/Pet.). The appropriate fractions were then combined and concentrated *in vacuo* to afford di-*tert*-butyl 1-(3-(*tert*-butoxy)-3-oxopropyl)hydrazine-1,2-dicarboxylate (1.11 g, 3.08 mmol, 59%) as a colourless oil. ^{1}H NMR (700 MHz, $CDCl_3$, rotamers) δ 6.39 (s, 0.70H), 6.08 (s, 0.20H), 3.71 (app. s, 2H), 2.52 (t, J = 6.6 Hz, 2H), 1.46–1.43 (m, 27H); ^{13}C NMR (150 MHz, $CDCl_3$) δ 168.9 (C), 168.6 (C), 152.4 (C), 79.0 (C), 78.6 (C), 78.1 (C), 44.3 (CH_2), 43.1 (CH_2), 31.8 (CH_2), 31.6 (CH_2), 25.6 (CH_3), 25.5 (CH_3); IR (thin film) 2975, 2931, 1707 cm^{-1}; LRMS (ES+) 361 (100, $[M+H]^+$); HRMS (ES+) calcd for $C_{17}H_{33}N_2O_6$ $[M+H]^+$ 361.2333, observed 361.2337.

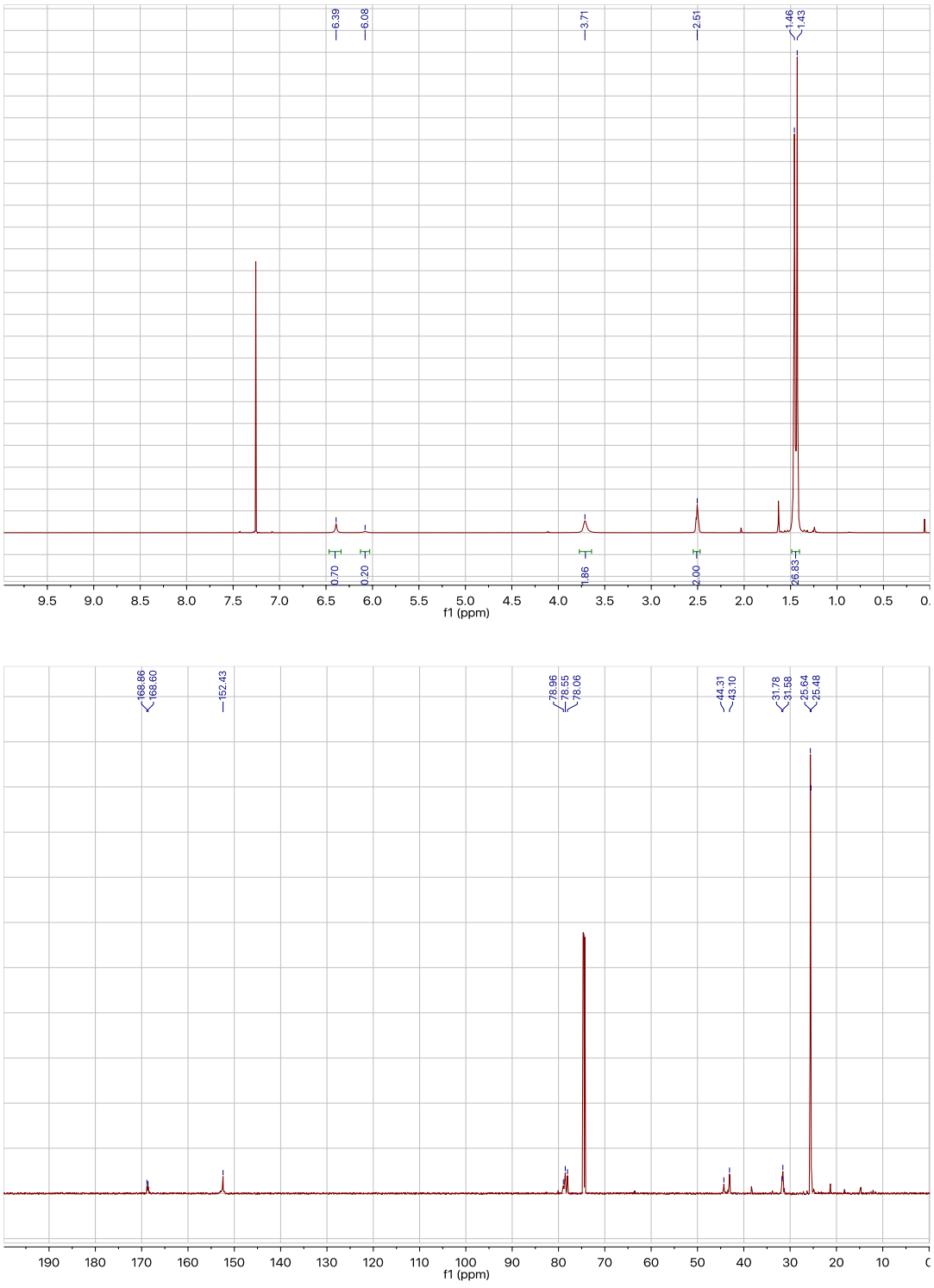

Figure **S15**. ^{1}H and ^{13}C NMR spectra for di-*tert*-butyl 1-(3-(*tert*-butoxy)-3-oxopropyl)hydrazine-1,2-dicarboxylate.

2-(2-(2-Methoxyethoxy)ethoxy)ethyl 4-methylbenzenesulfonate[4]

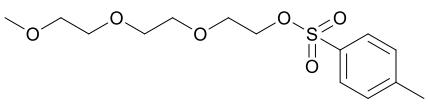

To a solution of triethylene glycol monomethyl ether (2.00 g, 12.2 mmol) and triethylamine (2.55 mL, 18.3 mmol) in dry THF (15 mL), was added 4-methylbenzenesulfonyl chloride (2.79 g, 14.6 mmol), and the reaction mixture was stirred for 21 h at 21 ˚C. Following this, the reaction mixture was diluted with water (15 mL) and extracted with EtOAc (3 × 15 mL). The organic extracts were combined and subsequently washed with brine (25 mL). The organic phase was dried over $MgSO_4$, concentrated *in vacuo* and the crude residue was purified by flash column chromatography (20–80% EtOAc/Pet.). The appropriate fractions were then combined and concentrated *in vacuo* to afford 2-(2-(2-methoxyethoxy)ethoxy)ethyl 4-methylbenzenesulfonate (3.74 g, 11.8 mmol, 96%) as a clear yellow oil. ^{1}H NMR (700 MHz, $CDCl_3$) δ 7.76 (d, *J* = 8.3 Hz, 2H), 7.31 (d, *J* = 8.3 Hz, 2H), 4.13–4.12 (m, 2H), 3.66–3.65 (m, 2H), 3.58–3.56 (m, 6H), 3.49 (m, 2H), 3.33 (s, 3H), 2.41 (s, 3H); ^{13}C NMR (150 MHz, $CDCl_3$) δ 144.9 (C), 133.1 (C), 130.0 (CH), 128.1 (CH), 72.0 (CH_2), 70.8 (CH_2), 70.7 (CH_2), 70.6 (CH_2), 69.4 (CH_2), 68.8 (CH_2), 59.1 (CH_3), 21.8 (CH_3); IR (thin film) 2877, 1598, 1452 cm^{-1}.

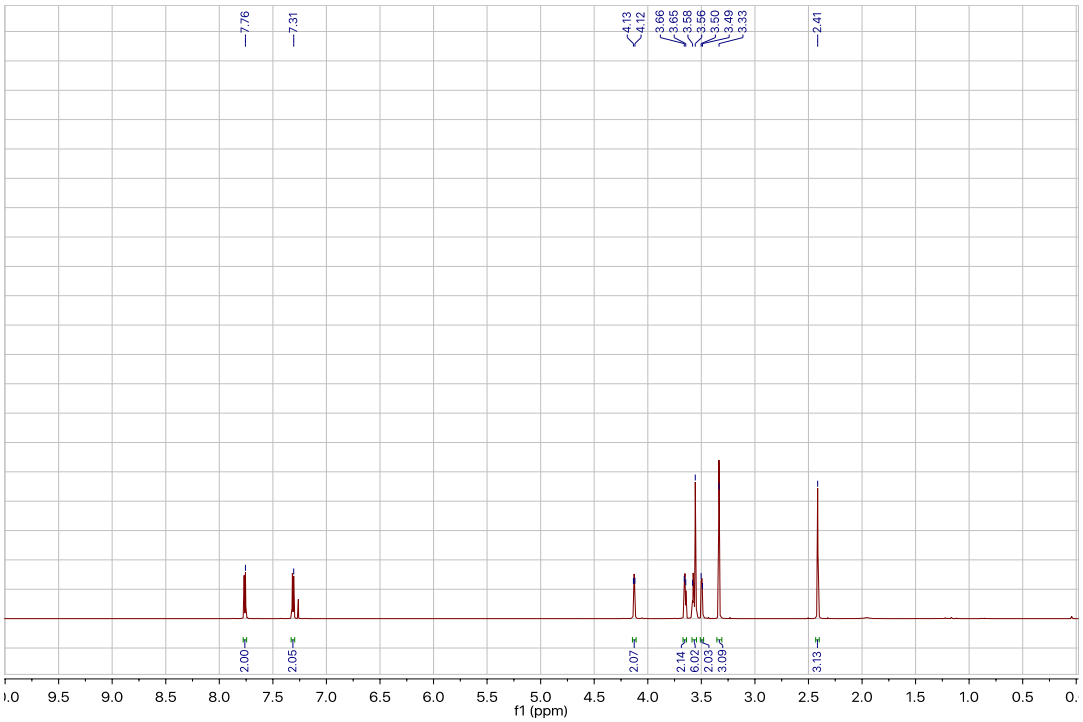

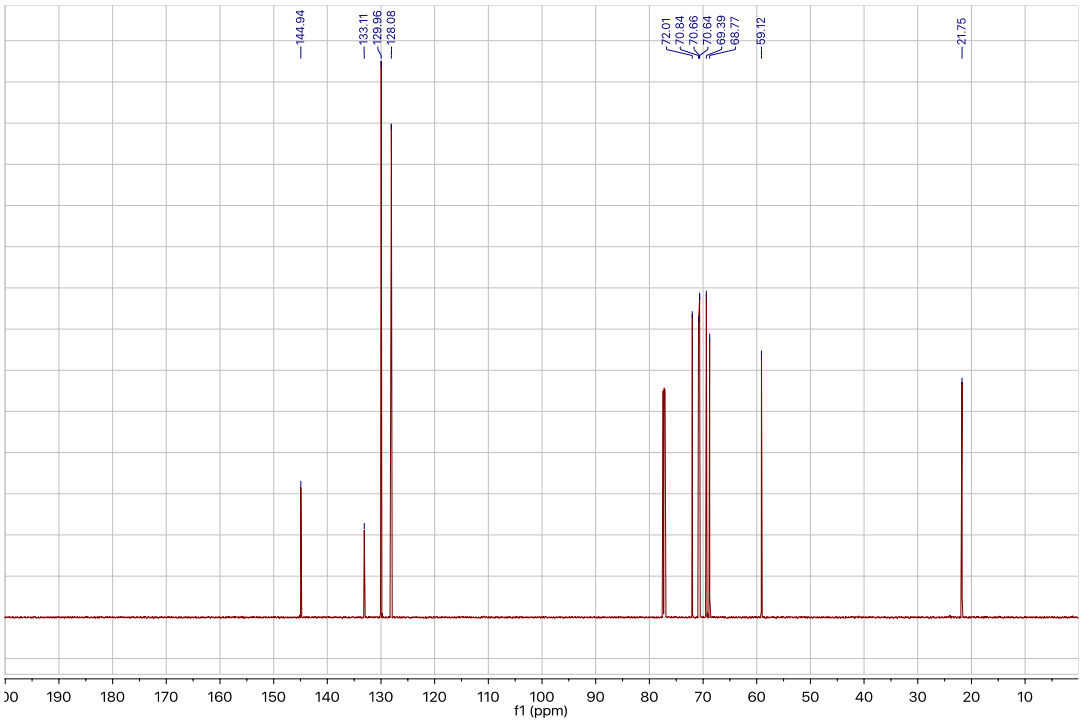

Figure **S16**. ^{1}H and ^{13}C NMR spectra for 2-(2-(2-methoxyethoxy)ethoxy)ethyl 4-methylbenzenesulfonate.

Tri-*tert*-butyl 2,5,8-trioxa-11,12-diazatetradecane-11,12,14-tricarboxylate 18

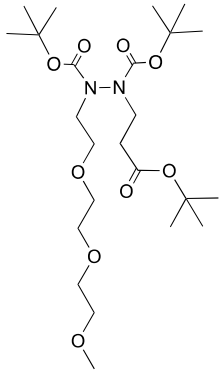

To a solution of di-*tert*-butyl 1-(3-(*tert*-butoxy)-3-oxopropyl)hydrazine-1,2-dicarboxylate (0.77 g, 2.1 mmol) and cesium carbonate (1.04 g, 3.19 mmol) in DMF (8 mL), was added 2-(2-(2-methoxyethoxy)ethoxy)ethyl 4-methylbenzenesulfonate (1.02 g, 3.21 mmol), and the reaction mixture was stirred at 21 ˚C for 72 h. Following this, the reaction mixture was diluted with water (8 mL) and extracted with EtOAc (3 × 15 mL). The organic extracts were combined and subsequently washed with sat. aq. LiCl solution (15 mL). The organic phase was dried over $MgSO_4$, concentrated *in vacuo* and the crude residue was purified by flash column chromatography (20–50% EtOAc/Pet.). The appropriate fractions were then combined and concentrated *in vacuo* to afford tri-*tert*-butyl 2,5,8-trioxa-11,12-diazatetradecane-11,12,14-tricarboxylate (0.92 g, 1.8 mmol, 85%) as a colourless oil. ^{1}H NMR (600 MHz, $CDCl_3$, rotamers) δ 3.78–3.59 (m, 12H), 3.56–3.53 (m, 2H), 3.37 (s, 3H), 2.61 (t, *J* = 7.8 Hz, 2H), 1.48–1.42 (m, 27H); ^{13}C NMR (150 MHz, $CDCl_3$) δ 171.4 (C), 171.2 (C), 171.1 (C), 155.8 (C), 155.2 (C), 155.2 (C), 155.0 (C), 154.6 (C), 154.5 (C), 81.6 (C), 81.5 (C), 81.4 (C), 81.4 (C), 81.2 (C), 81.2 (C), 81.1 (C), 80.7 (C), 80.6 (C), 80.4 (C), 72.0 (CH_2), 70.7 (CH_2), 70.7 (CH_2), 70.7 (CH_2), 70.6 (CH_2), 70.5 (CH_2), 70.4 (CH_2), 68.7 (CH_2), 68.5 (CH_2), 59.1 (CH_3), 51.2 (CH_2), 50.5 (CH_2), 50.3 (CH_2), 47.2 (CH_2), 46.1 (CH_2), 46.0 (CH_2), 34.4 (CH_2), 33.9 (CH_2), 33.9 (CH_2), 28.4 (CH_3), 28.4 (CH_3), 28.3 (CH_3), 28.2 (CH_3), 28.2 (CH_3); IR (thin film) 2973, 2928, 2872, 1705 cm^{-1}; LRMS (ES+) 507 (100, $[M+H]^+$); HRMS (ES+) calcd for $C_{25}H_{46}N_2O_9$ $[M+H]^+$ 507.3282, observed 507.3272.

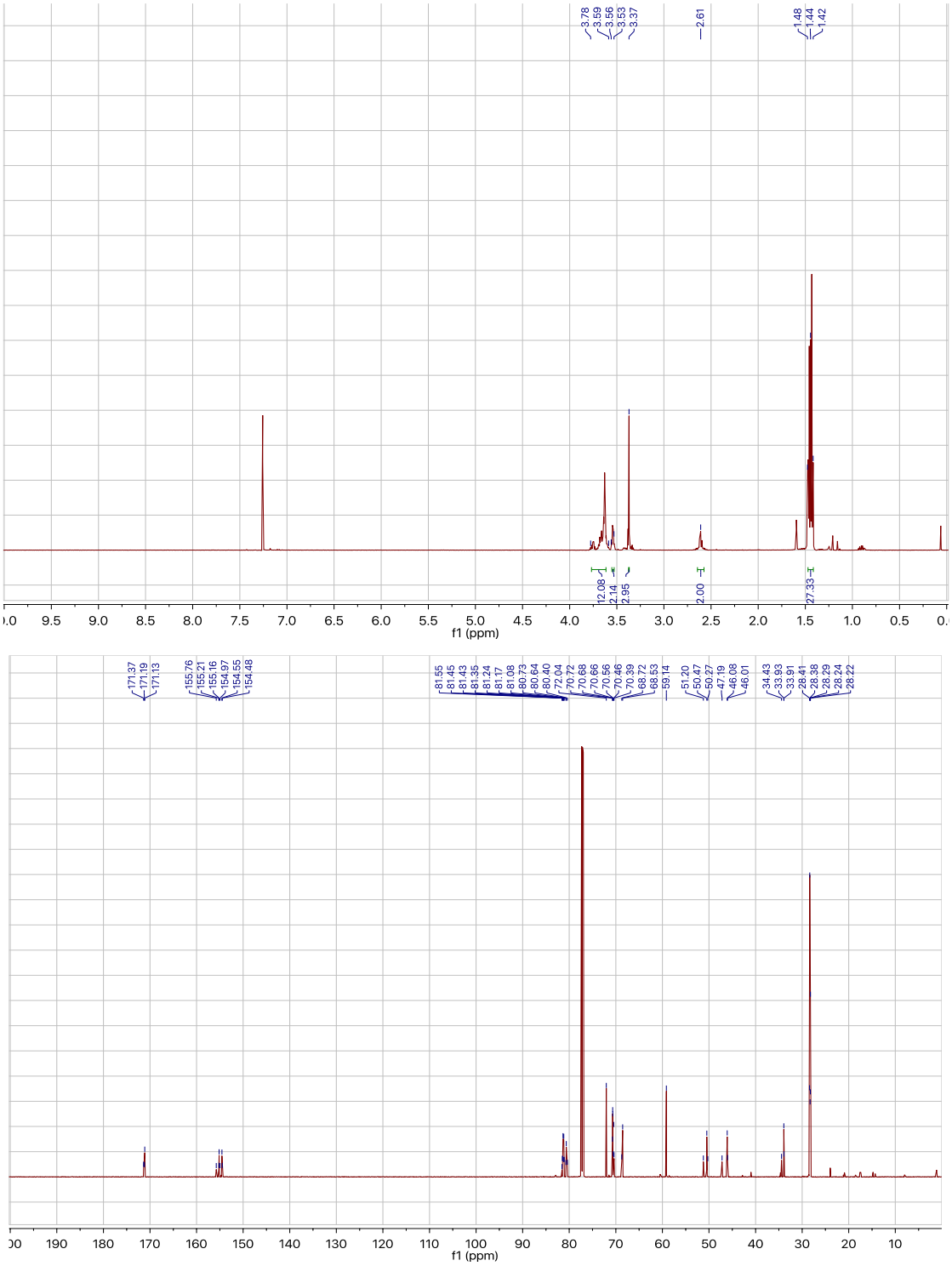

Figure **S17**. ^{1}H and ^{13}C NMR spectra for tri-*tert*-butyl 2,5,8-trioxa-11,12-diazatetradecane-11,12,14-tricarboxylate **18**.

3-(4,5-Dibromo-2-(2-(2-(2-methoxyethoxy)ethoxy)ethyl)-3,6-dioxo-3,6-dihydropyridazin-1(2*H*)-yl)propanoic acid 20

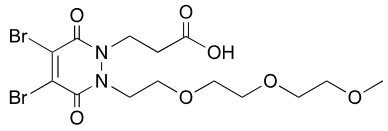

To a solution of tri-*tert*-butyl 2,5,8-trioxa-11,12-diazatetradecane-11,12,14-tricarboxylate **18** (1.54 g, 3.04 mmol) in AcOH (10 mL), was added dibromomaleic acid **19** (1.67 g, 6.10 mmol), and the reaction mixture was stirred under reflux for 24 h. Following this, the reaction mixture was concentrated *in vacuo* and the crude residue was purified by flash column chromatography (0–10% MeOH/CH_2Cl_2). The appropriate fractions were then combined and concentrated *in vacuo* to afford 3-(4,5-dibromo-2-(2-(2-(2-methoxyethoxy)ethoxy)ethyl)-3,6-dioxo-3,6-dihydropyridazin-1(2*H*)-yl)propanoic acid (1.09 g, 2.24 mmol, 74%) as a brown oil. ^{1}H NMR (700 MHz, $CDCl_3$) δ 4.49–4.47 (m, 2H), 4.28–4.27 (m, 2H), 3.77–3.76 (m, 2H), 3.61–3.56 (m, 8H), 3.41 (s, 3H), 2.82–2.80 (m, 2H); ^{13}C NMR (150 MHz, $CDCl_3$) δ 173.0 (C), 154.1 (C), 153.4 (C), 136.4 (C), 136.0 (C), 72.1 (CH_2), 70.9 (CH_2), 70.5 (CH_2), 70.3 (CH_2), 68.3 (CH_2), 59.0 (CH_3), 49.8 (CH_2), 44.6 (CH_2), 31.7 (CH_2); IR (thin film) 3452, 2918, 1723, 1628, 1574 cm^{-1}; LRMS (ES) 487 (100, $[M^{79}Br_2+H]^-$) ; HRMS (ES) calcd for $C_{14}H_{21}N_2O_7Br_2$ $[M^{79}Br_2+H]^-$ 486.9545, observed 486.9545.

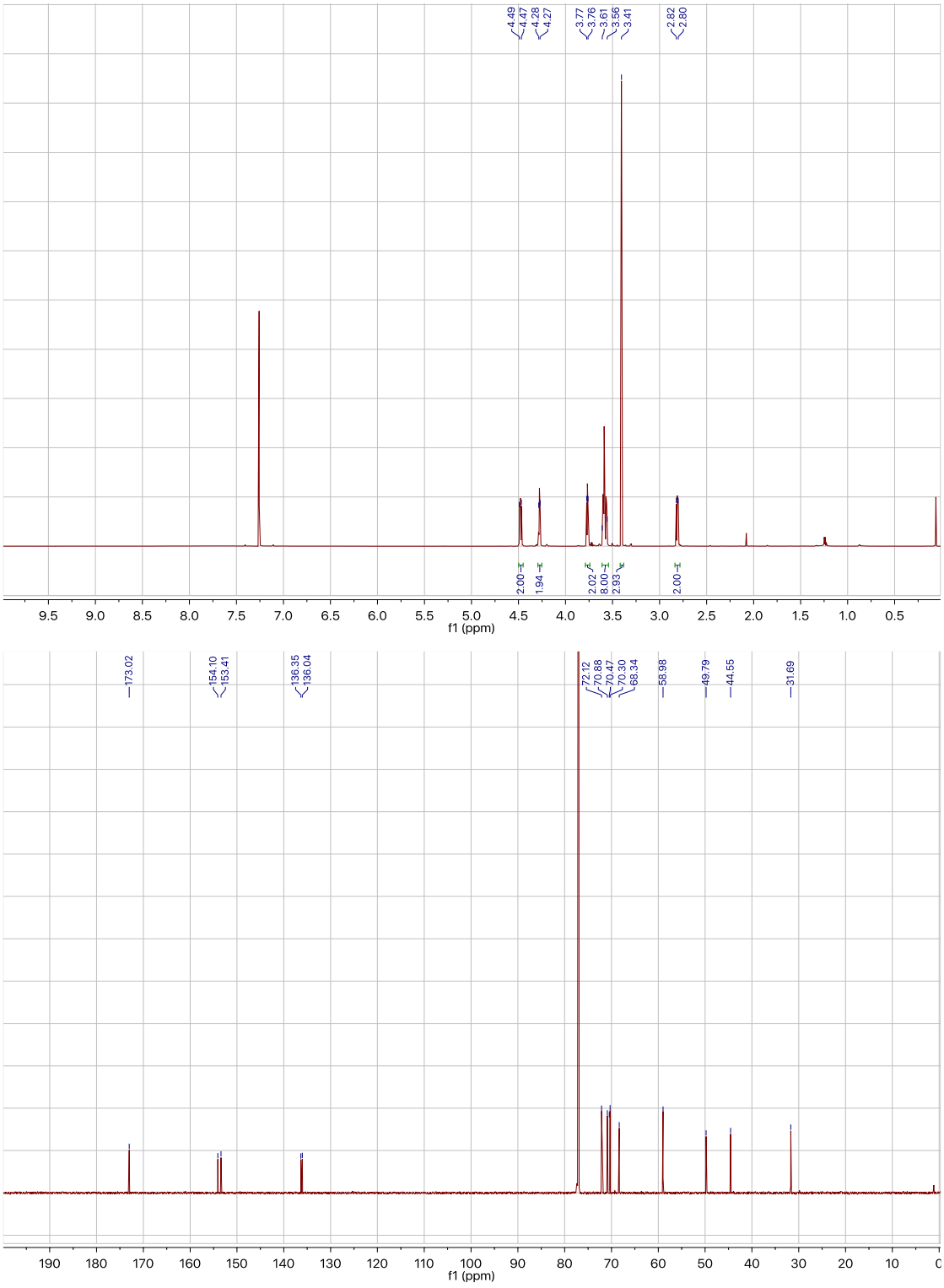

Figure **S18**. ^{1}H and ^{13}C NMR spectra for 3-(4,5-dibromo-2-(2-(2-(2-methoxyethoxy)ethoxy)ethyl)-3,6-dioxo-3,6-dihydropyridazin-1(2*H*)-yl)propanoic acid **20**.

_N_-(3-Azidopropyl)-3-(4,5-dibromo-2-(2-(2-(2-methoxyethoxy)ethoxy)ethyl)-3,6-dioxo-3,6-dihydropyridazin-1(2_H_)-yl)propanamide 21

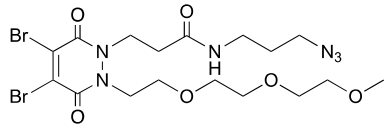

To a solution of 3-(4,5-dibromo-2-(2-(2-(2-methoxyethoxy)ethoxy)ethyl)-3,6-dioxo-3,6-dihydropyridazin-1(2*H*)-yl)propanoic acid **20** (0.15 g, 0.31 mmol) in THF (4 mL) stirring at 0 ˚C was added DCC (0.08 g, 0.4 mmol), and the reaction mixture was stirred at 0 ˚C for 30 mins. After this time, 3-azido-1-propanamine (0.04 g, 0.4 mmol) was added, and the reaction mixture was stirred at 21 ˚C for a further 23 h. Following this, the reaction mixture was filtered to remove insolubles and underwent 3 rounds of successive cooling on acetone/dry ice and filtrations before being concentrated *in vacuo*. The crude residue was purified by flash column chromatography (0–5% MeOH/CH_2Cl_2). The appropriate fractions were then combined and concentrated *in vacuo* to afford *N*-(3-azidopropyl)-3-(4,5-dibromo-2-(2-(2-(2-methoxyethoxy)ethoxy)ethyl)-3,6-dioxo-3,6-dihydropyridazin-1(2*H*)-yl)propanamide (0.09 g, 0.2 mmol, 51%) as a clear brown oil. ^{1}H NMR (700 MHz, $CDCl_3$) δ 6.40 (app. s, 1H), 4.46 (t, *J* = 7.0 Hz, 2H), 4.36 (t, *J* = 4.9 Hz, 2H), 3.74 (t, *J* = 4.9 Hz, 2H), 3.58–3.56 (m, 6H), 3.53–3.51 (m, 2H), 3.36 (s, 3H), 3.35 (app. d, 2H), 3.31 (q, *J* = 6.7 Hz, 2H), 2.66 (t, *J* = 7.0 Hz, 2H), 1.76 (p, *J* = 6.7 Hz, 2H); ^{13}C NMR (150 MHz, $CDCl_3$) δ 170.0 (C), 153.8 (C), 153.4 (C), 136.1 (C), 136.0 (C), 72.0 (CH_2), 70.6 (CH_2), 70.5 (CH_2), 70.5 (CH_2), 67.9 (CH_2), 59.1 (CH_3), 49.4 (CH_2), 48.8 (CH_2), 45.1 (CH_2), 37.4 (CH_2), 33.9 (CH_2), 28.9 (CH_2); IR (thin film) 2923, 2874, 2094, 1631 cm^{-1}; LRMS (ES+) 571 (100, [[M^{81}Br^{79}Br]+H]$^+$); HRMS (ES+) calcd for $C_{17}H_{27}N_6O_6Br_2$ [[M^{81}Br^{79}Br]+H]$^+$ 571.0333, observed 571.0337.

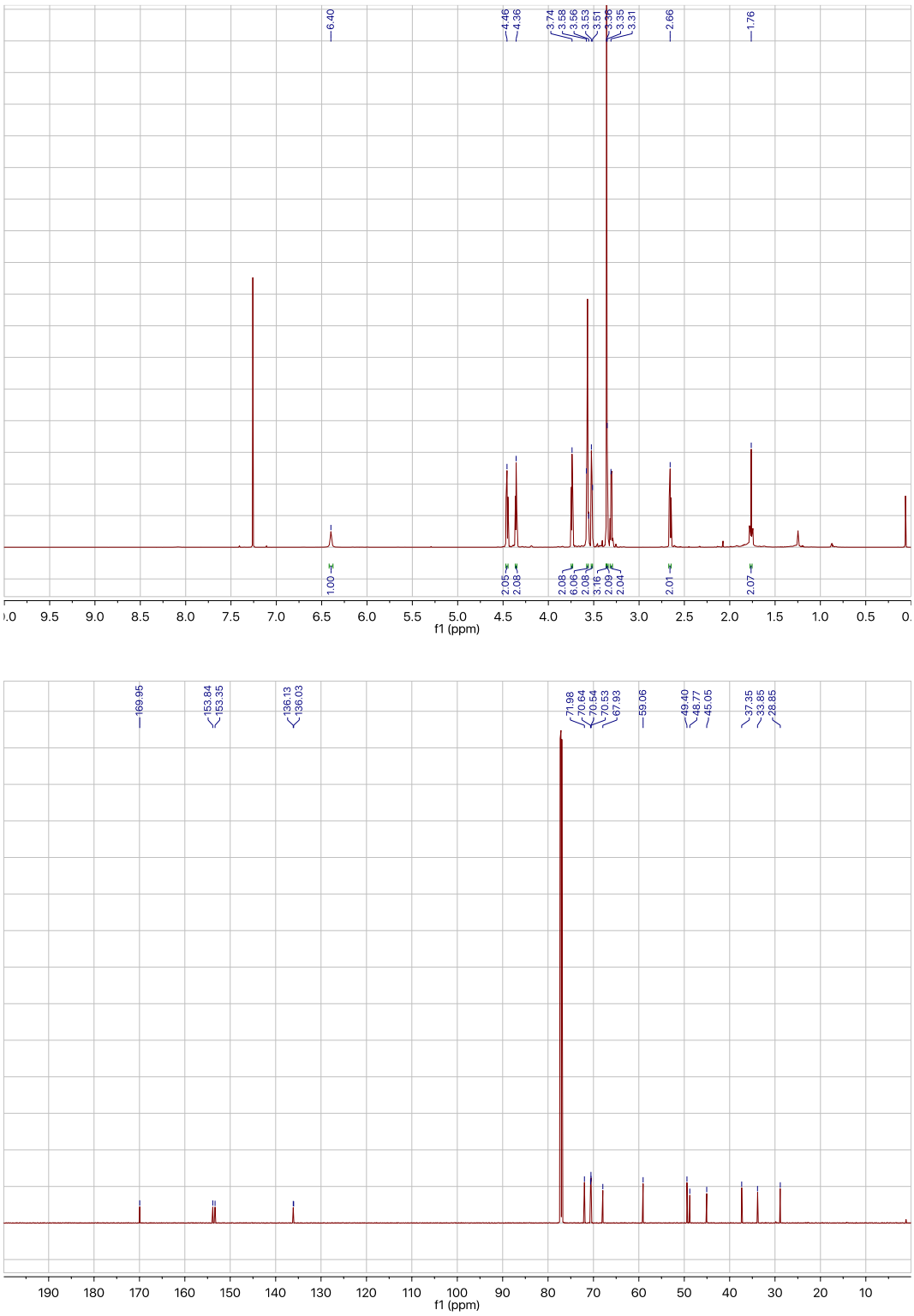

Figure **S19**. ^{1}H and ^{13}C NMR spectra for *N*-(3-azidopropyl)-3-(4,5-dibromo-2-(2-(2-(2-methoxyethoxy)ethoxy)ethyl)-3,6-dioxo-3,6-dihydropyridazin-1(2*H*)-yl)propanamide **21**.

3-(4,5-Dibromo-2-(2-(2-(2-methoxyethoxy)ethoxy)ethyl)-3,6-dioxo-3,6-dihydropyridazin-1(2*H*)-yl)-*N*-(prop-2-yn-1-yl)propanamide 22

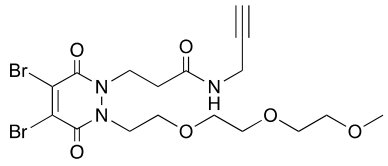

To a solution of 3-(4,5-dibromo-2-(2-(2-(2-methoxyethoxy)ethoxy)ethyl)-3,6-dioxo-3,6-dihydropyridazin-1(2*H*)-yl)propanoic acid **20** (0.10 g, 0.21 mmol) in THF (4 mL) stirring at 0 ˚C was added DCC (0.05 g, 0.2 mmol), and the reaction mixture was stirred at 0 ˚C for 30 mins. After this time, propargylamine (15 µL, 0.23 mmol) was added, and the reaction mixture was stirred at 21 ˚C for a further 20 h. Following this, the reaction mixture was filtered to remove insolubles and underwent 3 rounds of successive cooling on acetone/dry ice and filtrations before being concentrated *in vacuo*. The crude residue was purified by flash column chromatography (0–15% MeOH/CH_2Cl_2). The appropriate fractions were then combined and concentrated *in vacuo* to afford 3-(4,5-dibromo-2-(2-(2-(2-methoxyethoxy)ethoxy)ethyl)-3,6-dioxo-3,6-dihydropyridazin-1(2*H*)-yl)-*N*-(prop-2-yn-1-yl)propanamide (0.06 g, 0.1 mmol, 55%) as a green oil. ^{1}H NMR (700 MHz, $CDCl_3$) δ 6.78 (app. s, 1H), 4.46 (t, *J* = 7.1 Hz, 2H), 4.33 (t, *J* = 4.8 Hz, 2H), 4.00 (dd, *J* = 5.4, 2.5 Hz, 2H), 3.74 (t, *J* = 4.8 Hz, 2H), 3.59–3.56 (m, 6H), 3.53–3.52 (m, 2H), 3.36 (s, 3H), 2.71 (t, *J* = 7.1 Hz, 2H), 2.20 (t, *J* = 2.5 Hz, 1H); ^{13}C NMR (150 MHz, $CDCl_3$) δ 169.8 (C), 153.8 (C), 153.3 (C), 136.2 (C), 136.0 (C), 79.7 (C), 72.0 (CH_2), 71.5 (CH), 70.6 (CH_2), 70.5 (CH_2), 70.5 (CH_2), 68.0 (CH_2), 59.0 (CH_3), 49.1 (CH_2), 45.1 (CH_2), 33.3 (CH_2), 29.2 (CH_2); IR (thin film) 2873, 1629 cm^{-1}; LRMS (ES+) 526 (100, [[M^{81}Br^{79}Br]+H]$^+$); HRMS (ES+) calcd for $C_{17}H_{24}N_3O_6Br_2$ [[M^{81}Br^{79}Br]+H]$^+$ 526.0006, observed 526.0007.

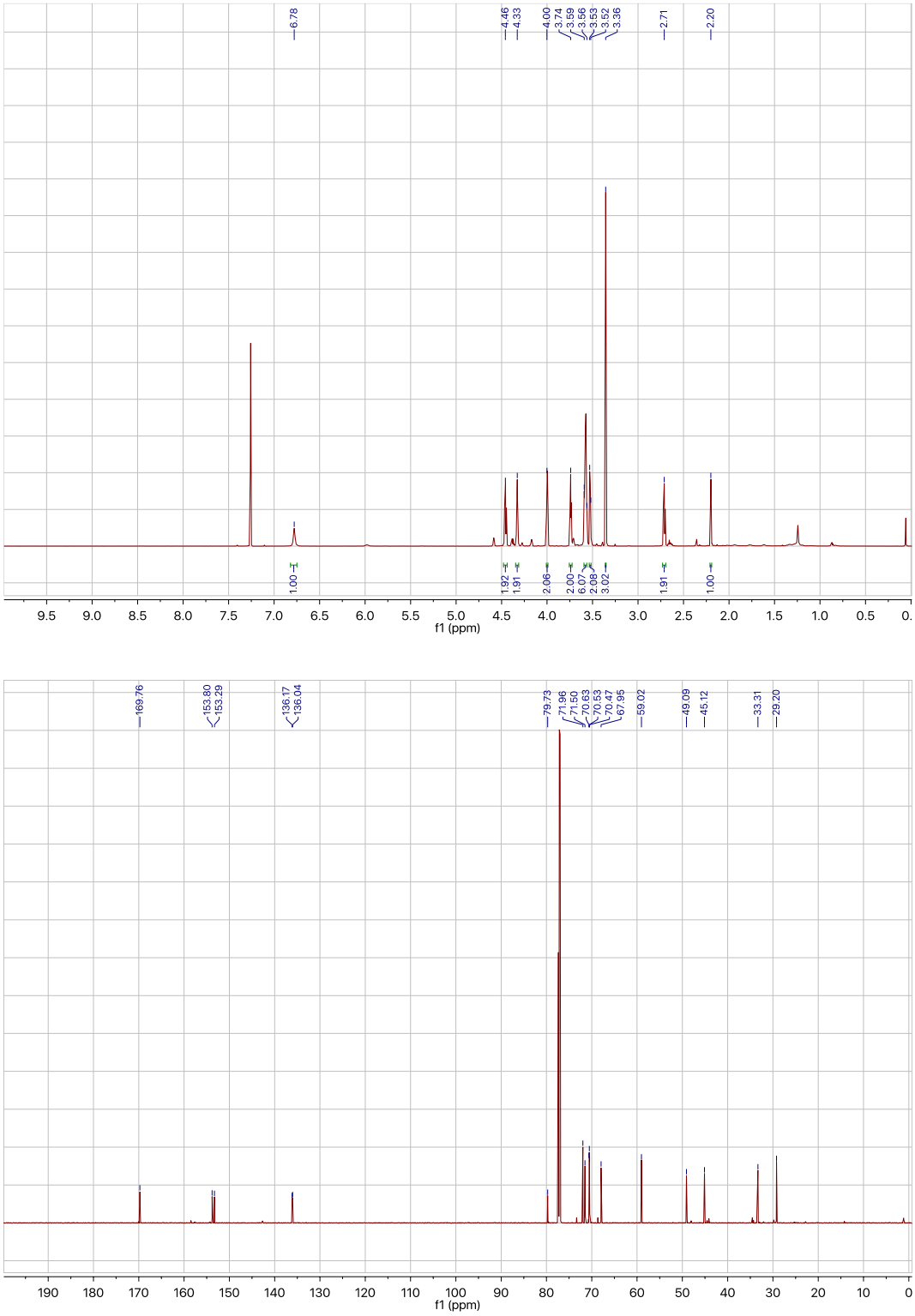

Figure **S20**. ^{1}H and ^{13}C NMR spectra for 3-(4,5-dibromo-2-(2-(2-(2-methoxyethoxy)ethoxy)ethyl)-3,6-dioxo-3,6-dihydropyridazin-1(2*H*)-yl)-*N*-(prop-2-yn-1-yl)propanamide **22**.

_N_-(3-Azidopropyl)-3-(2-(2-(2-(2-methoxyethoxy)ethoxy)ethyl)-3,6-dioxo-4,5-bis(_p_-tolylthio)-3,6-dihydropyridazin-1(2_H_)-yl)propanamide 24

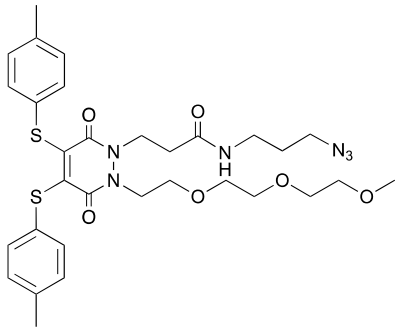

To a solution of 4-methylbenzenethiol **23** (0.03 g, 0.2 mmol) and triethylamine (75 µL, 0.54 mmol) in CH_2Cl_2 (2 mL) at 21 ˚C, was added *N*-(3-azidopropyl)-3-(4,5-dibromo-2-(2-(2-(2-methoxyethoxy)ethoxy)ethyl)-3,6-dioxo-3,6-dihydropyridazin-1(2*H*)-yl)propanamide **21** (0.05 g, 0.09 mmol), and the reaction mixture was stirred for 10 mins. Following this, the reaction mixture was diluted with CH_2Cl_2 (8 mL) and washed with water (3 × 8 mL) and brine (8 mL). The organic phase was then dried over $MgSO_4$, concentrated *in vacuo* and the crude residue was purified by flash column chromatography (0–5% MeOH/CH_2Cl_2). The appropriate fractions were then combined and concentrated *in vacuo* to afford *N*-(3-azidopropyl)-3-(2-(2-(2-(2-methoxyethoxy)ethoxy)ethyl)-3,6-dioxo-4,5-bis(*p*-tolylthio)-3,6-dihydropyridazin-1(2*H*)-yl)propanamide (0.05 g, 0.08 mmol, 85%) as a yellow oil. ^{1}H NMR (700 MHz, $CDCl_3$) δ 7.17–7.14 (m, 4H), 7.08–7.06 (m, 4H), 6.48 (app. s, 1H), 4.29 (t, *J* = 6.9 Hz, 2H), 4.16 (t, *J* = 5.0 Hz, 2H), 3.67 (t, *J* = 5.0 Hz, 2H), 3.59–3.56 (m, 6H), 3.52–3.51 (m, 2H), 3.34 (s, 3H), 3.32 (t, *J* = 6.6 Hz, 2H), 3.26 (q, *J* = 6.6 Hz, 2H), 2.59 (t, *J* = 6.9 Hz, 2H), 2.32 (s, 6H), 1.73 (p, *J* = 6.6 Hz, 2H); ^{13}C NMR (150 MHz, $CDCl_3$) δ 170.3 (C), 156.9 (C-), 156.4 (C), 142.3 (C), 142.1 (C), 138.1 (C), 138.1 (C), 131.3 (CH), 131.2 (CH), 129.9 (CH), 129.3 (C), 129.1 (C), 72.0 (CH_2), 70.6 (CH_2), 70.6 (CH_2), 70.5 (CH_2), 68.1 (CH_2), 59.0 (CH_3), 49.3 (CH_2), 47.8 (CH_2), 43.9 (CH_2), 37.3 (CH_2), 34.0 (CH_2), 28.8 (CH_2), 21.4 (CH_3); IR (thin film) 2921, 2869, 2094, 1621 cm^{-1}; LRMS (ES+) 657 (100, $[M+H]^+$); HRMS (ES+) calcd for $C_{31}H_{41}N_6O_6S_2$ $[M+H]^+$ 657.2524, observed 657.2527.

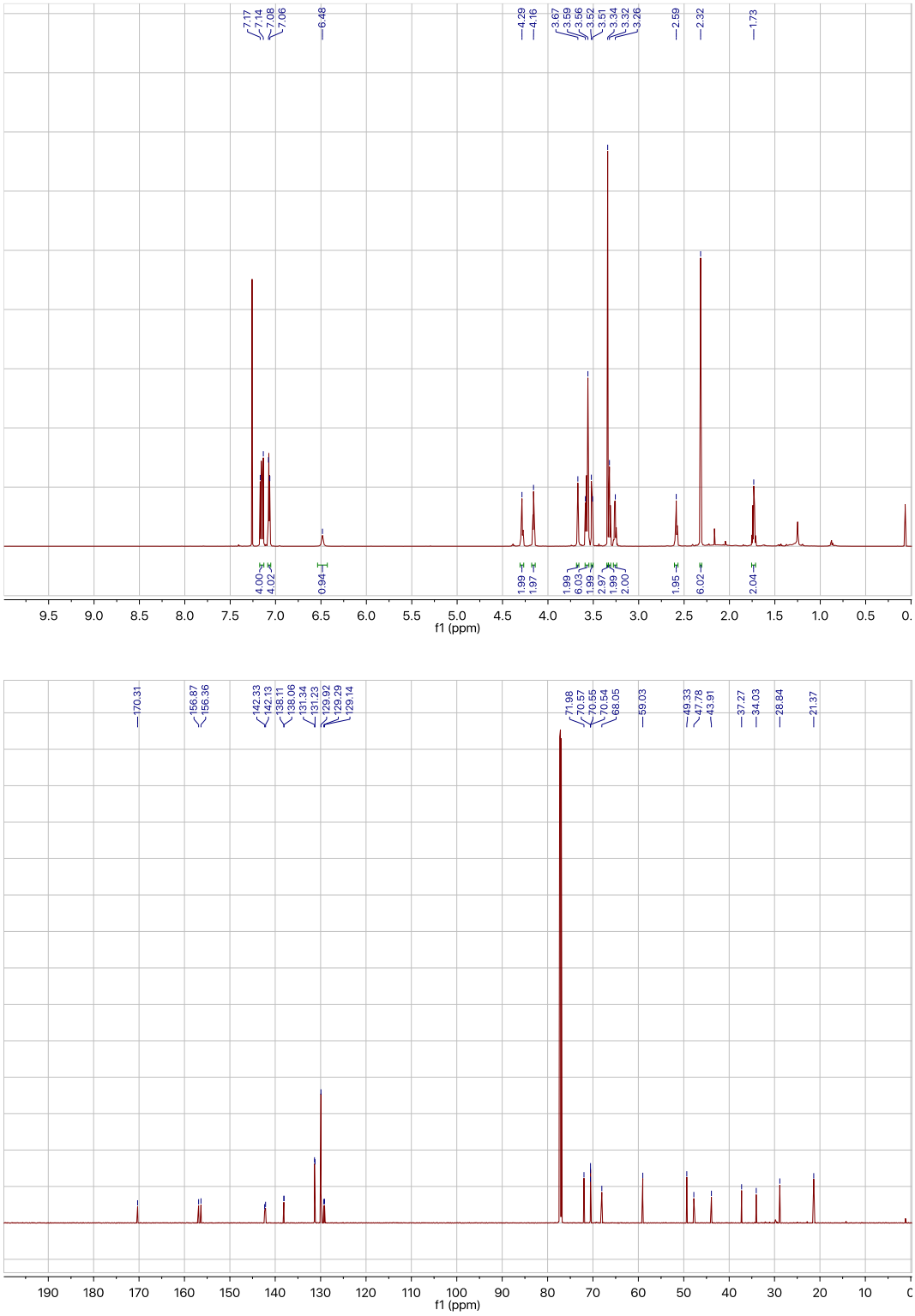

Figure **S21**. ^{1}H and ^{13}C NMR spectra for *N*-(3-azidopropyl)-3-(2-(2-(2-(2-methoxyethoxy)ethoxy)ethyl)-3,6-dioxo-4,5-bis(*p*-tolylthio)-3,6-dihydropyridazin-1(2*H*)-yl)propanamide **24**.

3-(2-(2-(2-(2-Methoxyethoxy)ethoxy)ethyl)-3,6-dioxo-4,5-bis(*p*-tolylthio)-3,6-dihydropyridazin-1(2*H*)-yl)-*N*-(prop-2-yn-1-yl)propanamide 25

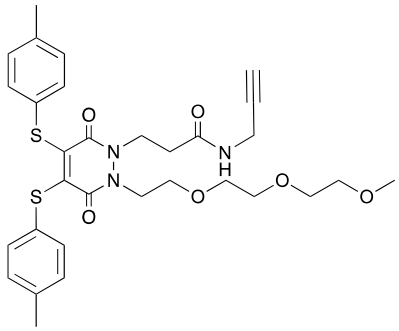

To a solution of 4-methylbenzenethiol **23** (0.01 g, 0.08 mmol) and triethylamine (17 µL, 0.12 mmol) in CH_2Cl_2 (3 mL) at 21 ˚C, was added 3-(4,5-dibromo-2-(2-(2-(2-methoxyethoxy)ethoxy)ethyl)-3,6-dioxo-3,6-dihydropyridazin-1(2*H*)-yl)-*N*-(prop-2-yn-1-yl)propanamide **22** (0.01 g, 0.02 mmol), and the reaction mixture was stirred for 10 mins. Following this, the reaction mixture was diluted with CH_2Cl_2 (8 mL) and washed with water (3 × 8 mL) and brine (8 mL). The organic phase was then dried over $MgSO_4$, concentrated *in vacuo* and the crude residue was purified by flash column chromatography (0–5% MeOH/CH_2Cl_2). The appropriate fractions were then combined and concentrated *in vacuo* to afford 3-(2-(2-(2-(2-methoxyethoxy)ethoxy)ethyl)-3,6-dioxo-4,5-bis(*p*-tolylthio)-3,6-dihydropyridazin-1(2*H*)-yl)-*N*-(prop-2-yn-1-yl)propanamide (0.01 g, 0.02 mmmol, 82%) as a yellow oil. ^{1}H NMR (700 MHz, $CDCl_3$)* δ 7.18–7.15 (m, 4H), 7.08–7.06 (m, 4H), 6.64 (app. s, 1H), 4.29 (t, *J* = 7.0 Hz, 2H), 4.13 (t, *J* = 4.9 Hz, 2H), 3.96 (dd, *J* = 5.3, 2.5 Hz, 2H), 3.68 (t, *J* = 4.9 Hz, 2H), 3.60–3.57 (m, 6H), 3.53–3.52 (m, 2H), 3.34 (s, 3H), 2.61 (t, *J* = 7.0 Hz, 2H), 2.32 (s, 6H), 2.18 (t, *J* = 2.5 Hz, 1H); ^{13}C NMR (150 MHz, $CDCl_3$) δ 169.9 (C), 156.9 (C), 156.3 (C), 142.4 (C), 142.3 (C), 138.1 (C), 138.0 (C), 131.3 (CH), 131.3 (CH), 129.9 (CH), 129.9 (CH), 129.4 (C), 129.3 (C), 79.8 (C), 72.0 (CH_2), 71.5 (CH), 70.5 (CH_2), 70.5 (CH_2), 68.2 (CH_2), 59.0 (CH_3), 48.4 (CH_2), 44.1 (CH_2), 33.5 (CH_2), 29.2 (CH_2), 21.4 (CH_3); IR (thin film) 2921, 2869, 1621 cm^{-1}; LRMS (ES+) 612 (100, $[M+H]^+$); HRMS (ES+) calcd for $C_{31}H_{38}N_3O_6S_2$ $[M+H]^+$ 612.2197, observed 612.2198.

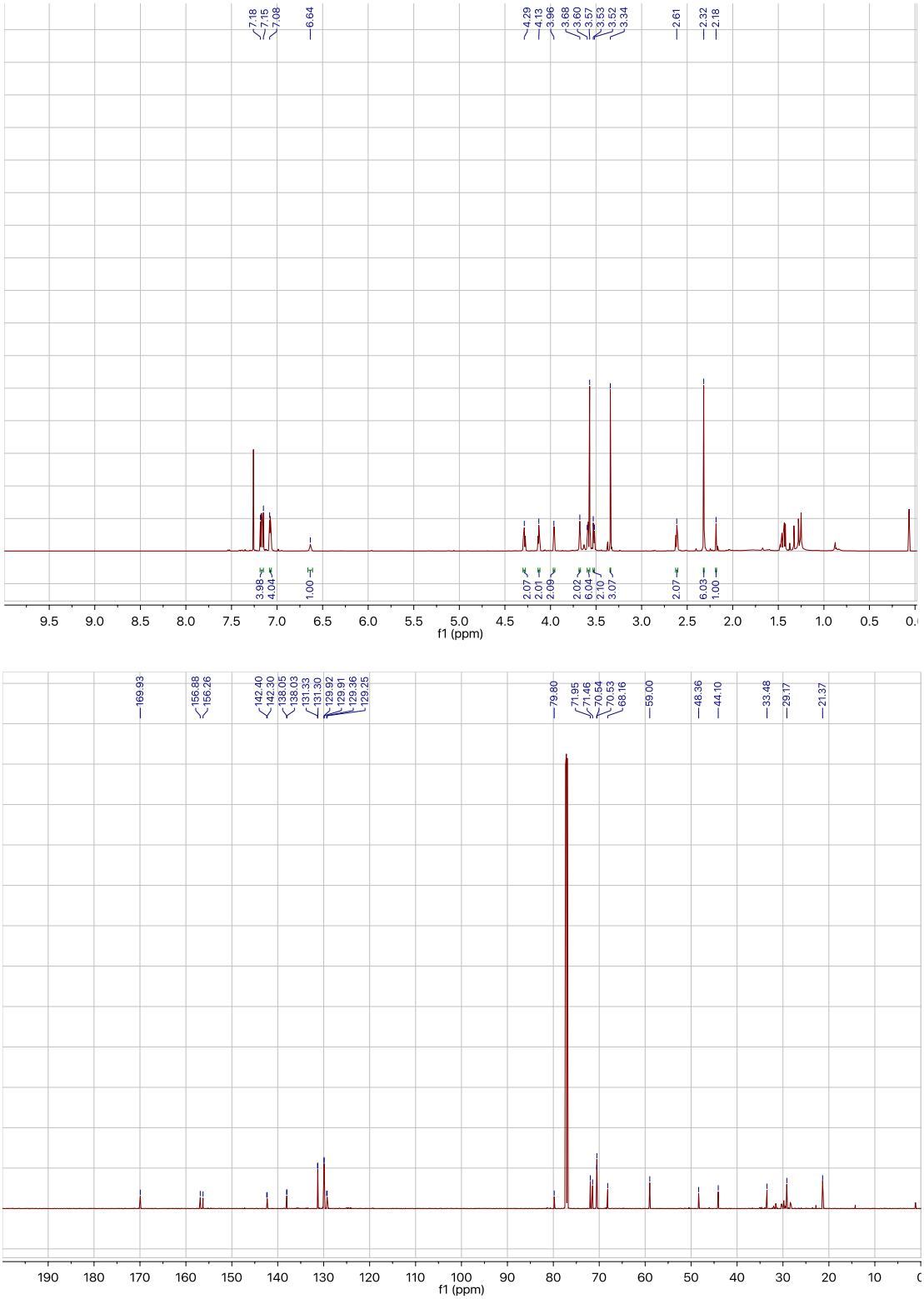

Figure **S22**. ^{1}H and ^{13}C NMR spectra for 3-(2-(2-(2-(2-methoxyethoxy)ethoxy)ethyl)-3,6-dioxo-4,5-bis(*p*-tolylthio)-3,6-dihydropyridazin-1(2*H*)-yl)-*N*-(prop-2-yn-1-yl)propanamide **25**. *Mixture of impurities at 1.48–1.25 ppm.

Incubations involving human serum albumin, maleimide and PDs 2–6

Human serum albumin control

Human serum albumin (20 µL, 3.8 mg/mL, 57 µM) in PBS (10 mM phosphate, 137 mM NaCl, 2.7 mM KCl, pH 7.4) was incubated at 37 ˚C for 4 h. The PBS was exchanged with ammonium acetate buffer (20 mM, pH 7.4) by repeated diafiltration (× 3) into VivaSpin sample concentrators (GE Healthcare, 10,000 MWCO). The sample was then analysed by LC-MS. Expected mass: 66,439 Da. Observed mass: 66,438 Da.

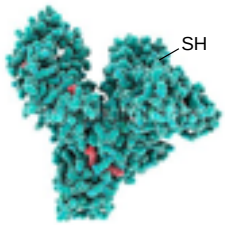

pH 7.4, 37 ˚C, 4 h

(a)

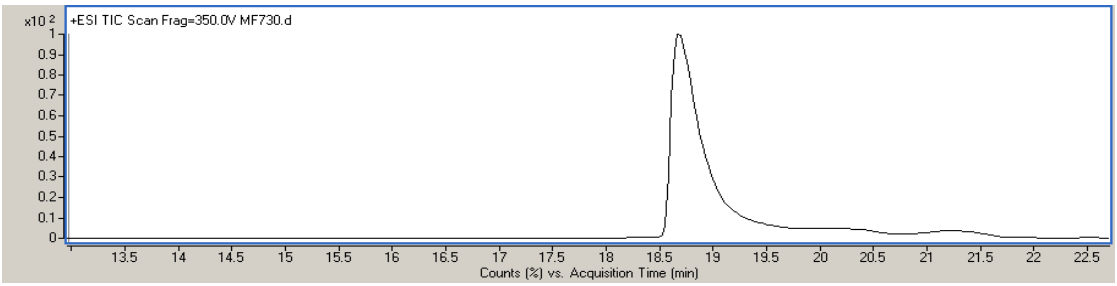

(b)

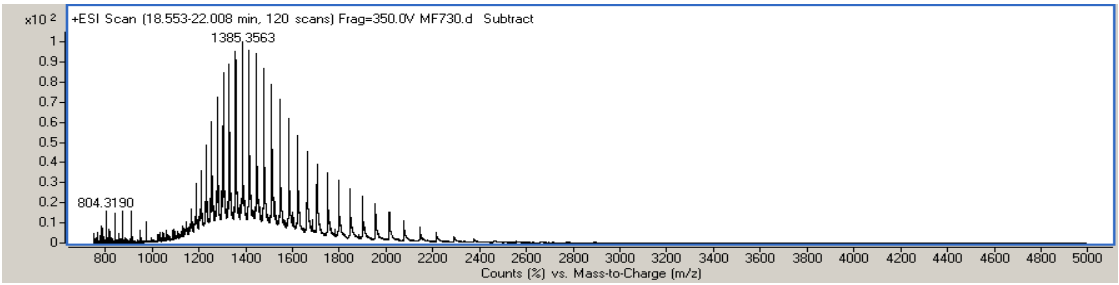

(c)

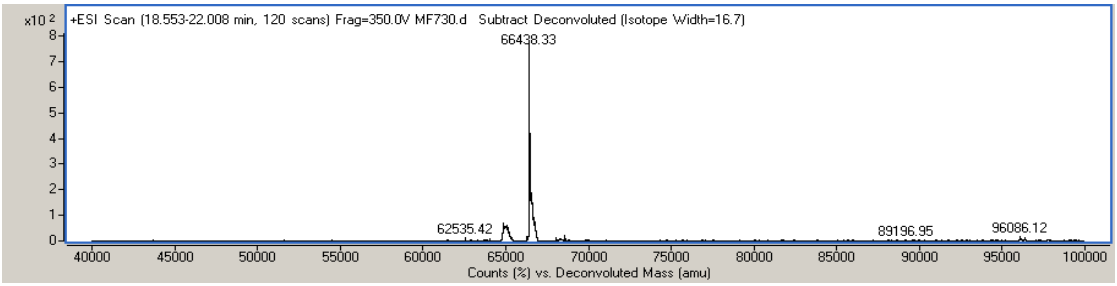

Figure **S23**. (a) TIC, (b) non-deconvoluted and (c) deconvoluted MS data for untreated human serum albumin used in the incubations with PDs **2–6** and maleimide.

Incubation of human serum albumin with mono-bromo PD (10 eq.)

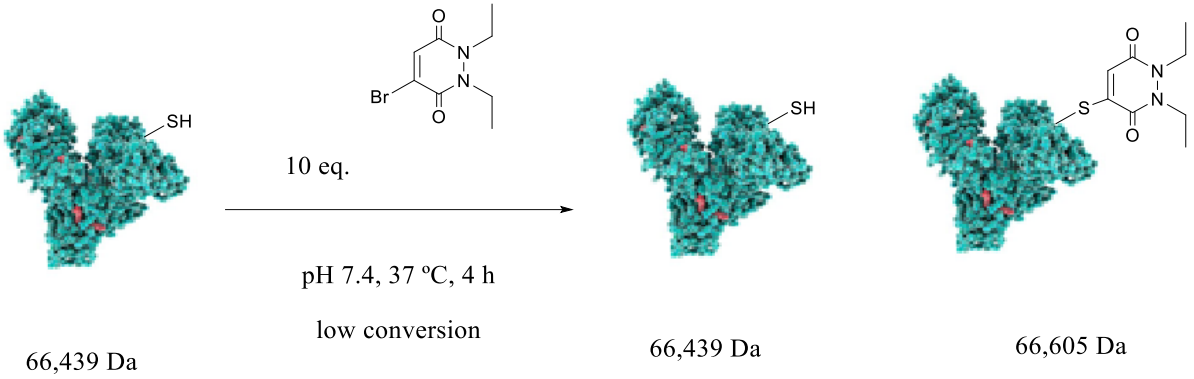

Mono-bromo PD (1.1 µL, 10 mM in MeCN, 10 eq.) was added to human serum albumin (20 µL, 3.8 mg/mL, 57 µM) in PBS (10 mM phosphate, 137 mM NaCl, 2.7 mM KCl, pH 7.4). The mixture was incubated at 37 ˚C for 4 h. Excess reagents were then removed by repeated diafiltration (× 3) into ammonium acetate buffer (20 mM, pH 7.4) using VivaSpin sample concentrators (GE Healthcare, 10,000 MWCO). The sample was then analysed by LC-MS. Expected mass: 66,605 Da. Observed masses: 66,606 and 66,440 Da.

(a)

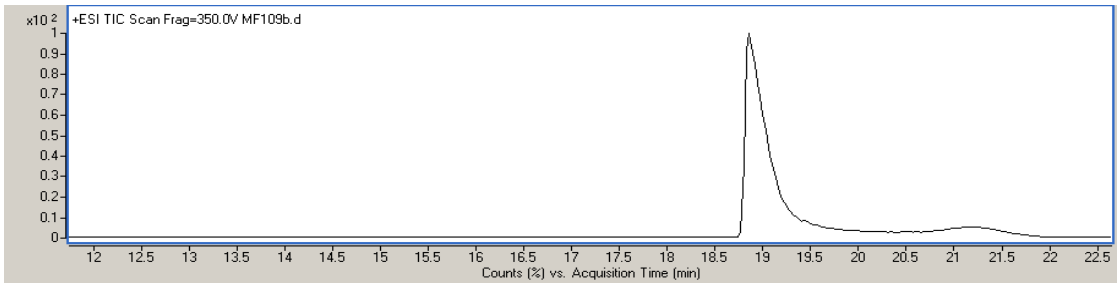

(b)

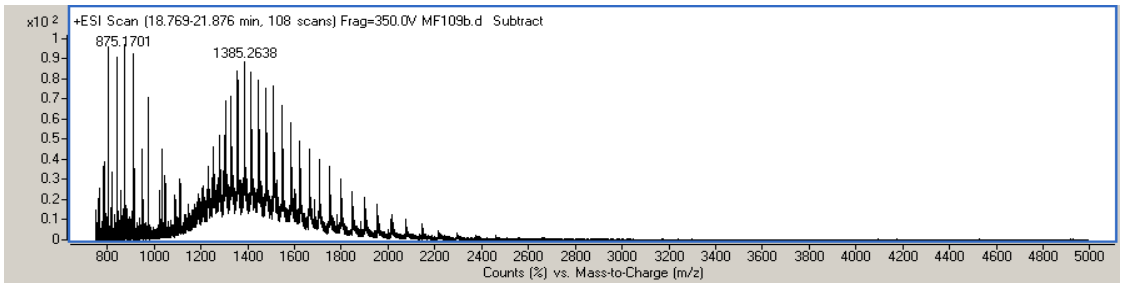

(c)

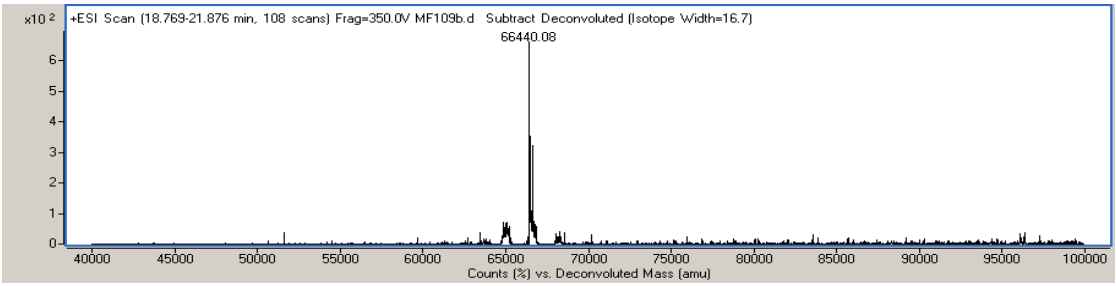

(d)

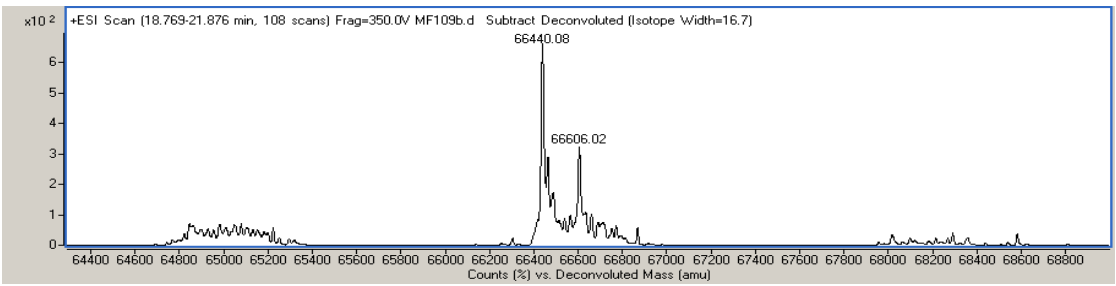

Figure **S24**. (a) TIC, (b) non-deconvoluted, (c) deconvoluted and (d) zoomed in of deconvolution MS data for human serum albumin incubated with mono-bromo PD (10 eq.).

Incubation of human serum albumin with di-bromo PD (10 eq.)

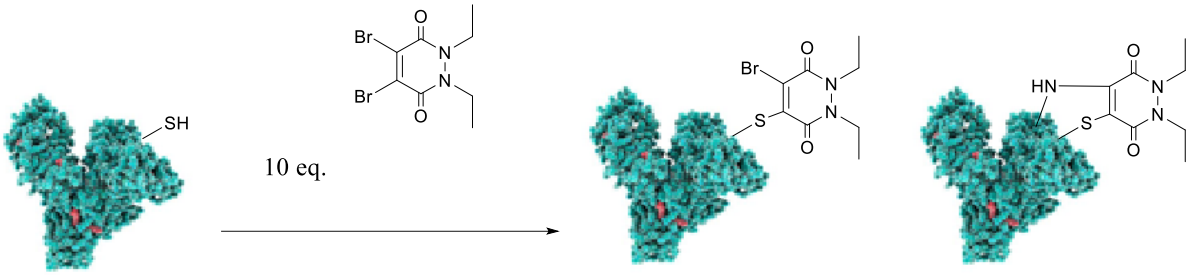

66,440 Da 66,685 Da 66,605 Da

Di-bromo PD (1.1 µL, 10 mM in MeCN, 10 eq.) was added to human serum albumin (20 µL, 3.8 mg/mL, 57 µM) in PBS (10 mM phosphate, 137 mM NaCl, 2.7 mM KCl, pH 7.4). The mixture was incubated at 37 ˚C for 4 h. Excess reagents were then removed by repeated diafiltration (× 3) into ammonium acetate buffer (20 mM, pH 7.4) using VivaSpin sample concentrators (GE Healthcare, 10,000 MWCO). The sample was then analysed by LC-MS. Expected mass: 66,685 Da. Observed masses: 66,685 and 66,605 Da.

(a)

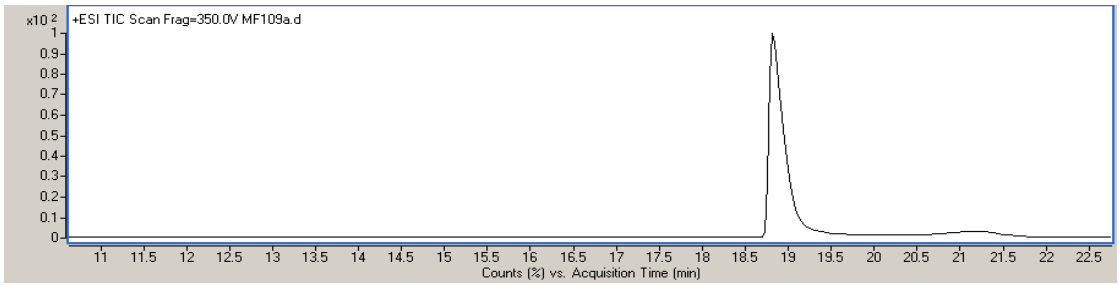

(b)

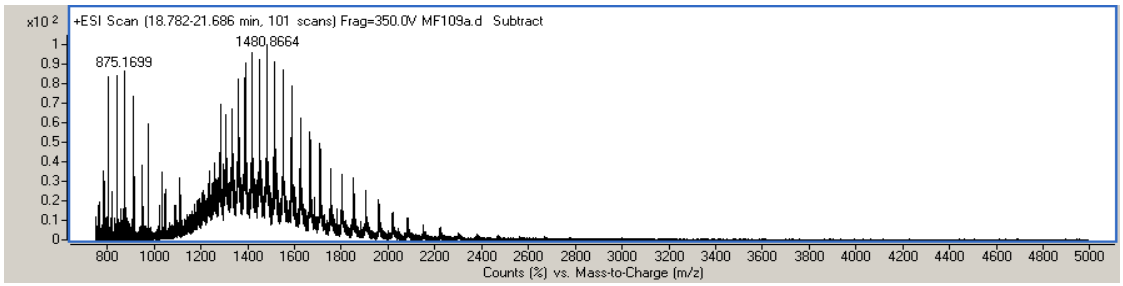

(c)

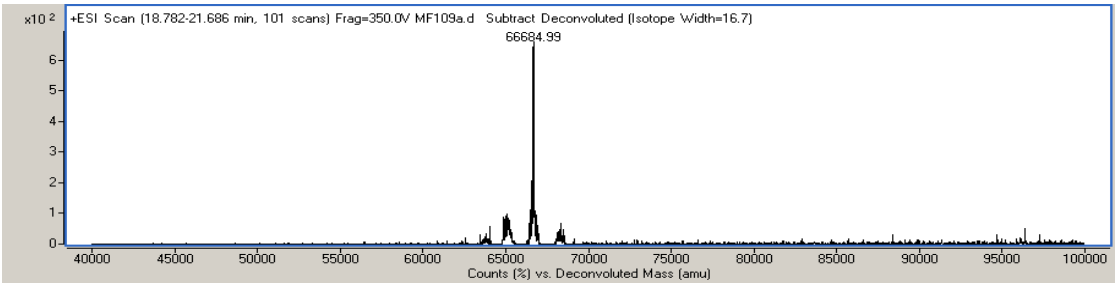

(d)

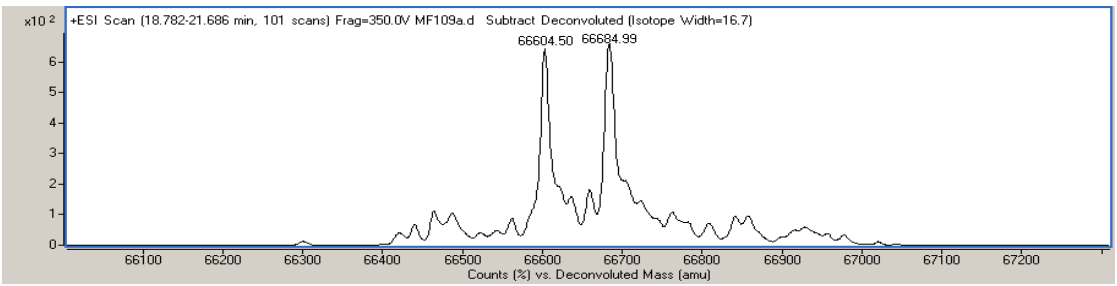

Figure **S25**. (a) TIC, (b) non-deconvoluted, (c) deconvoluted and (d) zoomed in of deconvolution MS data for human serum albumin incubated with di-bromo PD (10 eq.).

Incubation of human serum albumin with maleimide (10 eq.)

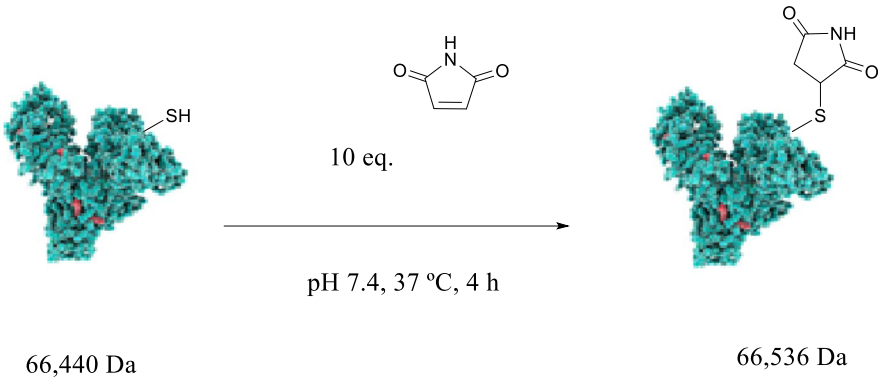

66,440 Da

66,536 Da

Maleimide (1.1 µL, 10 mM in MeCN, 10 eq.) was added to human serum albumin (20 µL, 3.8 mg/mL, 57 µM) in PBS (10 mM phosphate, 137 mM NaCl, 2.7 mM KCl, pH 7.4). The reaction was incubated at 37 ˚C for 4 h. Excess reagents were then removed by repeated diafiltration (× 3) into ammonium acetate buffer (20 mM, pH 7.4) using VivaSpin sample concentrators (GE Healthcare, 10,000 MWCO). The sample was then analysed by LC-MS. Expected mass: 66,536 Da. Observed mass: 66,536 Da.

(a)

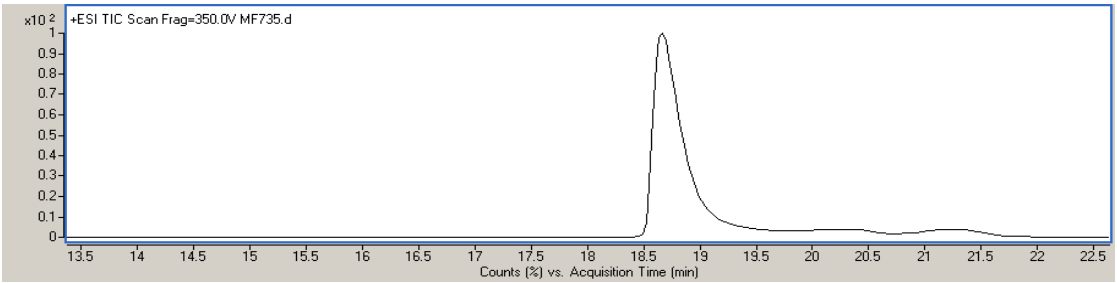

(b)

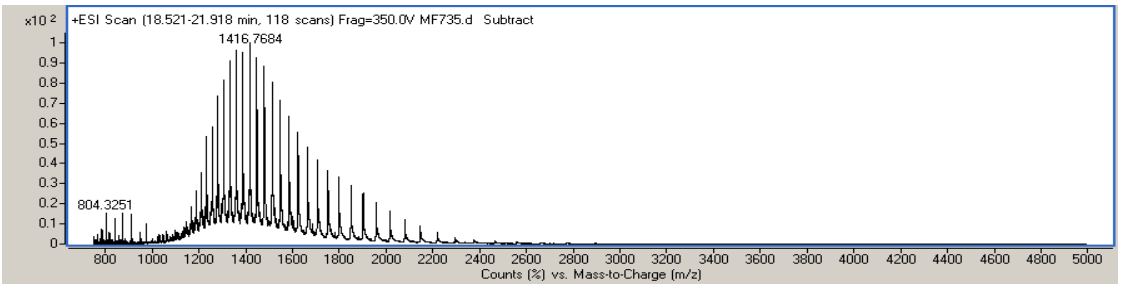

(c)

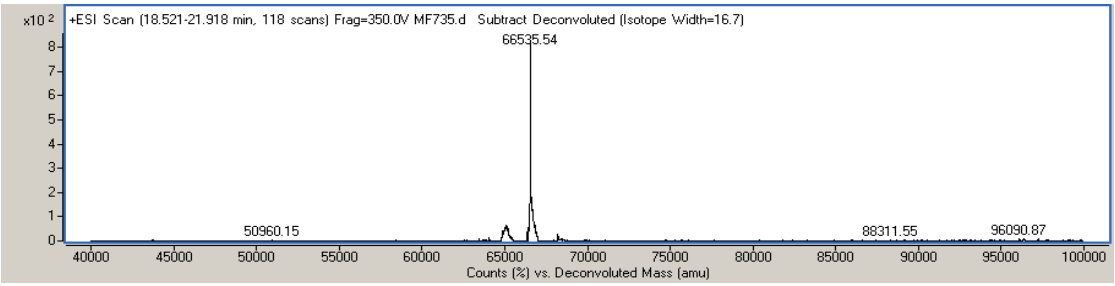

Figure **S26**. (a) TIC, (b) non-deconvoluted and (c) deconvoluted MS data for human serum albumin reacted with maleimide (10 eq.).

Incubation of human serum albumin with PD 2 (10 eq.)

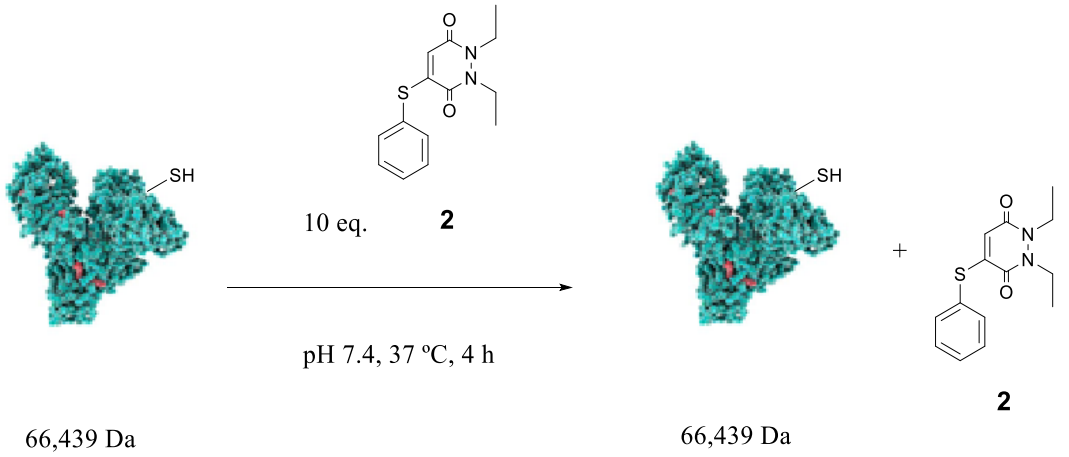

PD **2** (1.1 µL, 10 mM in MeCN, 10 eq.) was added to human serum albumin (20 µL, 3.8 mg/mL, 57 µM) in PBS (10 mM phosphate, 137 mM NaCl, 2.7 mM KCl, pH 7.4). The mixture was incubated at 37 ˚C for 4 h. Excess reagents were then removed by repeated diafiltration (× 3) into ammonium acetate buffer (20 mM, pH 7.4) using VivaSpin sample concentrators (GE Healthcare, 10,000 MWCO). The sample was then analysed by LC-MS. Expected mass: 66,438 Da. Observed mass: 66,439 Da.

(a)

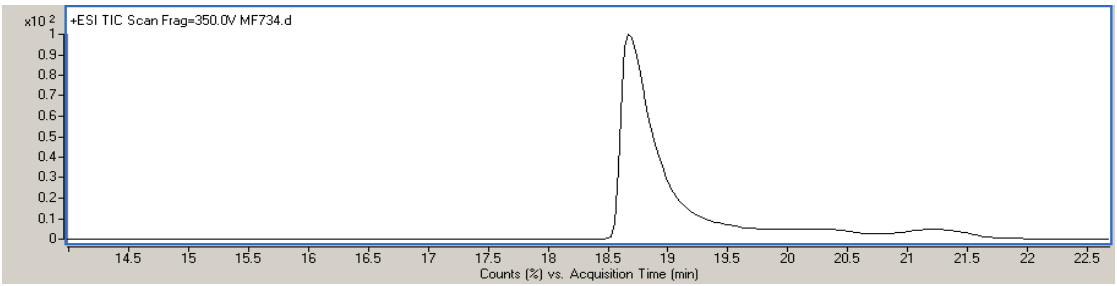

(b)

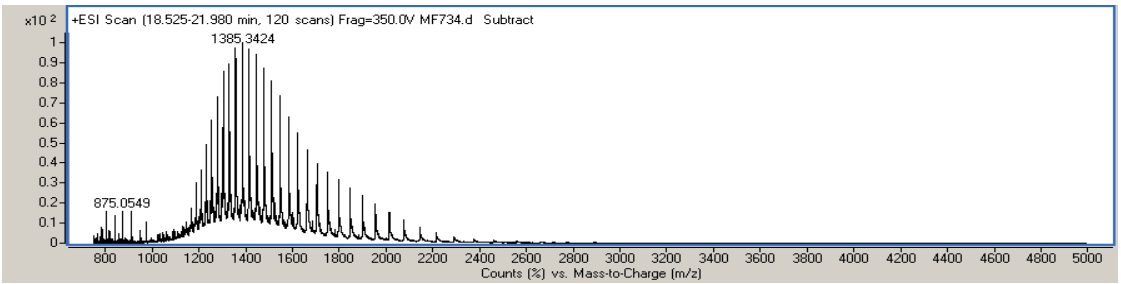

(c)

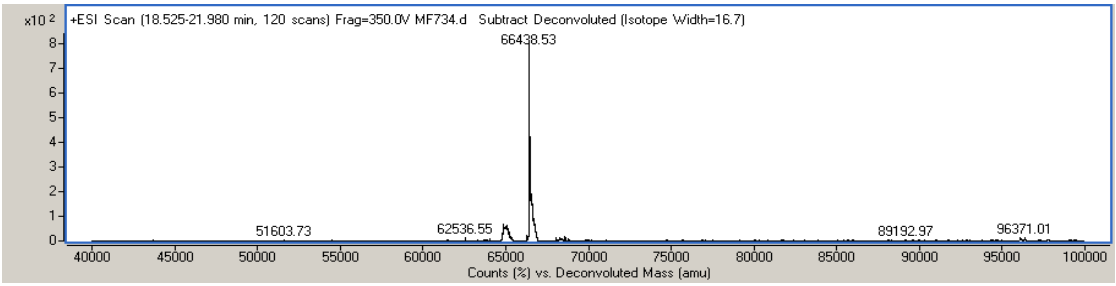

Figure **S27**. TIC, (b) non-deconvoluted and (c) deconvoluted MS data for human serum albumin incubated with PD **2** (10 eq.).

Incubation of human serum albumin with PD 3 (10 eq.)

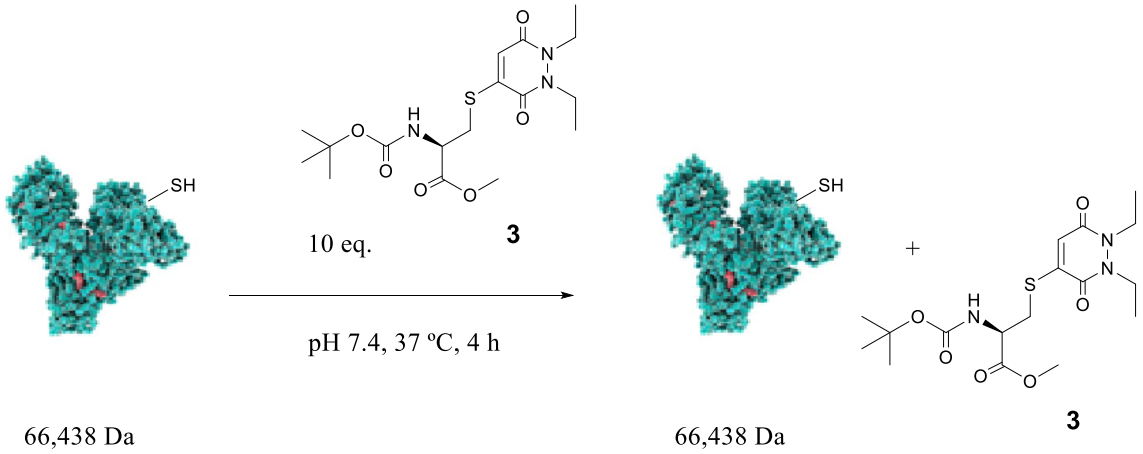

PD **3** (1.1 µL, 10 mM in MeCN, 10 eq.) was added to human serum albumin (20 µL, 3.8 mg/mL, 57 µM) in PBS (10 mM phosphate, 137 mM NaCl, 2.7 mM KCl, pH 7.4). The mixture was incubated at 37 ˚C for 4 h. Excess reagents were then removed by repeated diafiltration (× 3) into ammonium acetate buffer (20 mM, pH 7.4) using VivaSpin sample concentrators (GE Healthcare, 10,000 MWCO). The sample was then analysed by LC-MS. Expected mass: 66,438 Da. Observed mass: 66,438 Da.

(a)

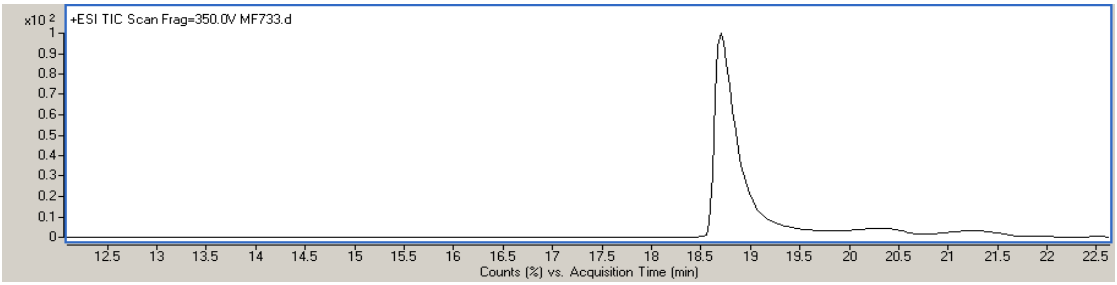

(b)

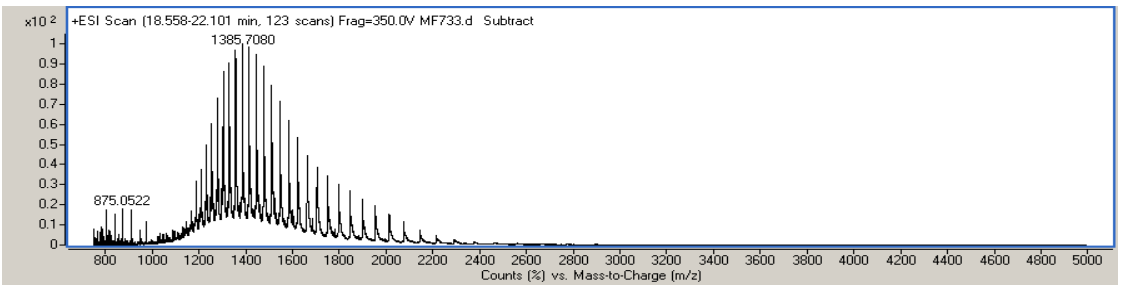

(c)

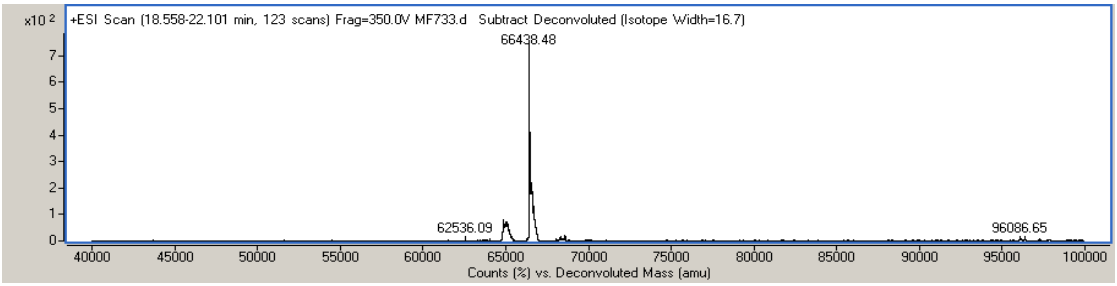

Figure **S28**. (a) TIC, (b) non-deconvoluted and (c) deconvoluted MS data for human serum albumin incubated with PD **3** (10 eq.).

Incubation of human serum albumin with PD 4 (10 eq.)

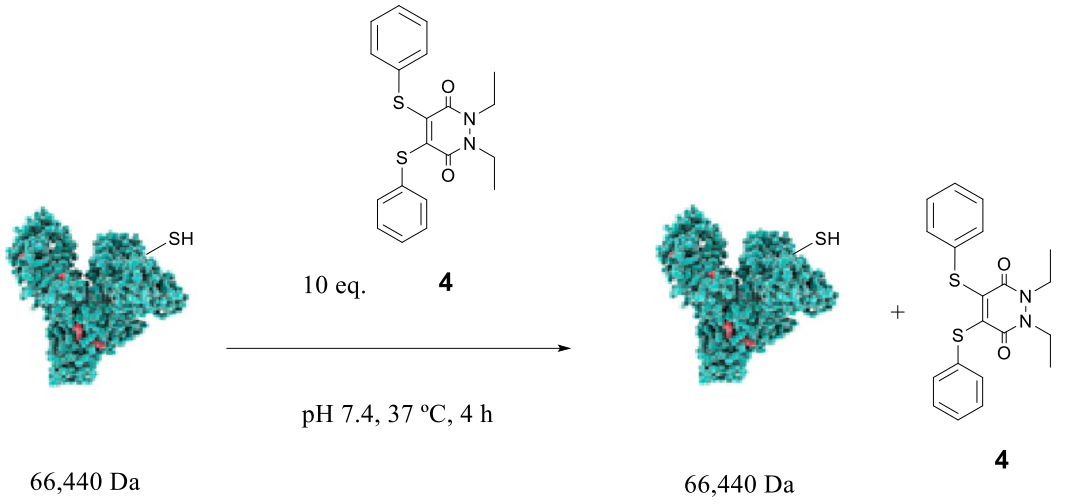

PD **4** (1.1 µL, 10 mM in MeCN, 10 eq.) was added to human serum albumin (20 µL, 3.8 mg/mL, 57 µM) in PBS (10 mM phosphate, 137 mM NaCl, 2.7 mM KCl, pH 7.4). The mixture was incubated at 37 ˚C for 4 h. Excess reagents were then removed by repeated diafiltration (× 3) into ammonium acetate buffer (20 mM, pH 7.4) using VivaSpin sample concentrators (GE Healthcare, 10,000 MWCO). The sample was then analysed by LC-MS. Expected mass: 66,438 Da. Observed mass: 66,440 Da.

(a)

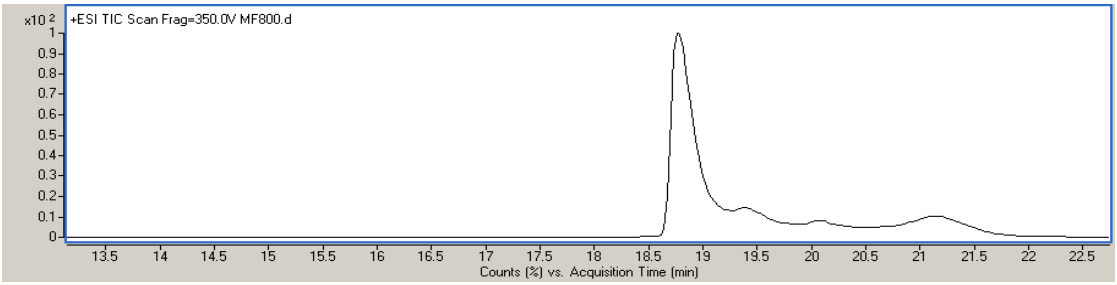

(b)

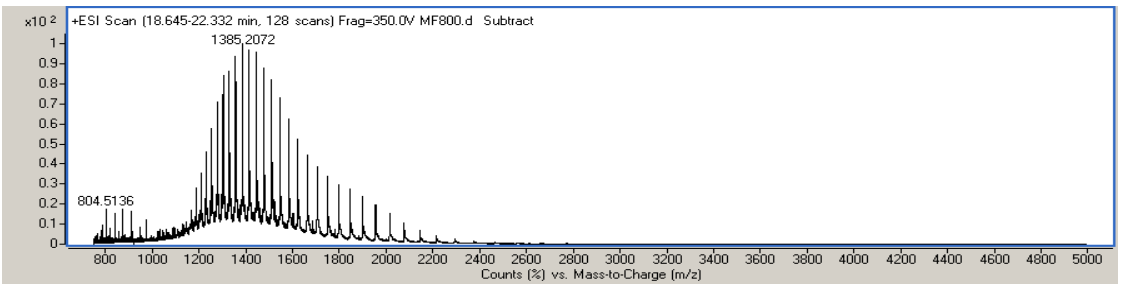

(c)

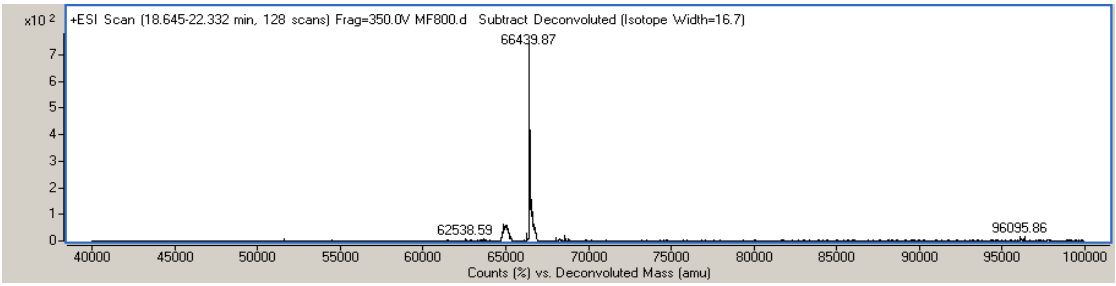

Figure **S29**. (a) TIC, (b) non-deconvoluted and (c) deconvoluted MS data for human serum albumin incubated with PD **4** (10 eq.).

Incubation of human serum albumin with PD 5 (10 eq.)

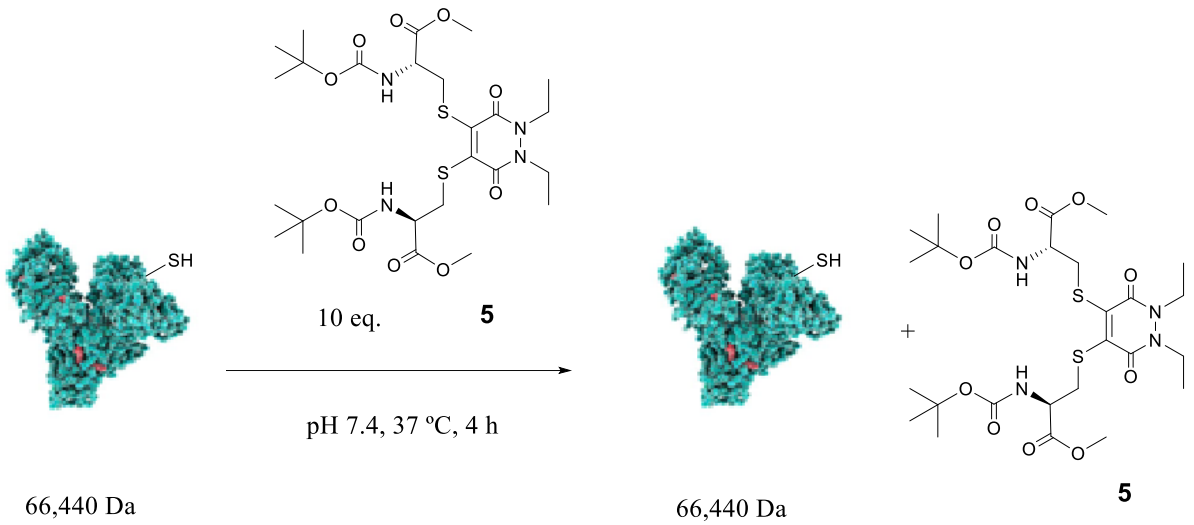

PD **5** (1.1 µL, 10 mM in MeCN, 10 eq.) was added to human serum albumin (20 µL, 3.8 mg/mL, 57 µM) in PBS (10 mM phosphate, 137 mM NaCl, 2.7 mM KCl, pH 7.4). The mixture was incubated at 37 ˚C for 4 h. Excess reagents were then removed by repeated diafiltration (× 3) into ammonium acetate buffer (20 mM, pH 7.4) using VivaSpin sample concentrators (GE Healthcare, 10,000 MWCO). The sample was then analysed by LC-MS. Expected mass: 66,438 Da. Observed mass: 66,440 Da.

(a)

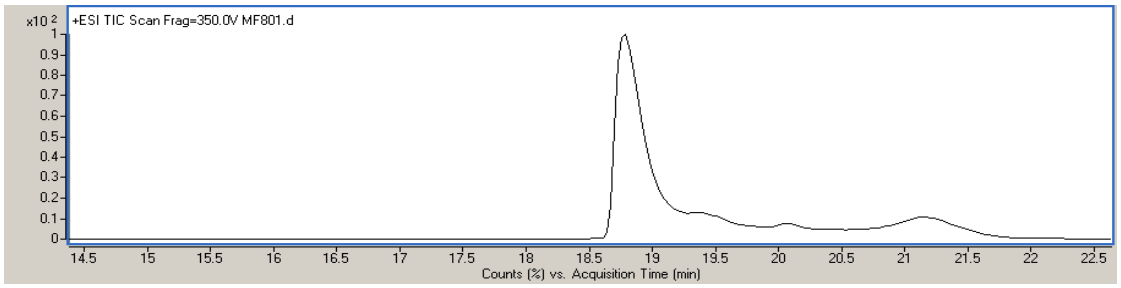

(b)

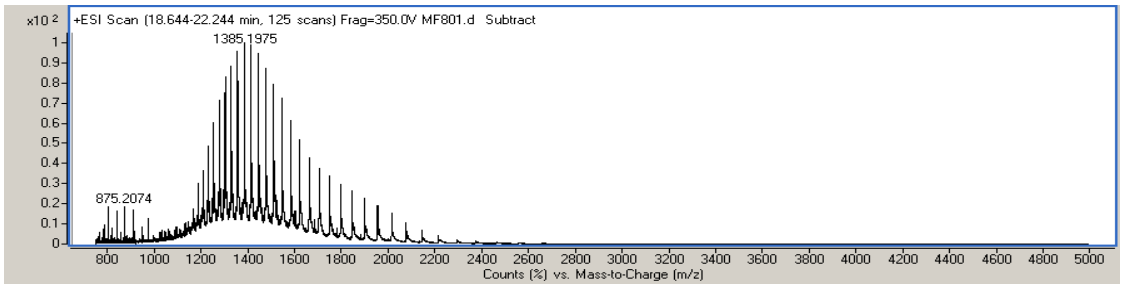

(c)

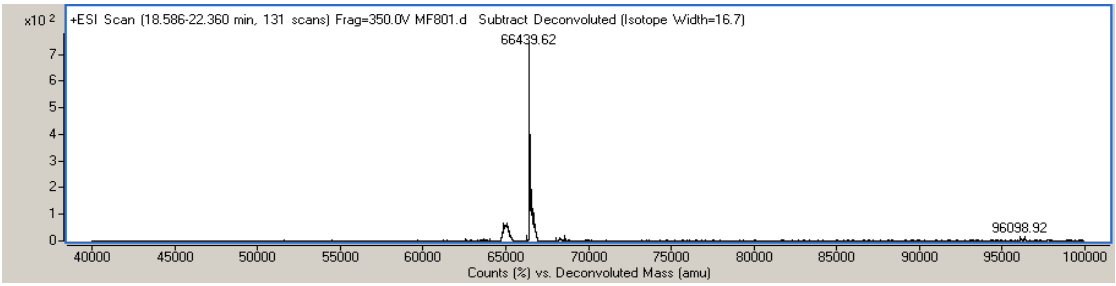

Figure **S30**. (a) TIC, (b) non-deconvoluted and (c) deconvoluted MS data for human serum albumin incubated with PD **5** (10 eq.).

Incubation of human serum albumin with PD 6 (10 eq.)

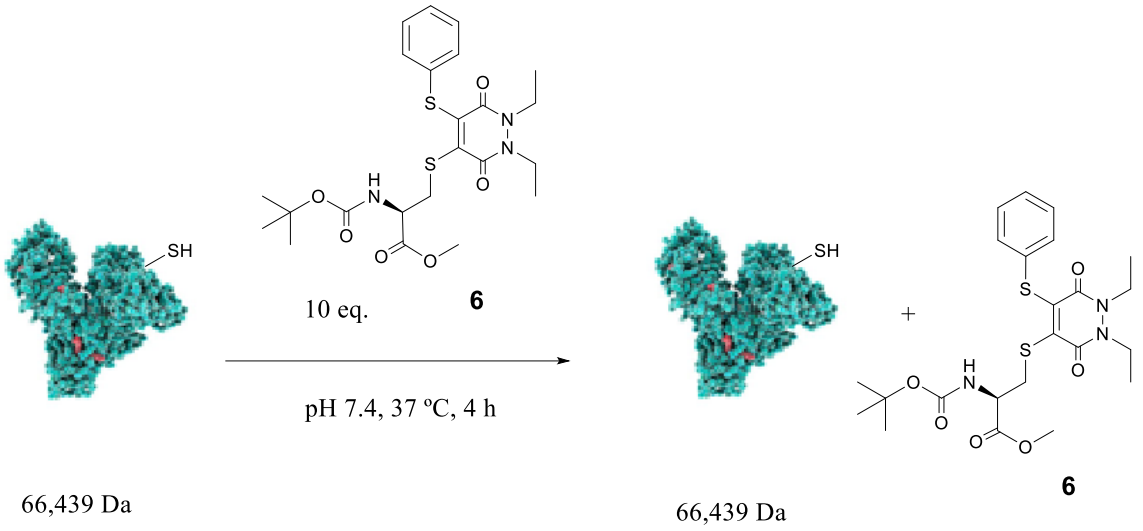

PD **6** (1.1 µL, 10 mM in MeCN, 10 eq.) was added to human serum albumin (20 µL, 3.8 mg/mL, 57 µM) in PBS (10 mM phosphate, 137 mM NaCl, 2.7 mM KCl, pH 7.4). The mixture was incubated at 37 °C for 4 h. Excess reagents were then removed by repeated diafiltration (× 3) into ammonium acetate buffer (20 mM, pH 7.4) using VivaSpin sample concentrators (GE Healthcare, 10,000 MWCO). The sample was then analysed by LC-MS. Expected mass: 66,438 Da. Observed mass: 66,439 Da.

(a)

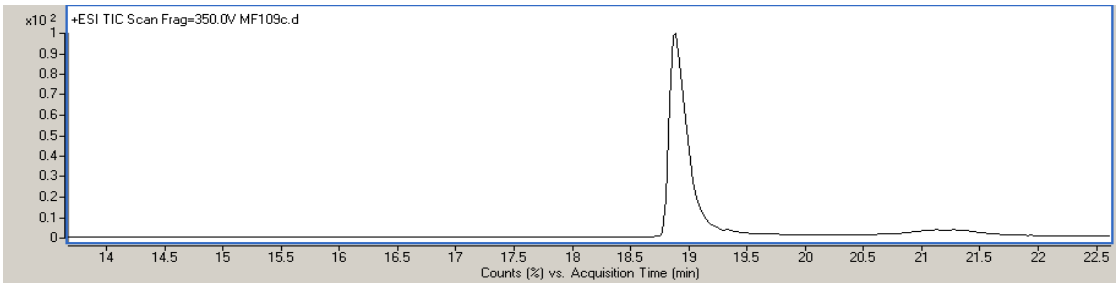

(b)

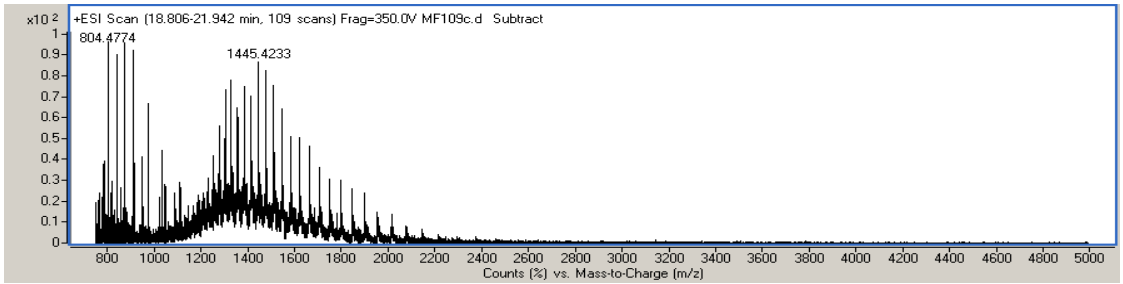

(c)

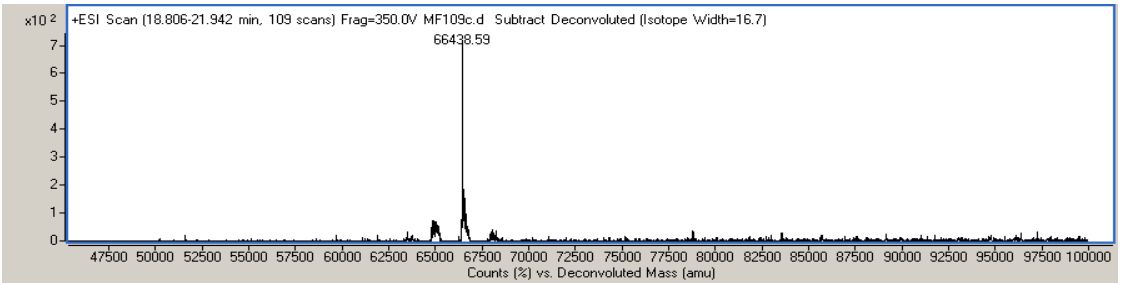

Figure **S31**. (a) TIC, (b) non-deconvoluted and (c) deconvoluted MS data for human serum albumin incubated with PD **6** (10 eq.).

Incubations involving GSH and PDs 2–6 at pH 6.5

Incubation of PD 2 with GSH (10 eq.)

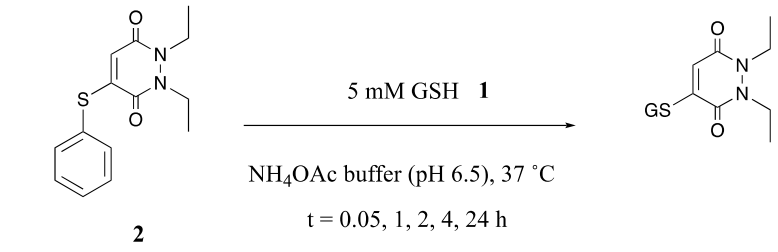

2

276 g/mol

UV r.t.: 1.77, 1.97 mins

473 g/mol

UV r.t.: 0.64, 0.78 mins

PD **2** (10 µL, 10 mM in MeCN, 1 eq.) was added to GSH **1** (190 µL, 5.3 mM, 10 eq.) in ammonium acetate buffer (50 mM, pH 6.5). The mixture was incubated at 37 ˚C for 24 h. The samples were analysed by LC-MS at t = 0.05, 1, 2, 4 and 24 h.

LC-MS data for t = 0.05 h

(a)

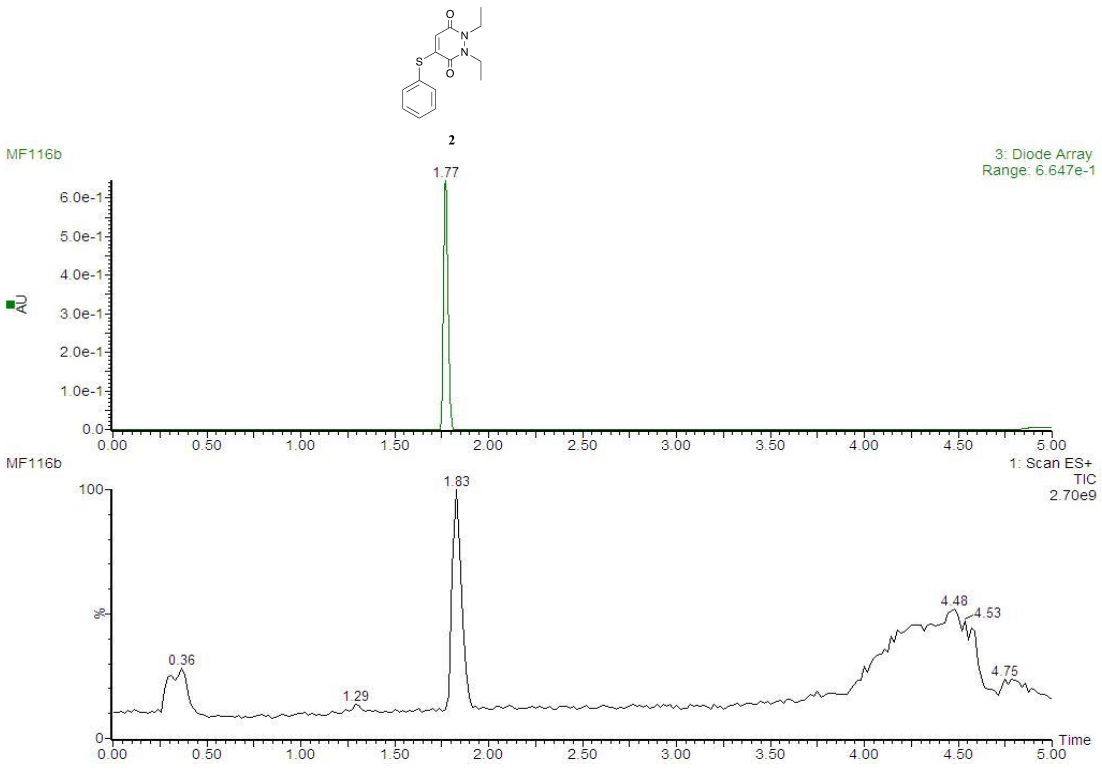

(b)

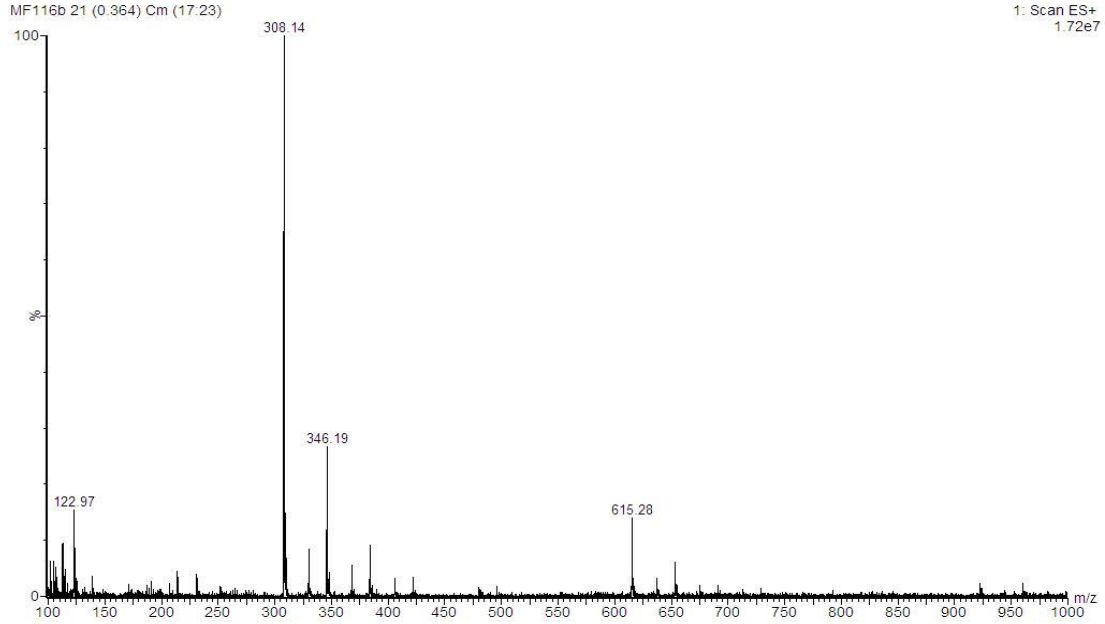

(c)

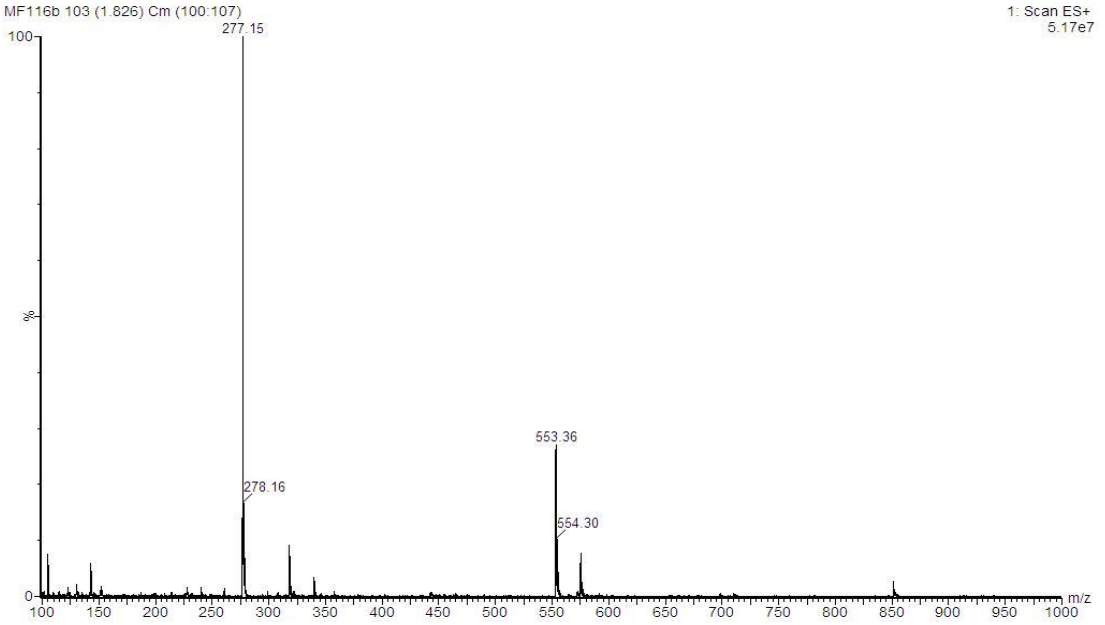

Figure **S32**. (a) TIC and UV trace at t = 0.05 h, (b) MS data at 0.36 mins in the TIC and (c) MS data at 1.77 mins in the UV for PD **2** incubated with GSH **1** (10 eq.) at pH 6.5.

LC-MS data for t = 1 h

(a)

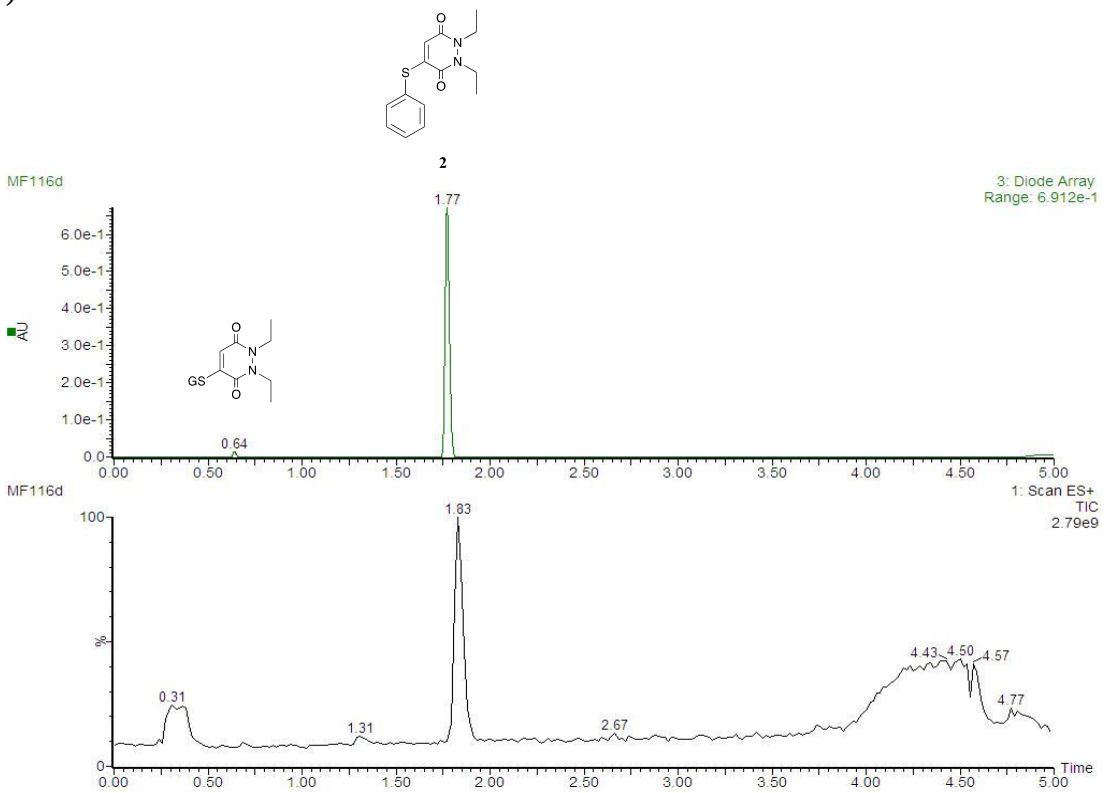

(b)

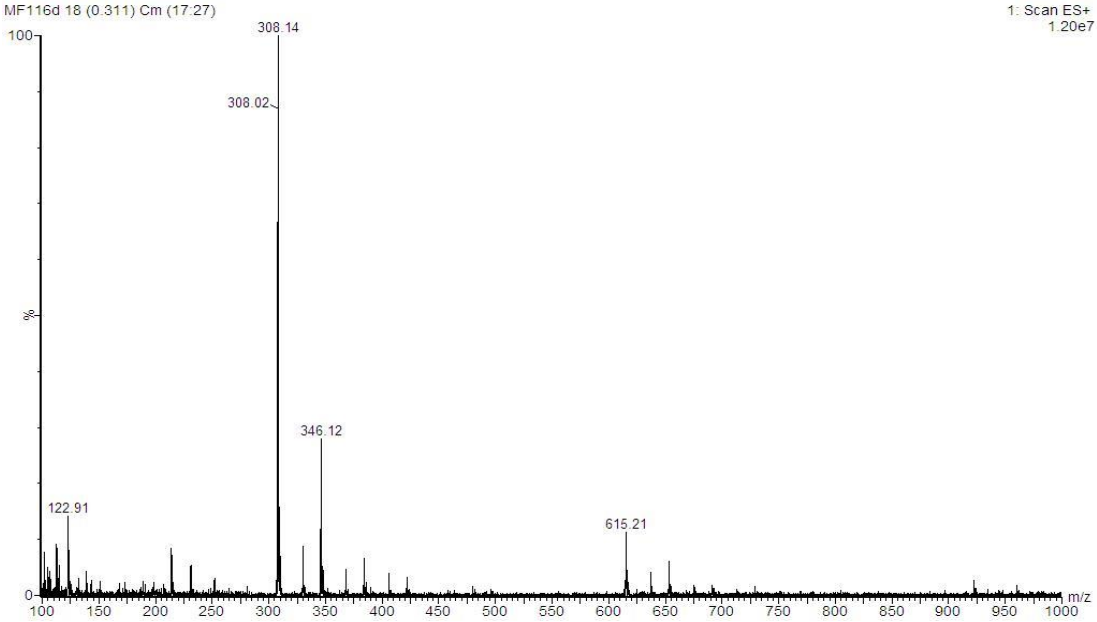

(c)

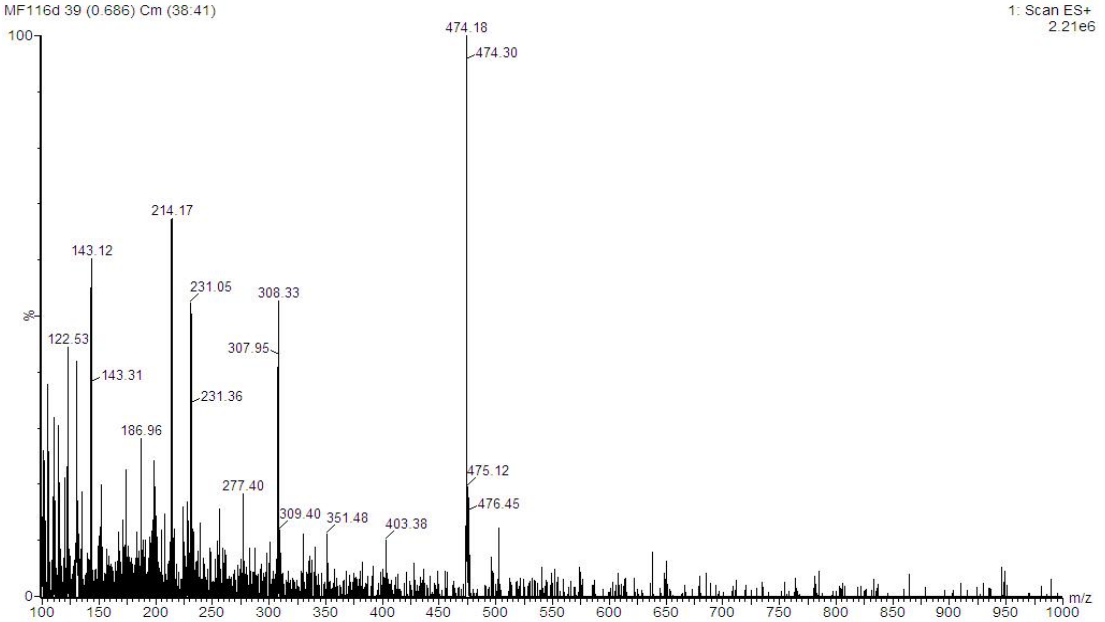

(d)

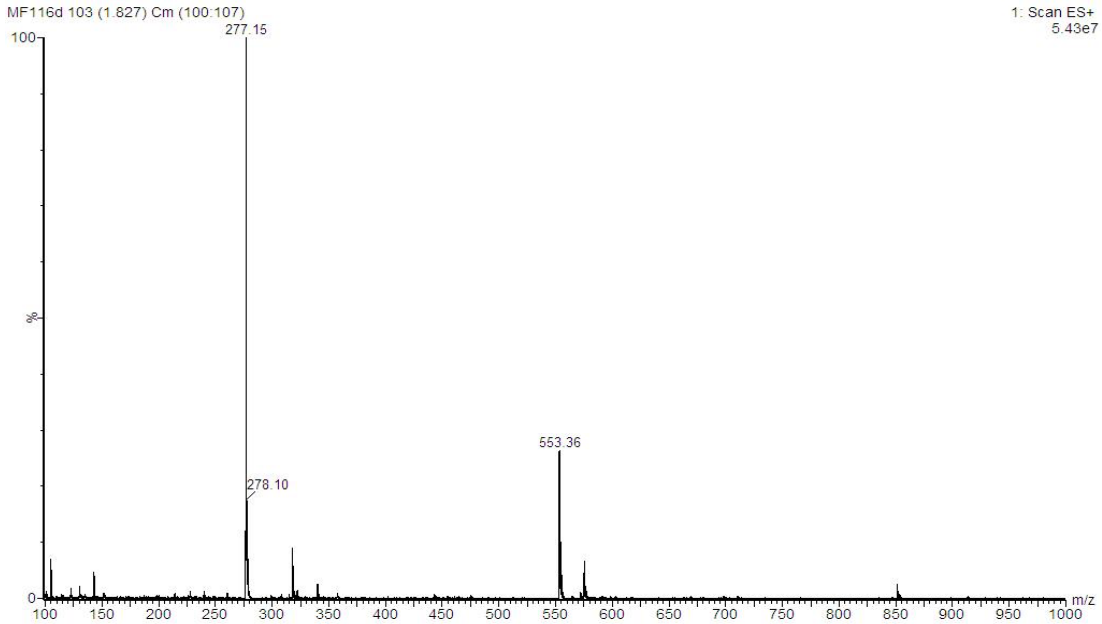

Figure **S33**. (a) TIC and UV trace at t = 1 h, (b) MS data at 0.31 mins in the TIC, (c) MS data at 0.64 mins in the UV and (d) at 1.77 mins in the UV for PD **2** incubated with GSH **1** (10 eq.) at pH 6.5.

LC-MS data for t = 2 h

(a)

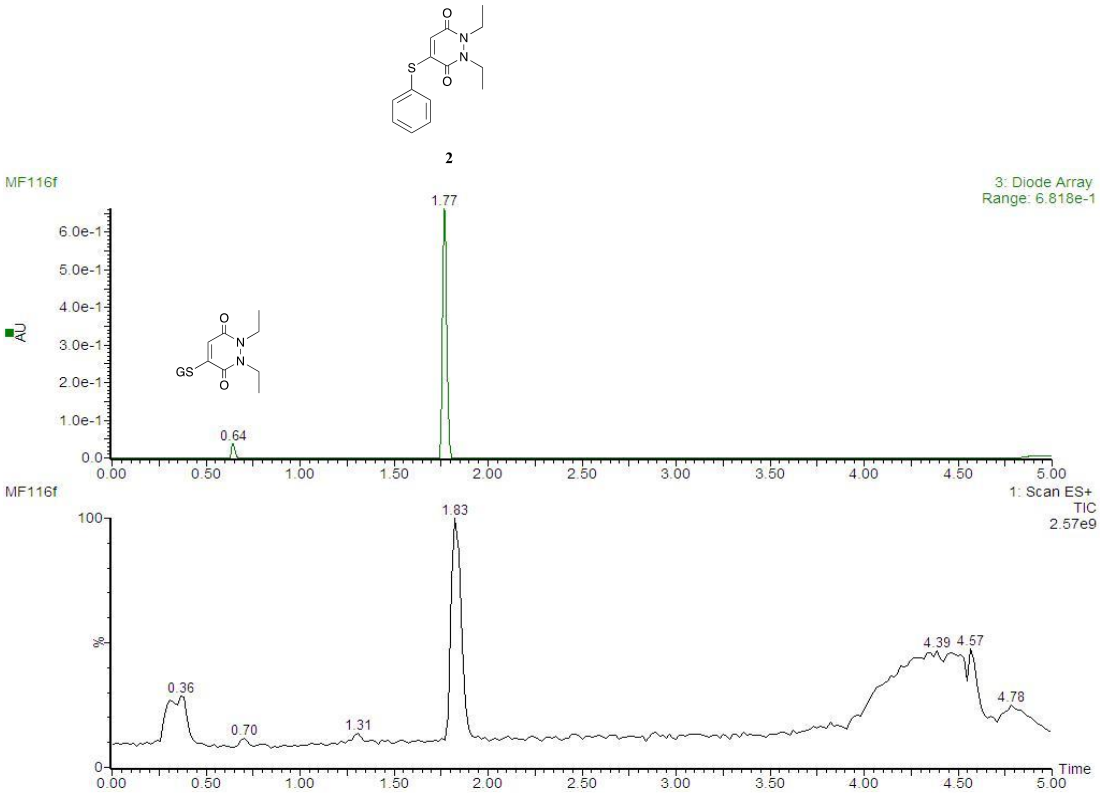

(b)

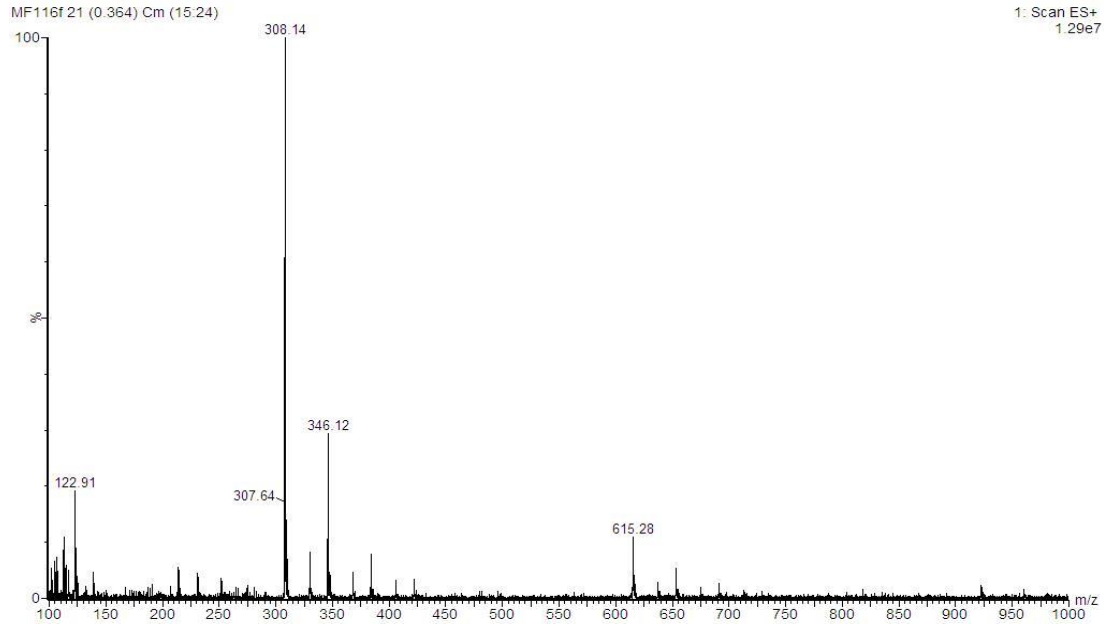

(c)

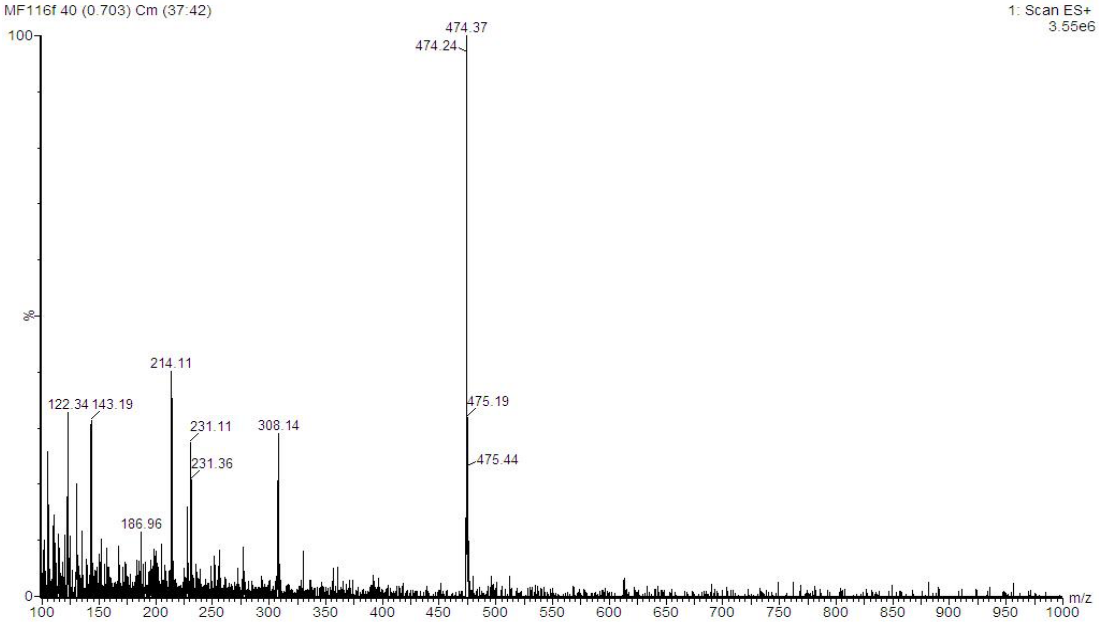

(d)

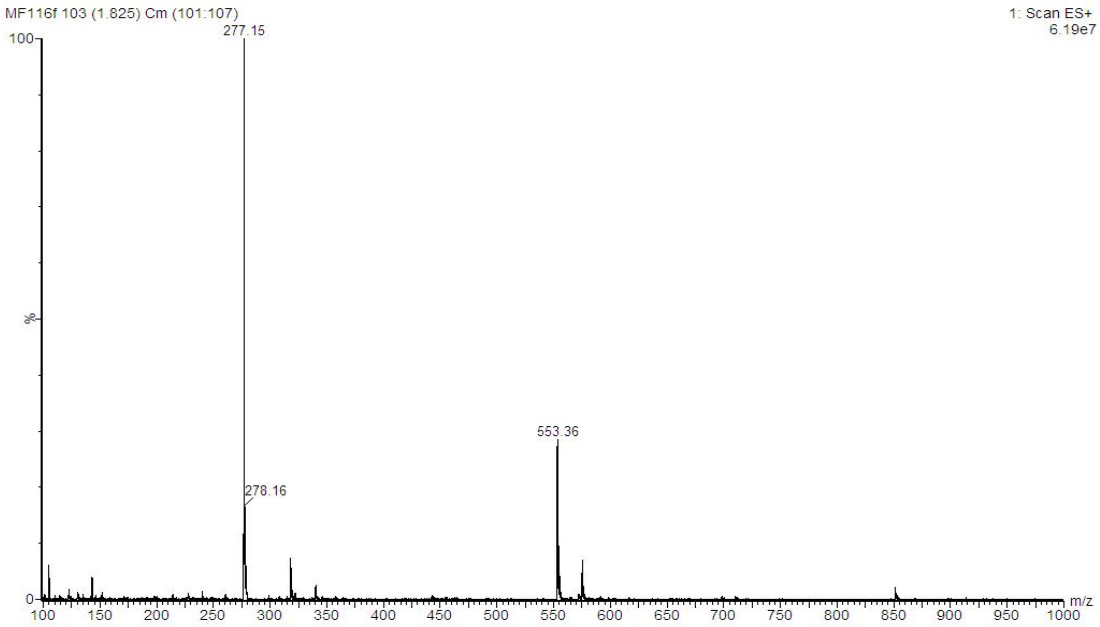

Figure **S34**. (a) TIC and UV trace at t = 2 h, (b) MS data at 0.36 mins in the TIC, (c) MS data at 0.64 mins in the UV and (d) at 1.77 mins in the UV for PD **2** incubated with GSH **1** (10 eq.) at pH 6.5.

LC-MS data for t = 4 h

(a)

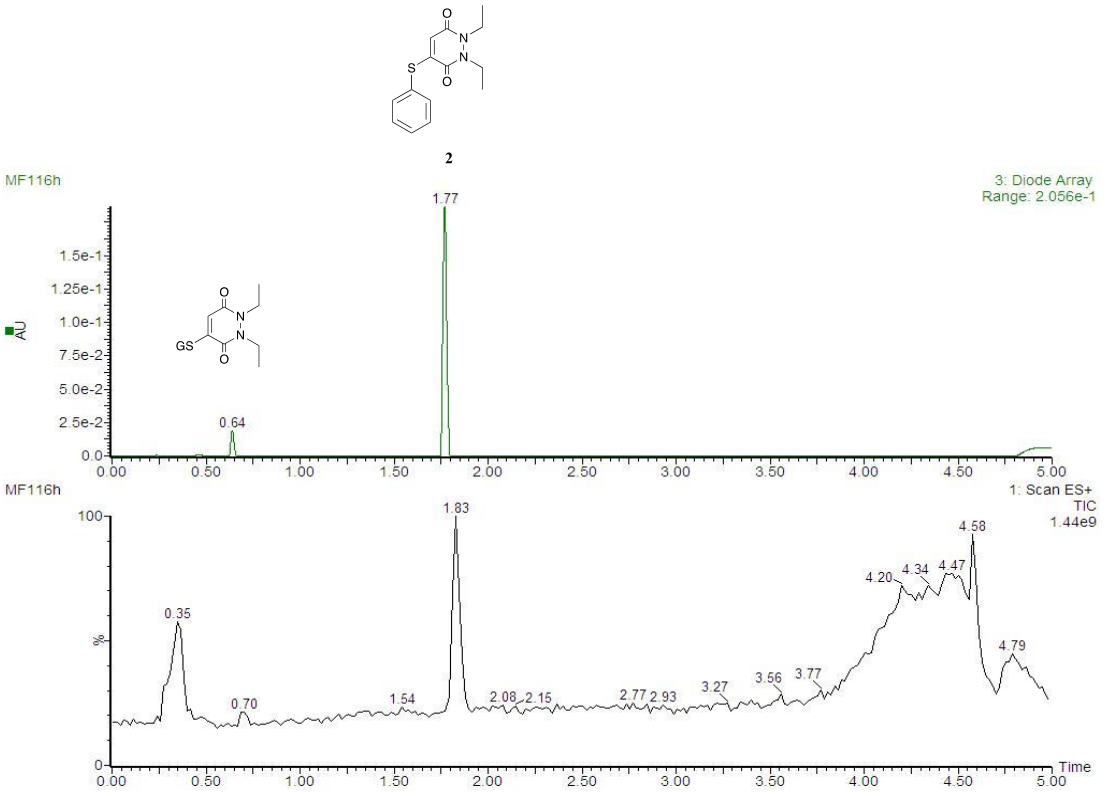

(b)

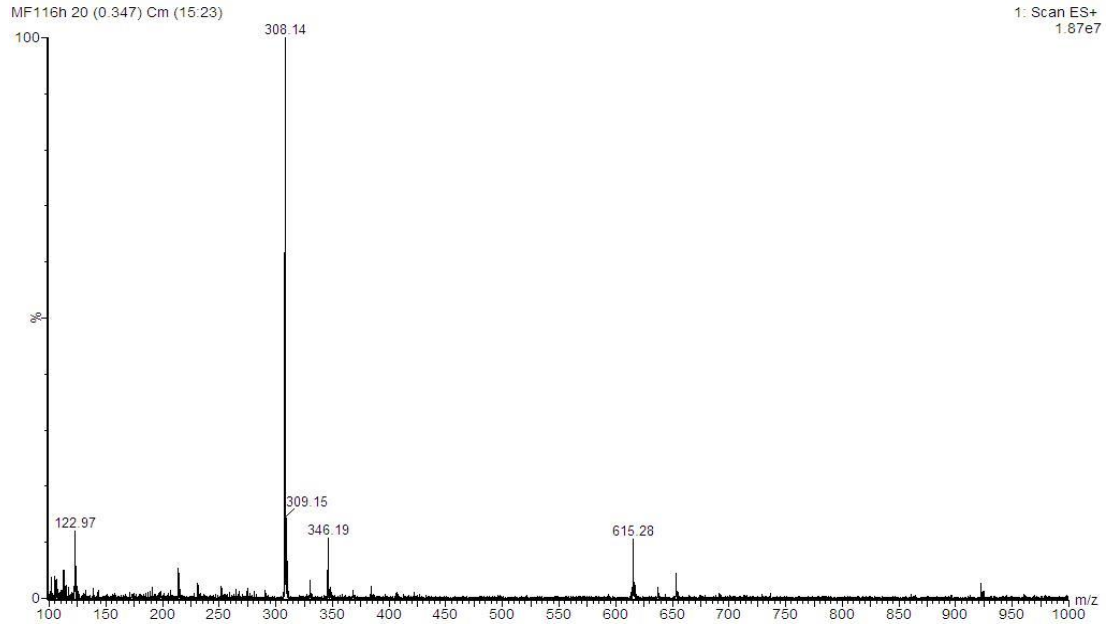

(c)

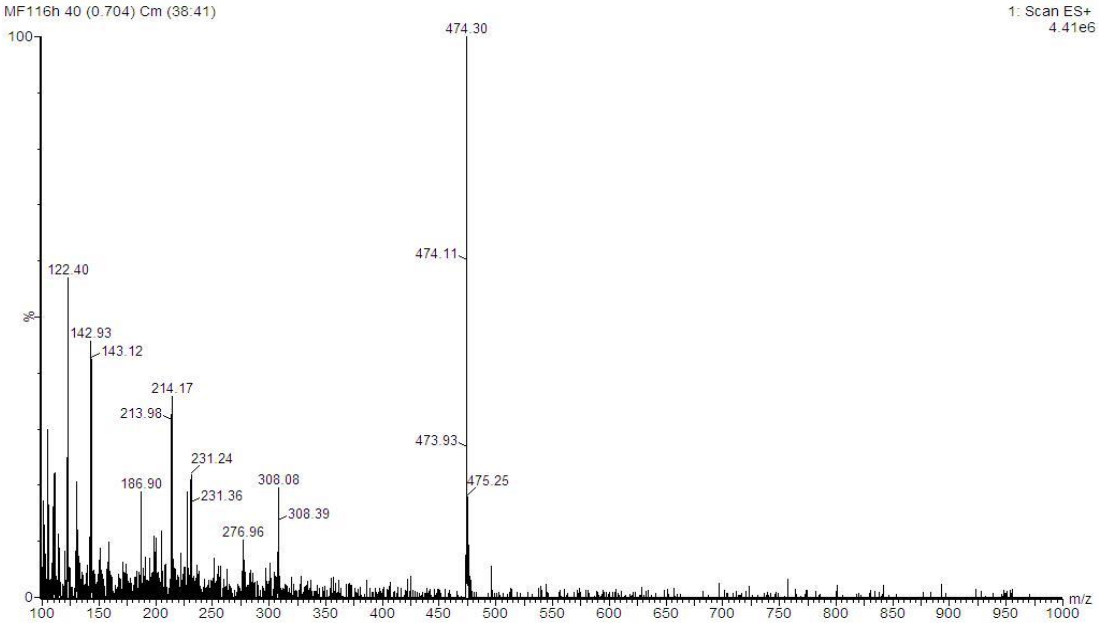

(d)

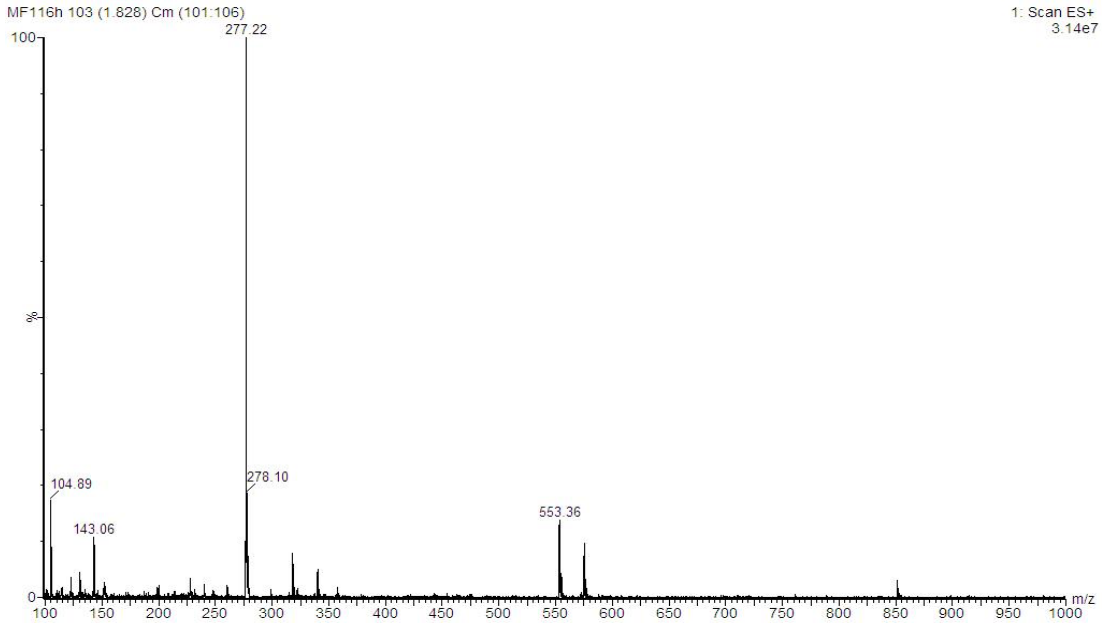

Figure **S35**. (a) TIC and UV trace at t = 4 h, (b) MS data at 0.35 mins in the TIC, (c) MS data at 0.64 mins in the UV and (d) at 1.77 mins in the UV for PD **2** incubated with GSH **1** (10 eq.) at pH 6.5.

LC-MS data for t = 24 h

(a)

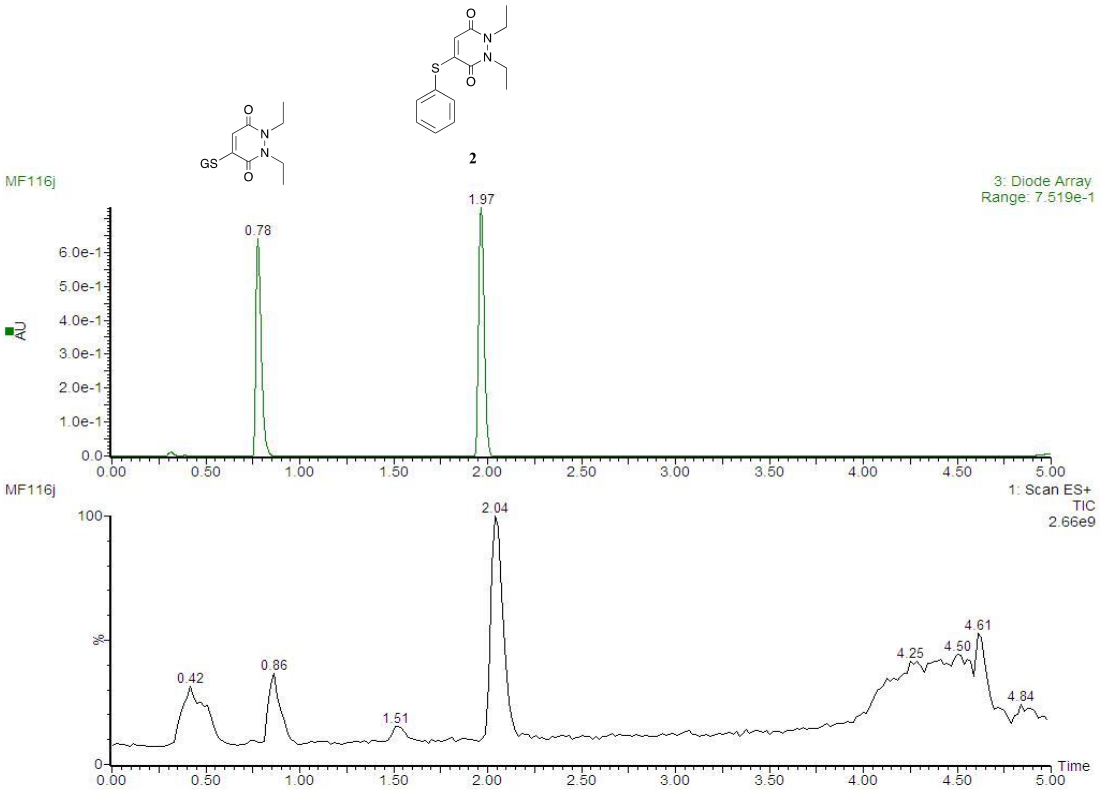

(b)

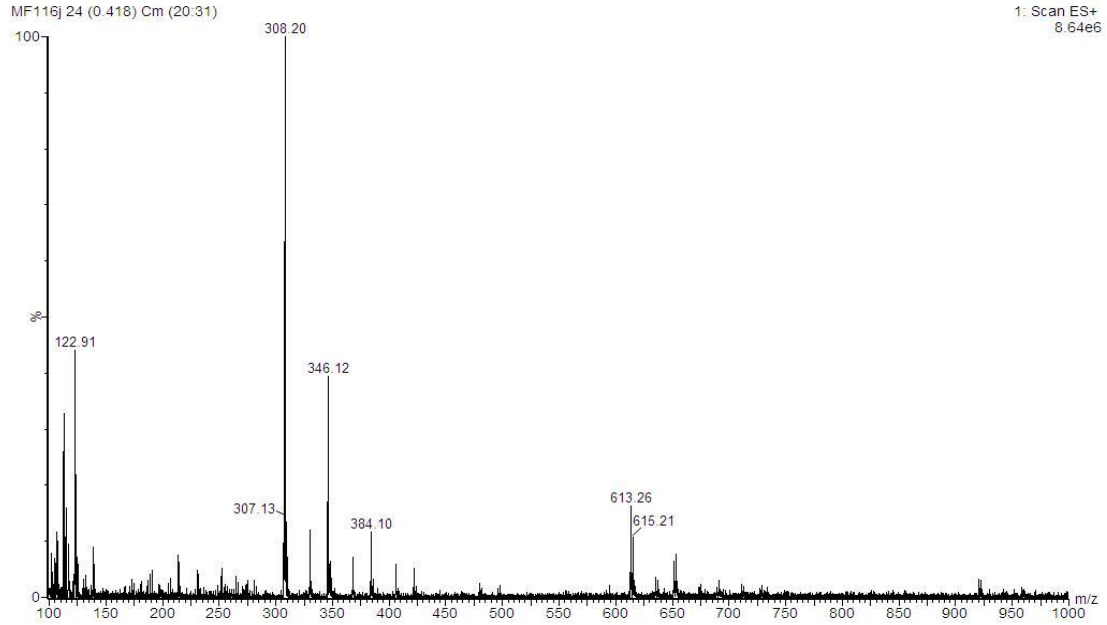

(c)

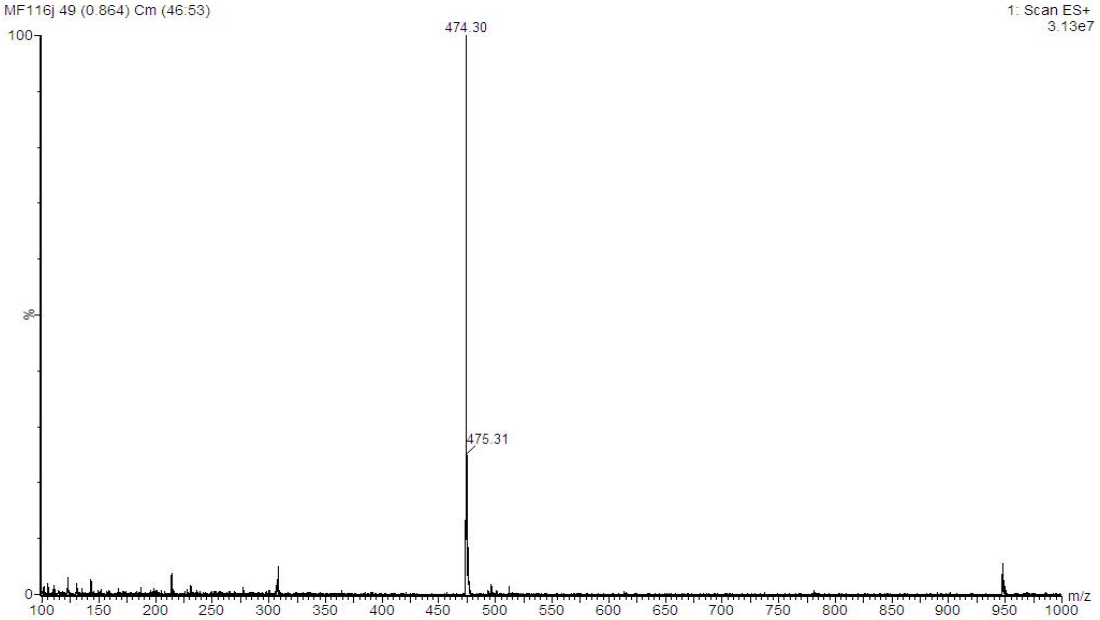

(d)

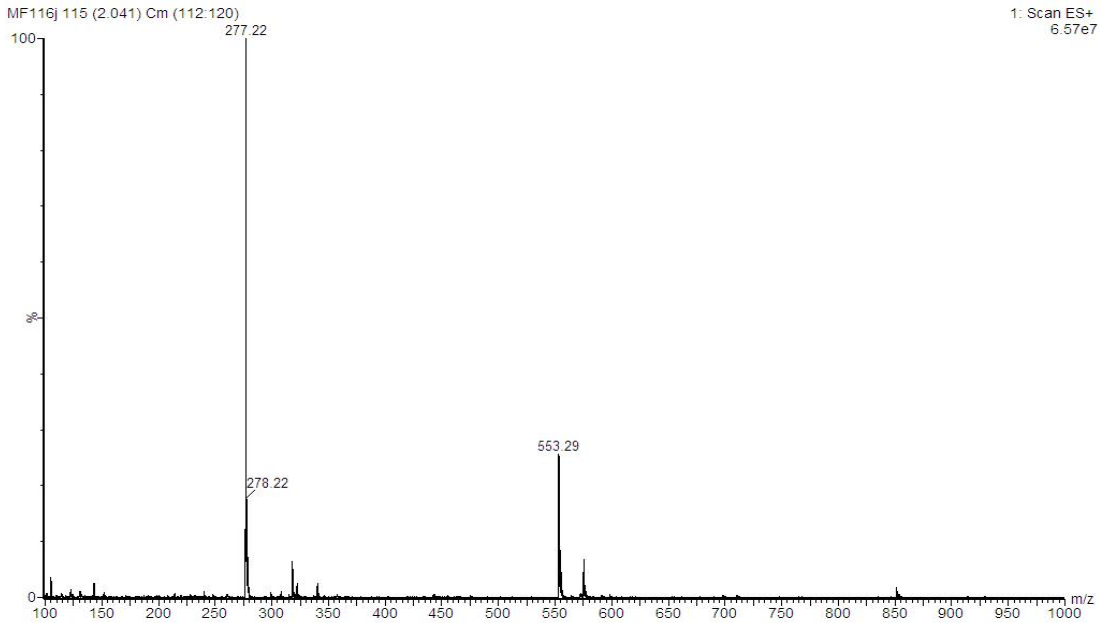

Figure **S36**. (a) TIC and UV trace at t = 24 h, (b) MS data at 0.42 mins in the TIC, (c) MS data at 0.78 mins in the UV and (d) at 1.97 mins in the UV for PD **2** incubated with GSH **1** (10 eq.) at pH 6.5.

Incubation of PD 3 with GSH (10 eq.)

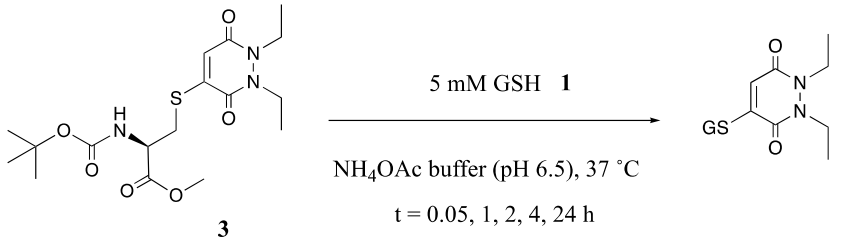

3

401 g/mol

473 g/mol

UV r.t.: 1.75–1.79 mins

UV r.t.: 0.69 mins

PD **3** (10 µL, 10 mM in MeCN, 1 eq.) was added to GSH **1** (190 µL, 5.3 mM, 10 eq.) in ammonium acetate buffer (50 mM, pH 6.5). The mixture was incubated at 37 ˚C for 24 h. The samples were analysed by LC-MS at t = 0.05, 1, 2, 4 and 24 h.

LC-MS data for t = 0.05 h

(a)

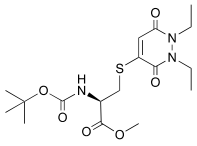

3

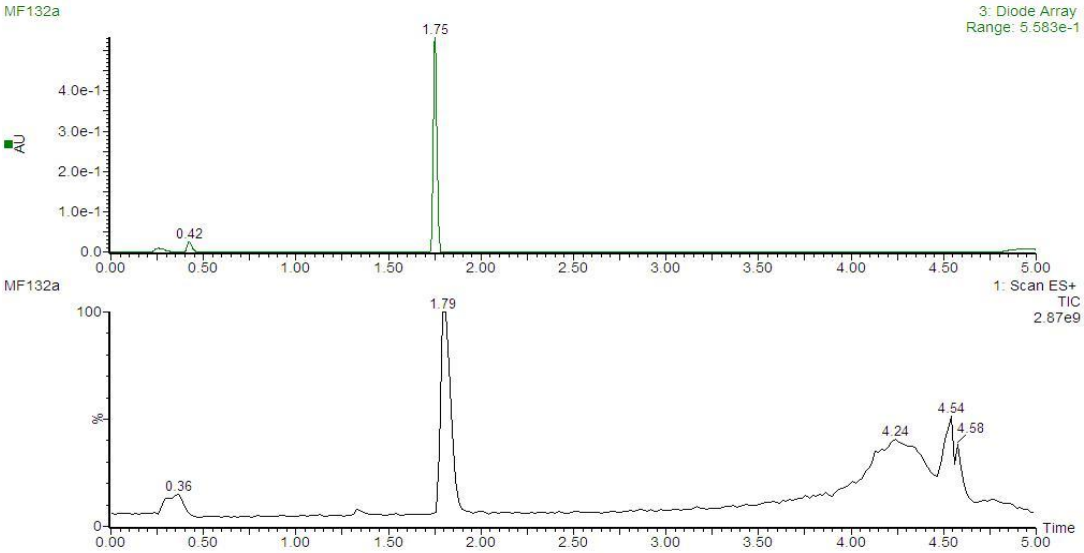

(b)

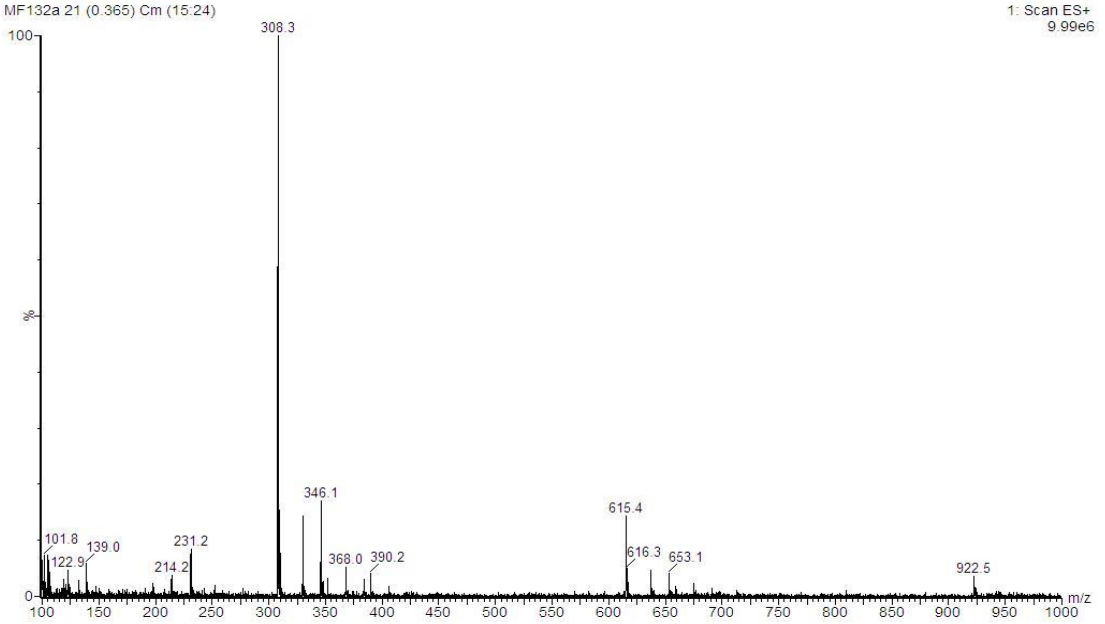

(c)

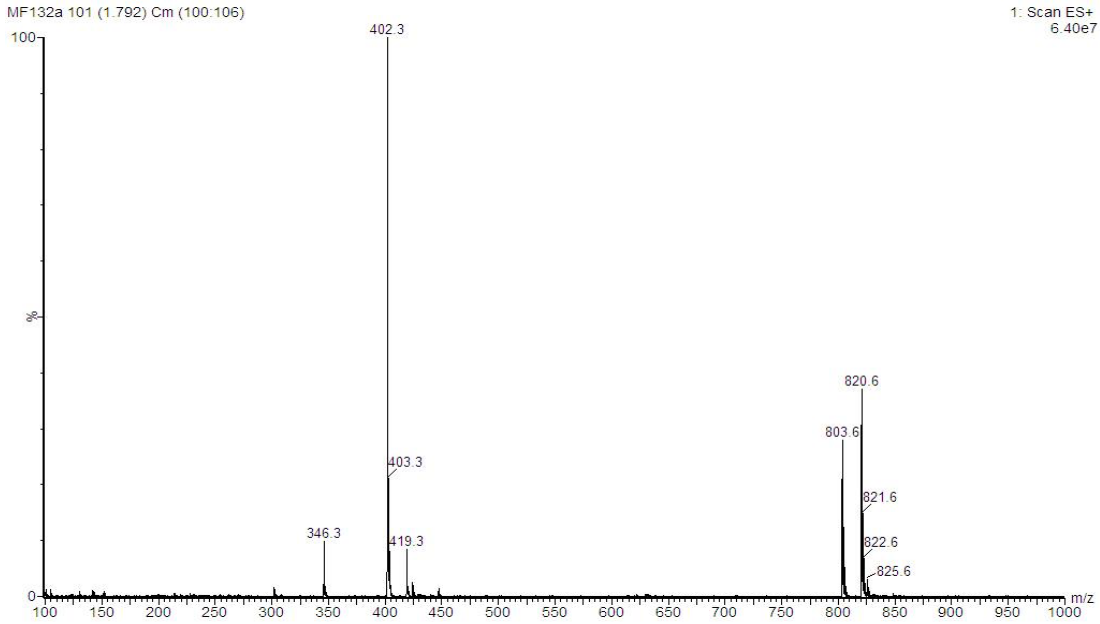

Figure **S37**. (a) TIC and UV trace at t = 0.05 h, (b) MS data at 0.42 mins in the UV and (c) MS data at 1.75 mins in the UV for PD **3** incubated with GSH **1** (10 eq.) at pH 6.5.

LC-MS data for t = 1 h

(a)

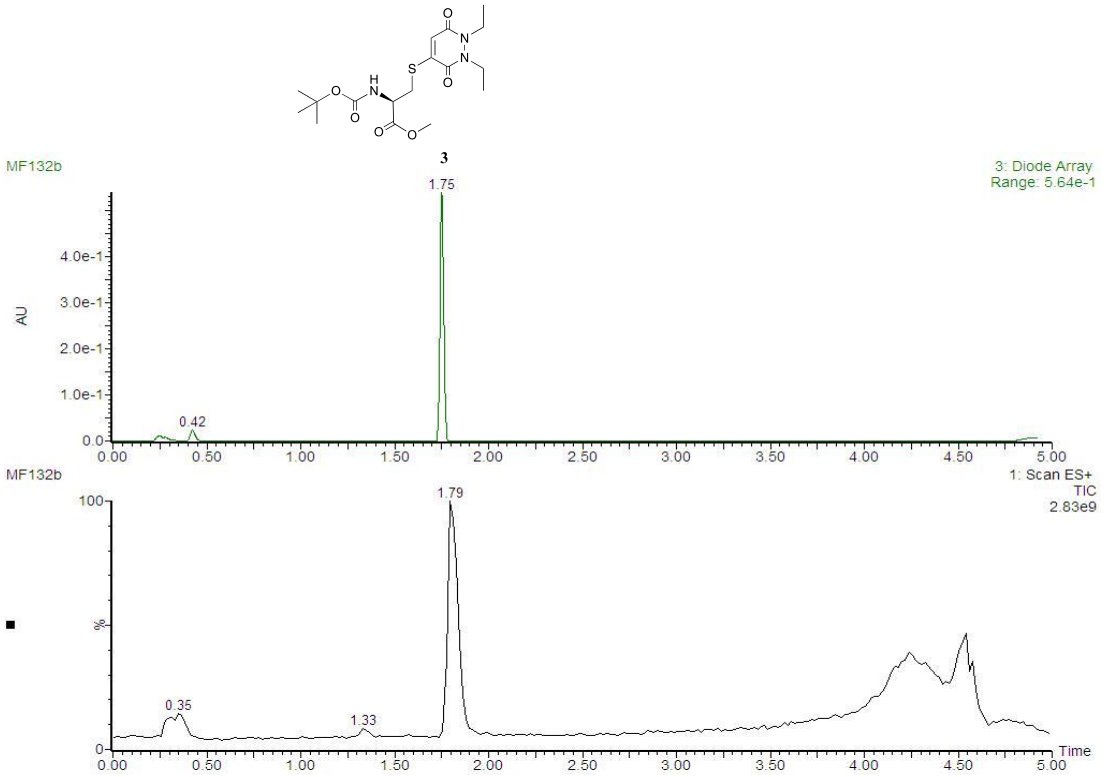
3
MF132b
3: Diode Array
Range: 5.64e-1
1.75
0.42
AU
MF132b
1: Scan ES+
TIC
2.83e9
1.79
0.35
1.33
%
Time

(b)

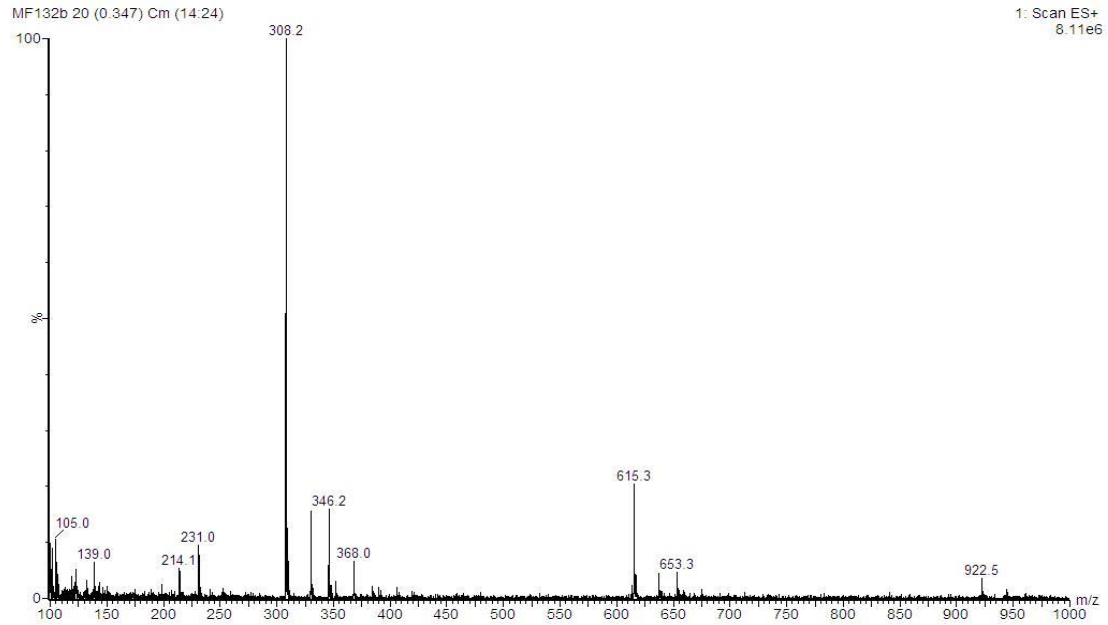
MF132b 20 (0.347) Cm (14:24)
1: Scan ES+
8.11e6
308.2
615.3
346.2
105.0
231.0
139.0
214.1
368.0
653.3
922.5
%
m/z

(c)

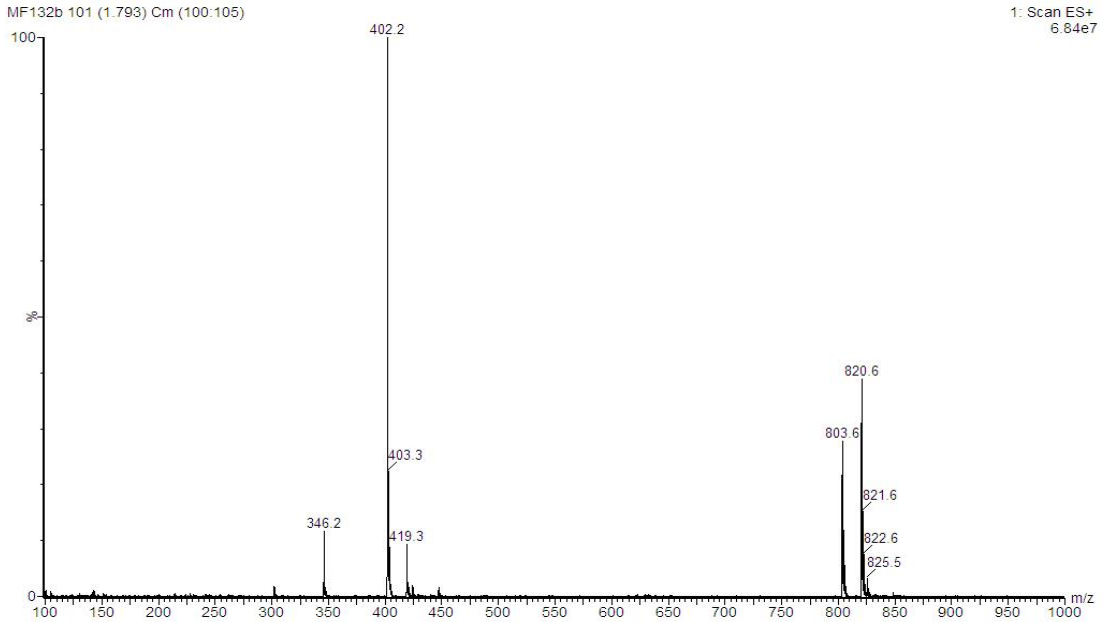

Figure **S38**. (a) TIC and UV trace at t = 1 h, (b) MS data at 0.42 mins in the UV and (c) MS data at 1.75 mins in the UV for PD **3** incubated with GSH **1** (10 eq.) at pH 6.5.

LC-MS data for t = 2 h

(a)

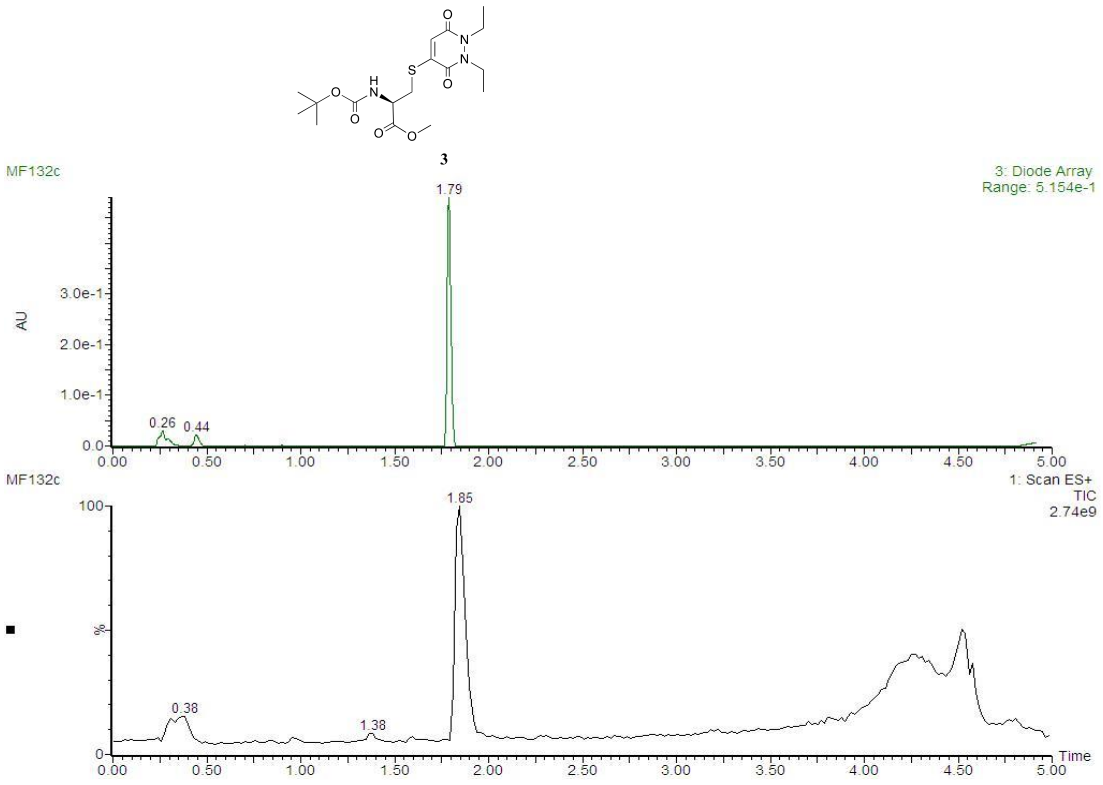

(b)

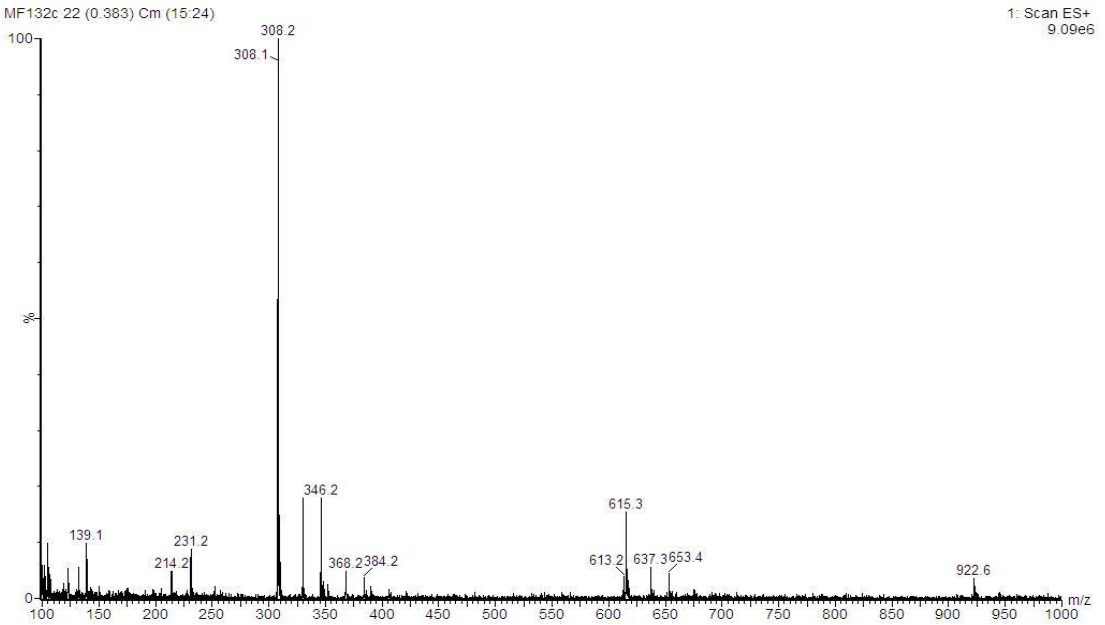

(c)

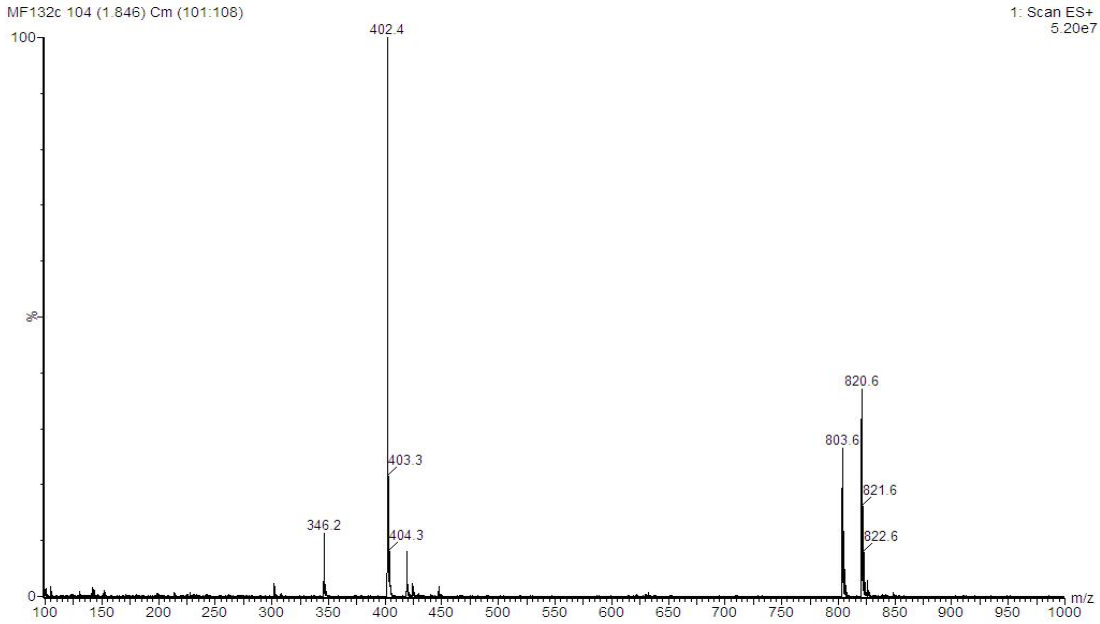

Figure **S39**. (a) TIC and UV trace at t = 2 h, (b) MS data at 0.26–0.44 mins in the UV and (c) MS data at 1.79 mins in the UV for PD **3** incubated with GSH **1** (10 eq.) at pH 6.5.

LC-MS data for t = 4 h

(a)

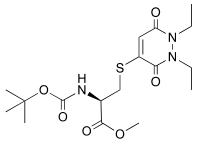

3

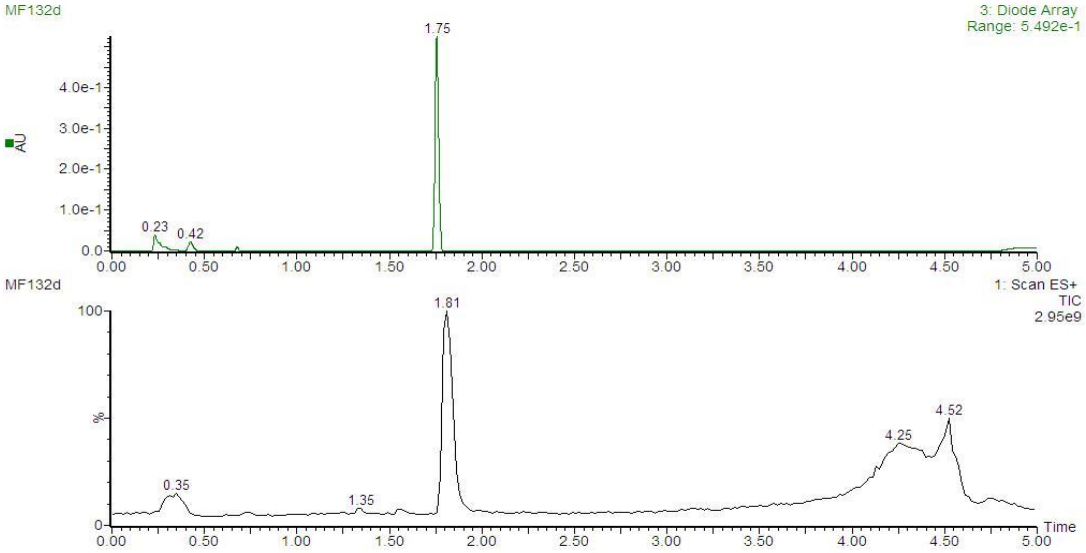
MF132d
3: Diode Array
Range: 5.492e-1
1.75
AU
0.23
0.42
MF132d
1: Scan ES+
TIC
2.95e9
1.81
%
4.52
4.25
0.35
1.35
Time

(b)

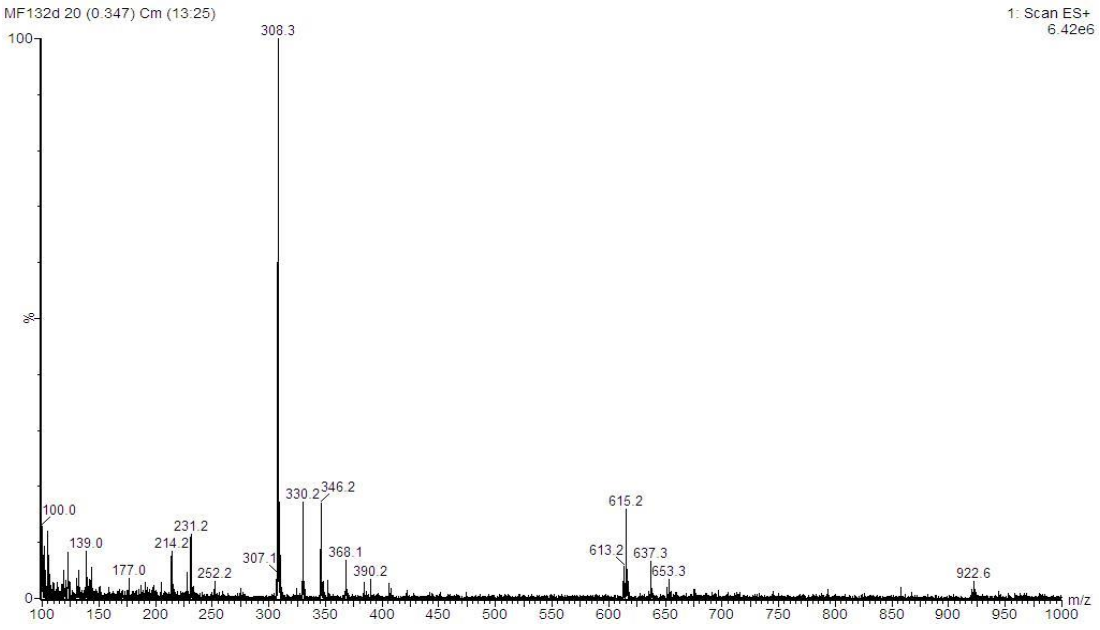
MF132d 20 (0.347) Cm (13:25)
1: Scan ES+
6.42e6
308.3
%
100.0
139.0
231.2
214.2
177.0
252.2
307.1
330.2
346.2
368.1
390.2
615.2
613.2
637.3
653.3
922.6
m/z

(c)

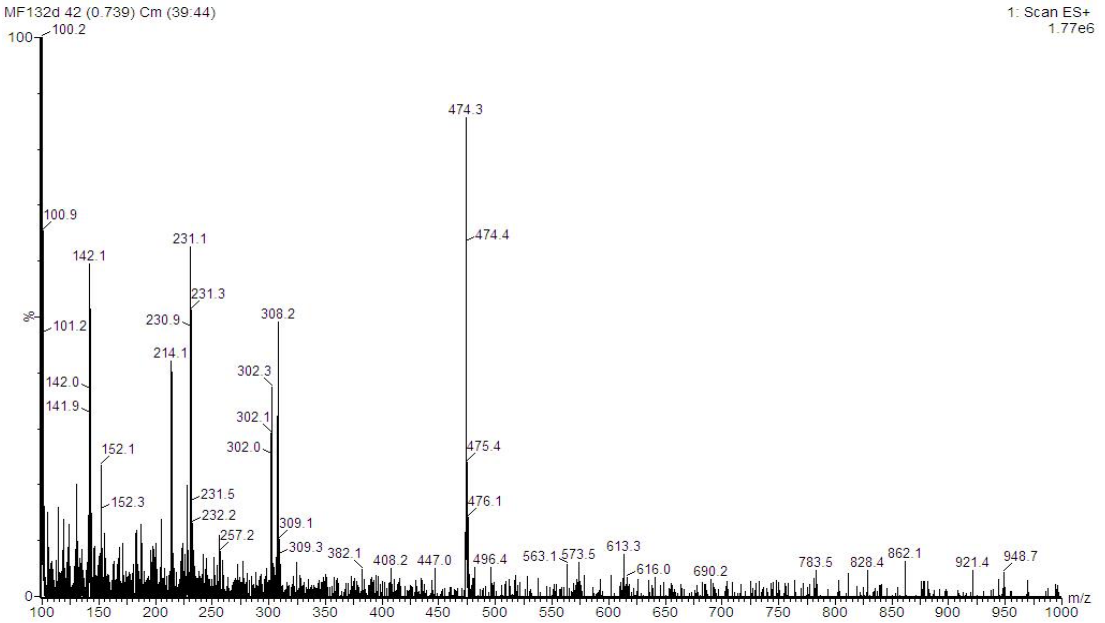

(d)

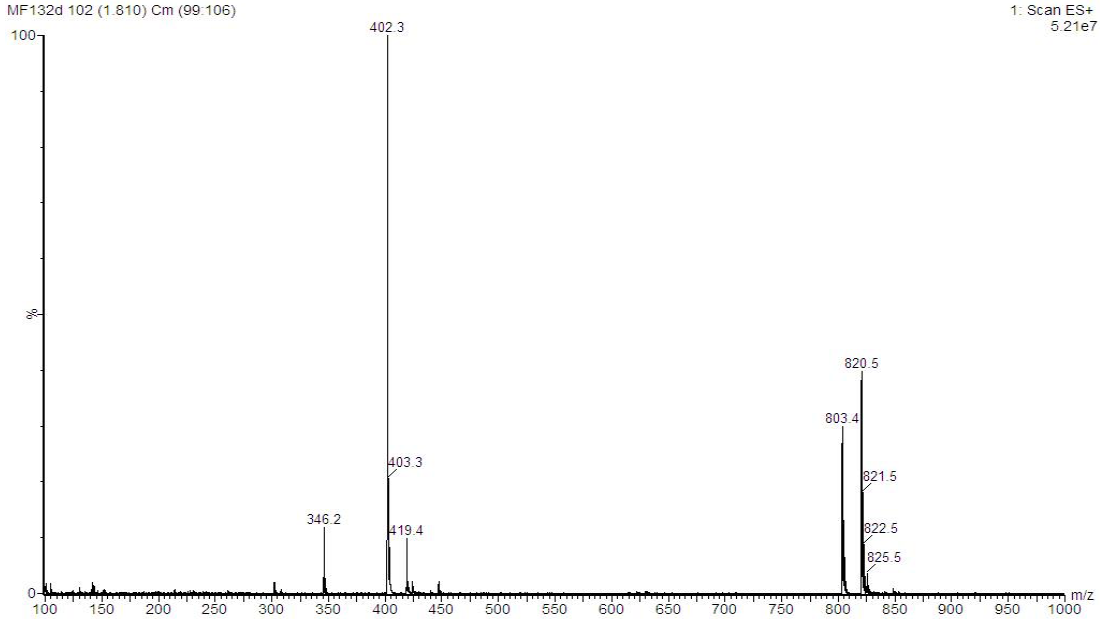

Figure **S40**. (a) TIC and UV trace at t = 4 h, (b) MS data at 0.26–0.42 mins in the UV, (c) MS data at 0.68 mins in the UV and (d) at 1.75 mins in the UV for PD **3** incubated with GSH **1** (10 eq.) at pH 6.5.

LC-MS data for t = 24 h

(a)

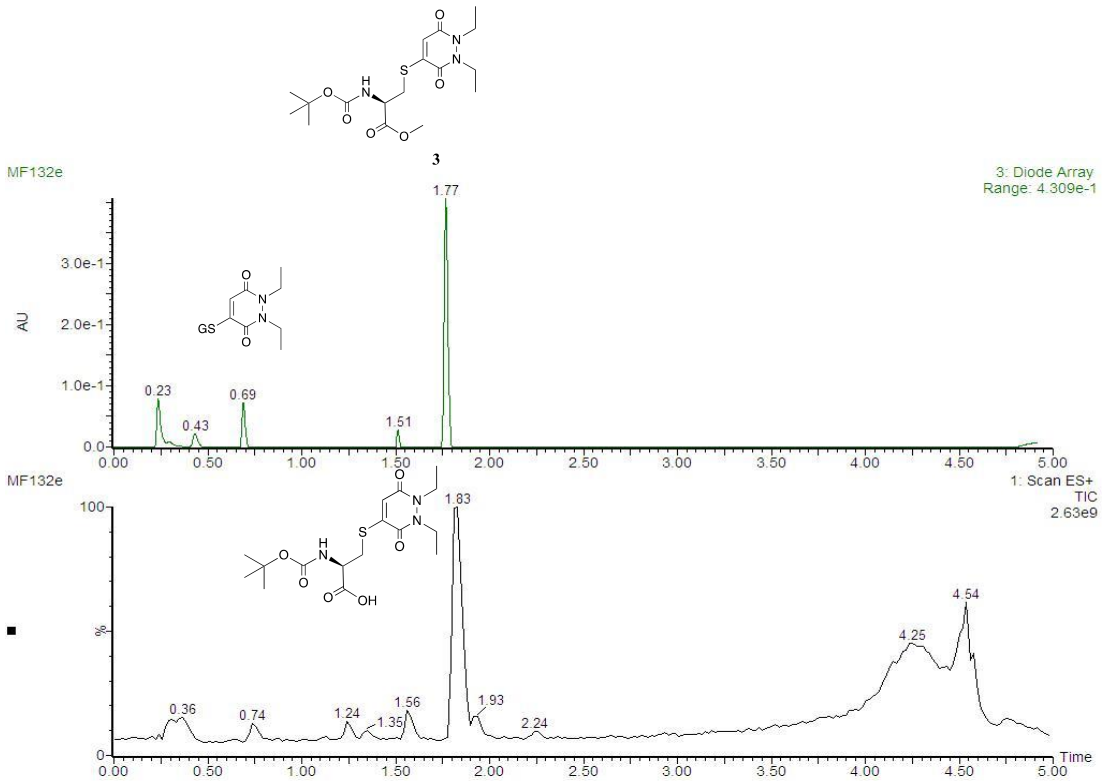
3
MF132e
3: Diode Array
Range: 4.309e-1
AU
GS
1.77
0.23
0.43
0.69
1.51
MF132e
1: Scan ES+
TIC
2.63e9
%
OH
1.83
4.54
4.25
0.36
0.74
1.24
1.35
1.56
1.93
2.24
Time

(b)

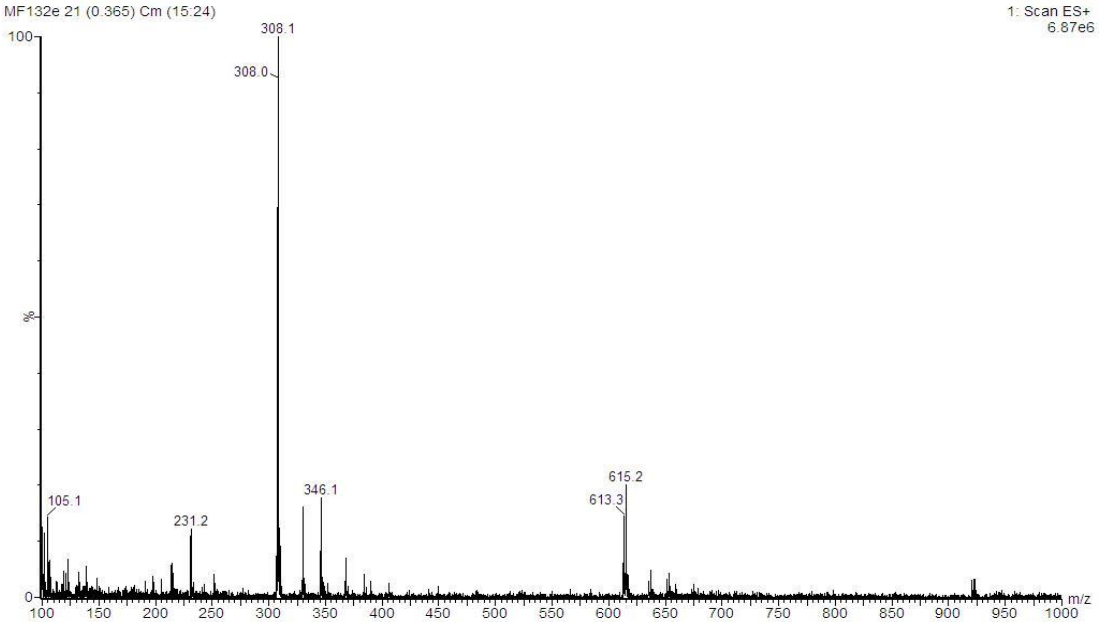
MF132e 21 (0.365) Cm (15:24)
1: Scan ES+
6.87e6
%
308.1
308.0
105.1
231.2
346.1
615.2
613.3
m/z

(c)

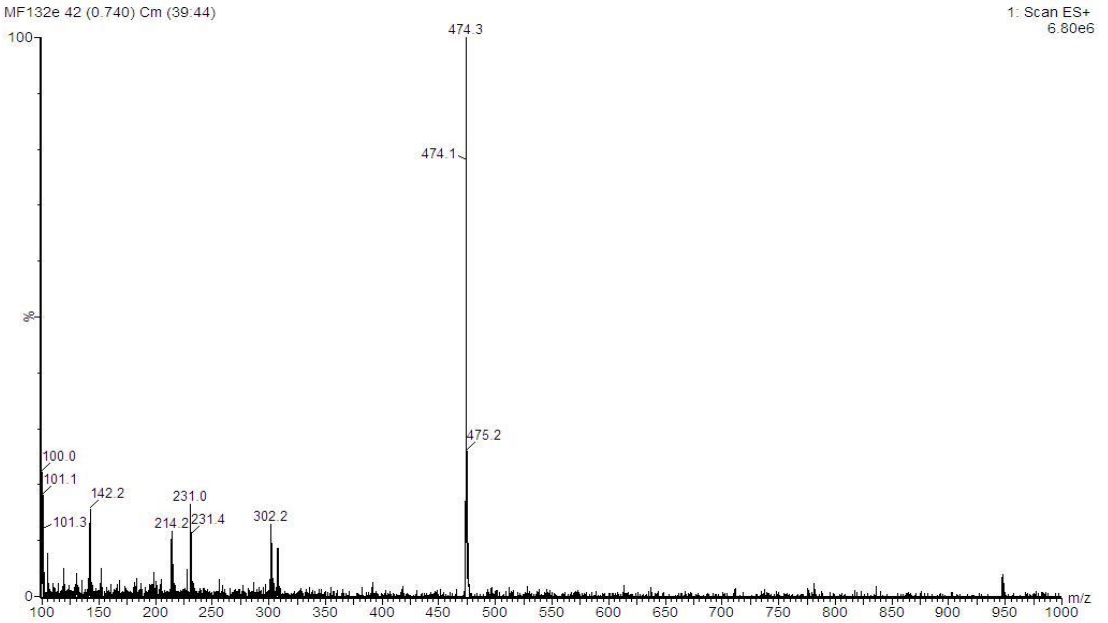
MF132e 42 (0.740) Cm (39:44)
1: Scan ES+
6.80e6
100
%
0
474.3
474.1
475.2
100.0
101.1
142.2
231.0
101.3
214.2
231.4
302.2
100
150
200
250
300
350
400
450
500
550
600
650
700
750
800
850
900
950
1000
m/z

(d)

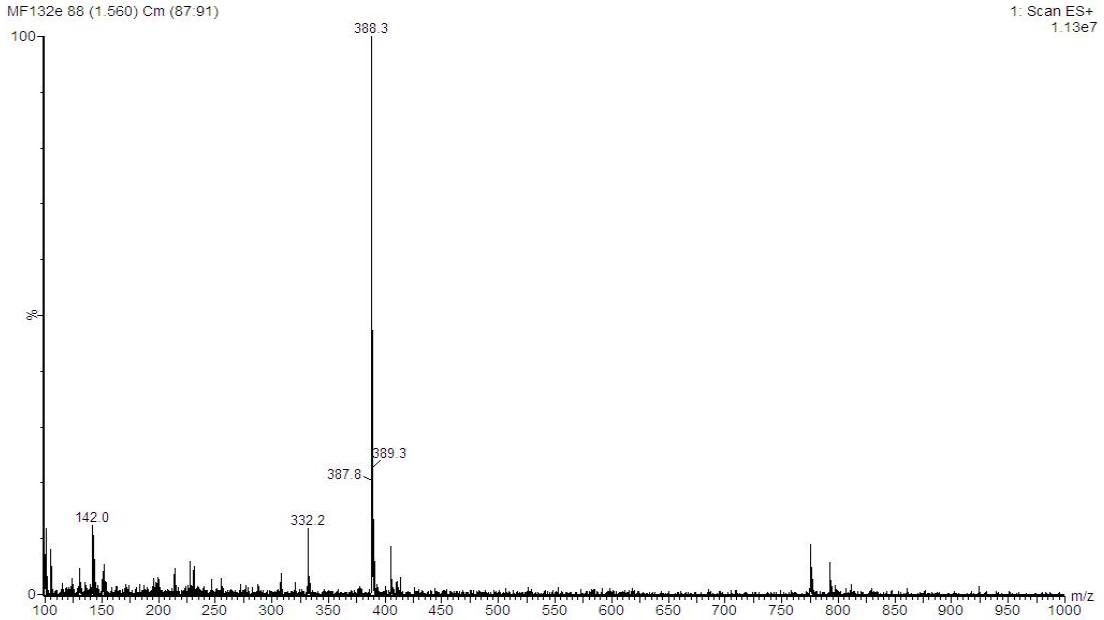
MF132e 88 (1.560) Cm (87:91)
1: Scan ES+
1.13e7
100
%
0
388.3
389.3
387.8
142.0
332.2
100
150
200
250
300
350
400
450
500
550
600
650
700
750
800
850
900
950
1000
m/z

(e)

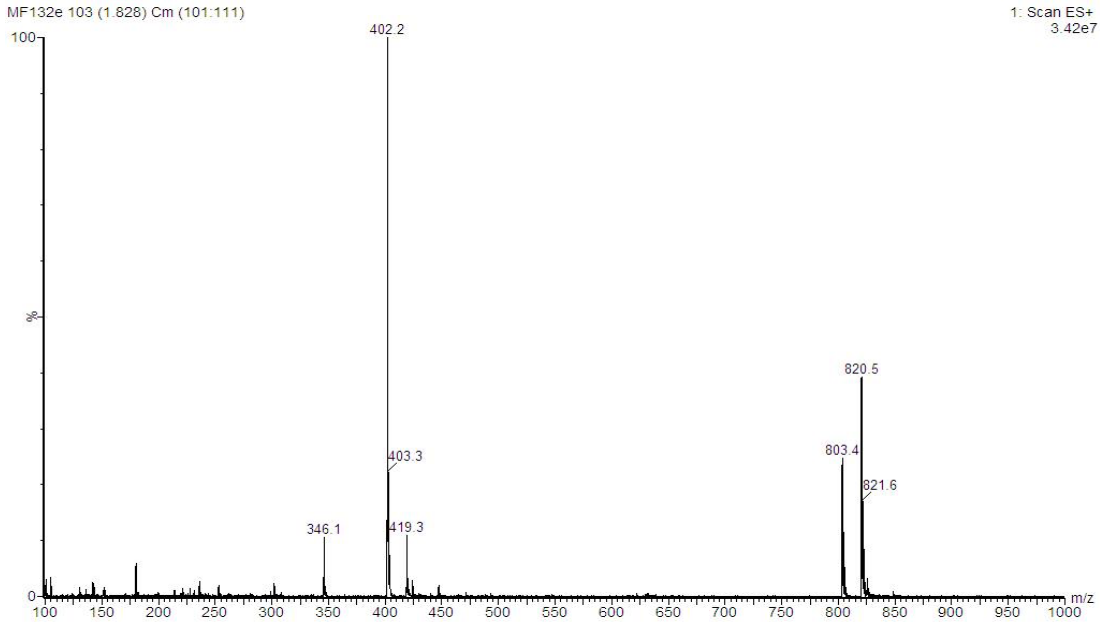

Figure **S41**. (a) TIC and UV trace at t = 24 h, (b) MS data at 0.26–0.43 mins in the UV, (c) MS data at 0.69 mins in the UV, (d) at 1.51 mins in the UV and (e) at 1.77 mins in the UV for PD **3** incubated with GSH **1** (10 eq.) at pH 6.5.

Incubation of PD 4 with GSH (10 eq.)

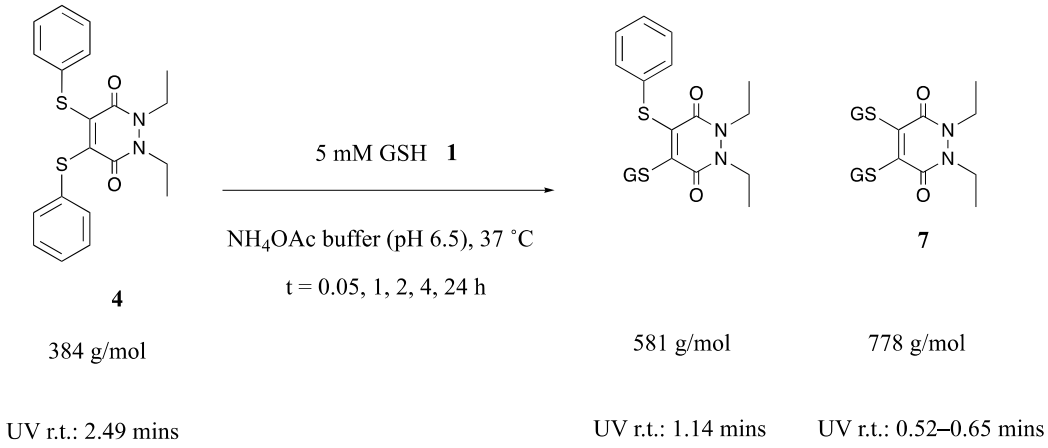

PD **4** (10 µL, 10 mM in MeCN, 1 eq.) was added to GSH **1** (190 µL, 5.3 mM, 10 eq.) in ammonium acetate buffer (50 mM, pH 6.5). The mixture was incubated at 37 ˚C for 24 h. The samples were analysed by LC-MS at t = 0.05, 1, 2, 4 and 24 h.

LC-MS data for t = 0.05 h

(a)

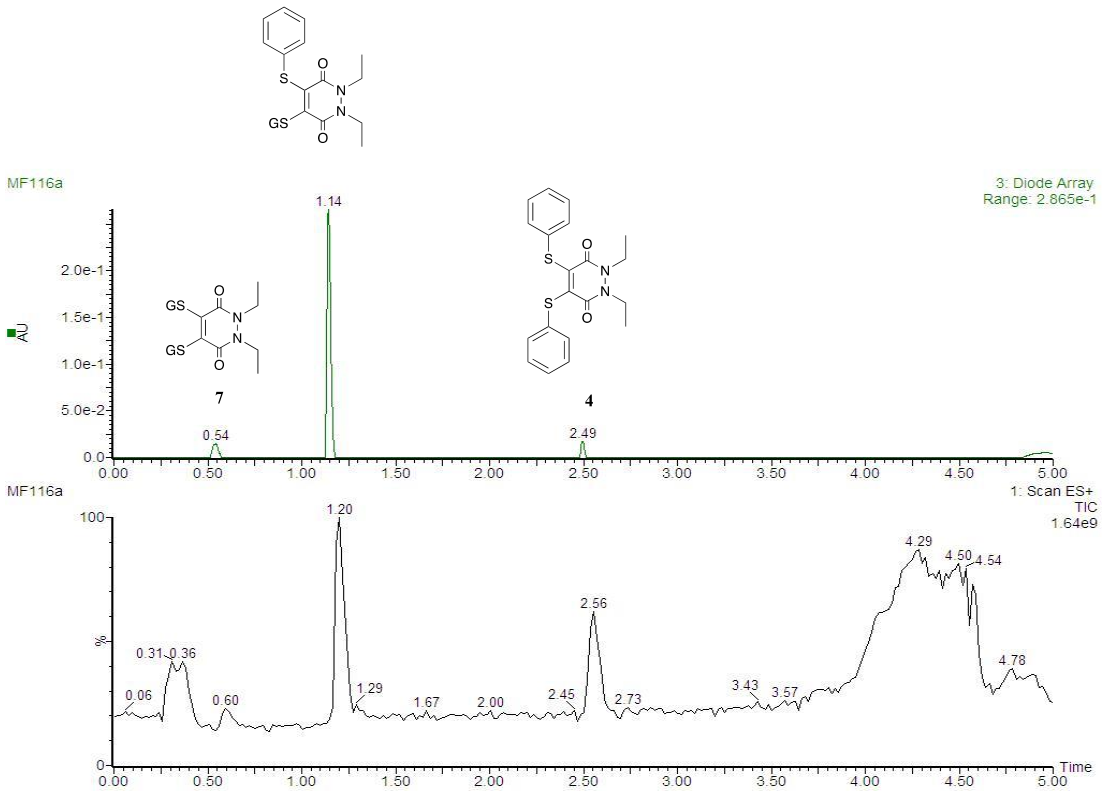

(b)

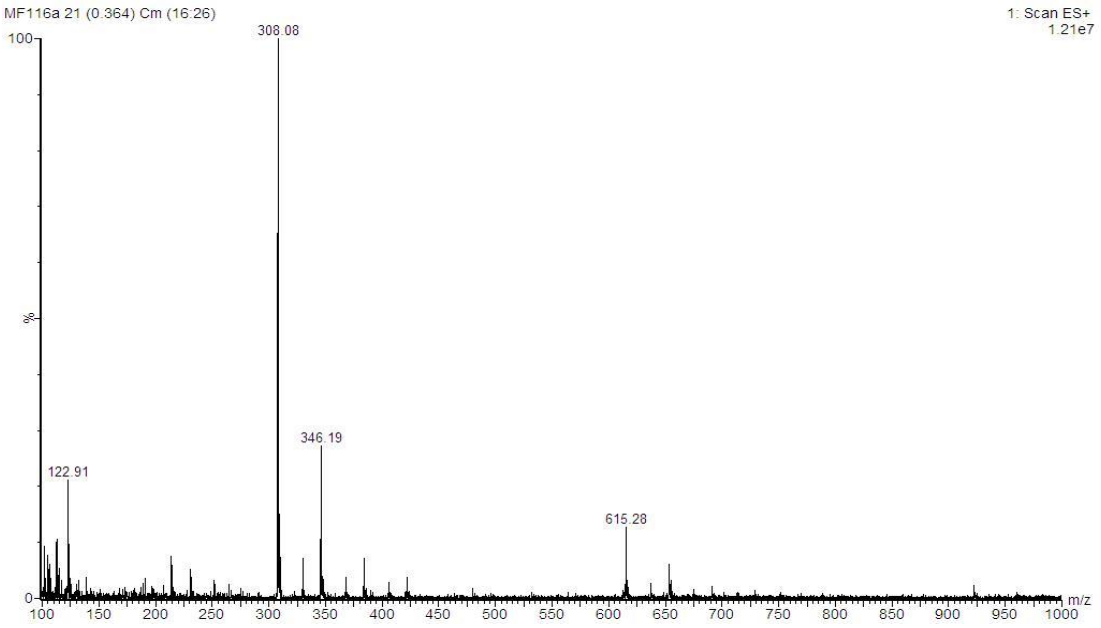
MF116a 21 (0.364) Cm (16:26)
1: Scan ES+
1.21e7
100
%
0
308.08
346.19
122.91
615.28
100 150 200 250 300 350 400 450 500 550 600 650 700 750 800 850 900 950 1000
m/z

(c)

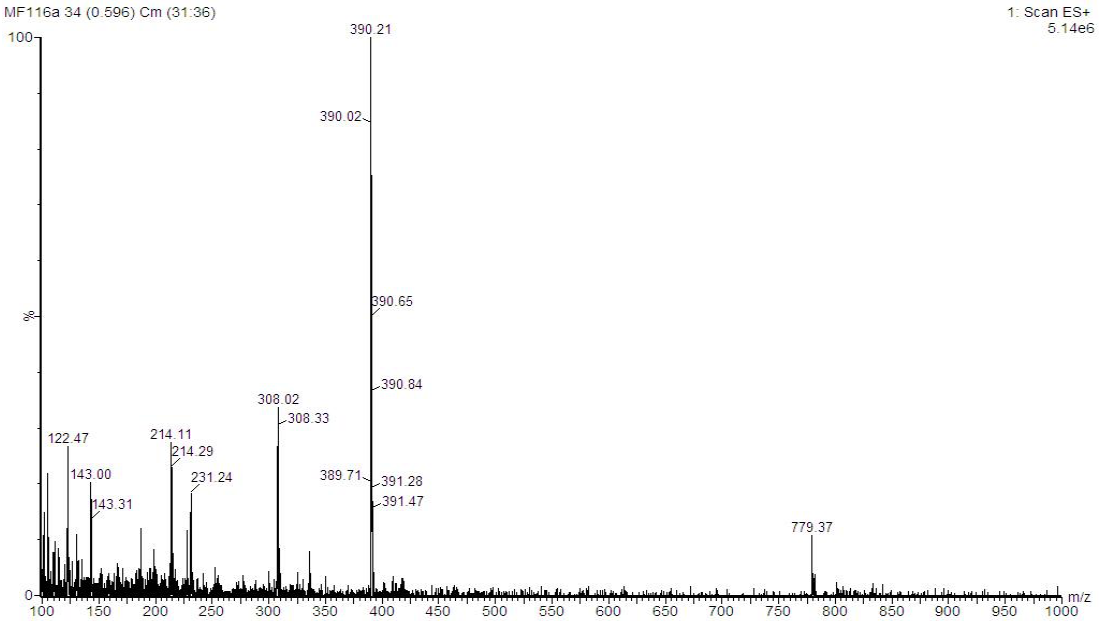
MF116a 34 (0.596) Cm (31:36)
1: Scan ES+
5.14e6
100
%
0
390.21
390.02
390.65
390.84
308.02
308.33
122.47
214.11
214.29
143.00
231.24
143.31
389.71
391.28
391.47
779.37
100 150 200 250 300 350 400 450 500 550 600 650 700 750 800 850 900 950 1000
m/z

(d)

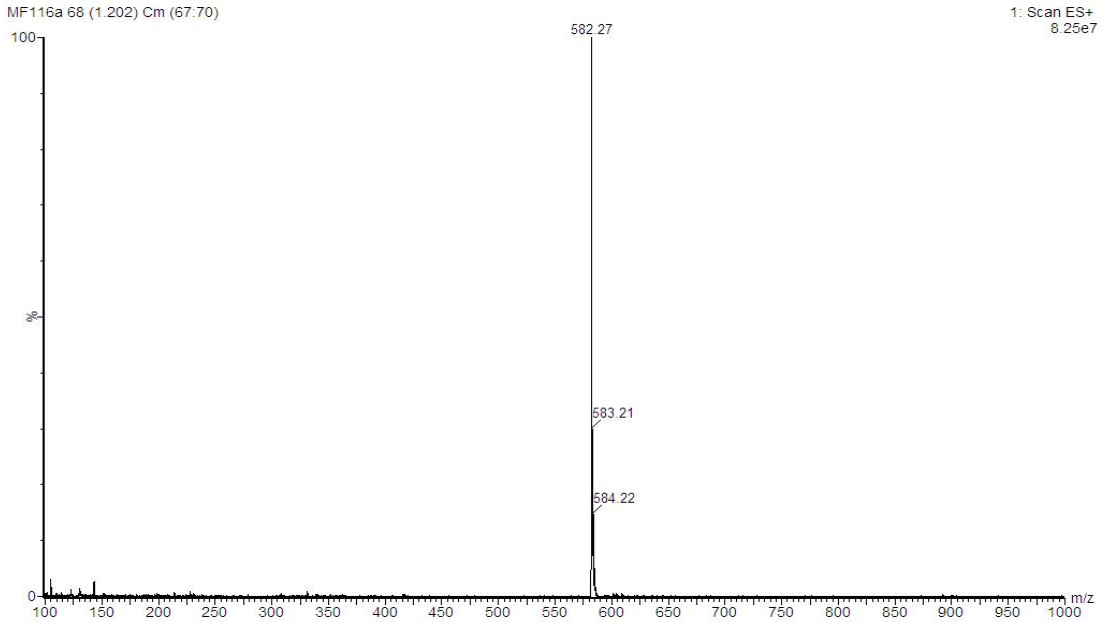

(e)

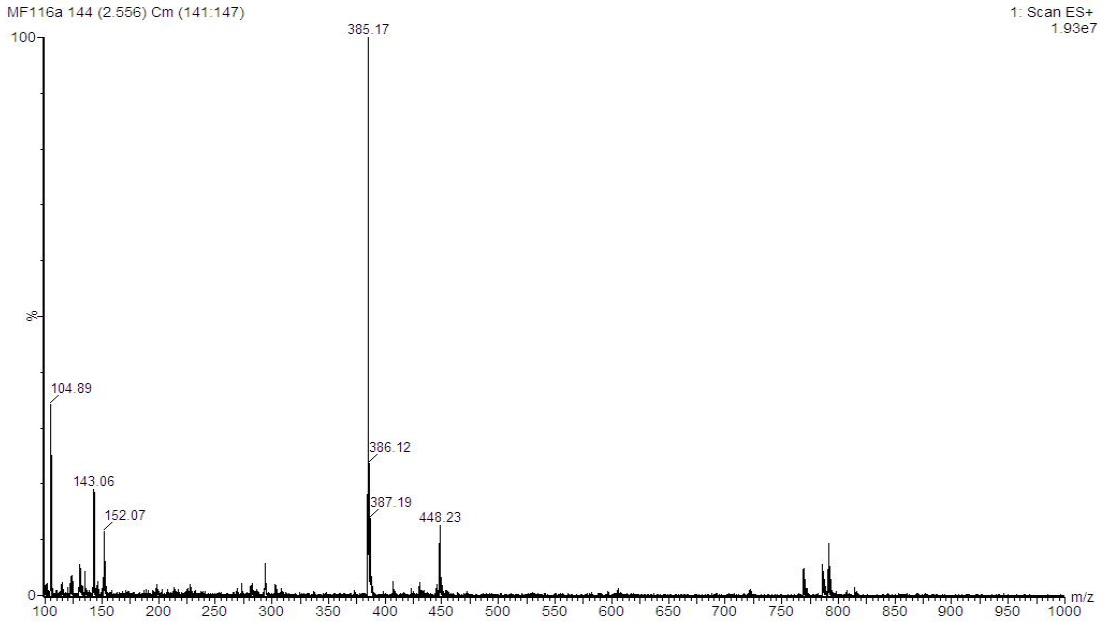

Figure **S42**. (a) TIC and UV trace at t = 0.05 h, (b) MS data at 0.36 mins in the TIC, (c) MS data at 0.54 mins in the UV, (d) at 1.14 mins in the UV and (e) at 2.49 mins in the UV for PD **4** incubated with GSH **1** (10 eq.) at pH 6.5.

LC-MS data for t = 1 h

(a)

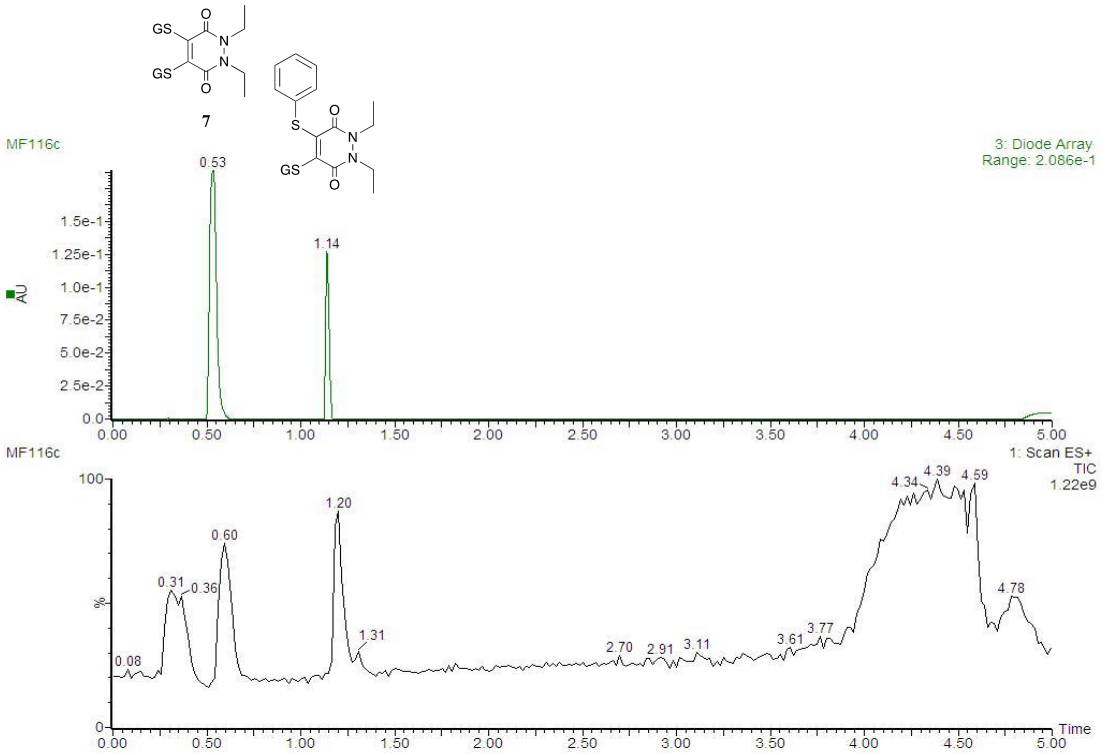
GS
GS
O
N
O
7
S
GS
MF116c
3: Diode Array
Range: 2.086e-1
0.53
1.14
AU
1.5e-1
1.25e-1
1.0e-1
7.5e-2
5.0e-2
2.5e-2
0.0
0.00
0.50
1.00
1.50
2.00
2.50
3.00
3.50
4.00
4.50
5.00
MF116c
1: Scan ES+
TIC
1.22e9
100
%
0
0.08
0.31
0.36
0.60
1.20
1.31
2.70
2.91
3.11
3.61
3.77
4.34
4.39
4.59
4.78
Time

(b)

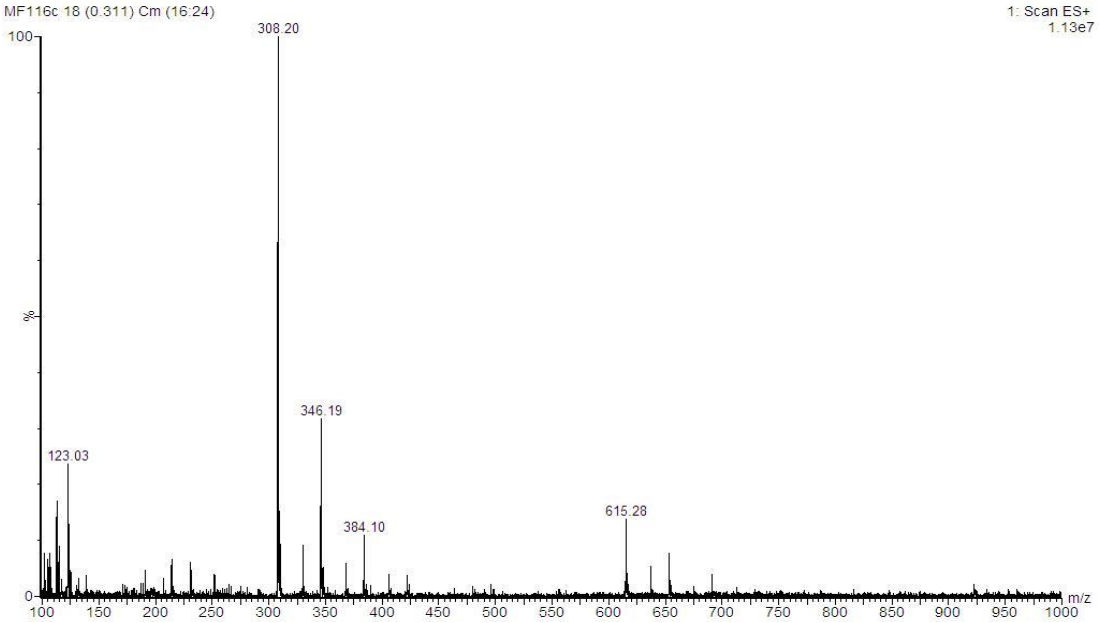
MF116c 18 (0.311) Cm (16:24)
1: Scan ES+
1.13e7
100
%
0
308.20
346.19
123.03
384.10
615.28
100
150
200
250
300
350
400
450
500
550
600
650
700
750
800
850
900
950
1000
m/z

(c)

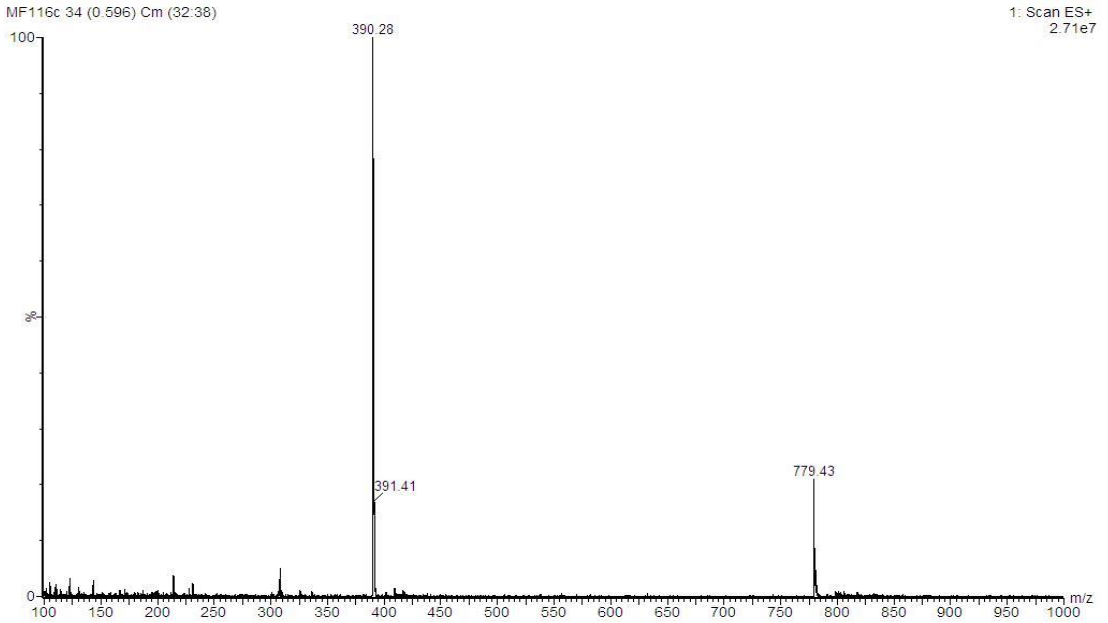

(d)

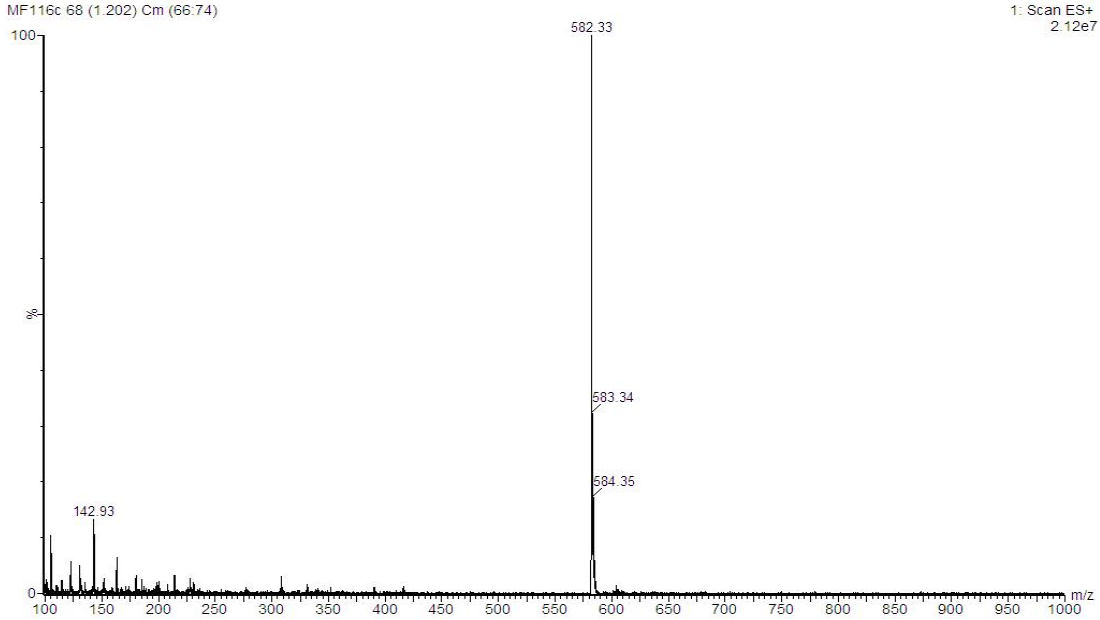

Figure **S43**. (a) TIC and UV trace at t = 1 h, (b) MS data at 0.36 mins in the TIC, (c) MS data at 0.53 mins in the UV and (d) at 1.14 mins in the UV for PD **4** incubated with GSH **1** (10 eq.) at pH 6.5.

LC-MS data for t = 2 h

(a)

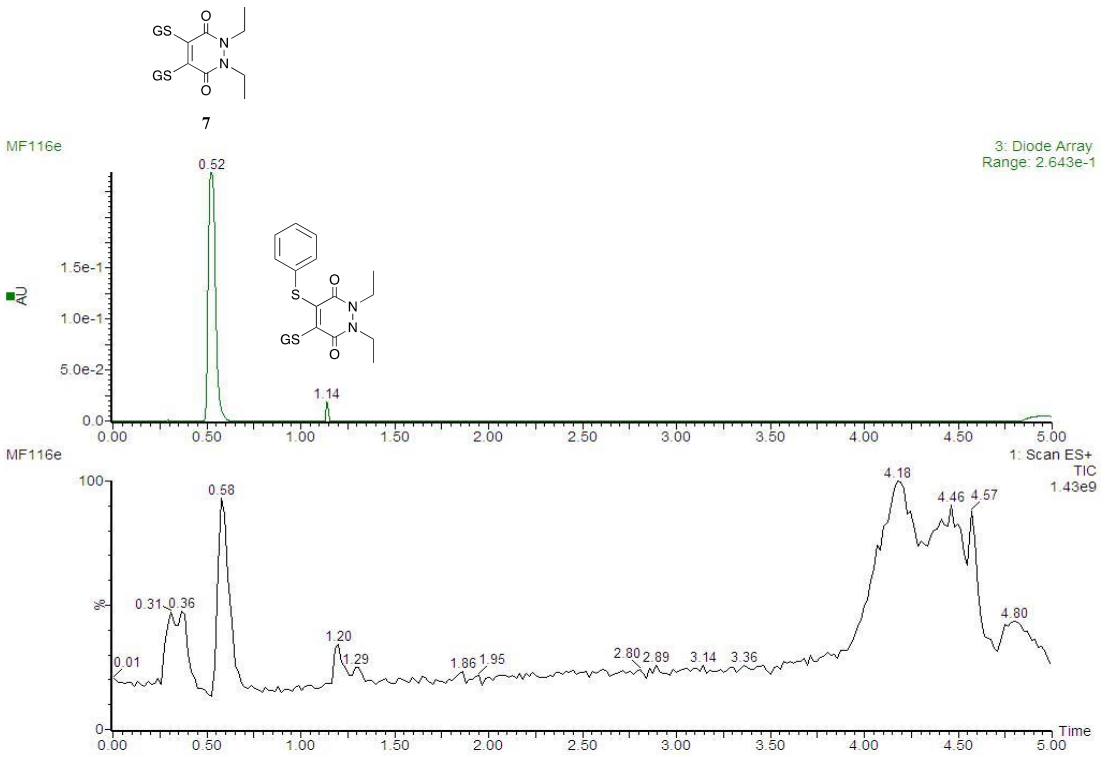
GS
GS
O
N
N
O
7
MF116e
3: Diode Array
Range: 2.643e-1
0.52
1.14
AU
1.5e-1
1.0e-1
5.0e-2
0.0
0.00
0.50
1.00
1.50
2.00
2.50
3.00
3.50
4.00
4.50
5.00
MF116e
1: Scan ES+
TIC
1.43e9
100
%
0
0.01
0.31
0.36
0.58
1.20
1.29
1.86
1.95
2.80
2.89
3.14
3.36
4.18
4.46
4.57
4.80
Time

(b)

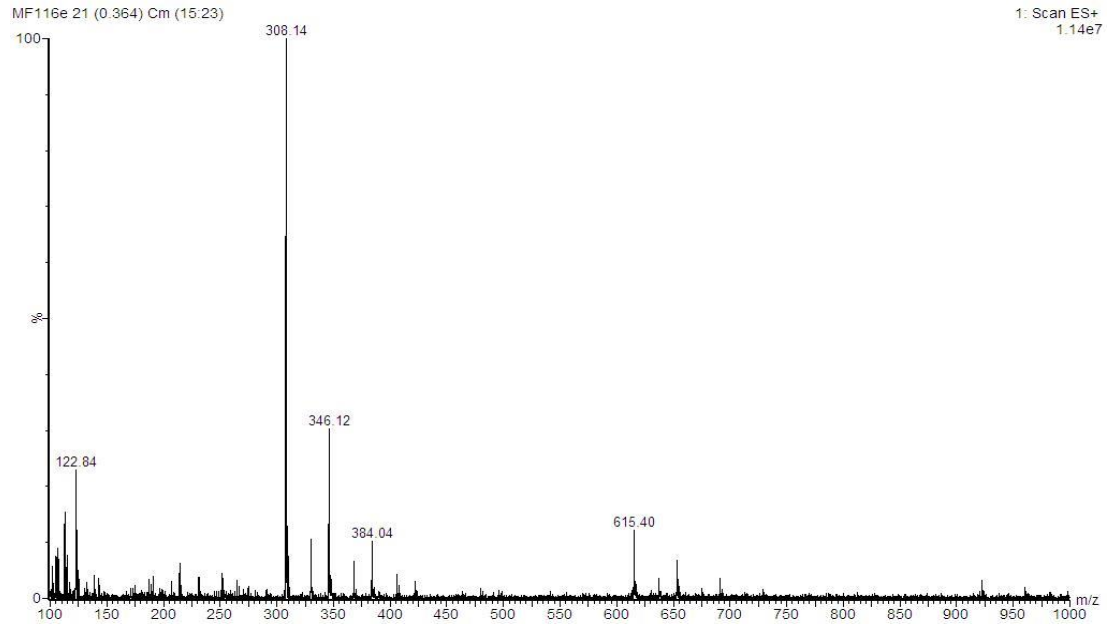
MF116e 21 (0.364) Cm (15:23)
1: Scan ES+
1.14e7
100
%
0
308.14
346.12
122.84
384.04
615.40
100
150
200
250
300
350
400
450
500
550
600
650
700
750
800
850
900
950
1000
m/z

(c)

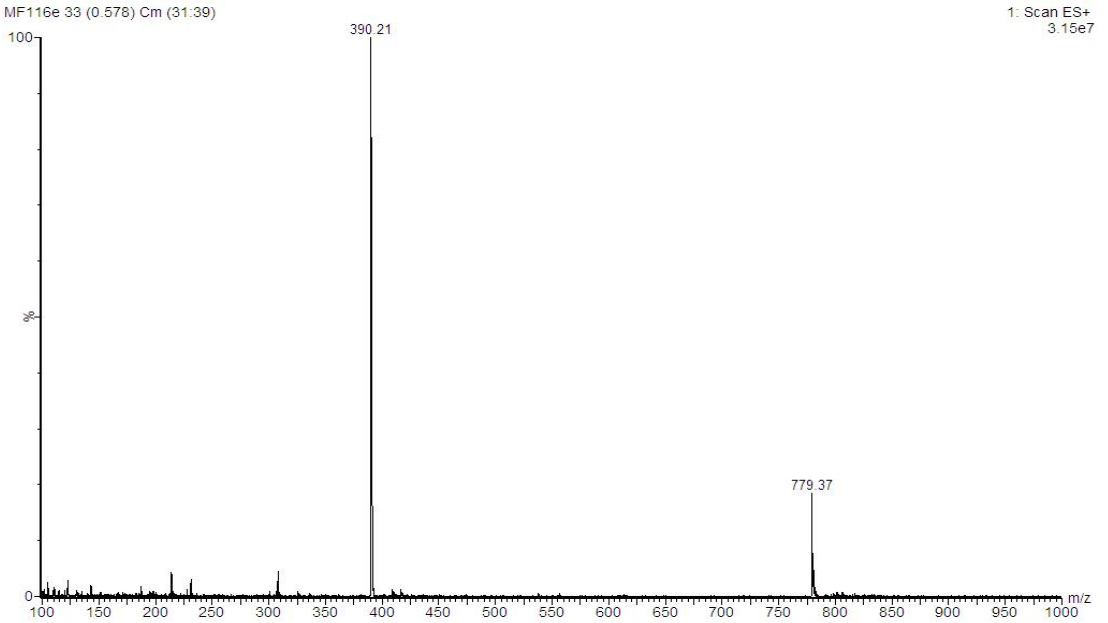

(d)

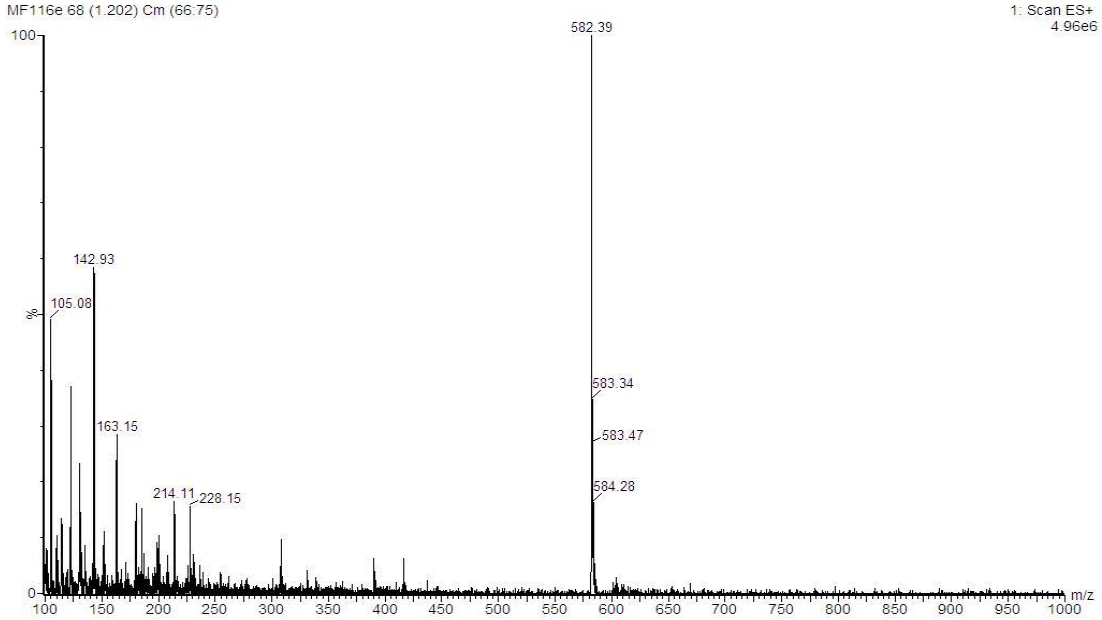

Figure **S44**. (a) TIC and UV trace at t = 2 h, (b) MS data at 0.36 mins in the TIC, (c) MS data at 0.52 mins in the UV and (d) at 1.14 mins in the UV for PD **4** incubated with GSH **1** (10 eq.) at pH 6.5.

LC-MS data for t = 4 h

(a)

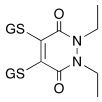
GS
GS
O
N
N
O

7

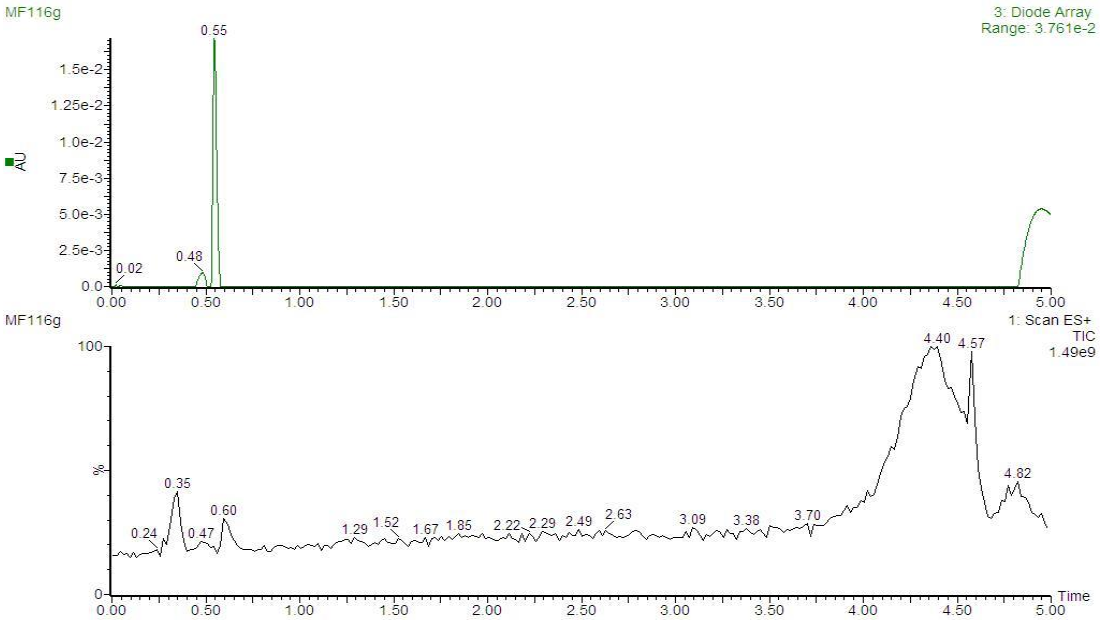
MF116g
3: Diode Array
Range: 3.761e-2
AU
0.55
0.48
0.02
MF116g
1: Scan ES+
TIC
1.49e9
%
4.40
4.57
4.82
0.35
0.60
0.24
0.47
1.29
1.52
1.67
1.85
2.22
2.29
2.49
2.63
3.09
3.38
3.70
Time

(b)

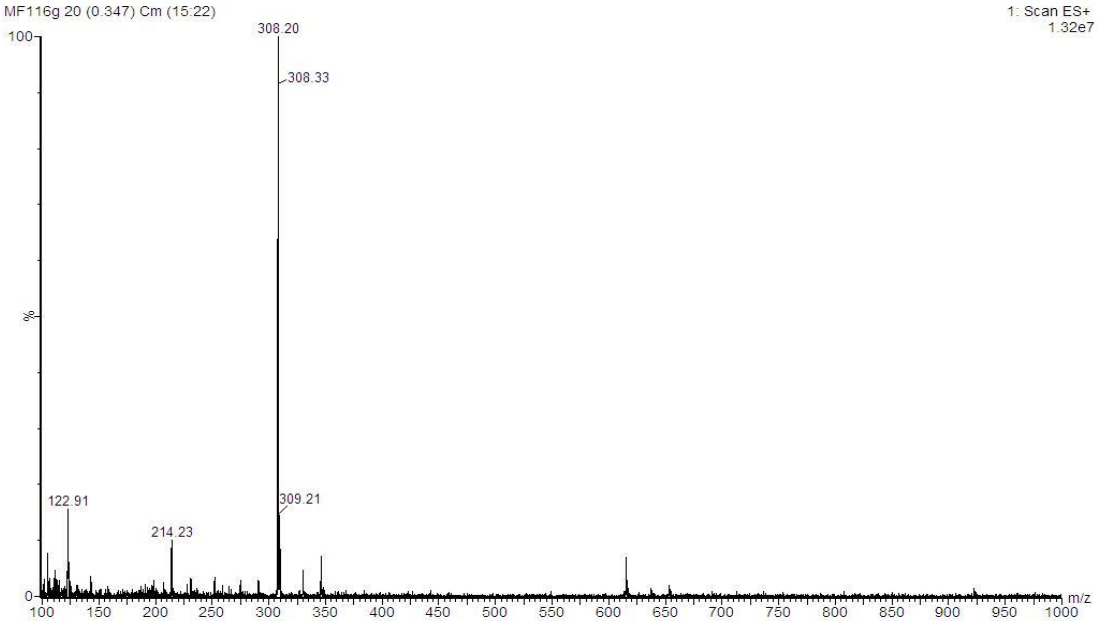
MF116g 20 (0.347) Cm (15:22)
1: Scan ES+
1.32e7
308.20
308.33
%
122.91
214.23
309.21
m/z

(c)

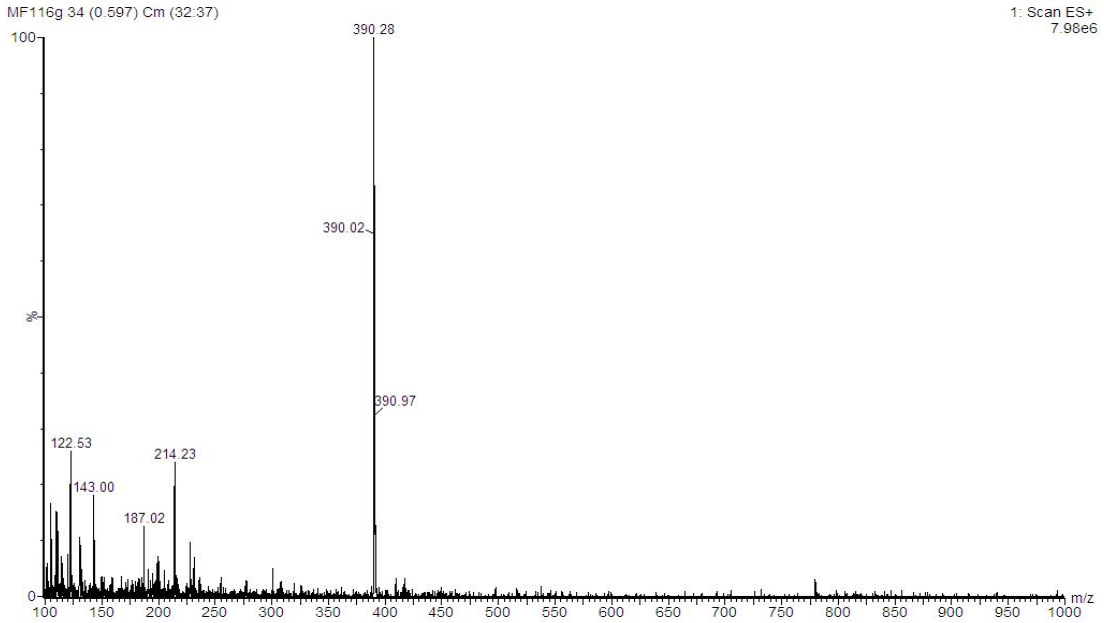

Figure **S45**. (a) TIC and UV trace at t = 4 h, (b) MS data at 0.35 mins in the TIC and (c) MS data at 0.55 mins in the UV for PD **4** incubated with GSH **1** (10 eq.) at pH 6.5.

LC-MS data for t = 24 h

(a)

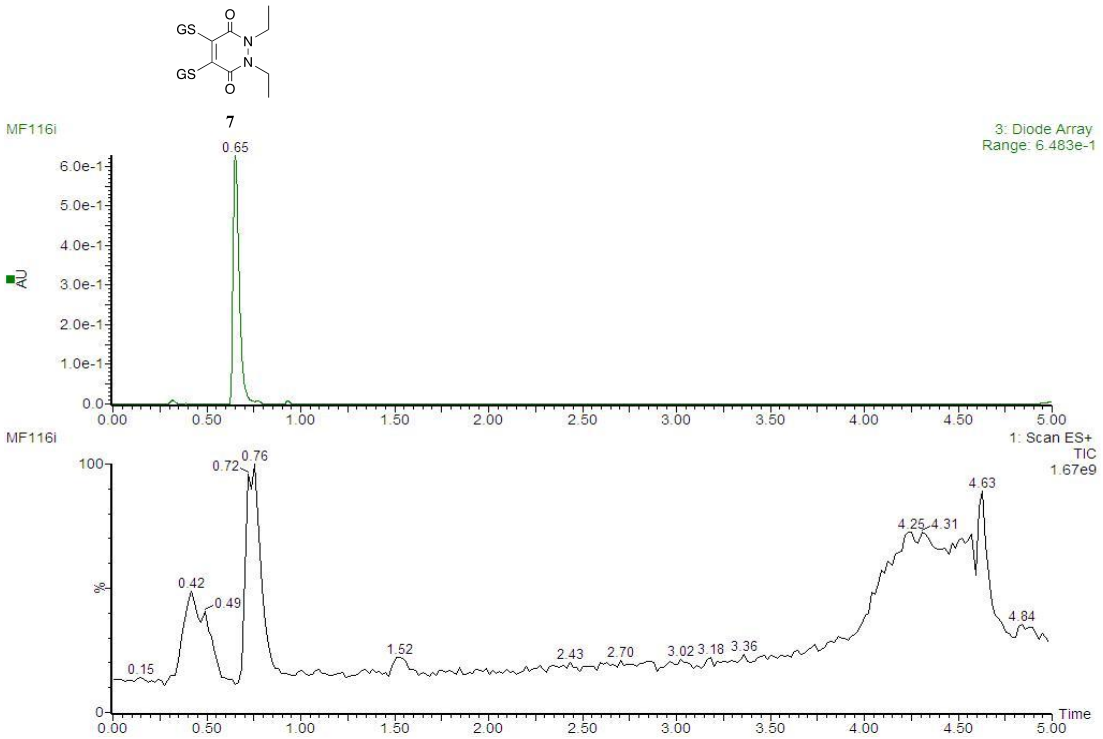

(b)

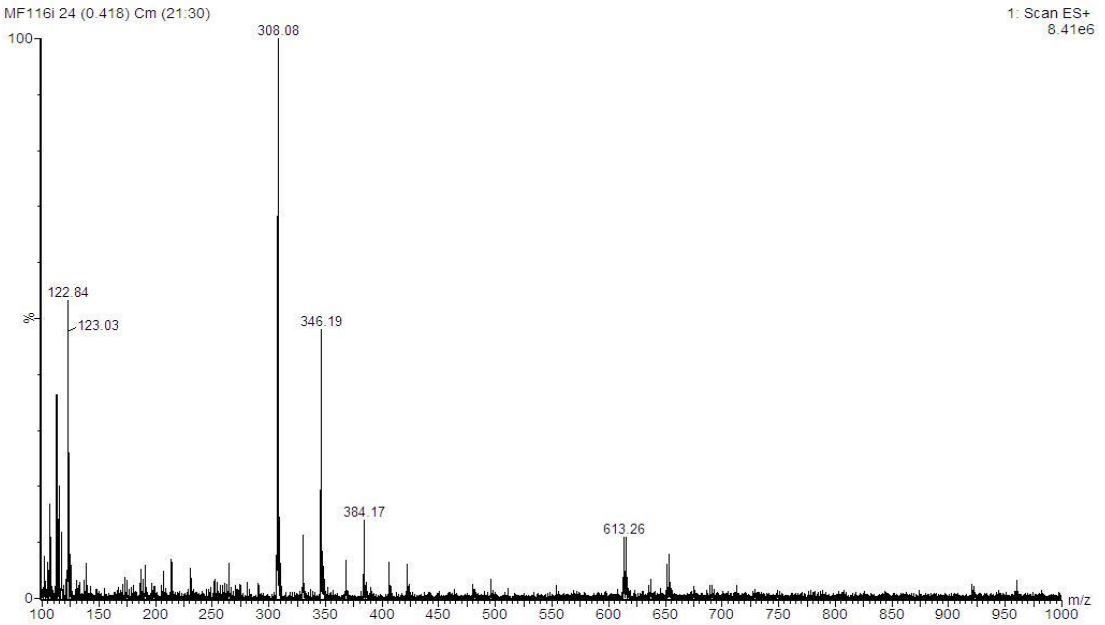

(c)

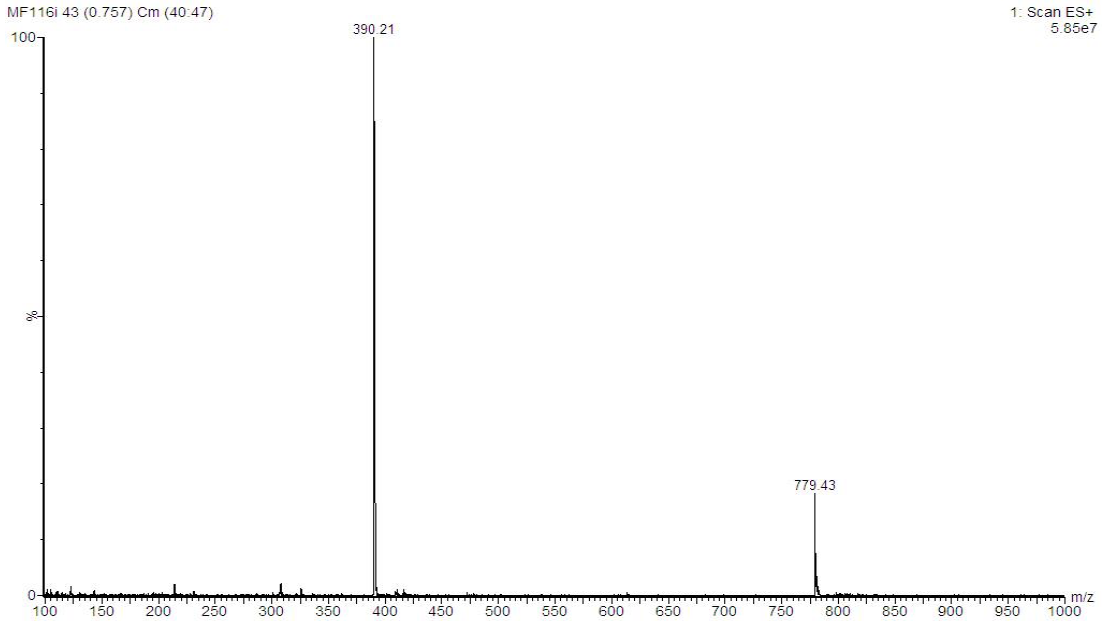

Figure **S46**. (a) TIC and UV trace at t = 24 h, (b) MS data at 0.42 mins in the TIC and (c) MS data at 0.65 mins in the UV for PD **4** incubated with GSH **1** (10 eq.) at pH 6.5.

Incubation of PD 5 with GSH (10 eq.)

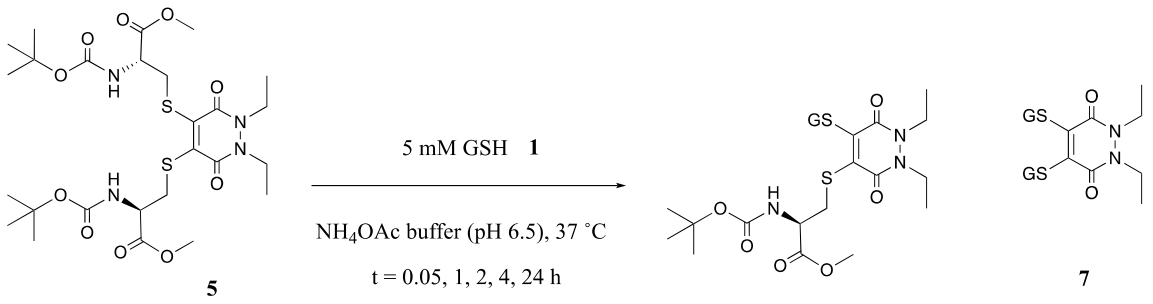

UV r.t.: 2.52, 2.53 mins

UV r.t.: 1.34, 1.35 mins

UV r.t.: 0.58, 0.59 mins

PD **5** (10 µL, 10 mM in MeCN, 1 eq.) was added to GSH **1** (190 µL, 5.3 mM, 10 eq.) in ammonium acetate buffer (50 mM, pH 6.5). The mixture was incubated at 37 ˚C for 24 h. The samples were analysed by LC-MS at t = 0.05, 1, 2, 4 and 24 h.

LC-MS data for t = 0.05 h

(a)

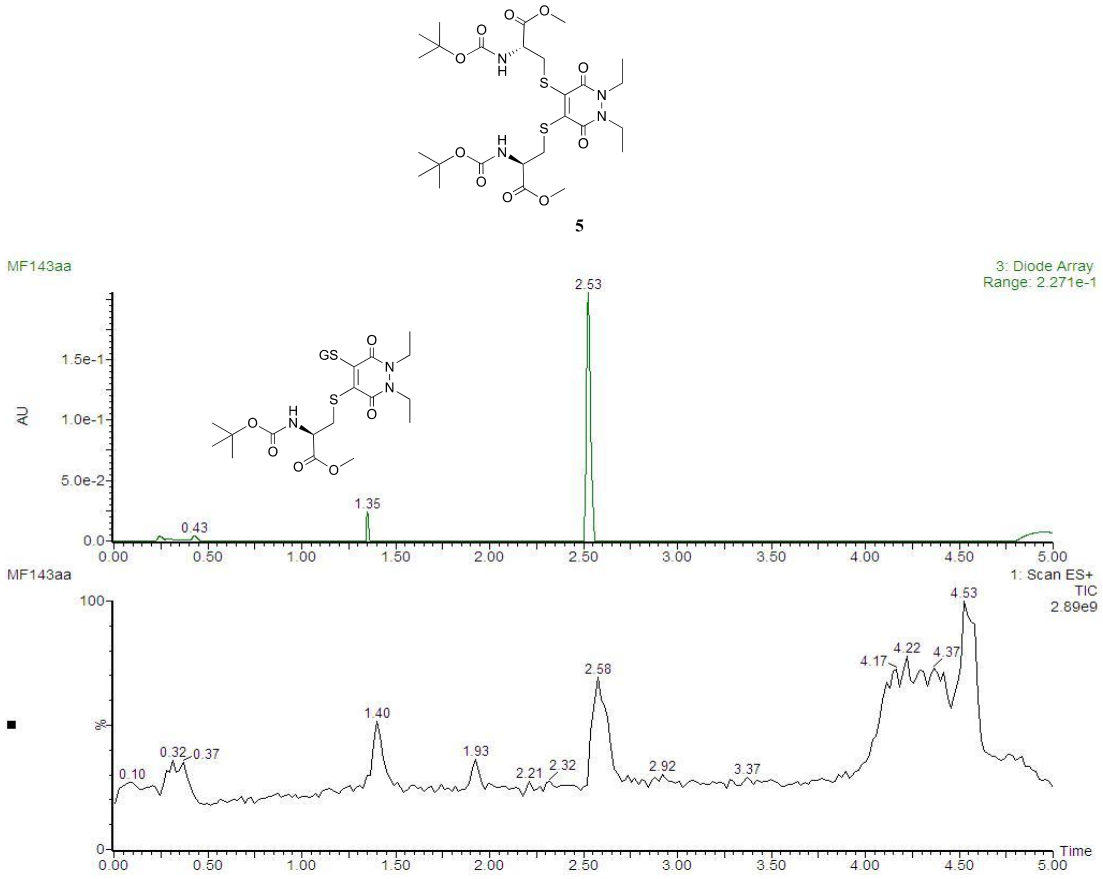

(b)

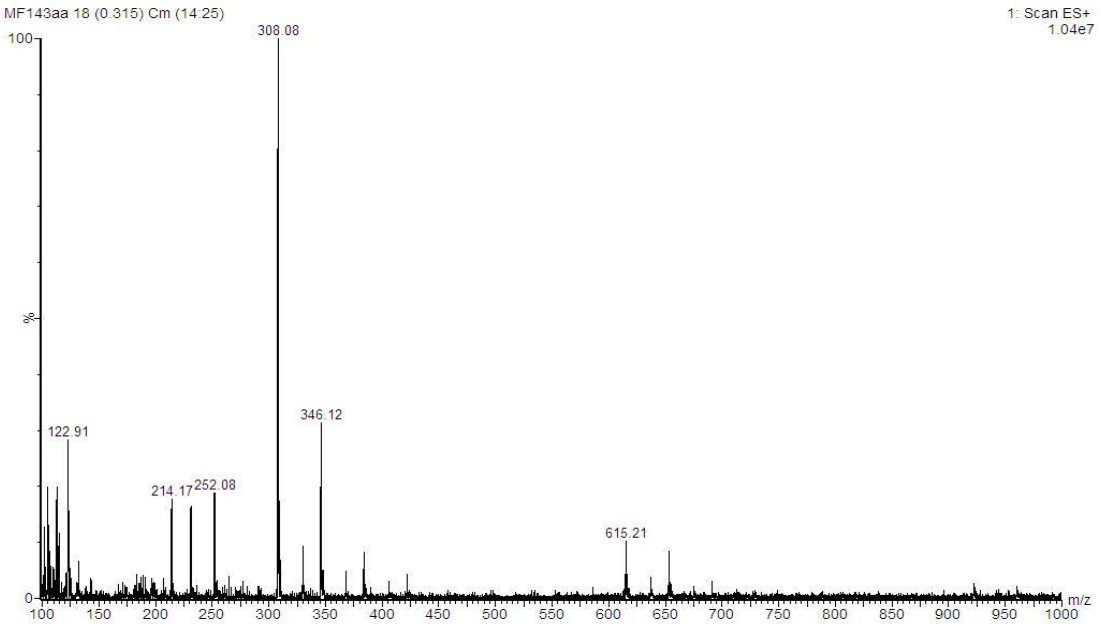
MF143aa 18 (0.315) Cm (14:25)
1: Scan ES+
1.04e7
100
%
0
308.08
346.12
122.91
214.17
252.08
615.21
100 150 200 250 300 350 400 450 500 550 600 650 700 750 800 850 900 950 1000
m/z

(c)

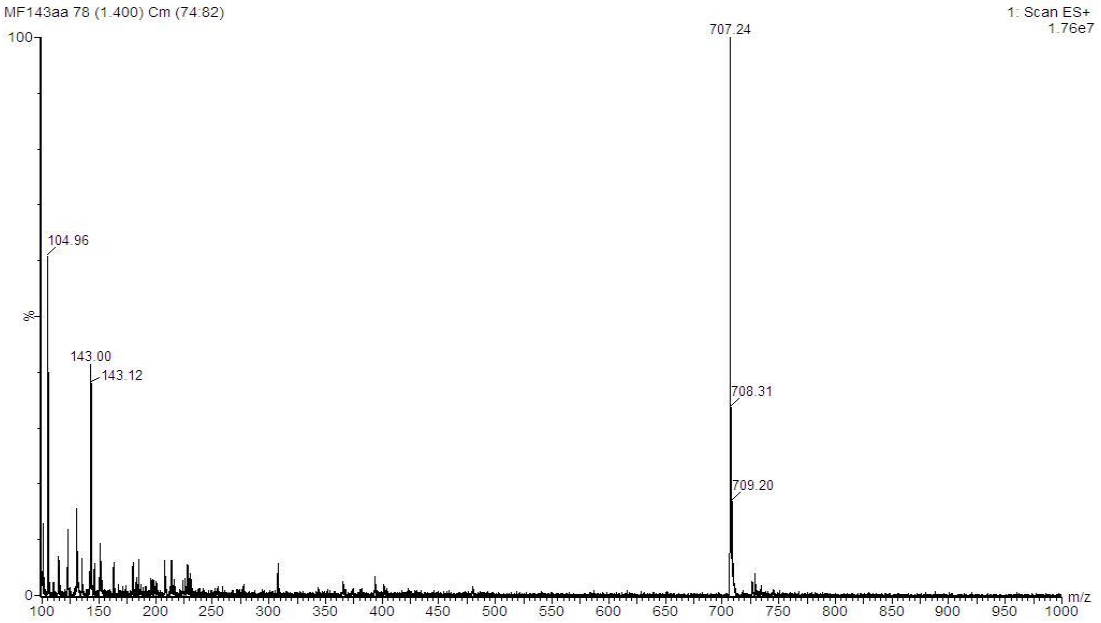
MF143aa 78 (1.400) Cm (74:82)
1: Scan ES+
1.76e7
100
%
0
707.24
104.96
143.00
143.12
708.31
709.20
100 150 200 250 300 350 400 450 500 550 600 650 700 750 800 850 900 950 1000
m/z

(d)

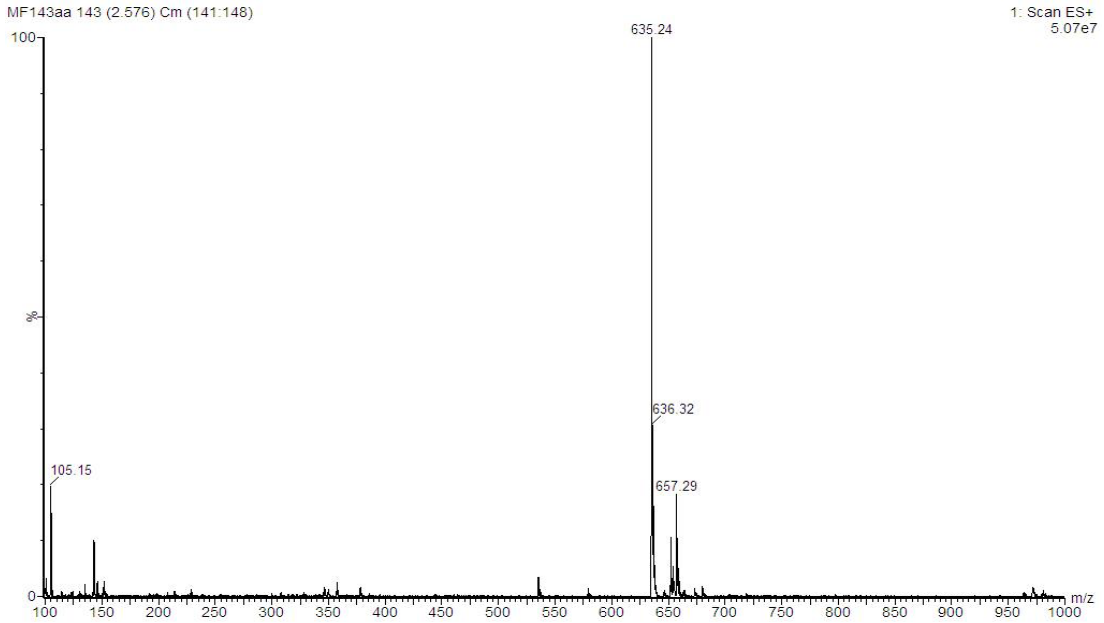

Figure **S47**. (a) TIC and UV trace at t = 0.05 h, (b) MS data at 0.43 mins in the TIC, (c) MS data at 1.35 mins in the UV and (d) at 2.53 mins in the UV for PD **5** incubated with GSH **1** (10 eq.) at pH 6.5.

LC-MS data for t = 1 h

(a)

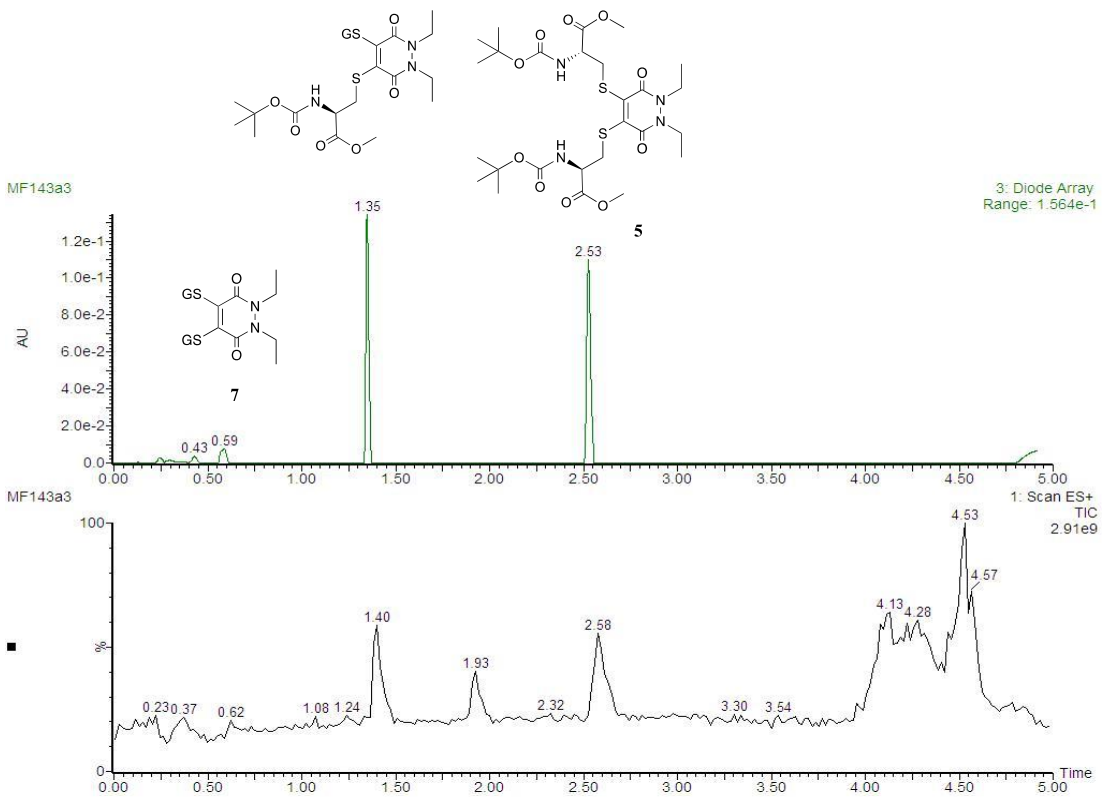
MF143a3
3: Diode Array
Range: 1.564e-1
5
7
AU
1.35
2.53
0.43
0.59
MF143a3
1: Scan ES+
TIC
2.91e9
4.53
4.57
4.13
4.28
1.40
1.93
2.58
2.32
0.23
0.37
0.62
1.08
1.24
3.30
3.54
%
Time

(b)

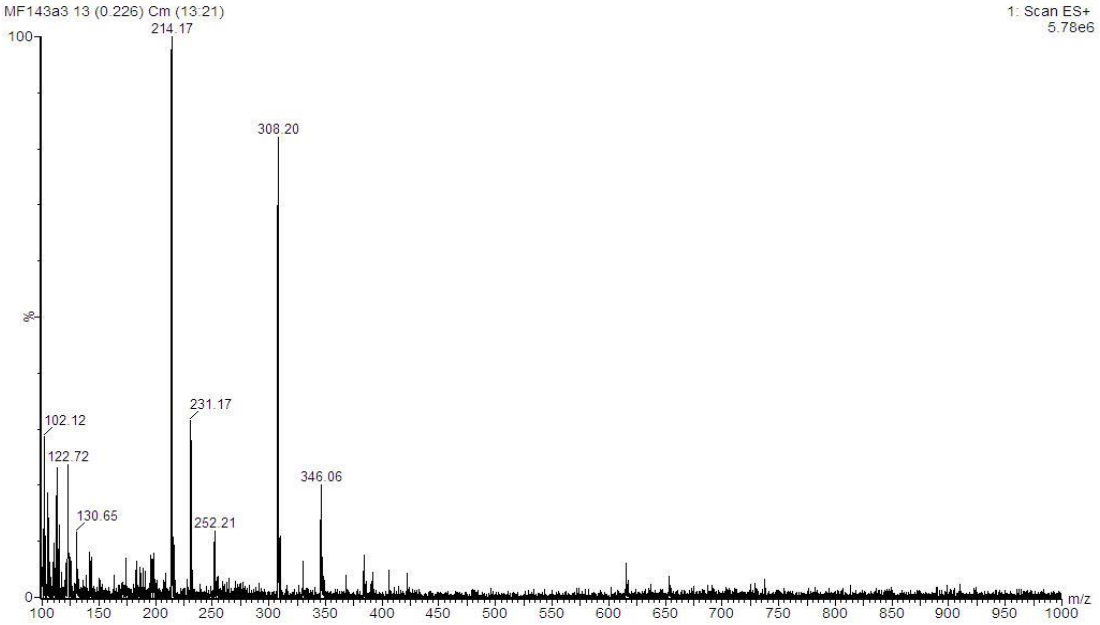
MF143a3 13 (0.226) Cm (13:21)
1: Scan ES+
5.78e6
214.17
308.20
231.17
102.12
122.72
346.06
130.65
252.21
%
m/z

(c)

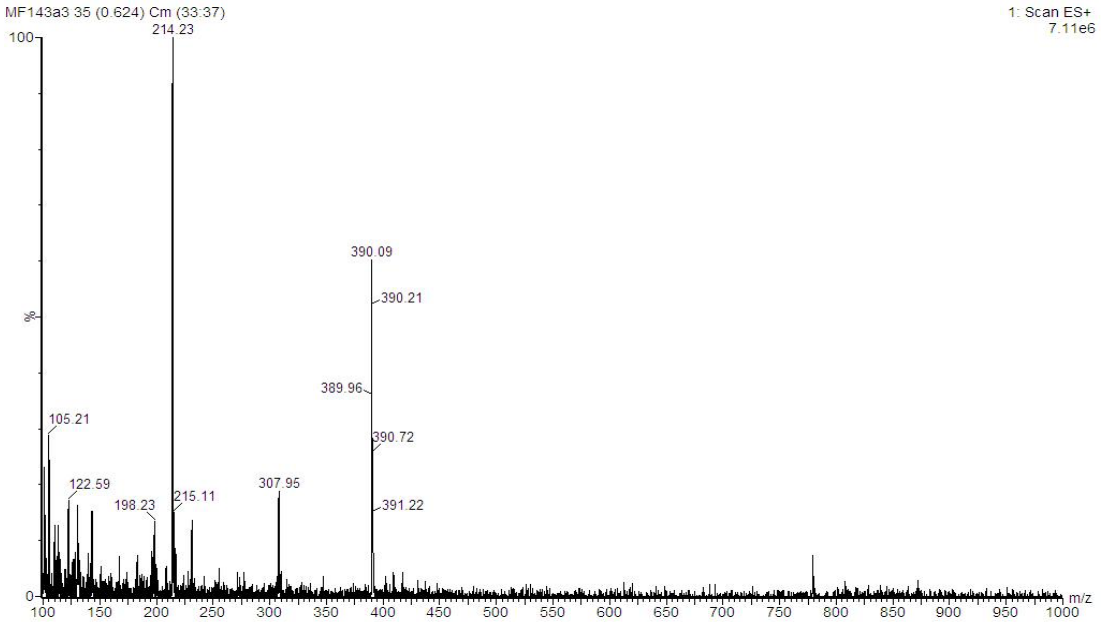
MF143a3 35 (0.624) Cm (33:37)
1: Scan ES+
7.11e6
100
%
0
214.23
390.09
390.21
389.96
105.21
390.72
122.59
307.95
198.23
215.11
391.22
m/z
100 150 200 250 300 350 400 450 500 550 600 650 700 750 800 850 900 950 1000

(d)

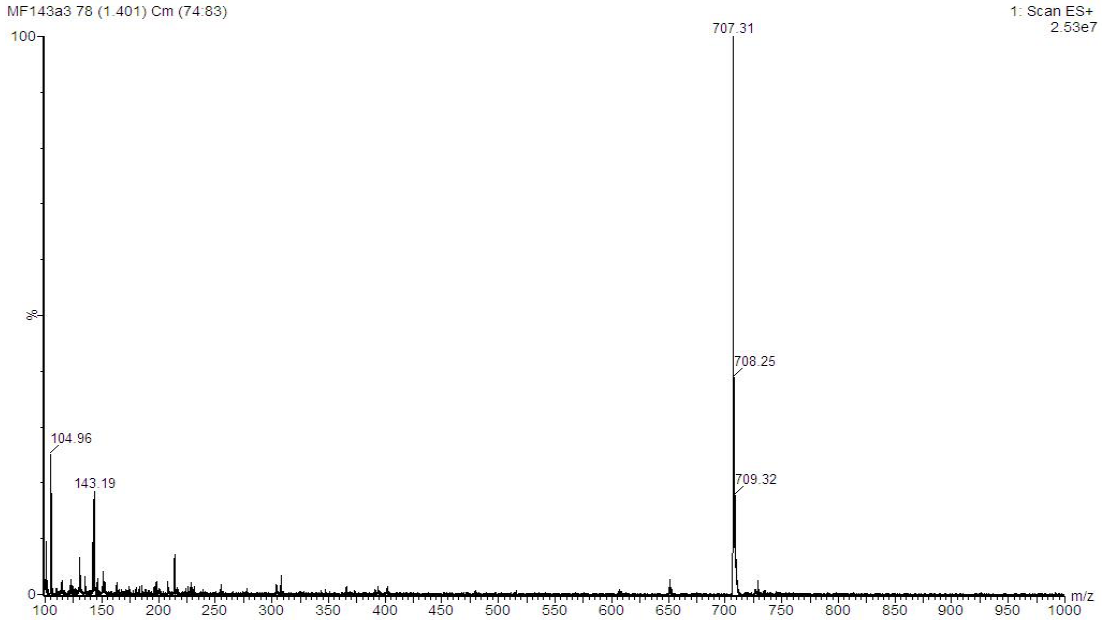
MF143a3 78 (1.401) Cm (74:83)
1: Scan ES+
2.53e7
100
%
0
707.31
708.25
104.96
143.19
709.32
m/z
100 150 200 250 300 350 400 450 500 550 600 650 700 750 800 850 900 950 1000

(e)

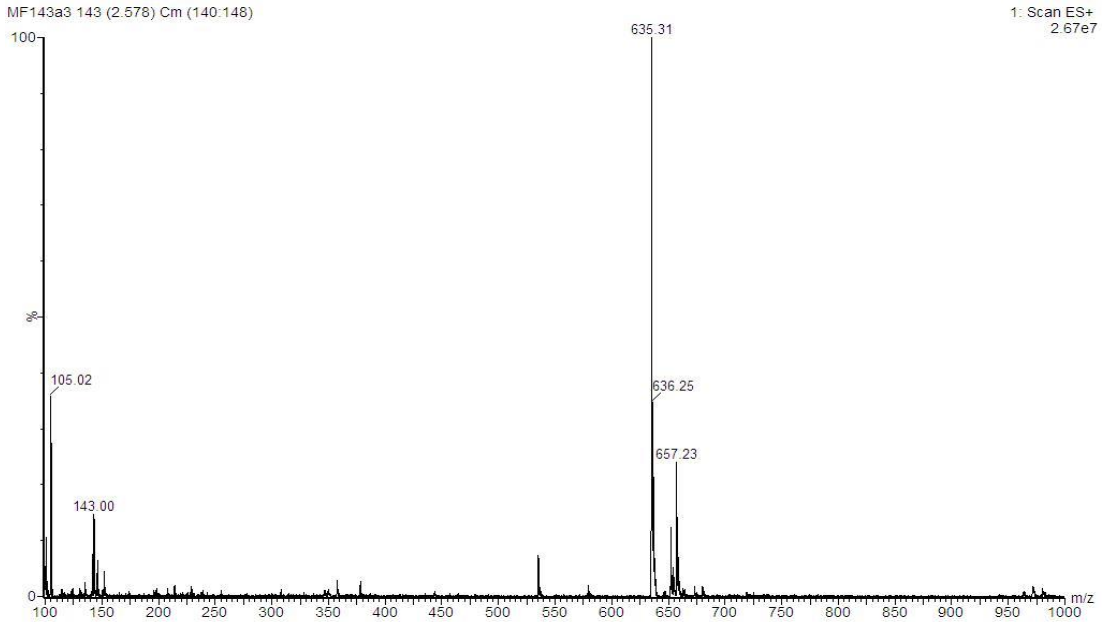

Figure **S48**. (a) TIC and UV trace at t = 1 h, (b) MS data at 0.43 mins in the TIC, (c) MS data at 0.59 mins in the UV, (d) at 1.35 mins in the UV and (e) at 2.53 mins in the UV for PD **5** incubated with GSH **1** (10 eq.) at pH 6.5.

LC-MS data for t = 2 h

(a)

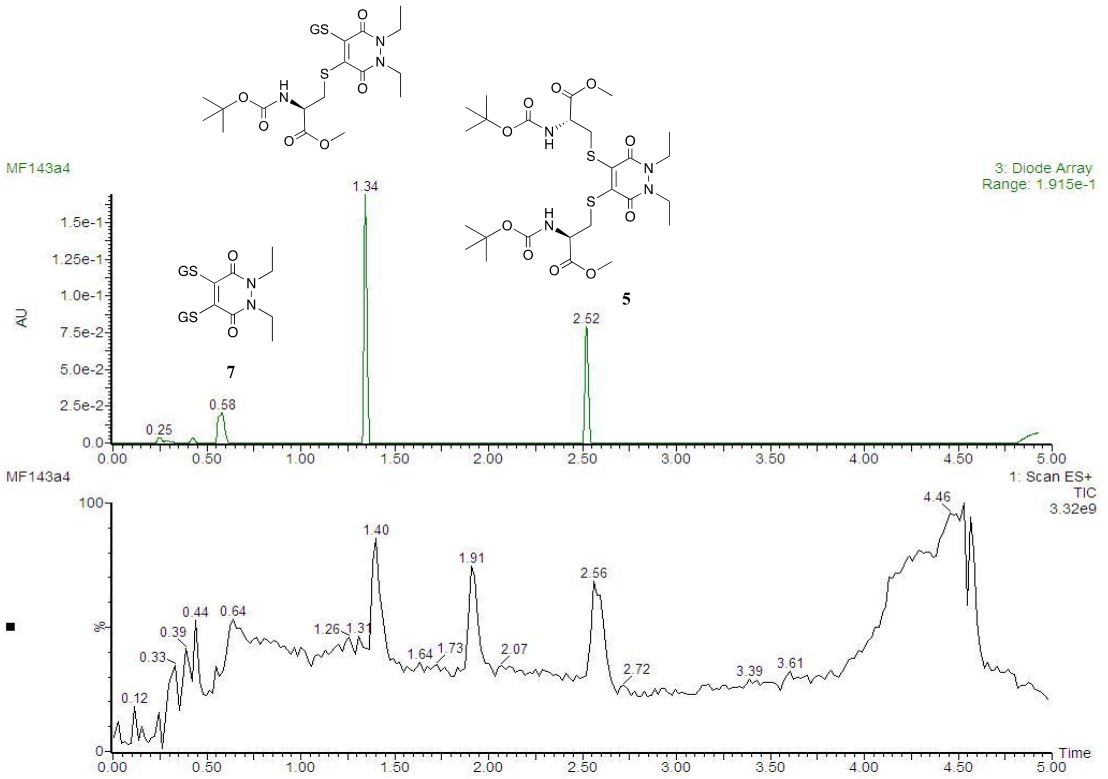
MF143a4
3: Diode Array
Range: 1.915e-1
AU
1.34
2.52
0.58
0.25
7
5
MF143a4
1: Scan ES+
TIC
3.32e9
%
4.46
1.40
1.91
2.56
0.44
0.64
0.39
0.33
0.12
1.26
1.31
1.64
1.73
2.07
2.72
3.39
3.61
Time

(b)

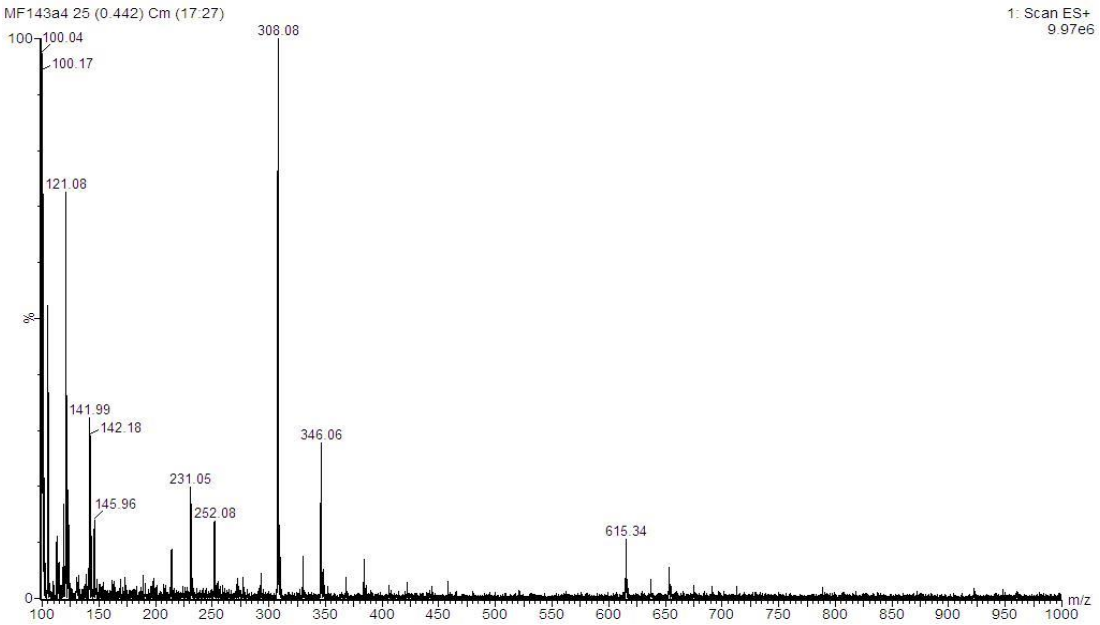
MF143a4 25 (0.442) Cm (17:27)
1: Scan ES+
9.97e6
100.04
100.17
308.08
121.08
141.99
142.18
346.06
231.05
145.96
252.08
615.34
%
m/z

(c)

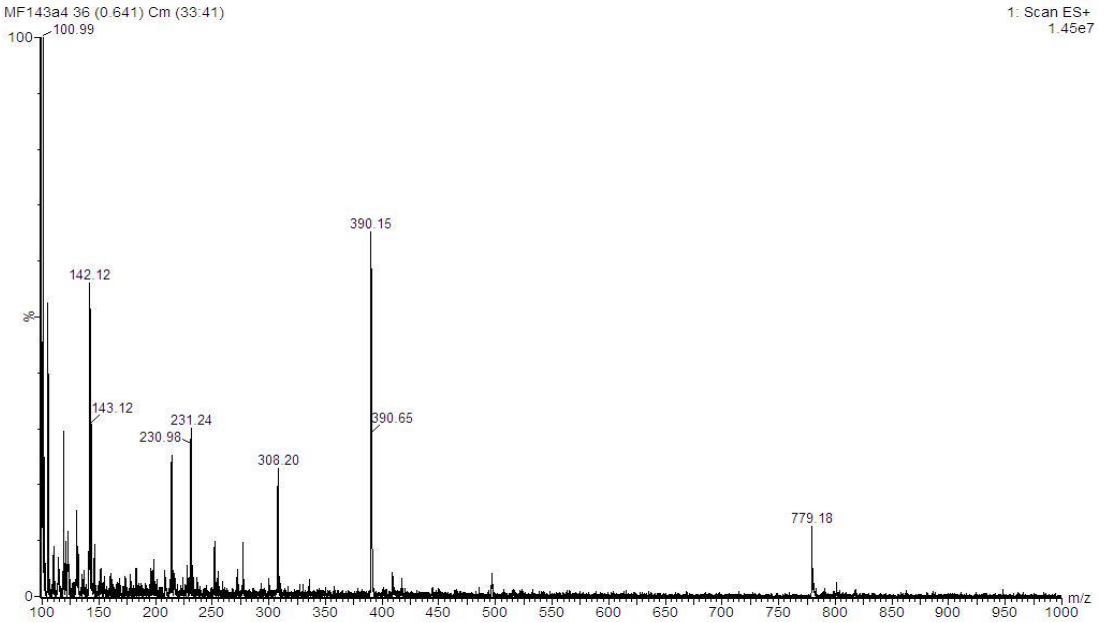
MF143a4 36 (0.641) Cm (33:41)
1: Scan ES+
1.45e7
100.99
390.15
142.12
143.12
231.24
230.98
390.65
308.20
779.18
%
m/z

(d)

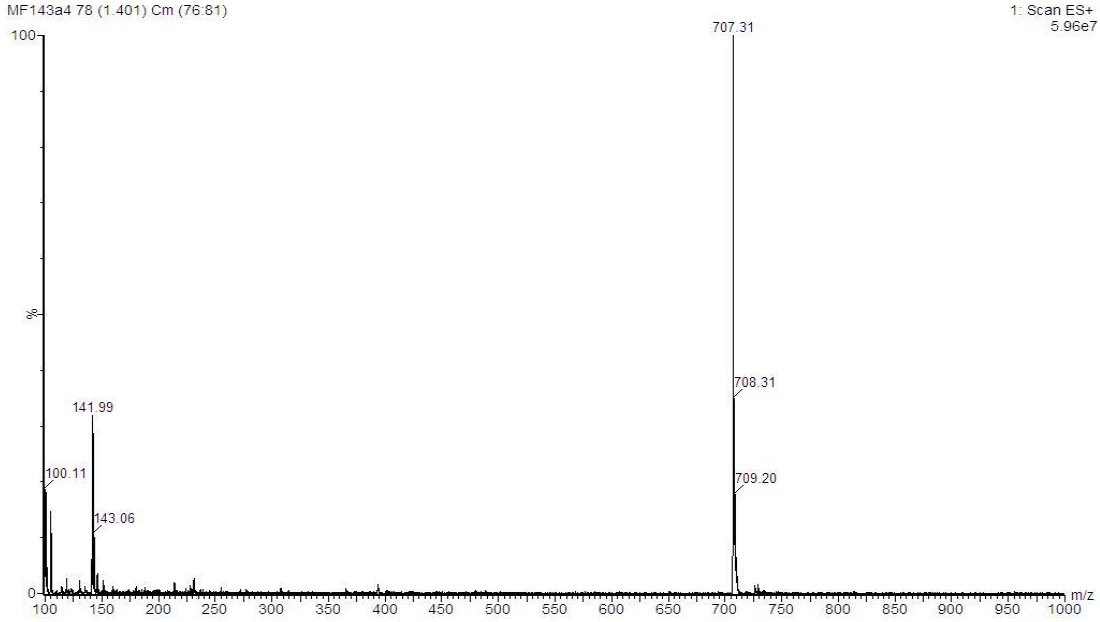
MF143a4 78 (1.401) Cm (76:81)
1: Scan ES+
5.96e7
707.31
708.31
141.99
100.11
709.20
143.06
%
m/z

(e)

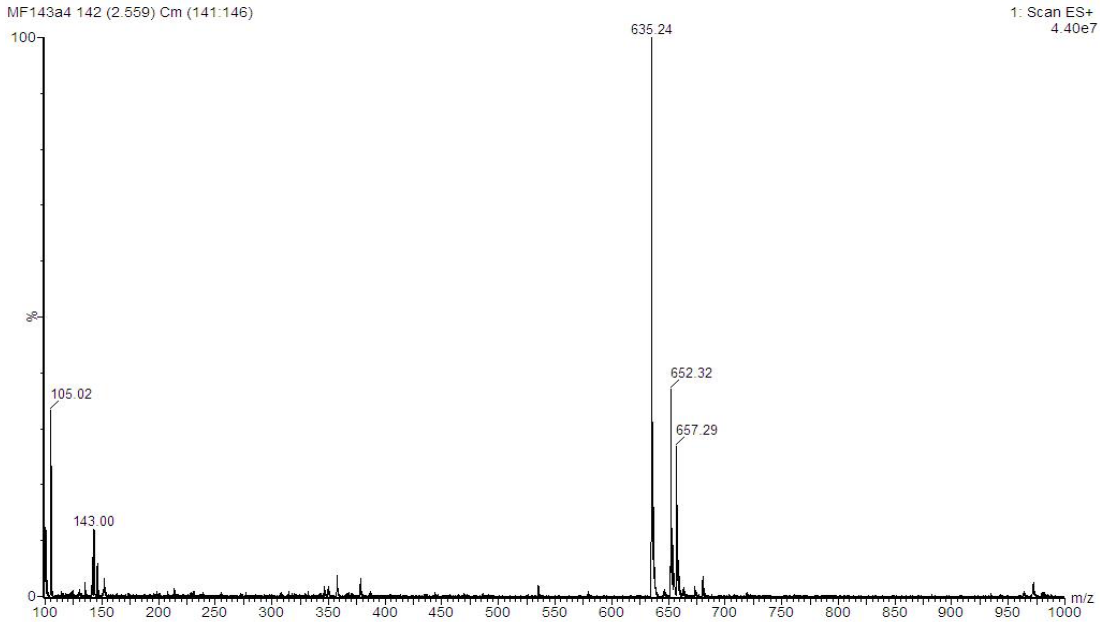

Figure **S49**. (a) TIC and UV trace at t = 2 h, (b) MS data at 0.25–0.44 mins in the UV, (c) MS data at 0.58 mins in the UV, (d) at 1.34 mins in the UV and (e) at 2.52 mins in the UV for PD **5** incubated with GSH **1** (10 eq.) at pH 6.5.

LC-MS data for t = 4 h

(a)

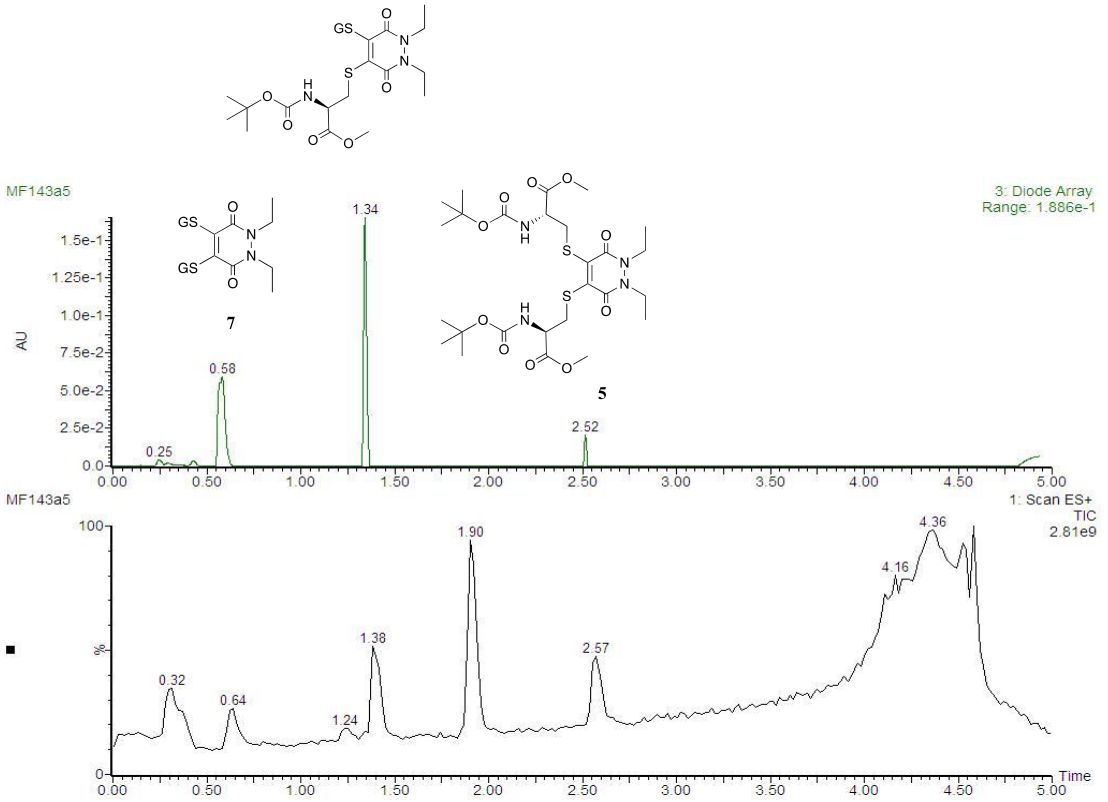
MF143a5
3: Diode Array
Range: 1.886e-1
AU
7
5
0.25
0.58
1.34
2.52
MF143a5
1: Scan ES+
TIC
2.81e9
%
0.32
0.64
1.24
1.38
1.90
2.57
4.16
4.36
Time

(b)

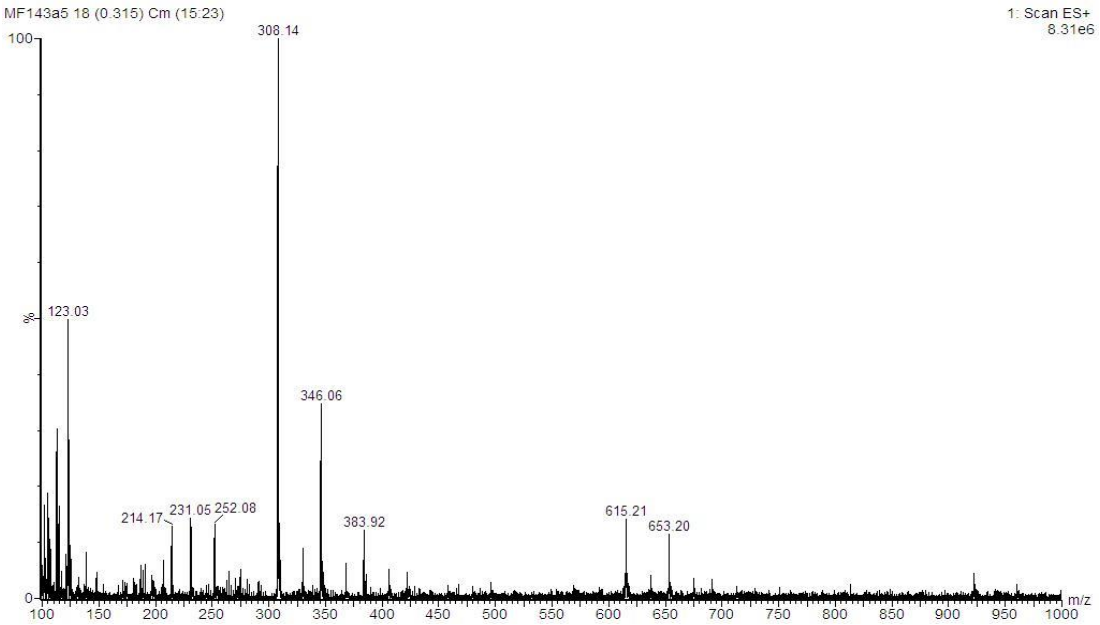
MF143a5 18 (0.315) Cm (15:23)
1: Scan ES+
8.31e6
%
308.14
123.03
346.06
214.17
231.05
252.08
383.92
615.21
653.20
m/z

(c)

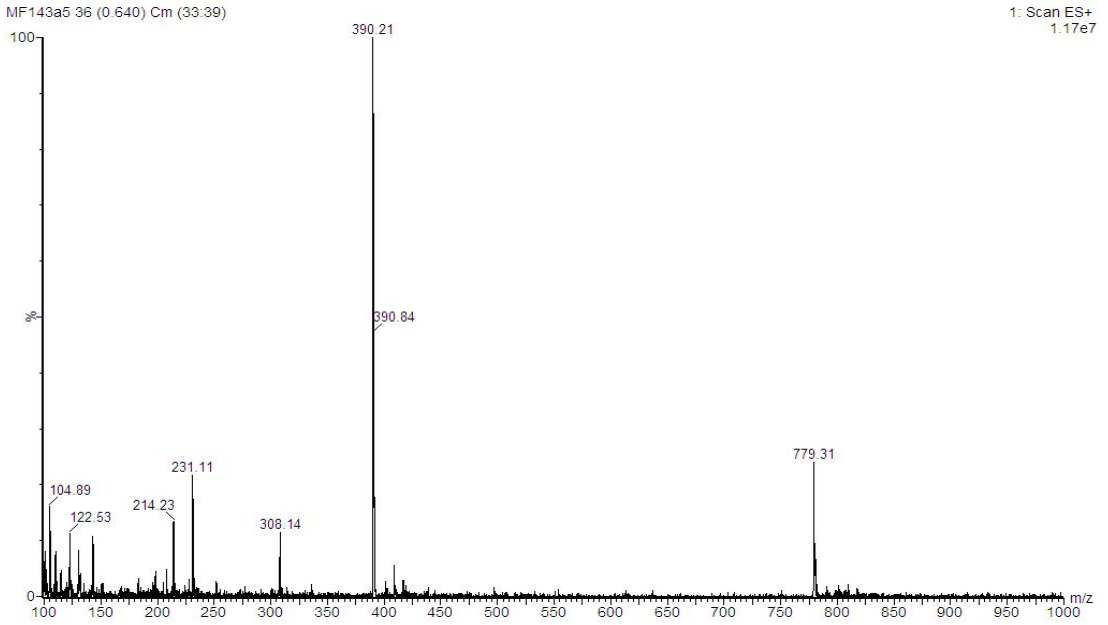
MF143a5 36 (0.640) Cm (33:39)
1: Scan ES+
1.17e7
100
%
0
390.21
390.84
779.31
231.11
104.89
214.23
122.53
308.14
m/z
100 150 200 250 300 350 400 450 500 550 600 650 700 750 800 850 900 950 1000

(d)

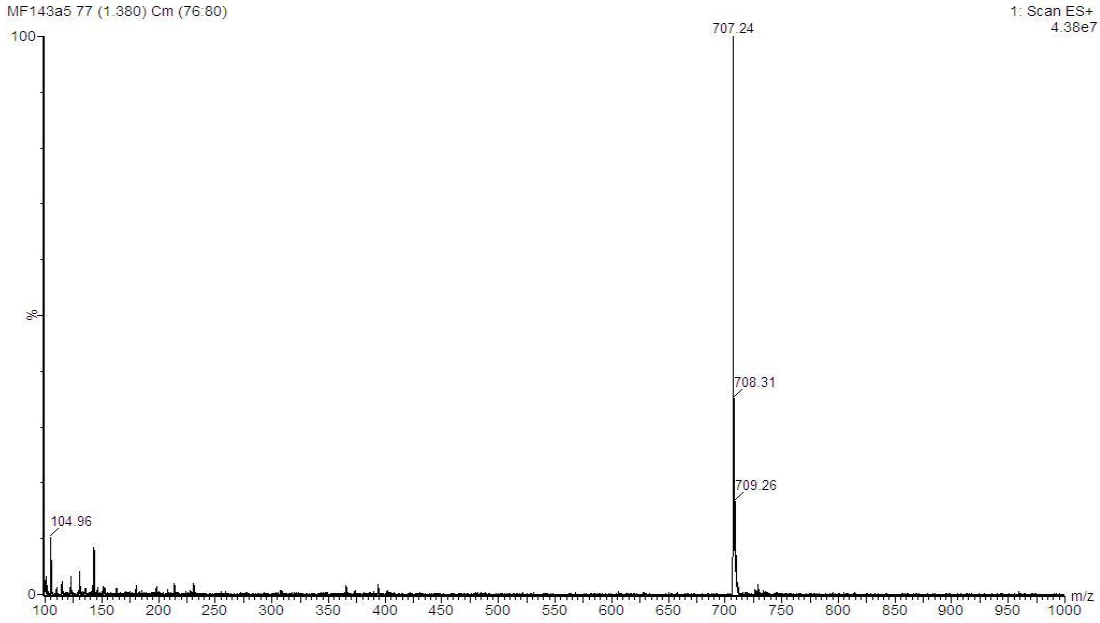
MF143a5 77 (1.380) Cm (76:80)
1: Scan ES+
4.38e7
100
%
0
707.24
708.31
709.26
104.96
m/z
100 150 200 250 300 350 400 450 500 550 600 650 700 750 800 850 900 950 1000

(e)

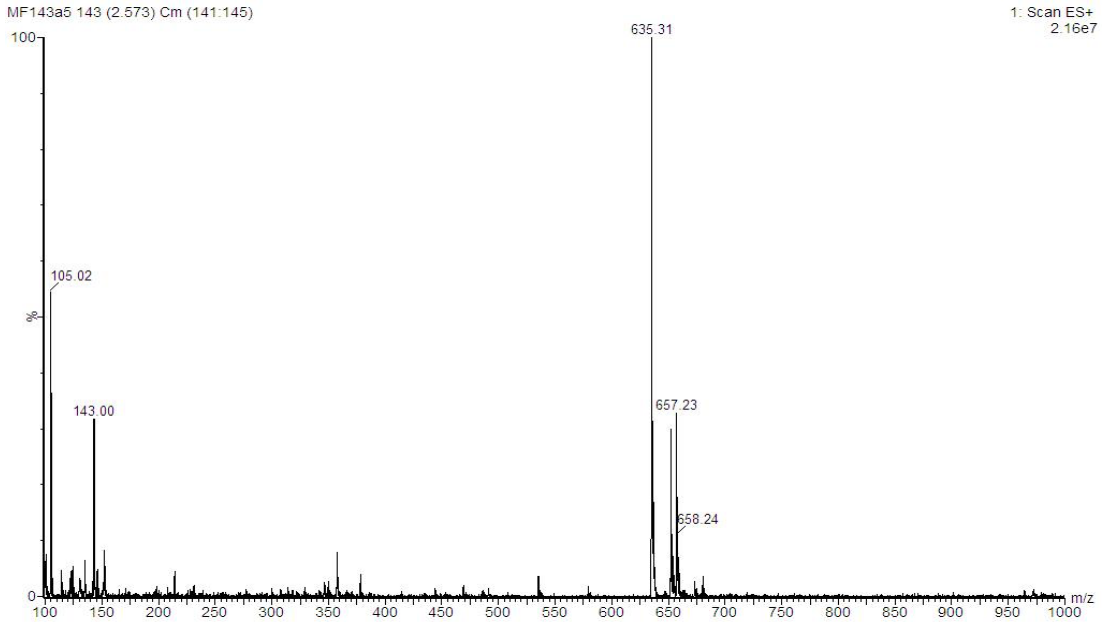

Figure **S50**. (a) TIC and UV trace at t = 4 h, (b) MS data at 0.25–0.44 mins in the UV, (c) MS data at 0.58 mins in the UV, (d) at 1.34 mins in the UV and (e) at 2.52 mins in the UV for PD **5** incubated with GSH **1** (10 eq.) at pH 6.5.

LC-MS data for t = 24 h

(a)

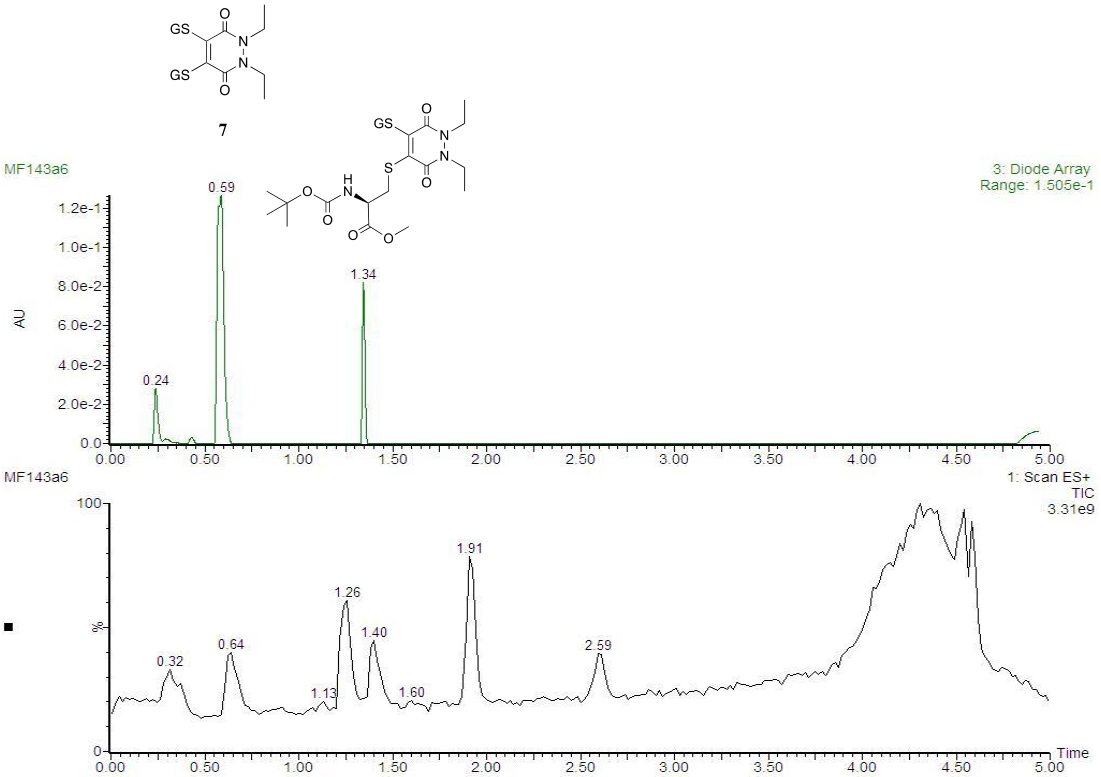
7
MF143a6
3: Diode Array
Range: 1.505e-1
AU
0.59
1.34
0.24
MF143a6
1: Scan ES+
TIC
3.31e9
%
1.91
1.26
1.40
0.64
0.32
2.59
1.13
1.60
Time

(b)

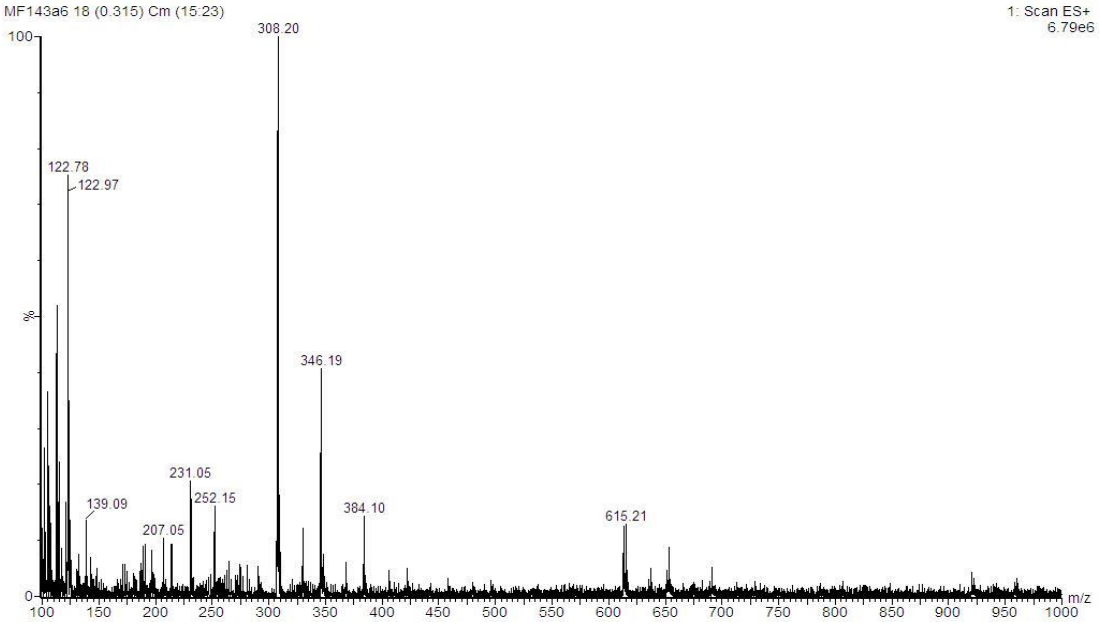
MF143a6 18 (0.315) Cm (15:23)
1: Scan ES+
6.79e6
308.20
122.78
122.97
346.19
231.05
252.15
139.09
207.05
384.10
615.21
%
m/z

(c)

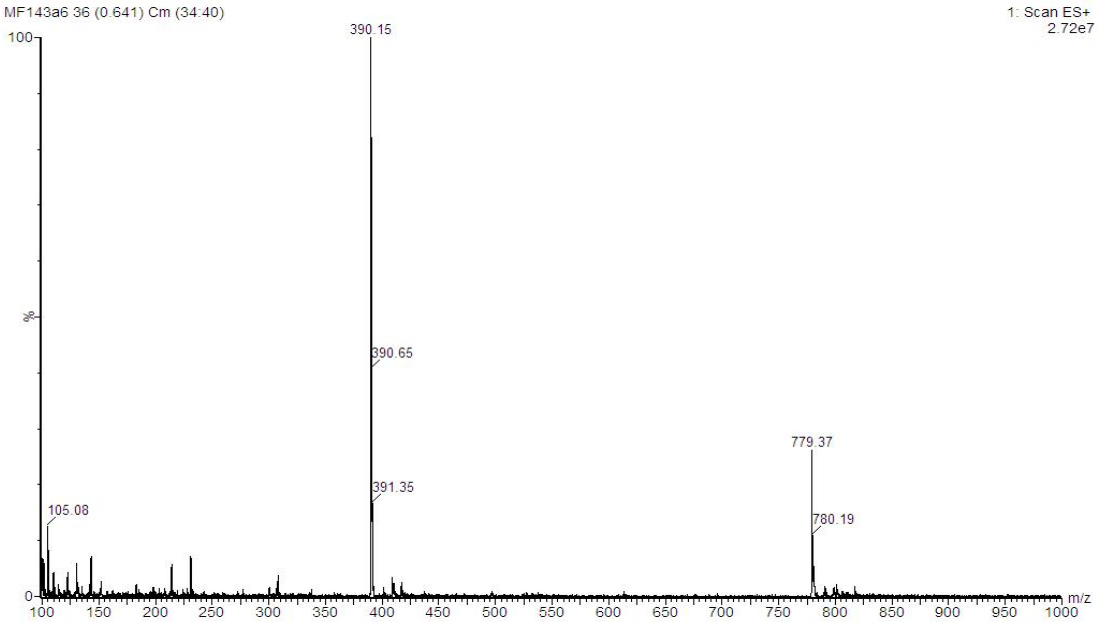

(d)

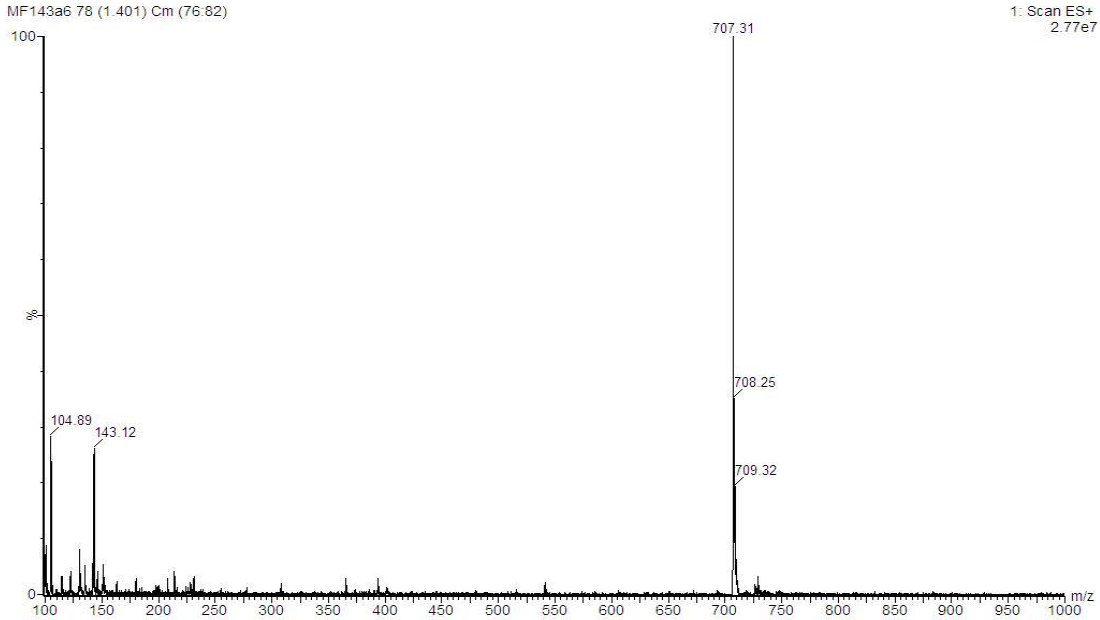

Figure **S51**. (a) TIC and UV trace at t = 24 h, (b) MS data at 0.24–0.44 mins in the UV, (c) MS data at 0.59 mins in the UV and (d) at 1.34 mins in the UV for PD **5** incubated with GSH **1** (10 eq.) at pH 6.5.

Incubation of PD 6 with GSH (10 eq.)

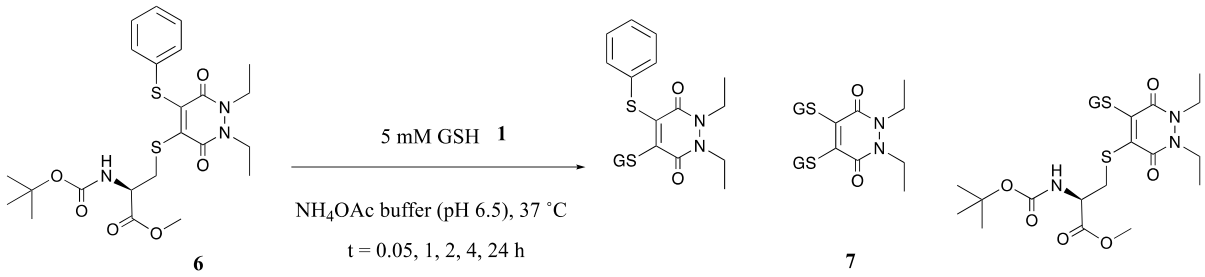

PD **6** (10 µL, 10 mM in MeCN, 1 eq.) was added to GSH **1** (190 µL, 5.3 mM, 10 eq.) in ammonium acetate buffer (50 mM, pH 6.5). The mixture was incubated at 37 ˚C for 24 h. The samples were analysed by LC-MS at t = 0.05, 1, 2, 4 and 24 h.

LC-MS data for t = 0.05 h

(a)

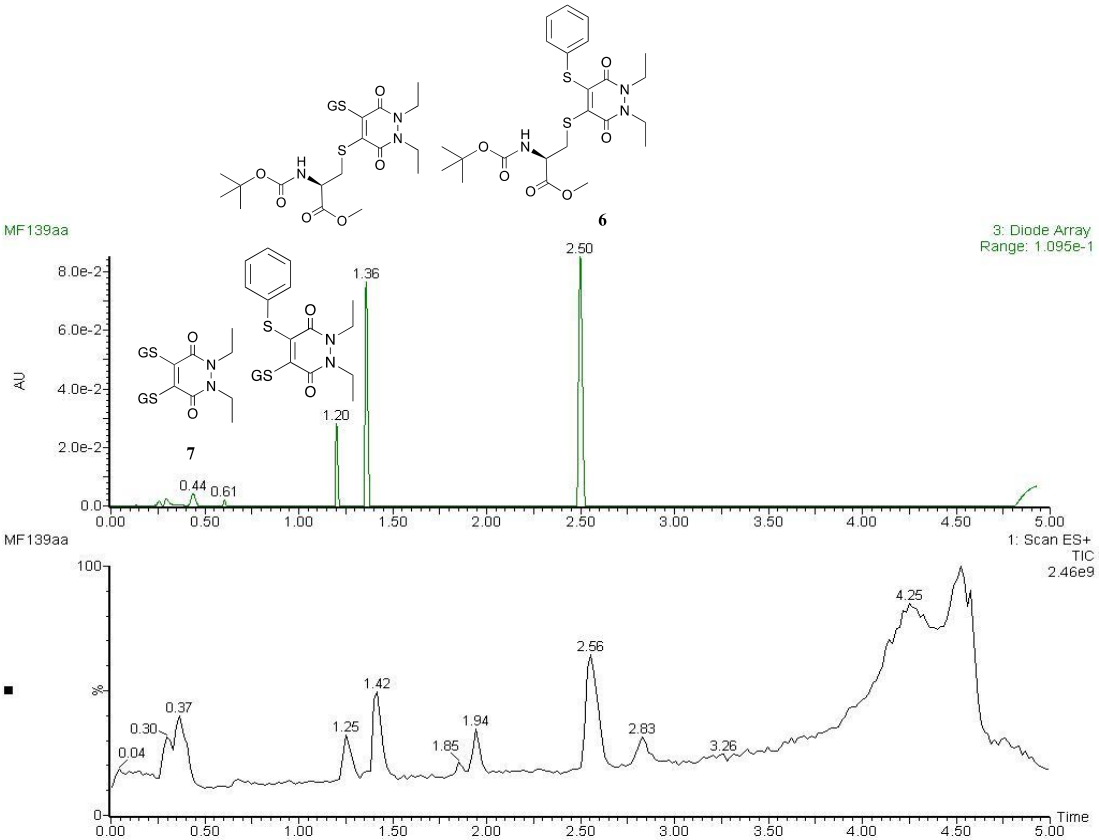

(b)

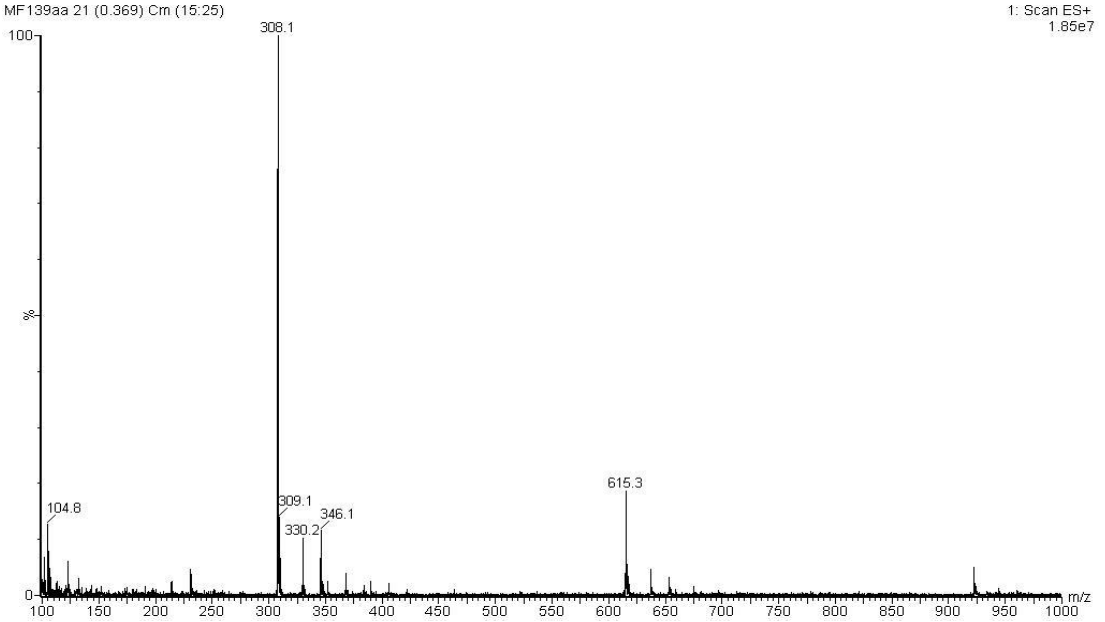
MF139aa 21 (0.369) Cm (15:25)
1: Scan ES+
1.85e7
100
%
0
308.1
615.3
104.8
309.1
346.1
330.2
m/z
100 150 200 250 300 350 400 450 500 550 600 650 700 750 800 850 900 950 1000

(c)

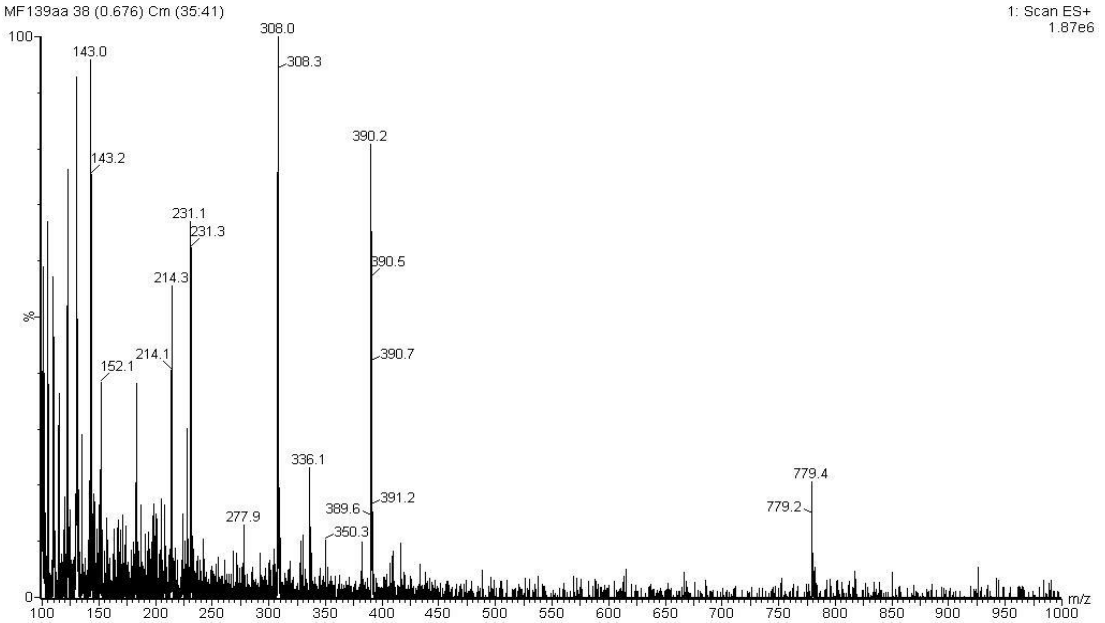
MF139aa 38 (0.676) Cm (35:41)
1: Scan ES+
1.87e6
100
%
0
308.0
308.3
143.0
390.2
143.2
231.1
231.3
390.5
214.3
390.7
214.1
152.1
336.1
779.4
779.2
391.2
389.6
277.9
350.3
m/z
100 150 200 250 300 350 400 450 500 550 600 650 700 750 800 850 900 950 1000

(d)

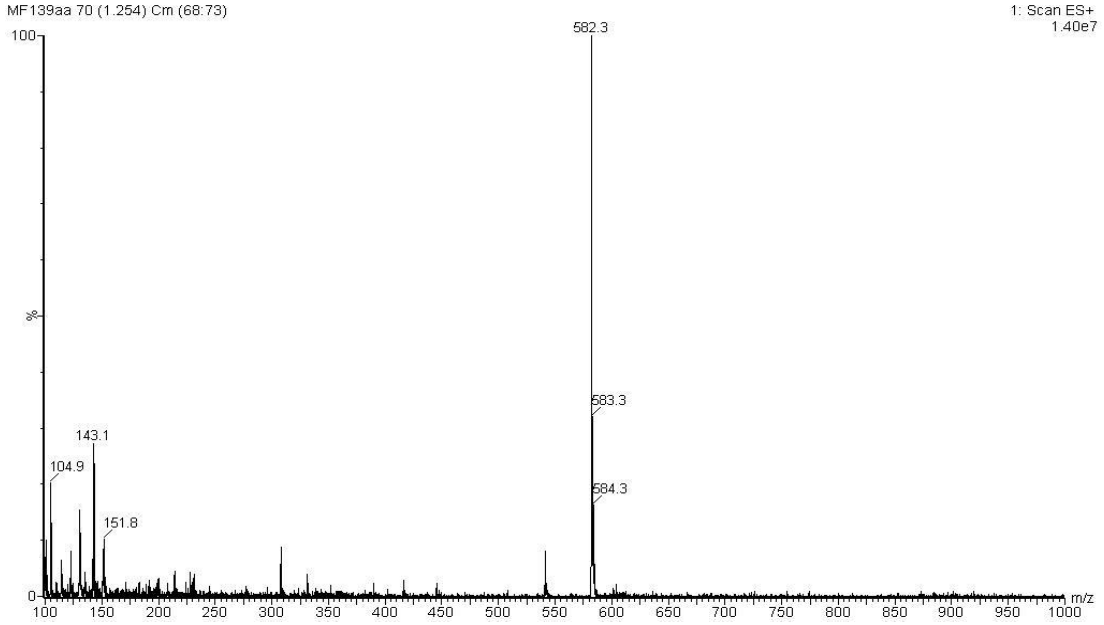
MF139aa 70 (1.254) Cm (68:73)
1: Scan ES+
1.40e7
100
%
0
582.3
583.3
584.3
143.1
104.9
151.8
100 150 200 250 300 350 400 450 500 550 600 650 700 750 800 850 900 950 1000
m/z

(e)

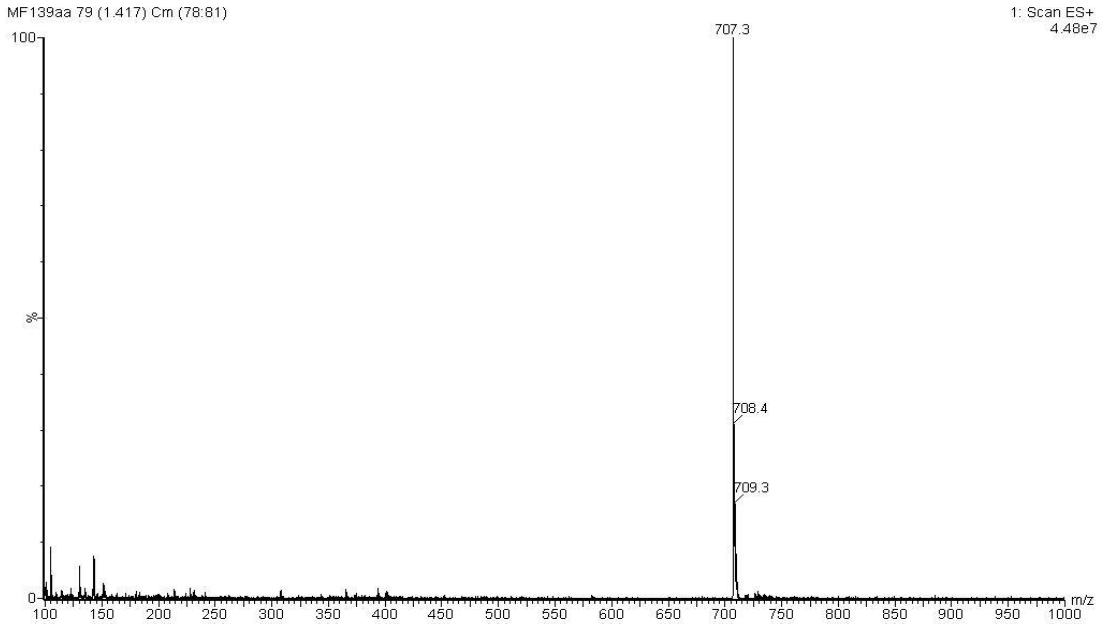
MF139aa 79 (1.417) Cm (78:81)
1: Scan ES+
4.48e7
100
%
0
707.3
708.4
709.3
100 150 200 250 300 350 400 450 500 550 600 650 700 750 800 850 900 950 1000
m/z

(f)

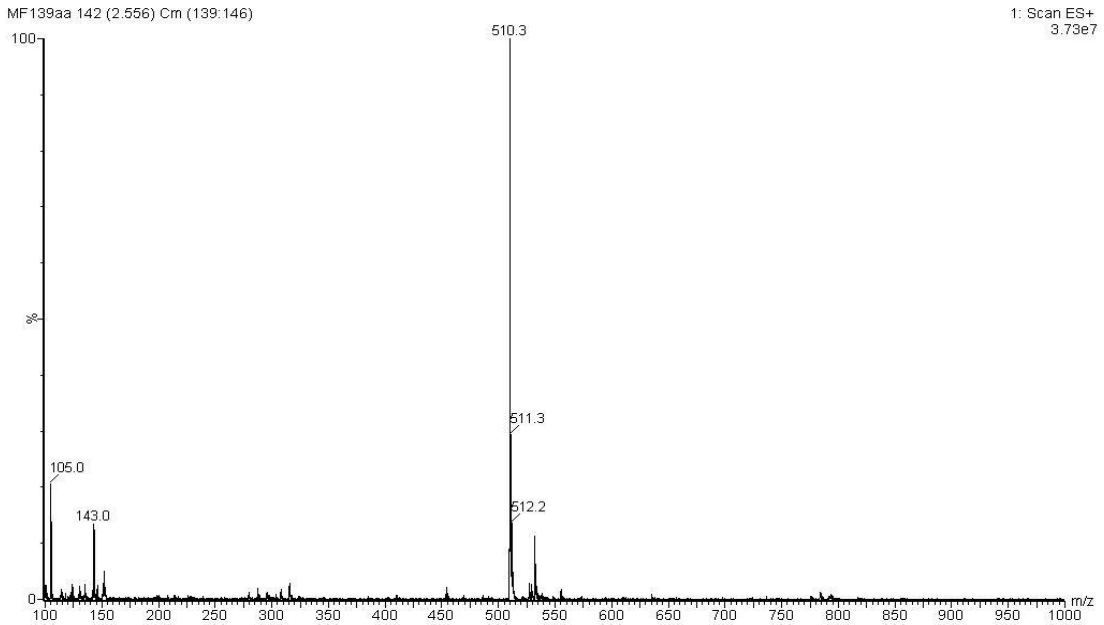

Figure **S52**. (a) TIC and UV trace at t = 0.05 h, (b) MS data at 0.24–0.44 mins in the UV, (c) MS data at 0.61 mins in the UV, (d) at 1.20 mins in the UV, (e) at 1.36 mins in the UV and (f) at 2.50 mins in the UV for PD **6** incubated with GSH **1** (10 eq.) at pH 6.5.

LC-MS data for t = 1 h

(a)

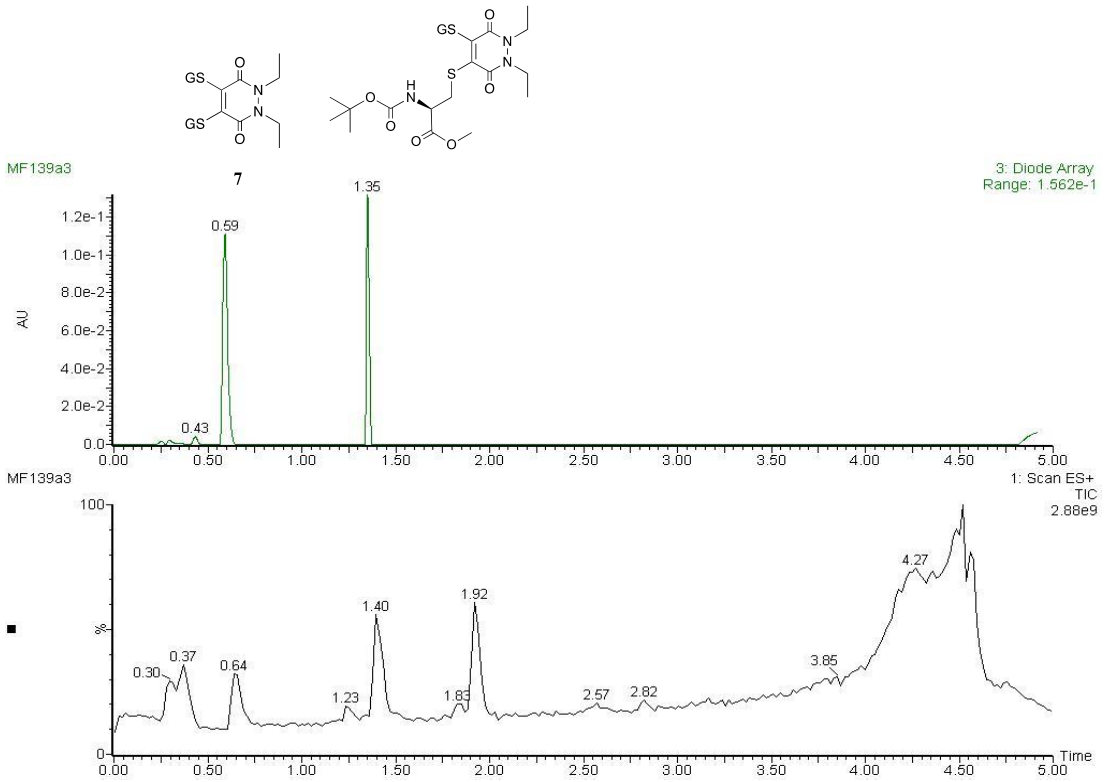
GS
GS
GS
S
7
MF139a3
3: Diode Array
Range: 1.562e-1
AU
1.35
0.59
0.43
MF139a3
1: Scan ES+
TIC
2.88e9
%
4.27
1.92
1.40
0.37
0.64
0.30
3.85
1.23
1.85
2.57
2.82
Time

(b)

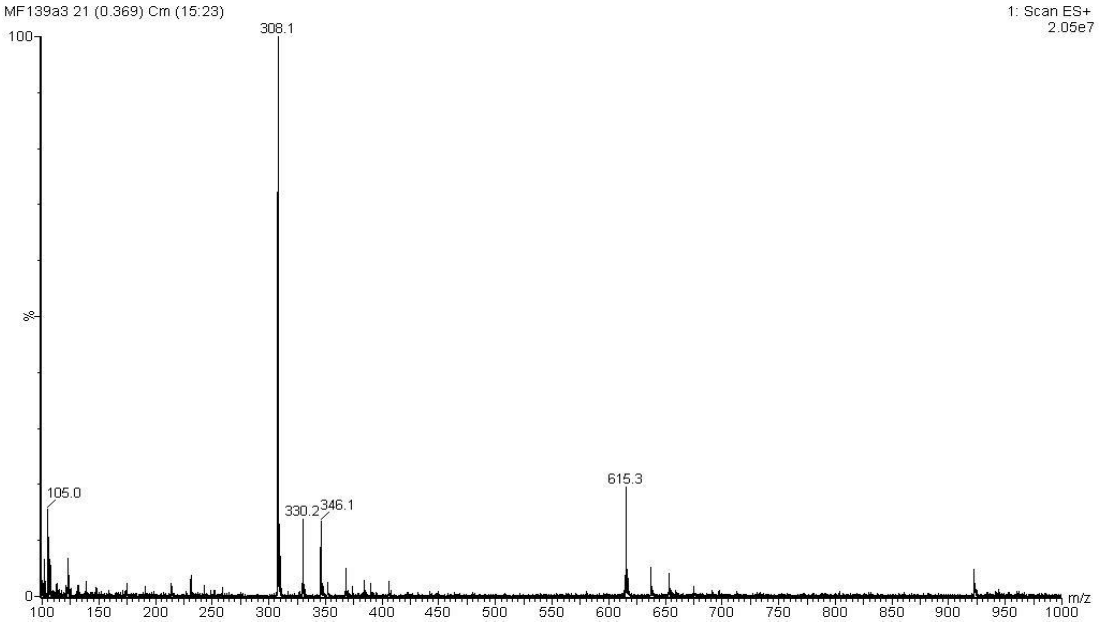
MF139a3 21 (0.369) Cm (15:23)
1: Scan ES+
2.05e7
%
308.1
105.0
330.2
346.1
615.3
m/z

(c)

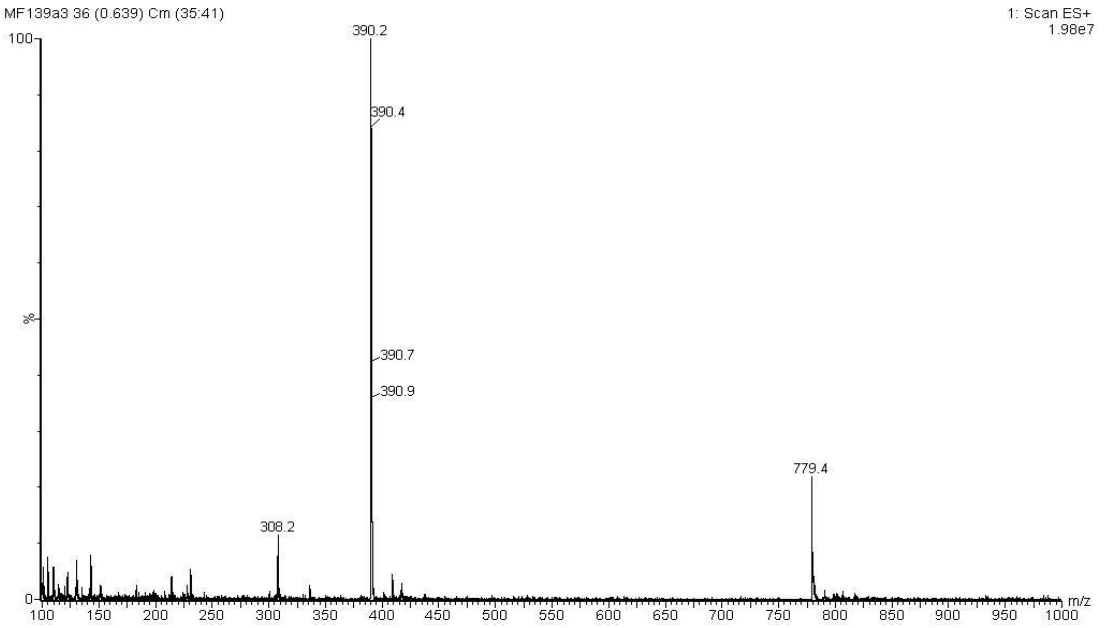

(d)

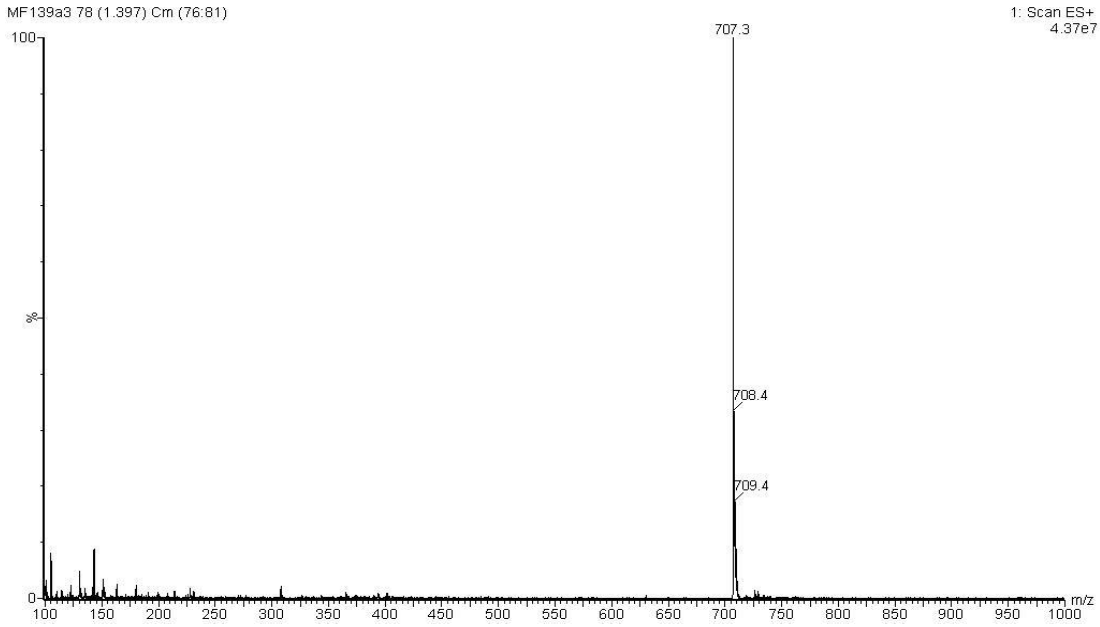

Figure **S53**. (a) TIC and UV trace at t = 1 h, (b) MS data at 0.24–0.43 mins in the UV, (c) MS data at 0.59 mins in the UV and (d) at 1.35 mins in the UV for PD **6** incubated with GSH **1** (10 eq.) at pH 6.5.

LC-MS data for t = 2 h

(a)

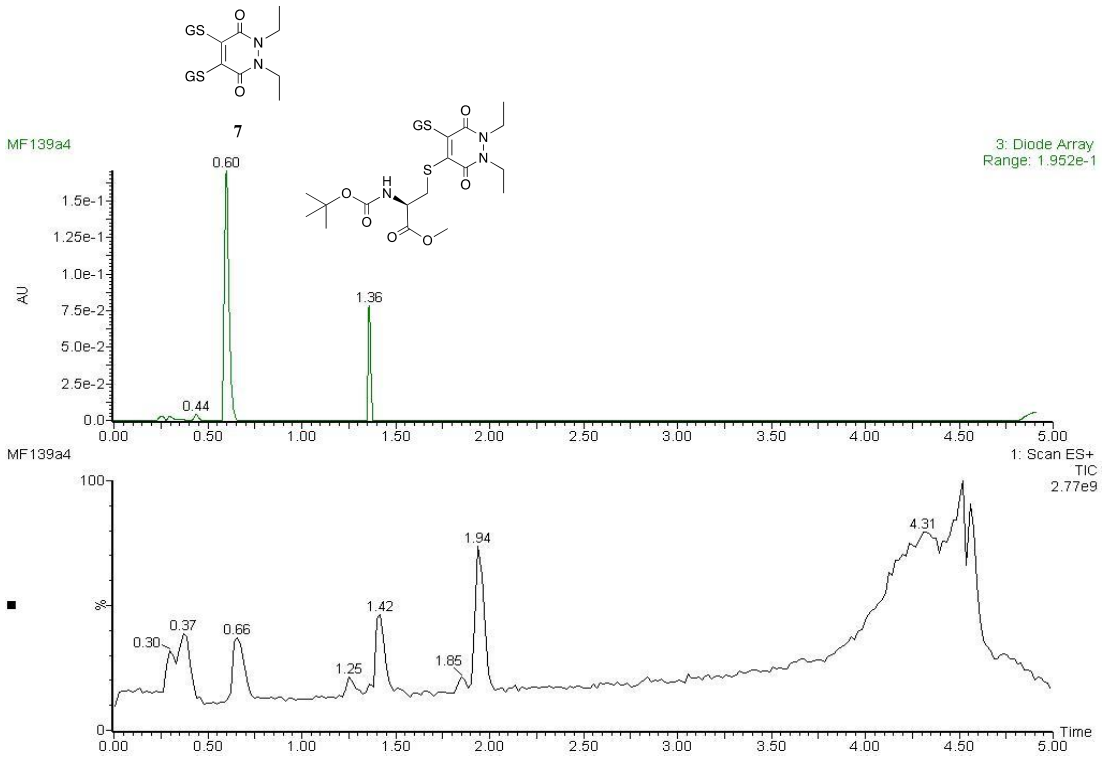
7
MF139a4
3: Diode Array
Range: 1.952e-1
0.60
1.36
0.44
AU
MF139a4
1: Scan ES+
TIC
2.77e9
1.94
4.31
1.42
0.37
0.66
0.30
1.25
1.85
%
Time

(b)

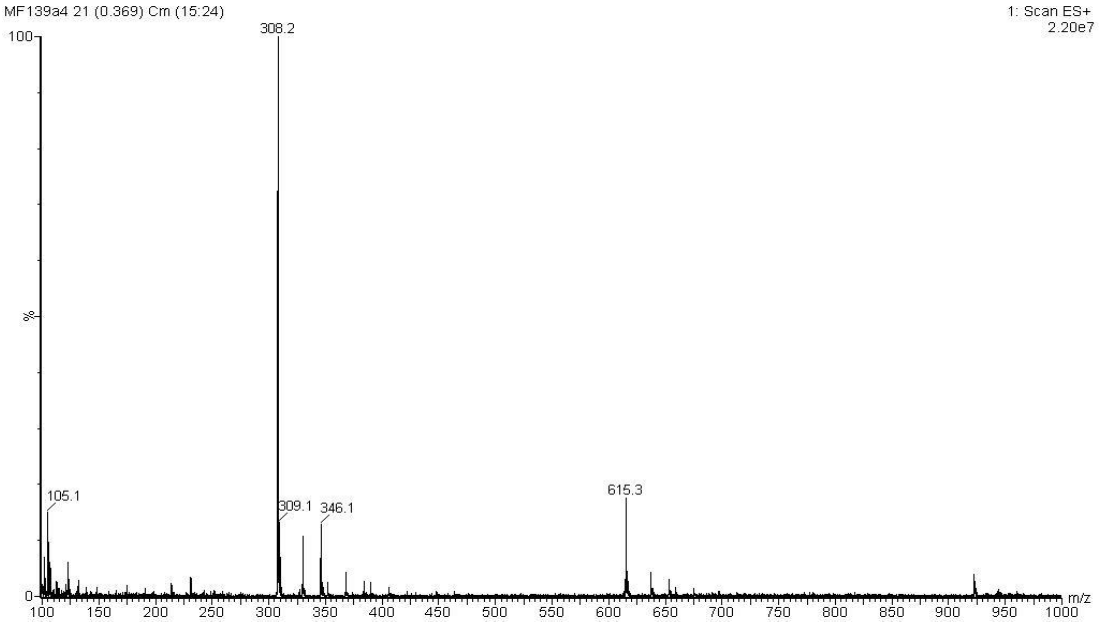
MF139a4 21 (0.369) Cm (15:24)
1: Scan ES+
2.20e7
308.2
105.1
309.1
346.1
615.3
%
m/z

(c)

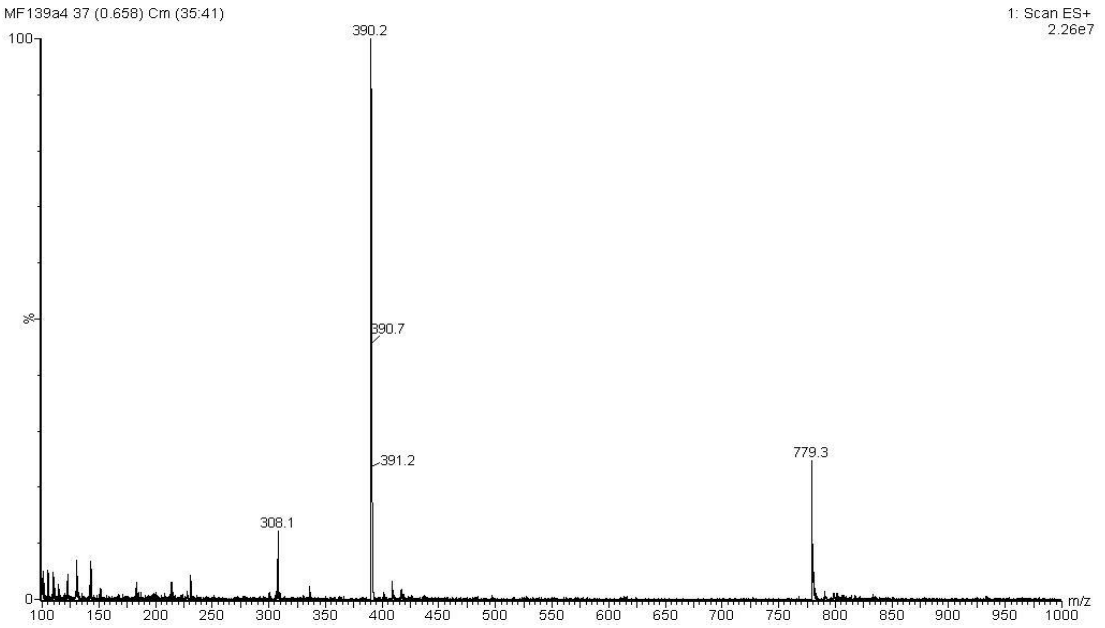

(d)

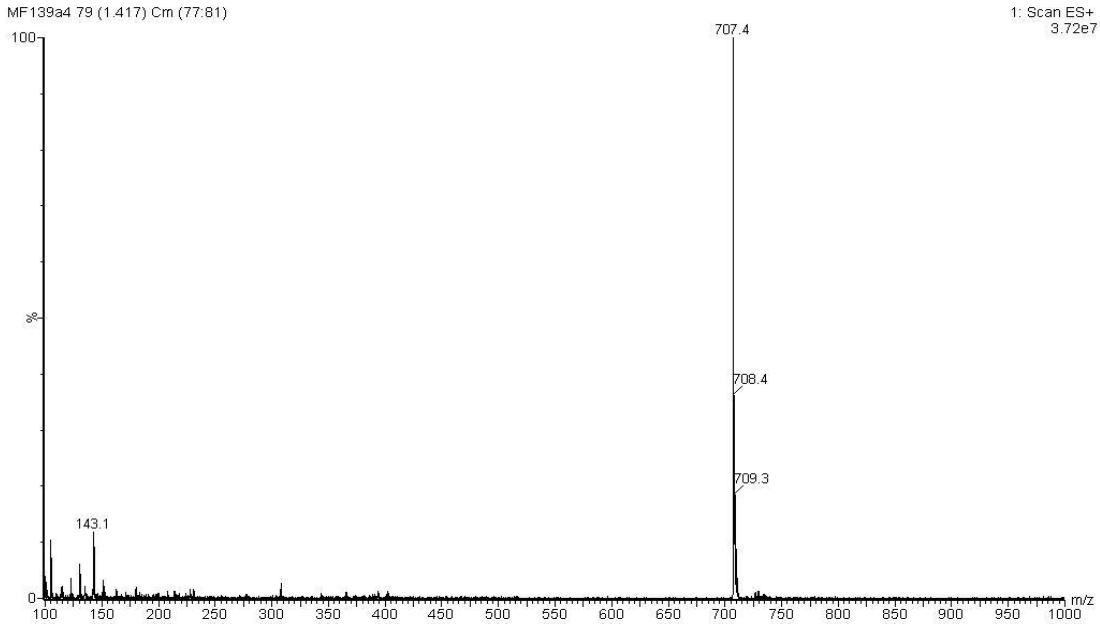

Figure **S54**. (a) TIC and UV trace at t = 2 h, (b) MS data at 0.24–0.44 mins in the UV, (c) MS data at 0.60 mins in the UV and (d) at 1.36 mins in the UV for PD **6** incubated with GSH **1** (10 eq.) at pH 6.5.

LC-MS data for t = 4 h

(a)

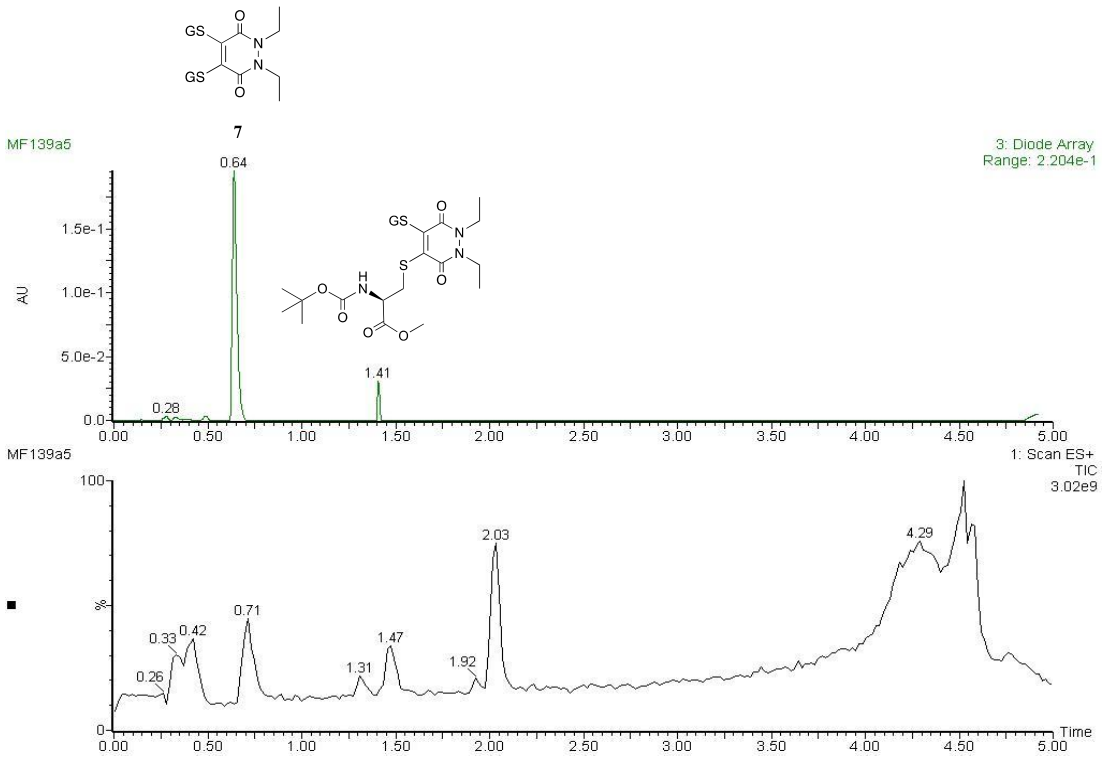
7
MF139a5
3: Diode Array
Range: 2.204e-1
0.64
1.41
0.28
AU
MF139a5
1: Scan ES+
TIC
3.02e9
2.03
4.29
0.71
0.33
0.42
1.47
0.26
1.31
1.92
%
Time

(b)

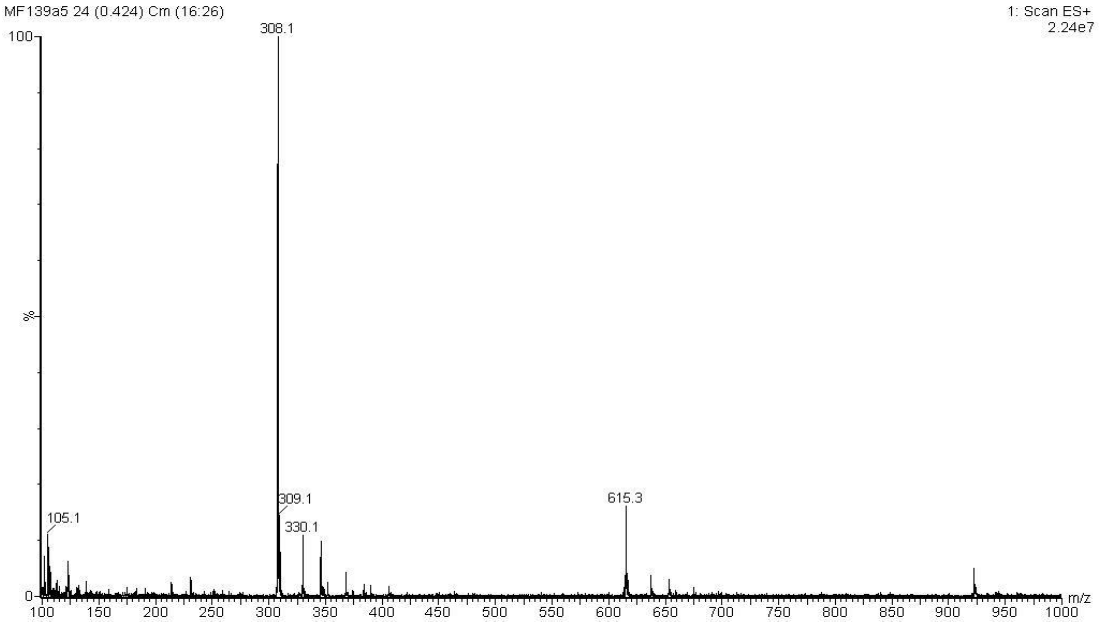
MF139a5 24 (0.424) Cm (16:26)
1: Scan ES+
2.24e7
308.1
309.1
330.1
615.3
105.1
%
m/z

(c)

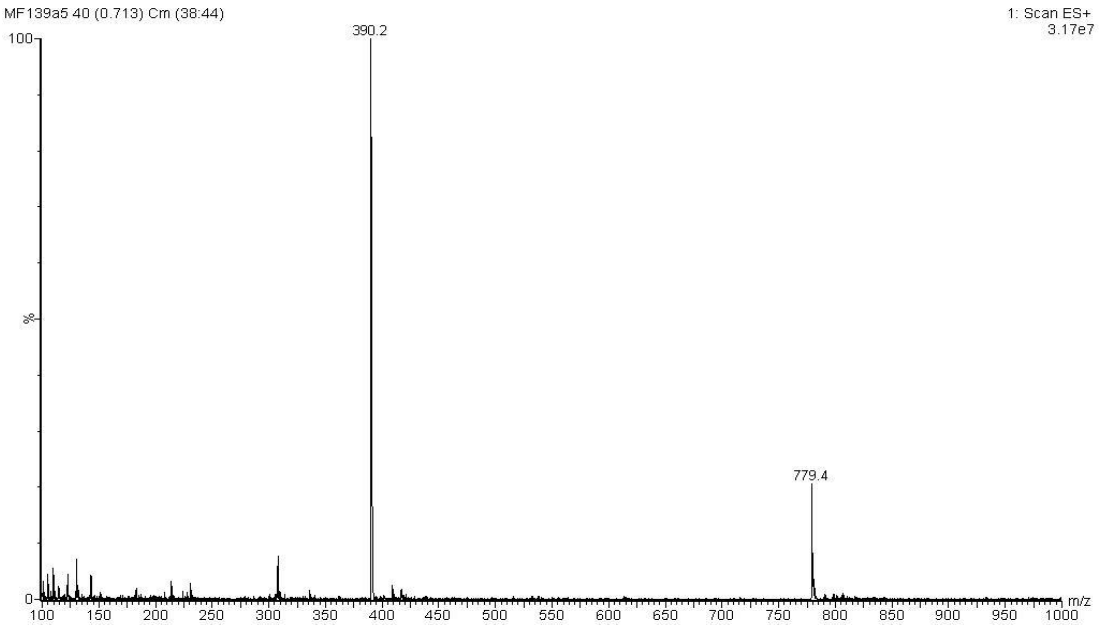

(d)

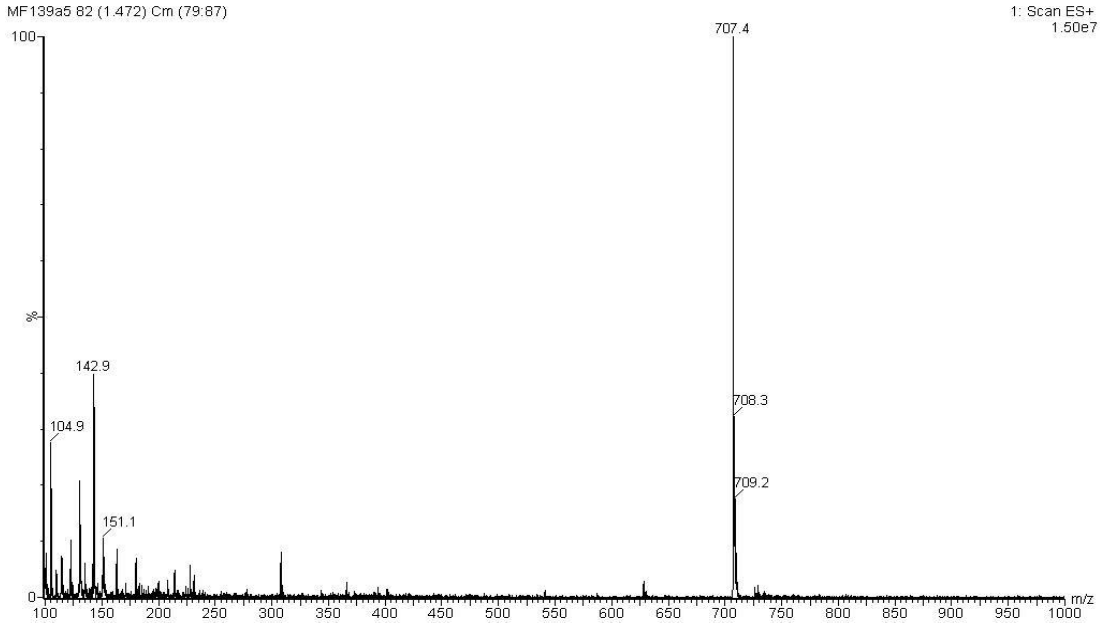

Figure **S55**. (a) TIC and UV trace at t = 4 h, (b) MS data at 0.28–0.44 mins in the UV, (c) MS data at 0.64 mins in the UV and (d) at 1.41 mins in the UV for PD **6** incubated with GSH **1** (10 eq.) at pH 6.5.

LC-MS data for t = 24 h

(a)

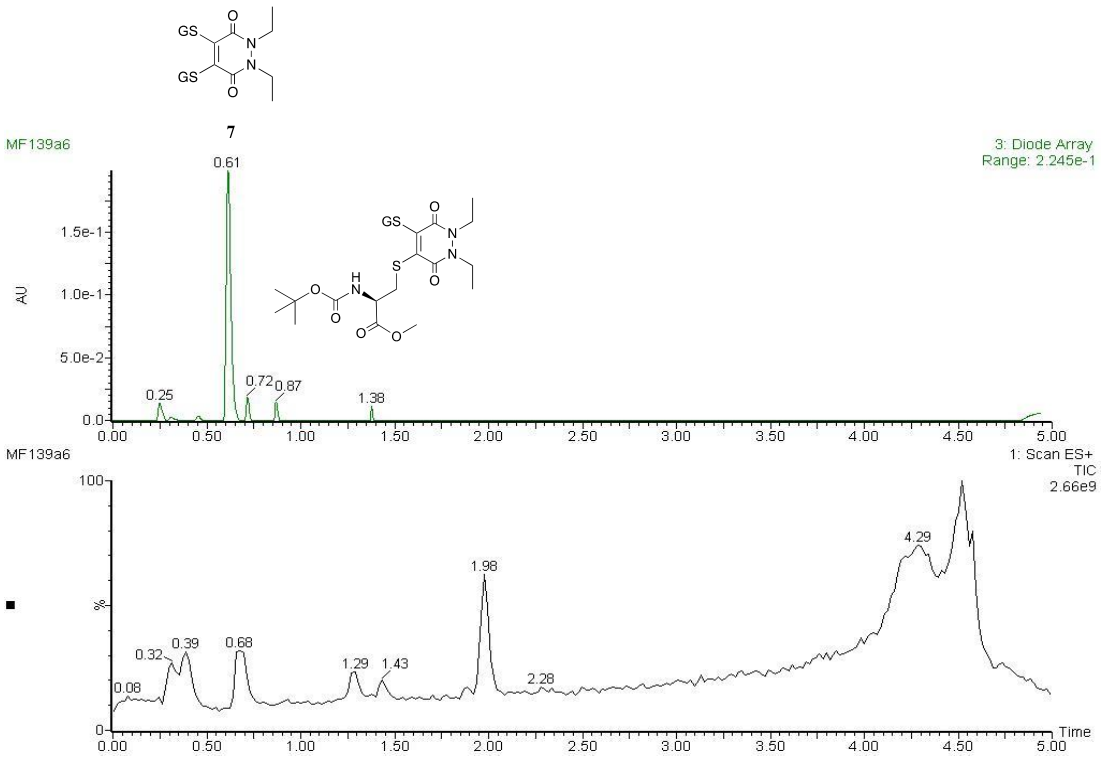
7
MF139a6
3: Diode Array
Range: 2.245e-1
AU
0.61
0.25
0.72
0.87
1.38
MF139a6
1: Scan ES+
TIC
2.66e9
%
0.08
0.32
0.39
0.68
1.29
1.43
1.98
2.28
4.29
Time

(b)

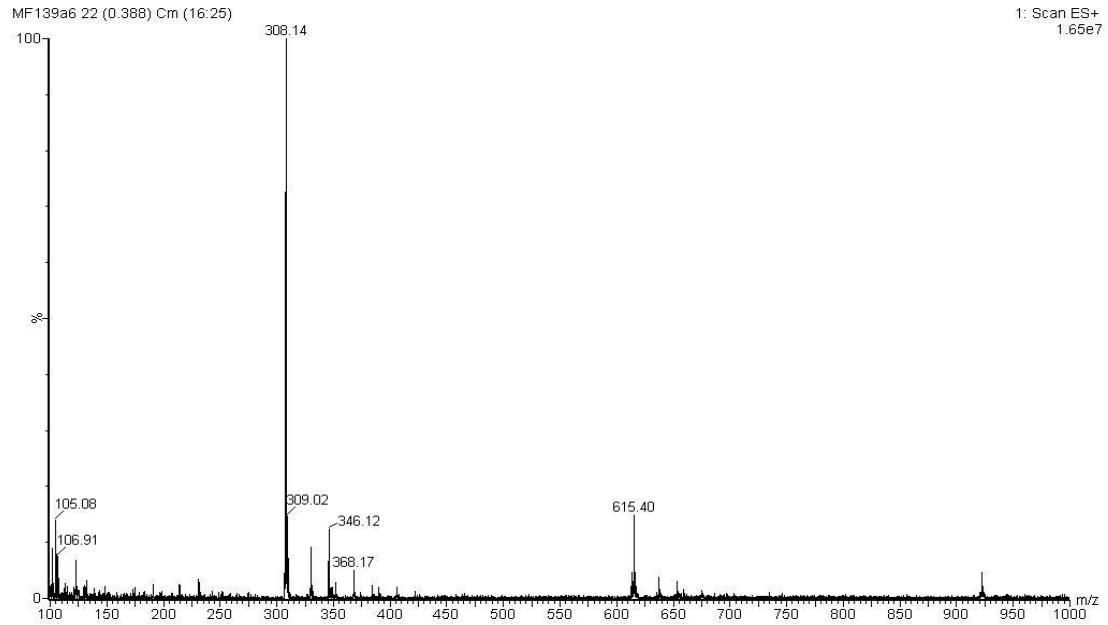
MF139a6 22 (0.388) Cm (16:25)
1: Scan ES+
1.65e7
308.14
%
105.08
106.91
309.02
346.12
368.17
615.40
m/z

(c)

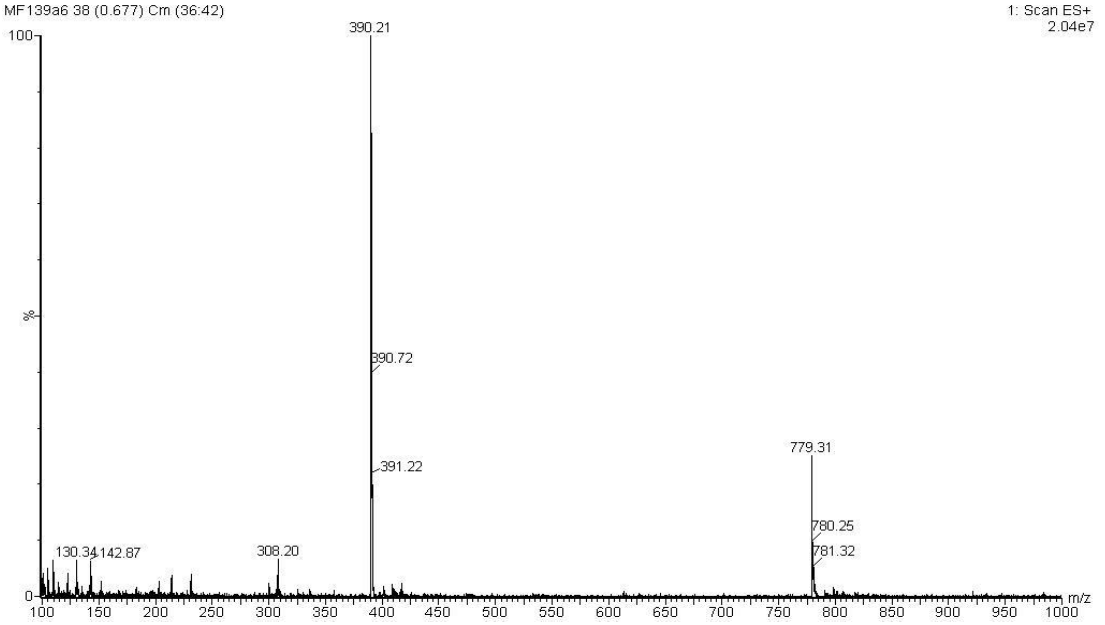
MF139a6 38 (0.677) Cm (36:42)
1: Scan ES+
2.04e7
100
%
0
390.21
390.72
391.22
779.31
780.25
781.32
130.34
142.87
308.20
100 150 200 250 300 350 400 450 500 550 600 650 700 750 800 850 900 950 1000
m/z

(d)

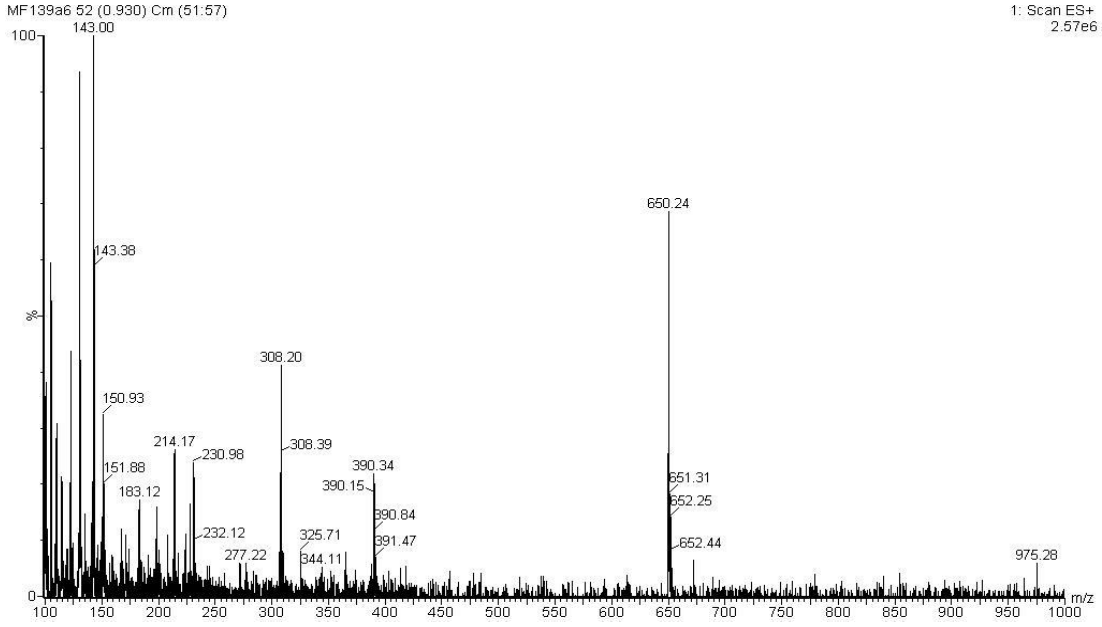
MF139a6 52 (0.930) Cm (51:57)
1: Scan ES+
2.57e6
100
%
0
143.00
143.38
650.24
308.20
150.93
214.17
230.98
308.39
390.34
151.88
390.15
651.31
652.25
183.12
390.84
232.12
325.71
391.47
277.22
344.11
652.44
975.28
100 150 200 250 300 350 400 450 500 550 600 650 700 750 800 850 900 950 1000
m/z

(e)

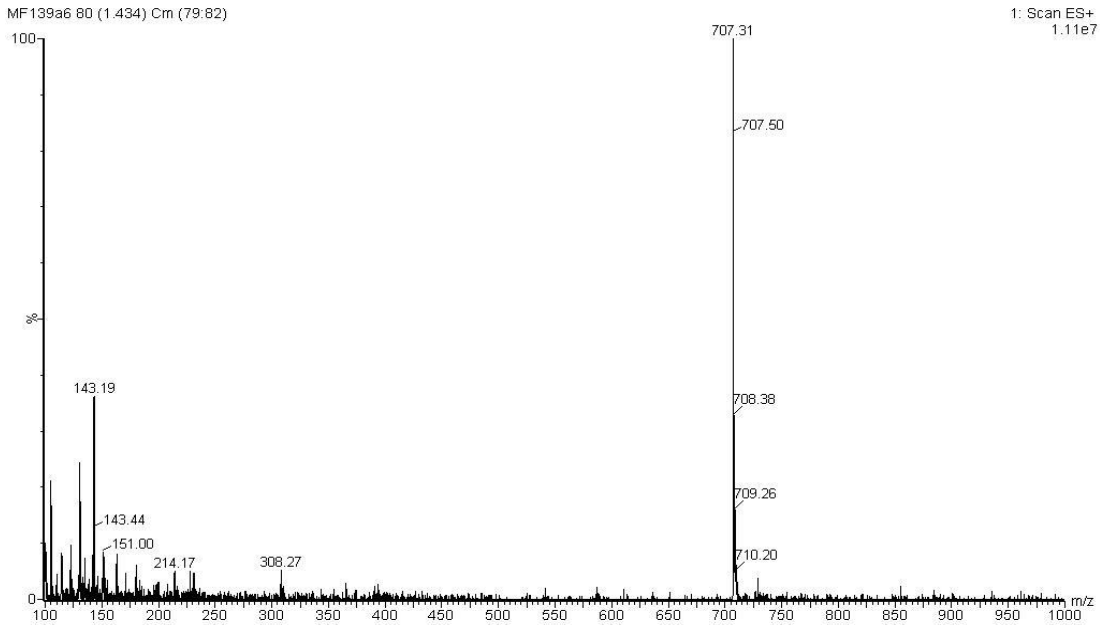

Figure **S56**. (a) TIC and UV trace at t = 24 h, (b) MS data at 0.25–0.44 mins in the UV, (c) MS data at 0.61–0.72 mins in the UV, (d) at 0.87 mins in the UV and (e) at 1.38 mins in the UV for PD **6** incubated with GSH **1** (10 eq.) at pH 6.5.

Incubations involving GSH and PDs 2–6 at pH 5.0

Incubation of PD 2 with GSH (10 eq.)

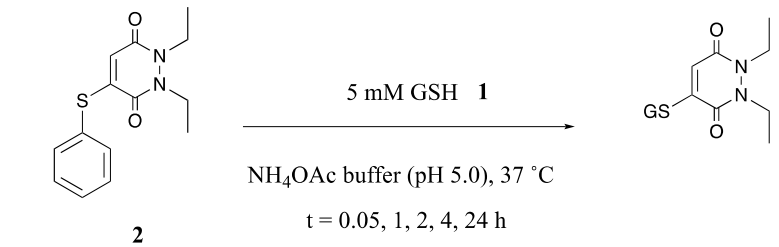

2

276 g/mol

UV r.t.: 1.80–1.97 mins

473 g/mol

UV r.t.: 0.69 mins

PD **2** (10 µL, 10 mM in MeCN, 1 eq.) was added to GSH **1** (190 µL, 5.3 mM, 10 eq.) in ammonium acetate buffer (50 mM, pH 5.0). The mixture was incubated at 37 ˚C for 24 h. The samples were analysed by LC-MS at t = 0.05, 1, 2, 4 and 24 h.

LC-MS data for t = 0.05 h

(a)

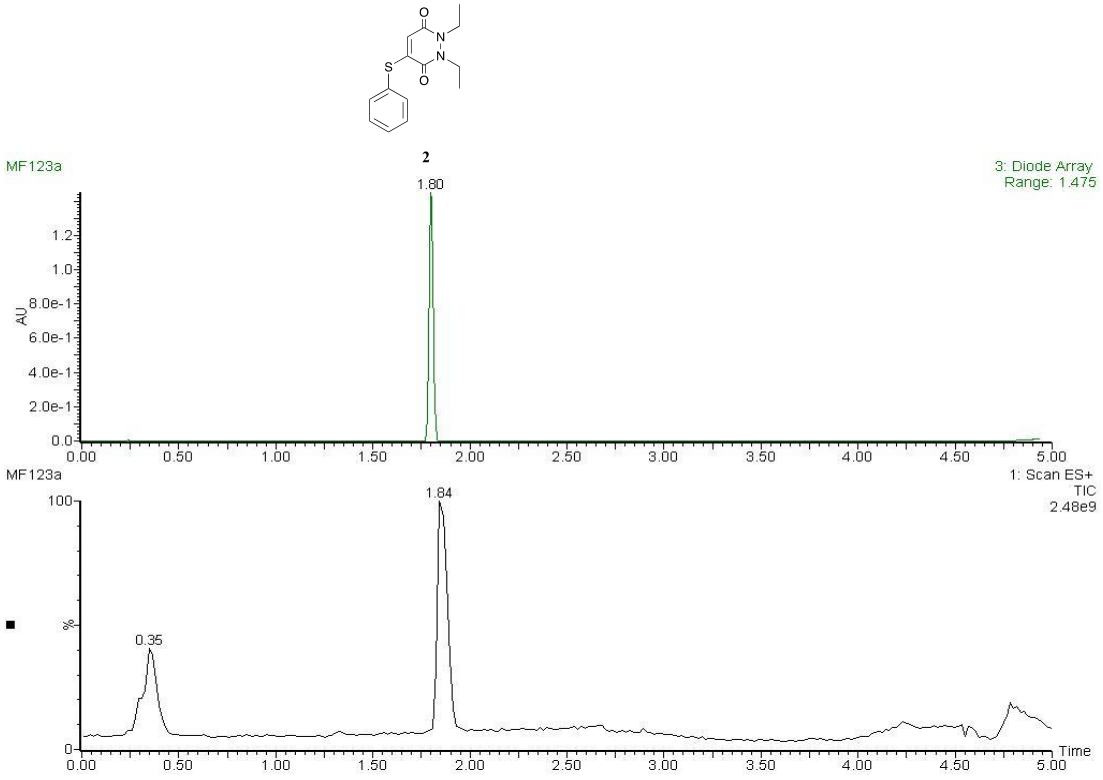

(b)

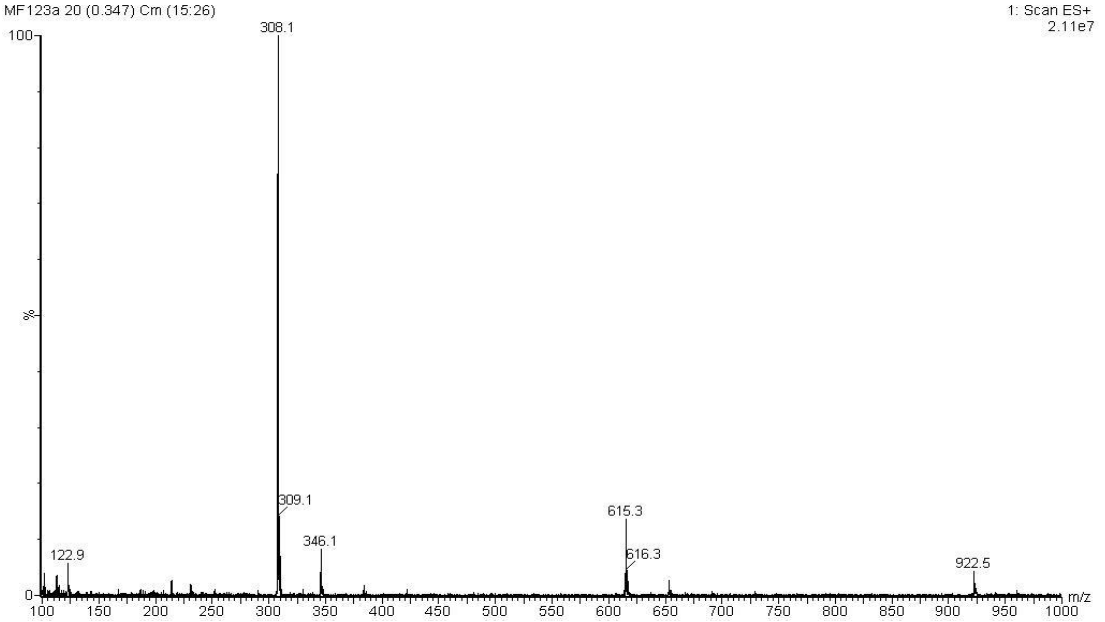

(c)

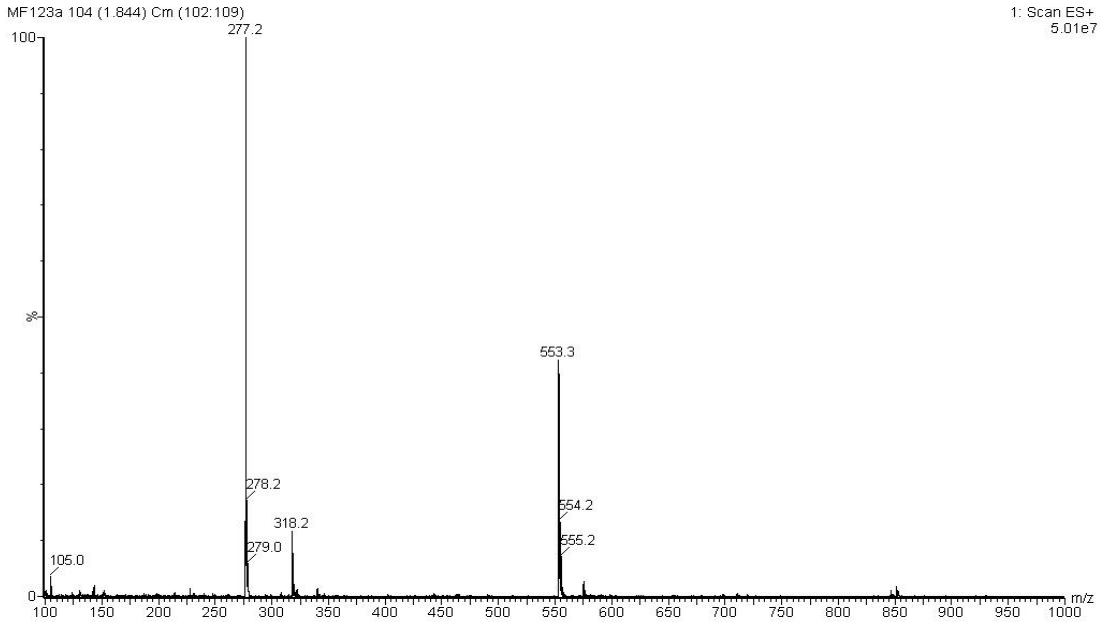

Figure **S57**. (a) TIC and UV trace at t = 0.05 h, (b) MS data at 0.35 mins in the TIC and (c) MS data at 1.80 mins in the UV for PD **2** incubated with GlSH **1** (10 eq.) at pH 5.0.

LC-MS data for t = 1 h

(a)

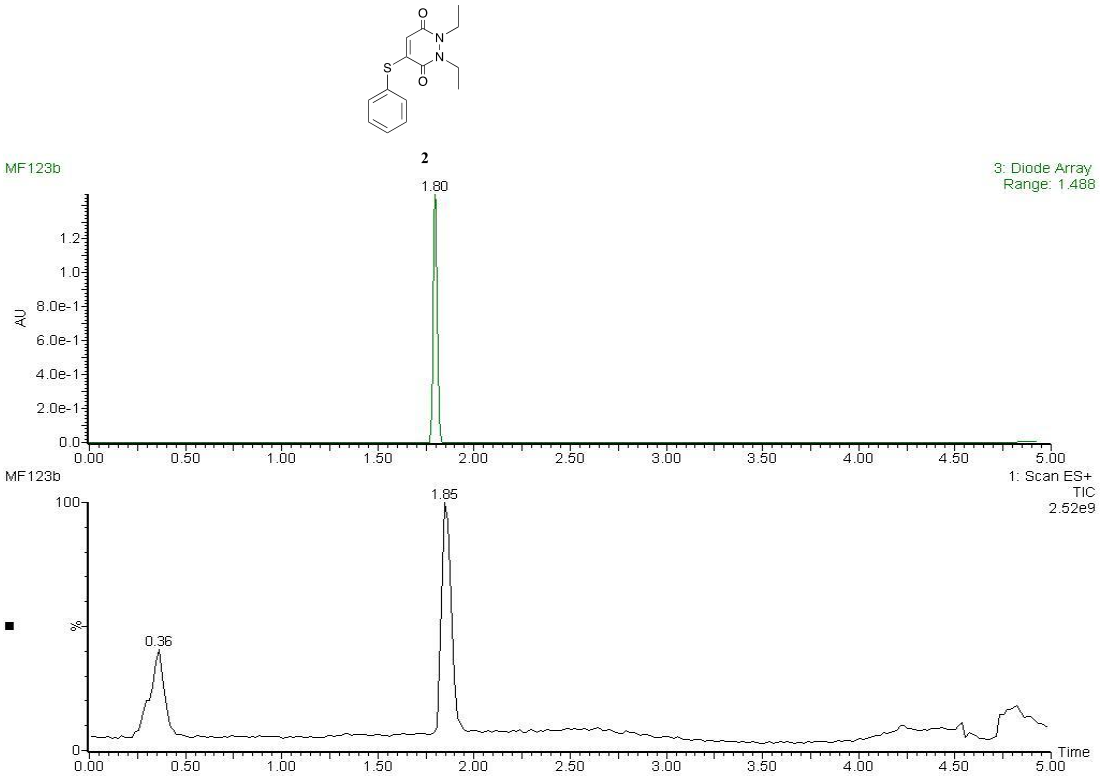
2
MF123b
3: Diode Array
Range: 1.488
1.80
AU
MF123b
1: Scan ES+
TIC
2.52e9
1.85
0.36
%
Time

(b)

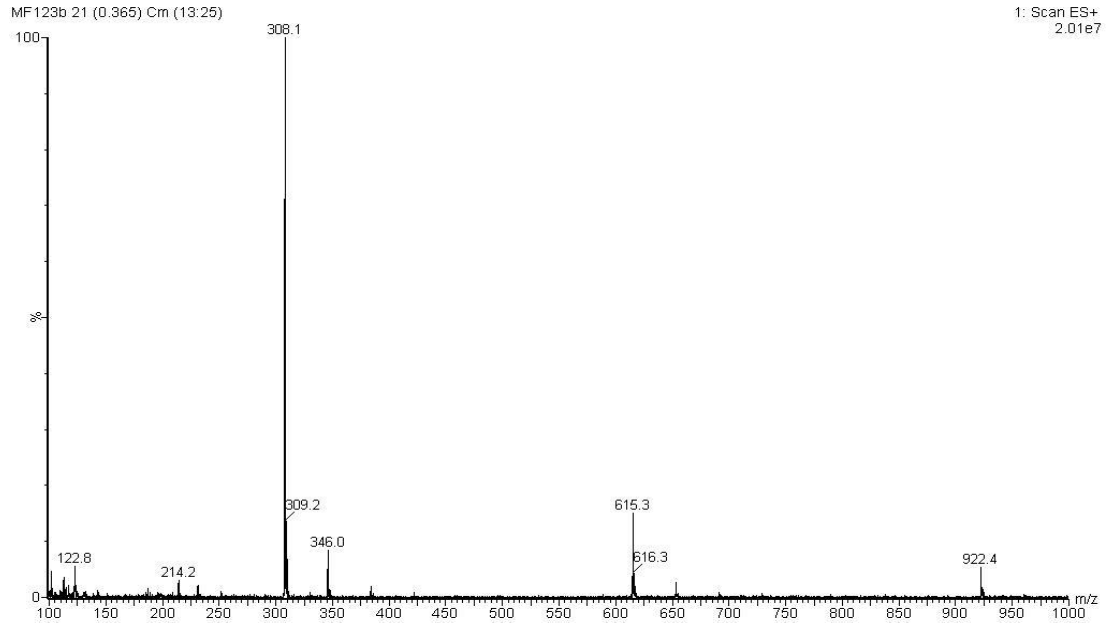
MF123b 21 (0.365) Cm (13:25)
1: Scan ES+
2.01e7
308.1
309.2
615.3
346.0
616.3
122.8
214.2
922.4
%
m/z

(c)

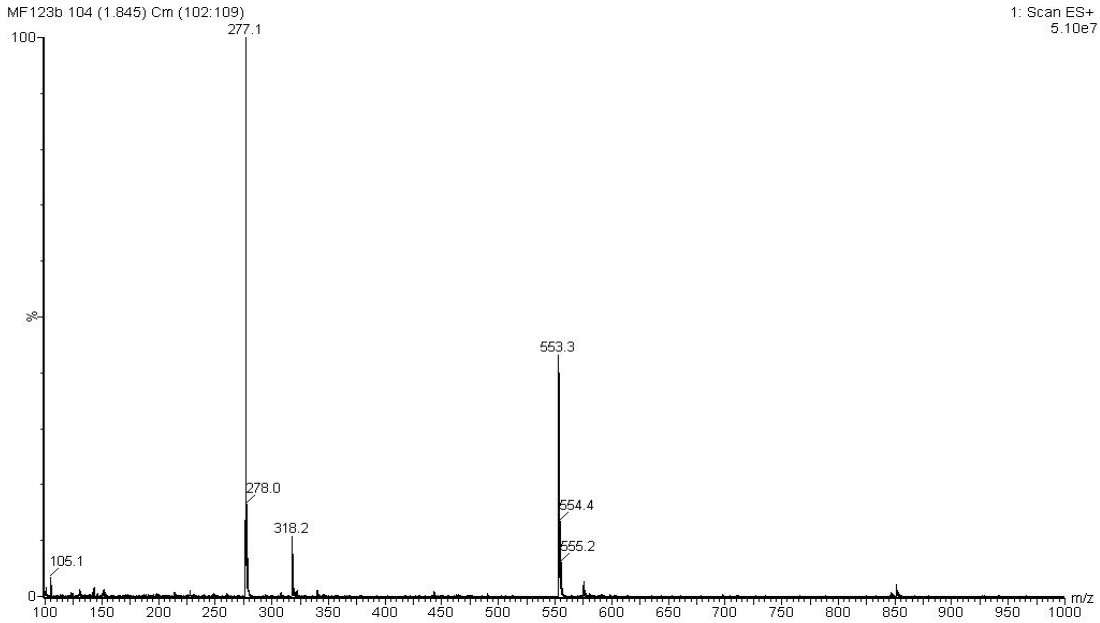

Figure **S58**. (a) TIC and UV trace at t = 1 h, (b) MS data at 0.36 mins in the TIC and (c) MS data at 1.80 mins in the UV for PD **2** incubated with GSH **1** (10 eq.) at pH 5.0.

LC-MS data for t = 2 h

(a)

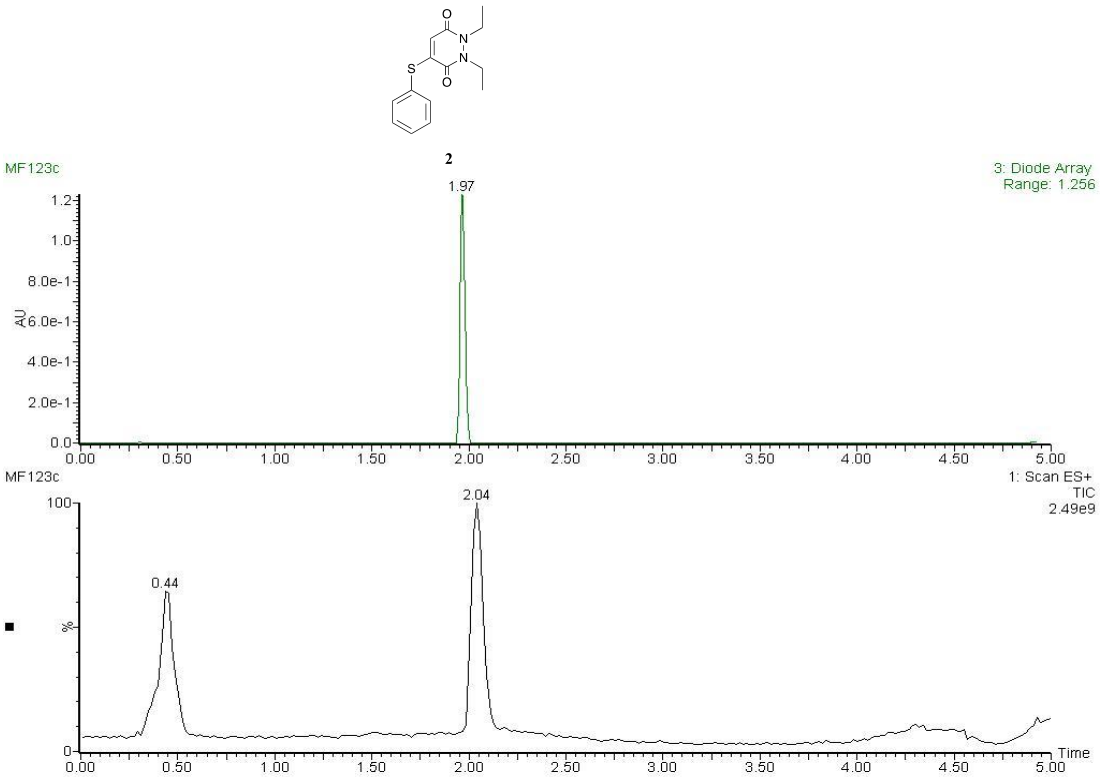
2
MF123c
3: Diode Array
Range: 1.256
1.97
AU
MF123c
1: Scan ES+
TIC
2.49e9
2.04
0.44
%
Time

(b)

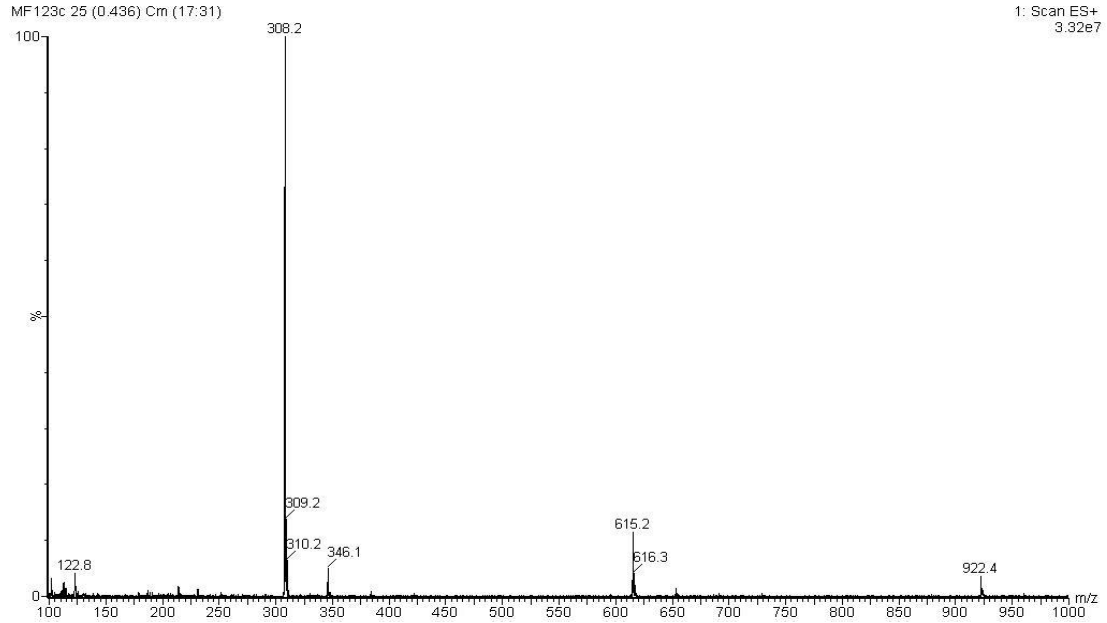
MF123c 25 (0.436) Cm (17:31)
1: Scan ES+
3.32e7
308.2
309.2
310.2
346.1
122.8
615.2
616.3
922.4
%
m/z

(c)

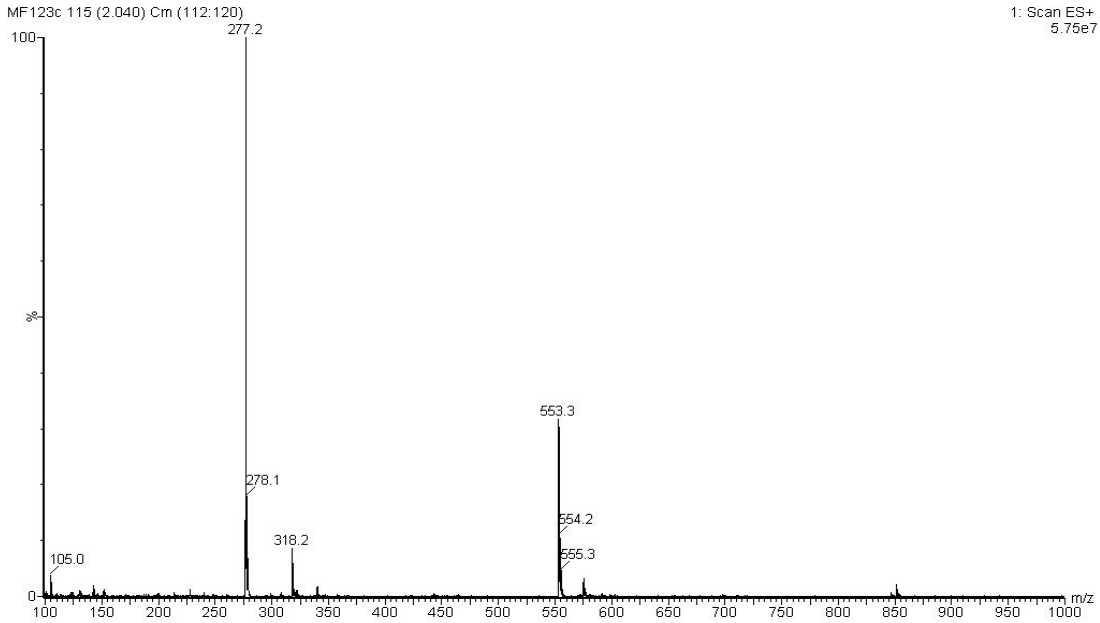

Figure **S59**. (a) TIC and UV trace at t = 2 h, (b) MS data at 0.44 mins in the TIC and (c) MS data at 1.97 mins in the UV for PD **2** incubated with GSH **1** (10 eq.) at pH 5.0.

LC-MS data for t = 4 h

(a)

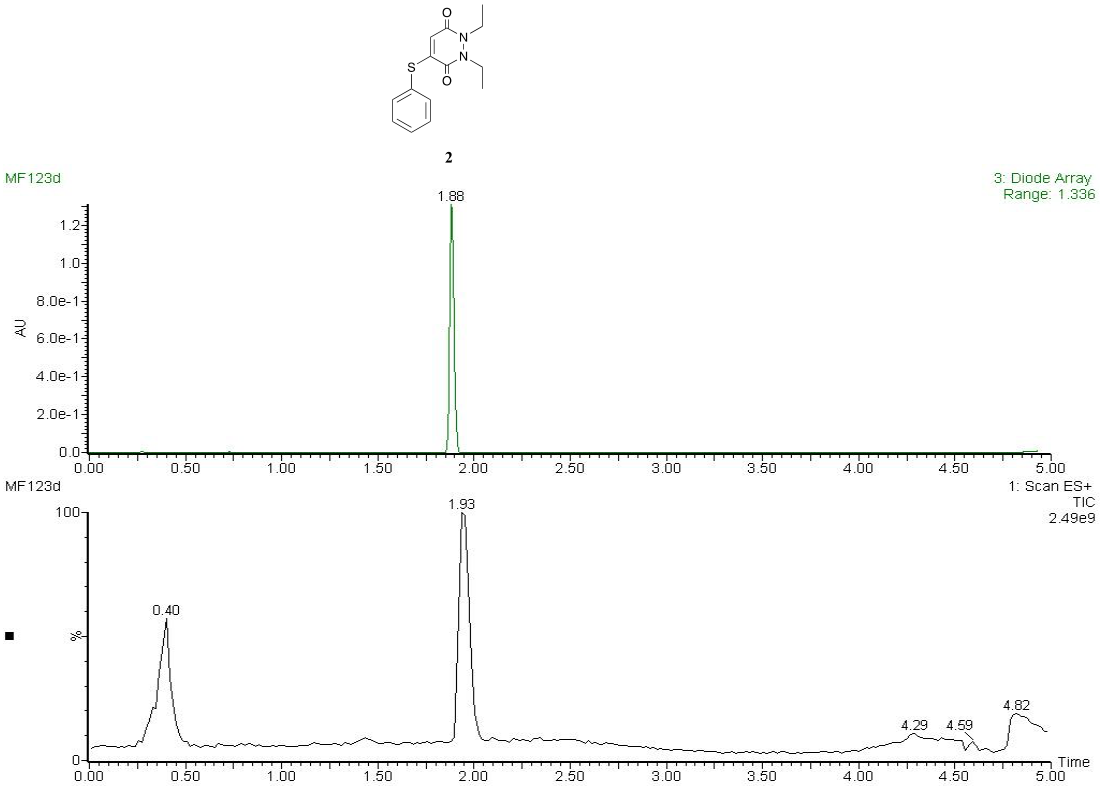

(b)

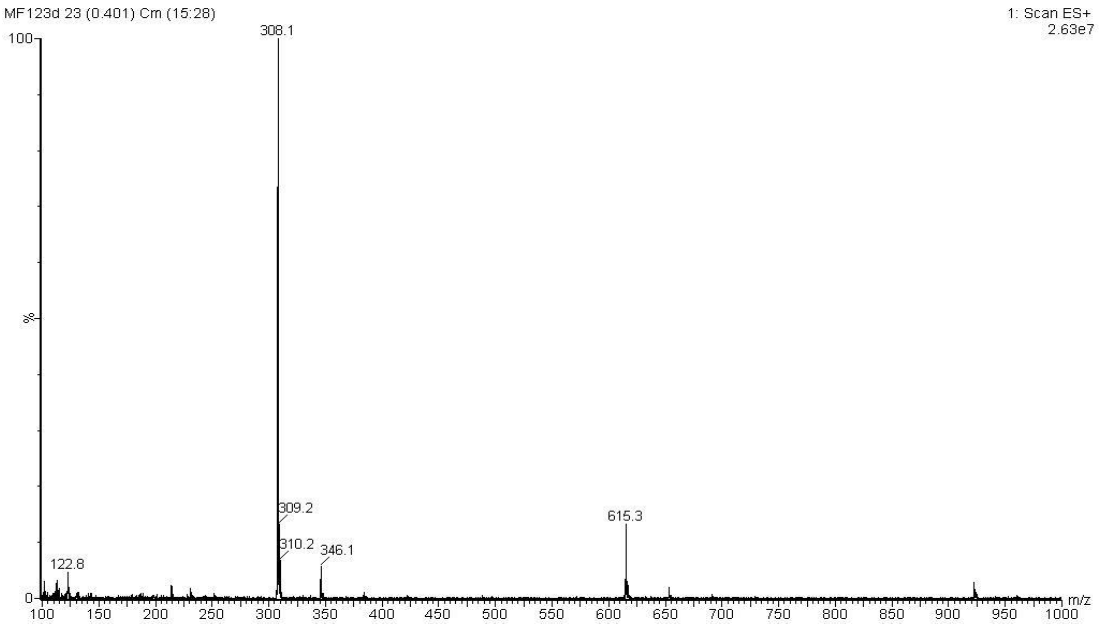

(c)

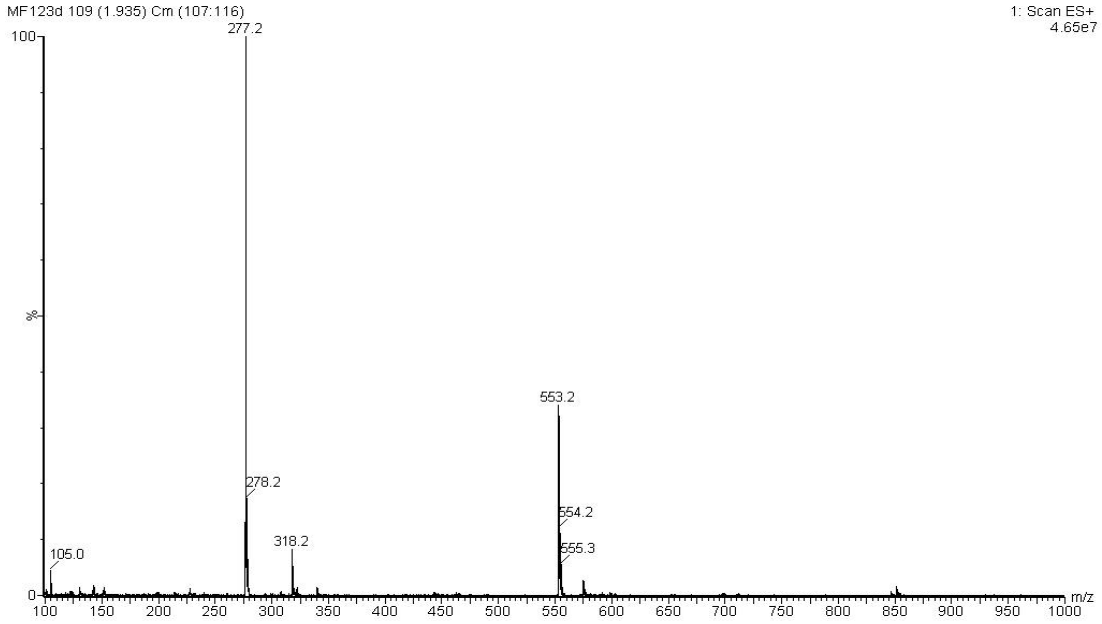

Figure **S60**. (a) TIC and UV trace at t = 4 h, (b) MS data at 0.40 mins in the TIC and (c) MS data at 1.88 mins in the UV for PD **2** incubated with GSH **1** (10 eq.) at pH 5.0.

LC-MS data for t = 24 h

(a)

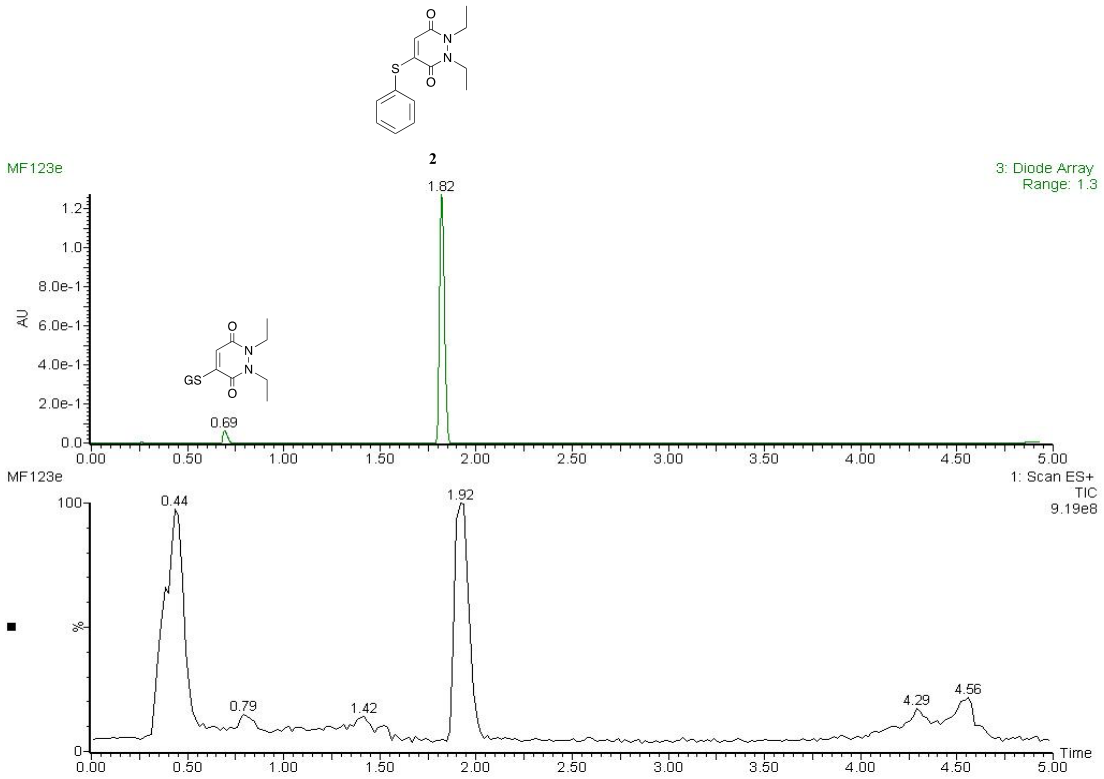
2
MF123e
3: Diode Array
Range: 1.3
1.82
AU
GS
0.69
MF123e
1: Scan ES+
TIC
9.19e8
0.44
1.92
0.79
1.42
4.29
4.56
%
Time

(b)

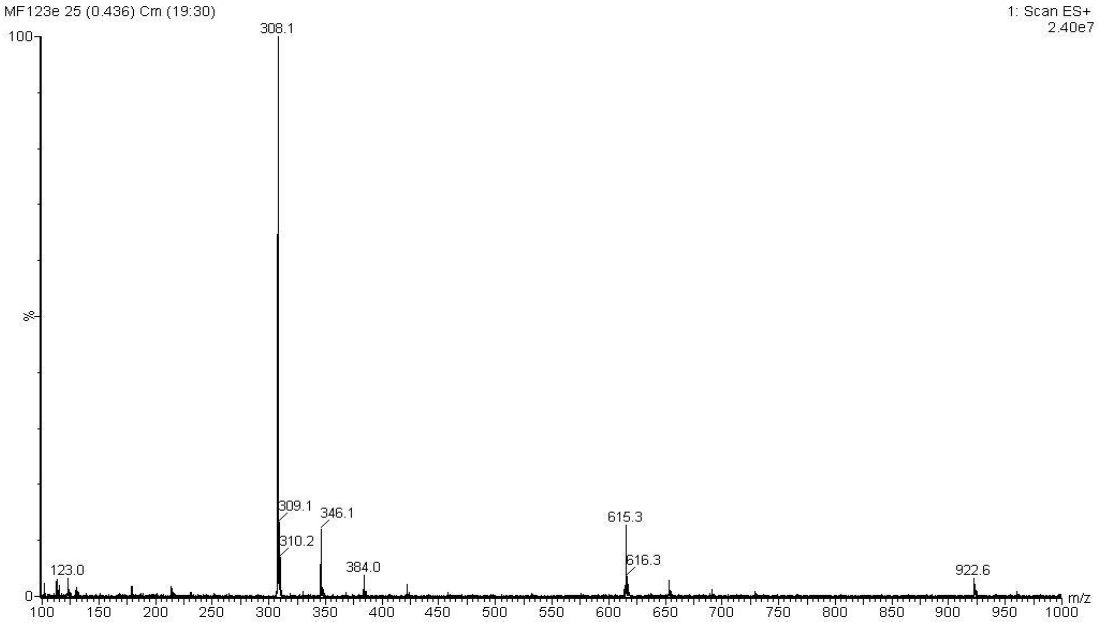
MF123e 25 (0.436) Cm (19:30)
1: Scan ES+
2.40e7
308.1
309.1
346.1
310.2
615.3
616.3
123.0
384.0
922.6
%
m/z

(c)

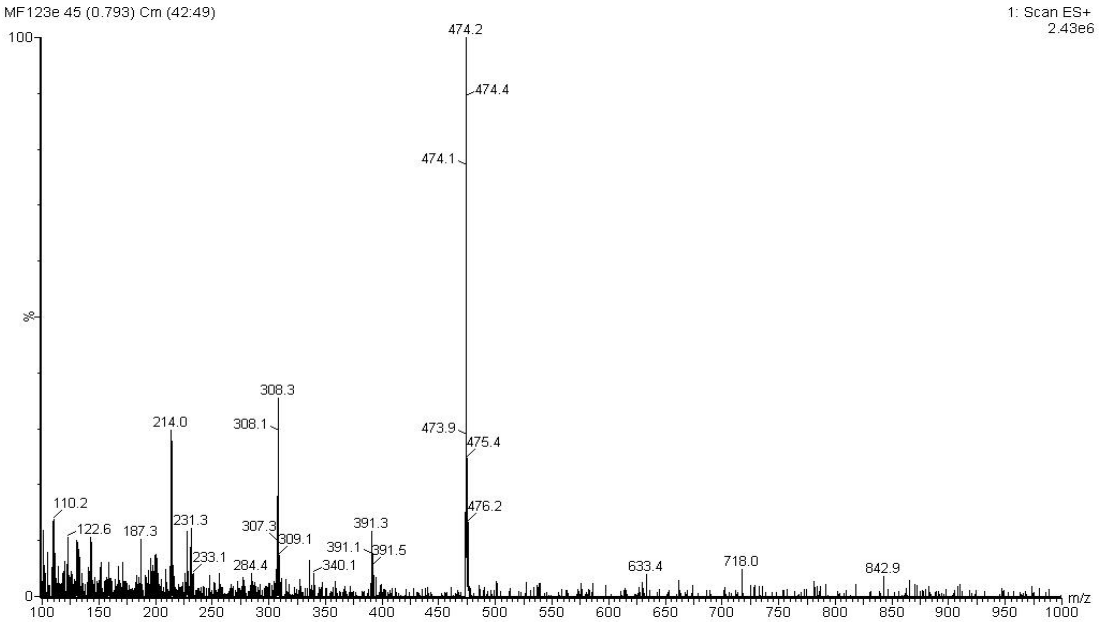

(d)

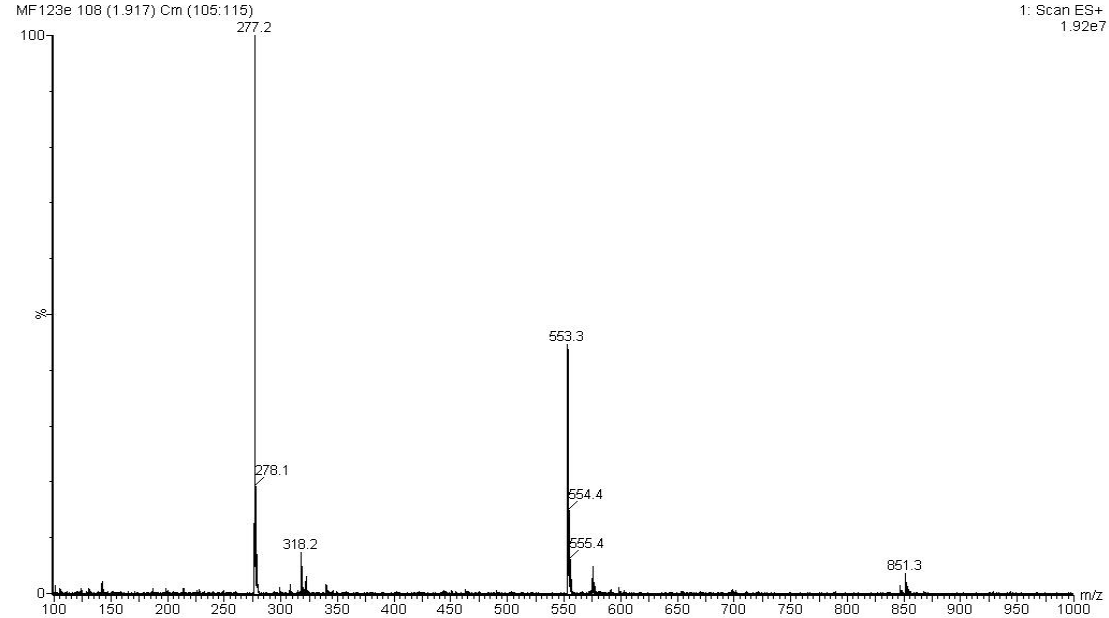

Figure **S61**. (a) TIC and UV trace at t = 24 h, (b) MS data at 0.44 mins in the TIC, (c) MS data at 0.69 mins in the UV and (d) at 1.82 mins in the UV for PD **2** incubated with GSH **1** (10 eq.) at pH 5.0.

Incubation of PD 3 with GSH (10 eq.)

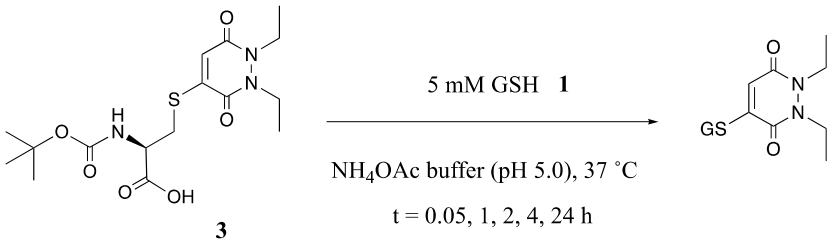

3

401 g/mol

473 g/mol

UV r.t.: 1.75, 1.86 mins

UV r.t.: 0.67 mins

PD **3** (10 µL, 10 mM in MeCN, 1 eq.) was added to GSH **1** (190 µL, 5.3 mM, 10 eq.) in ammonium acetate buffer (50 mM, pH 5.0). The mixture was incubated at 37 ˚C for 24 h. The samples were analysed by LC-MS at t = 0.05, 1, 2, 4 and 24 h.

LC-MS data for t = 0.05 h

(a)

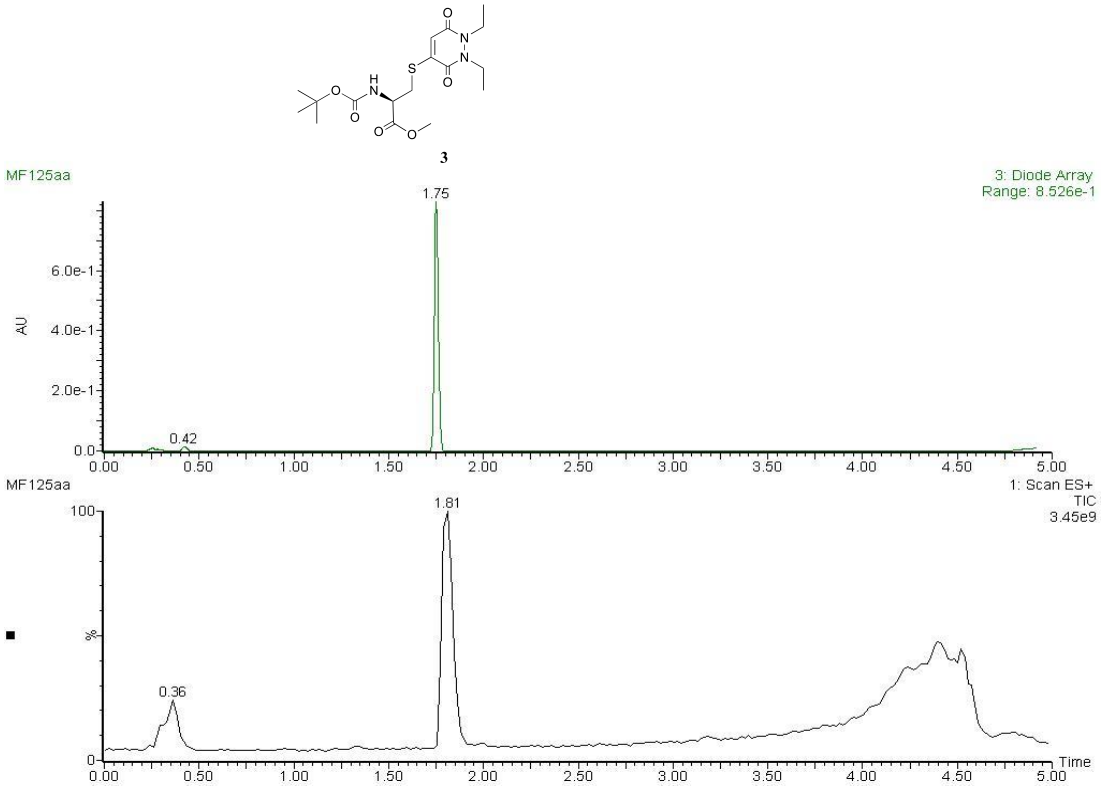

(b)

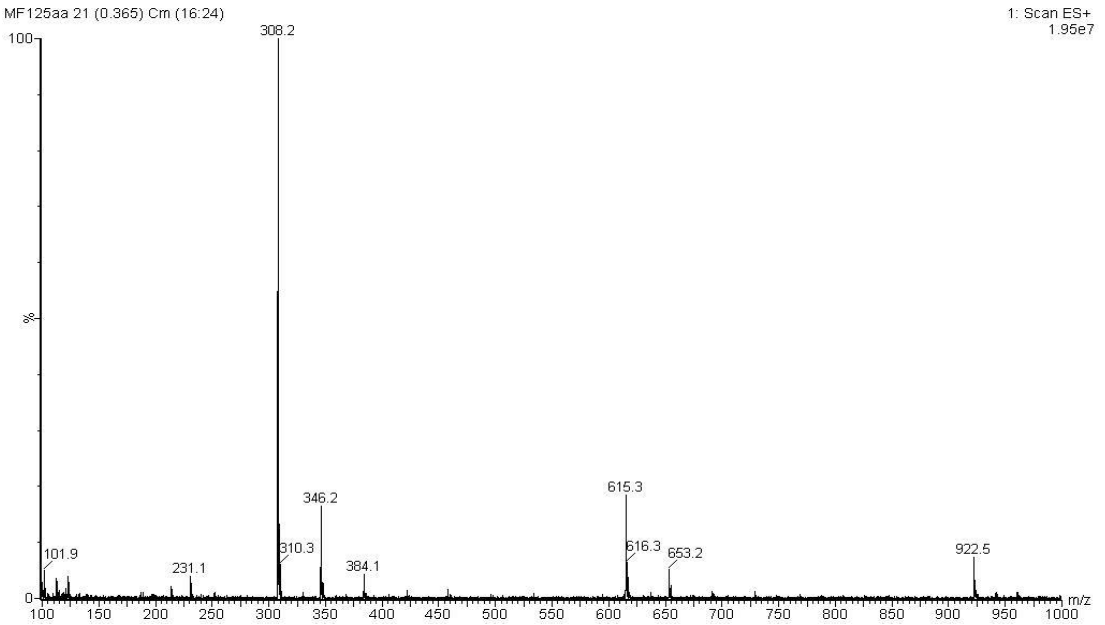

(c)

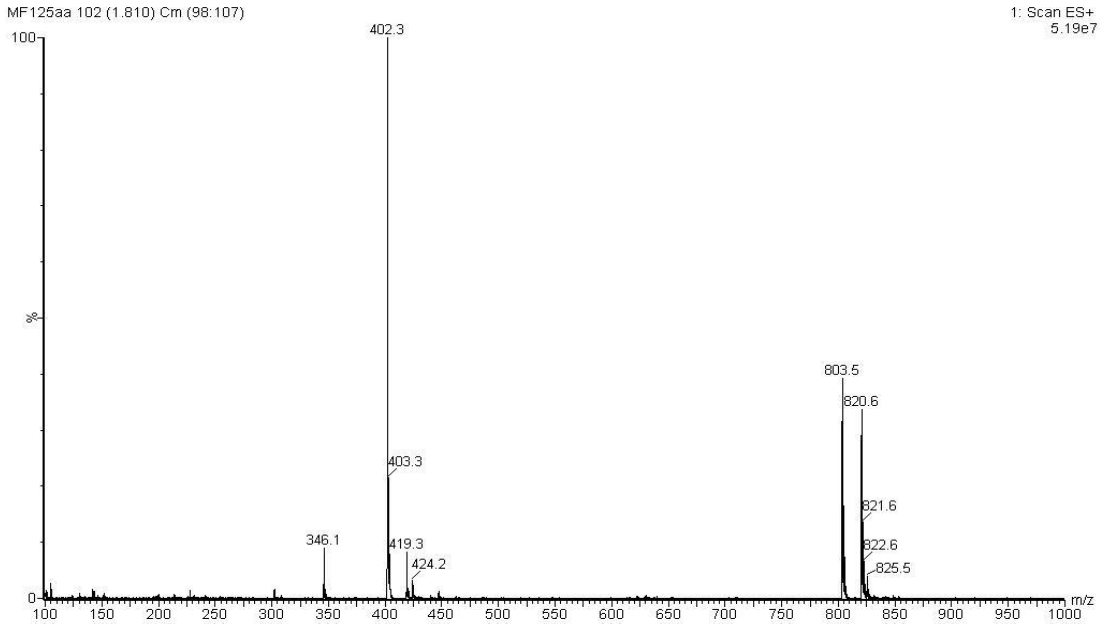

Figure **S62**. (a) TIC and UV trace at t = 0.05 h, (b) MS data at 0.24–0.42 mins in the UV, and (c) MS data at 1.75 mins in the UV for PD **3** incubated with GSH **1** (10 eq.) at pH 5.0.

LC-MS data for t = 1 h

(a)

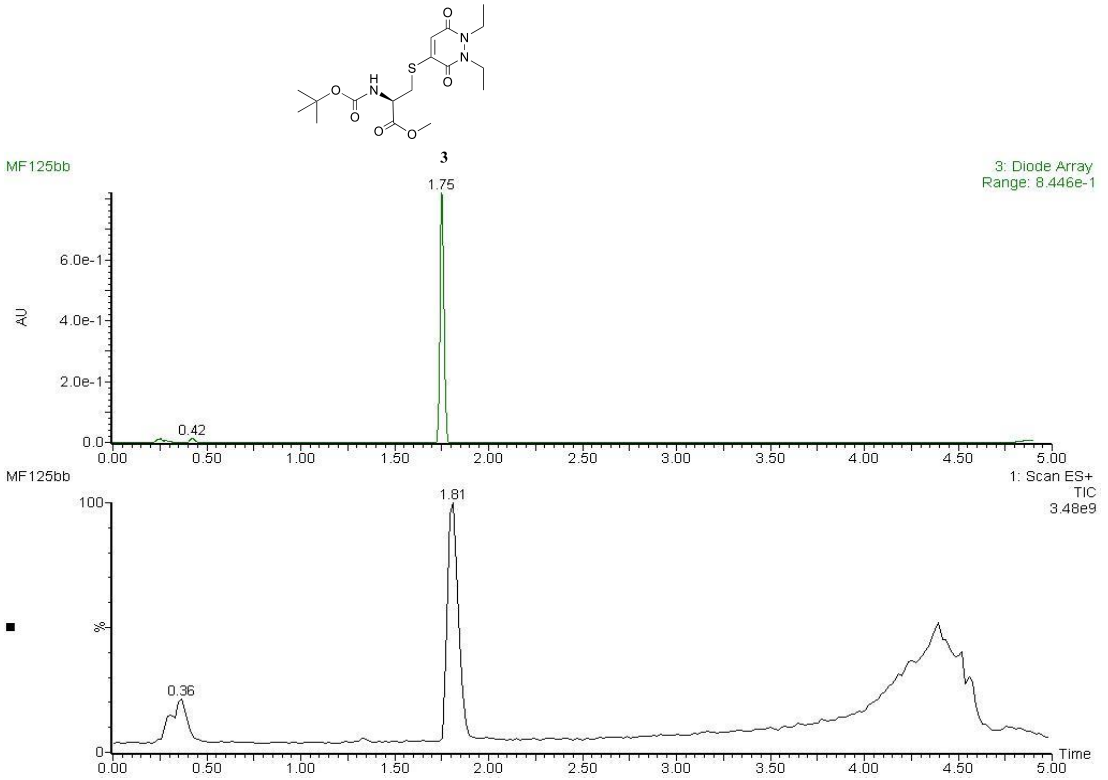
3
MF125bb
3: Diode Array
Range: 8.446e-1
1.75
AU
0.42
MF125bb
1: Scan ES+
TIC
3.48e9
1.81
%
0.36
Time

(b)

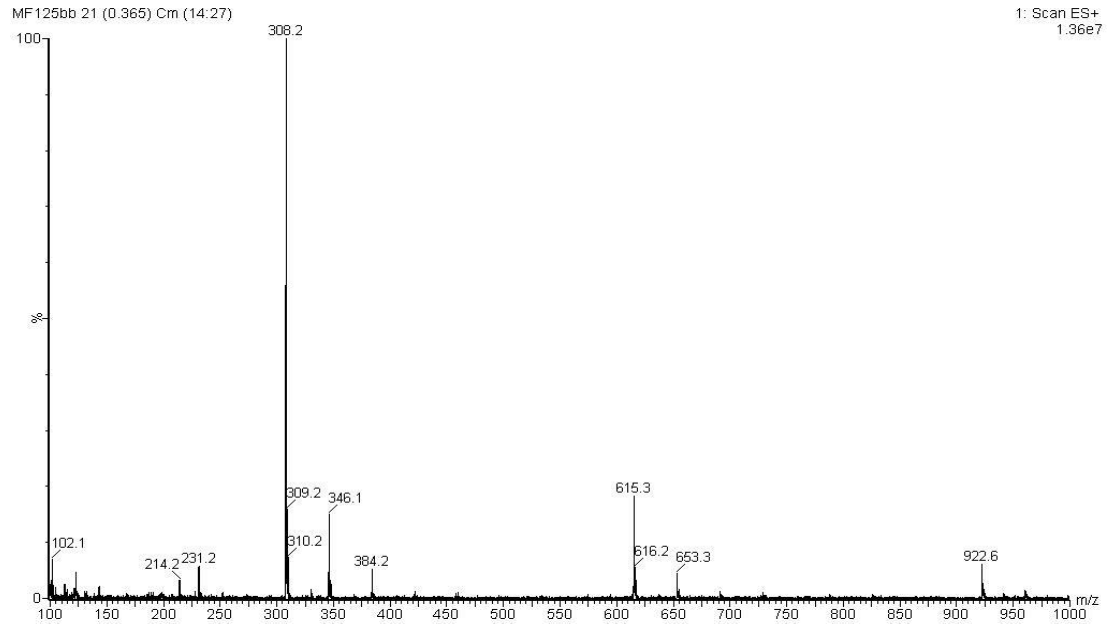
MF125bb 21 (0.365) Cm (14:27)
1: Scan ES+
1.36e7
308.2
%
309.2
346.1
615.3
102.1
310.2
616.2
653.3
214.2
231.2
384.2
922.6
m/z

(c)

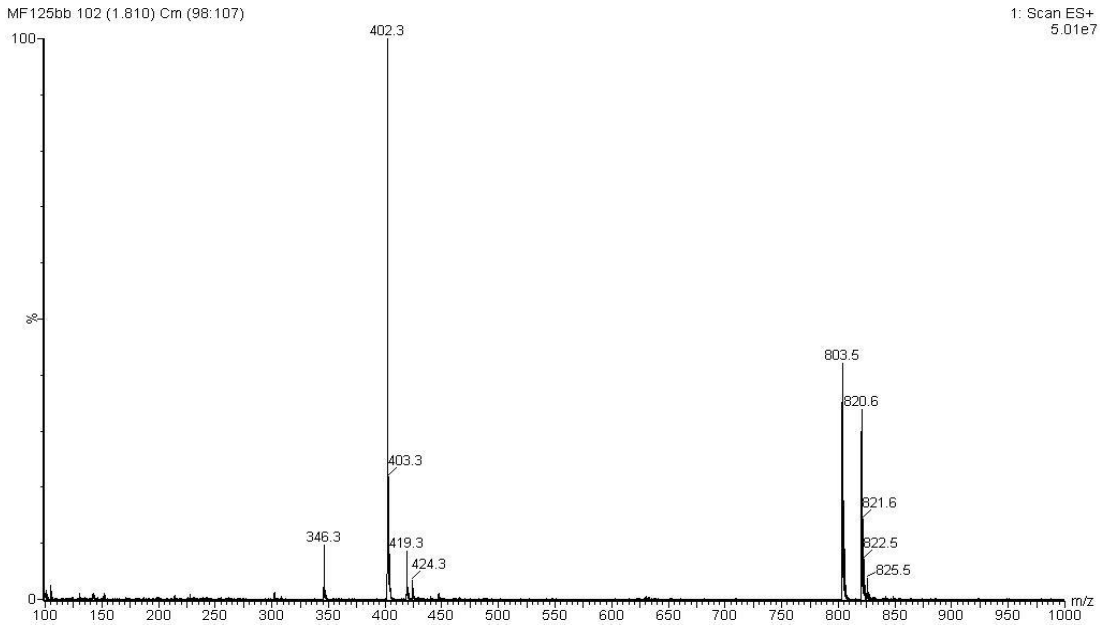

Figure **S63**. (a) TIC and UV trace at t = 1 h, (b) MS data at 0.24–0.42 mins in the UV, and (c) MS data at 1.75 mins in the UV forPD **3** incubated with GSH **1** (10 eq.) at pH 5.0.

LC-MS data for t = 2 h

(a)

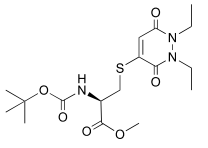

3

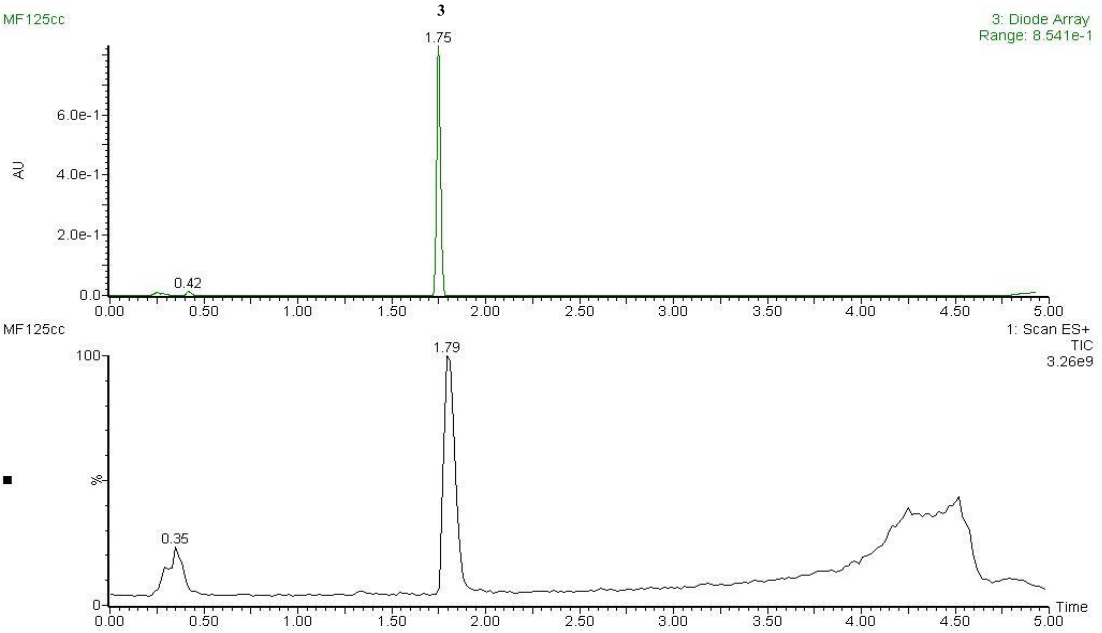
MF125cc
3: Diode Array
Range: 8.541e-1
1.75
6.0e-1
4.0e-1
2.0e-1
0.0
AU
0.42
0.00
0.50
1.00
1.50
2.00
2.50
3.00
3.50
4.00
4.50
5.00
MF125cc
1: Scan ES+
TIC
3.26e9
100
%
1.79
0.35
0
Time

(b)

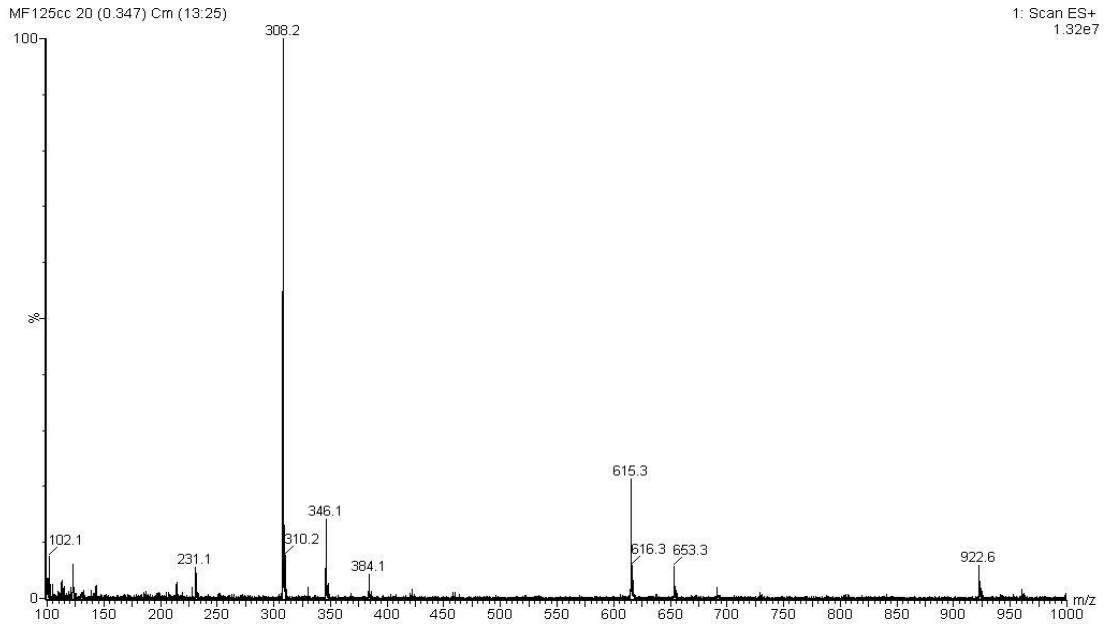
MF125cc 20 (0.347) Cm (13:25)
1: Scan ES+
1.32e7
100
%
308.2
615.3
346.1
102.1
310.2
231.1
384.1
616.3
653.3
922.6
0
100
150
200
250
300
350
400
450
500
550
600
650
700
750
800
850
900
950
1000
m/z

(c)

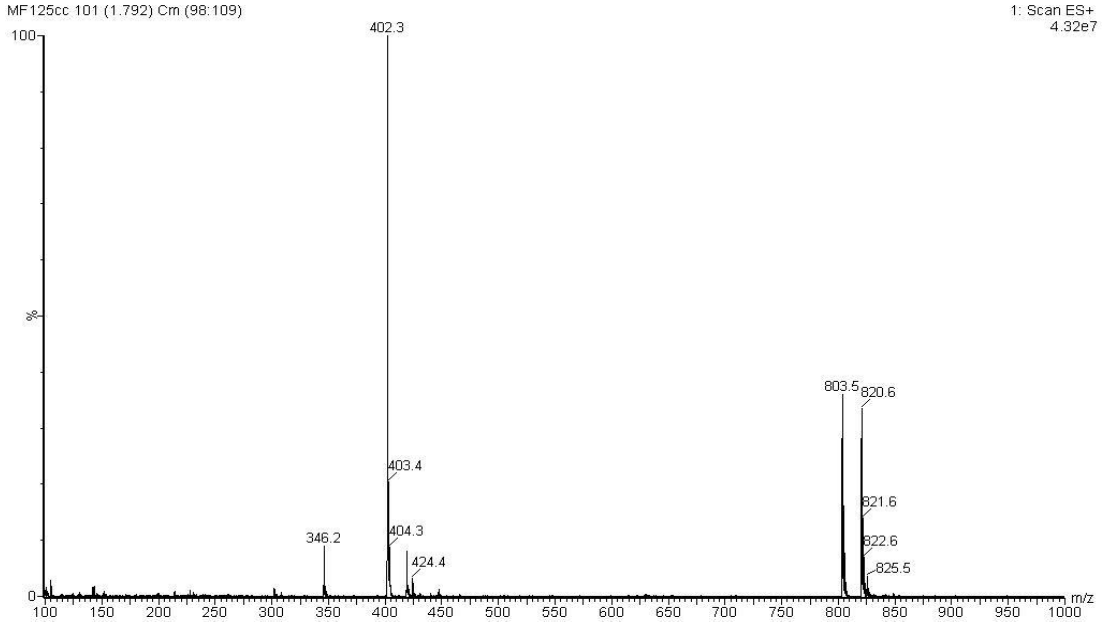

Figure **S64**. (a) TIC and UV trace at t = 2 h, (b) MS data at 0.24–0.42 mins in the UV, and (c) MS data at 1.75 mins in the UV for PD **3** incubated with GSH **1** (10 eq.) at pH 5.0.

LC-MS data for t = 4 h

(a)

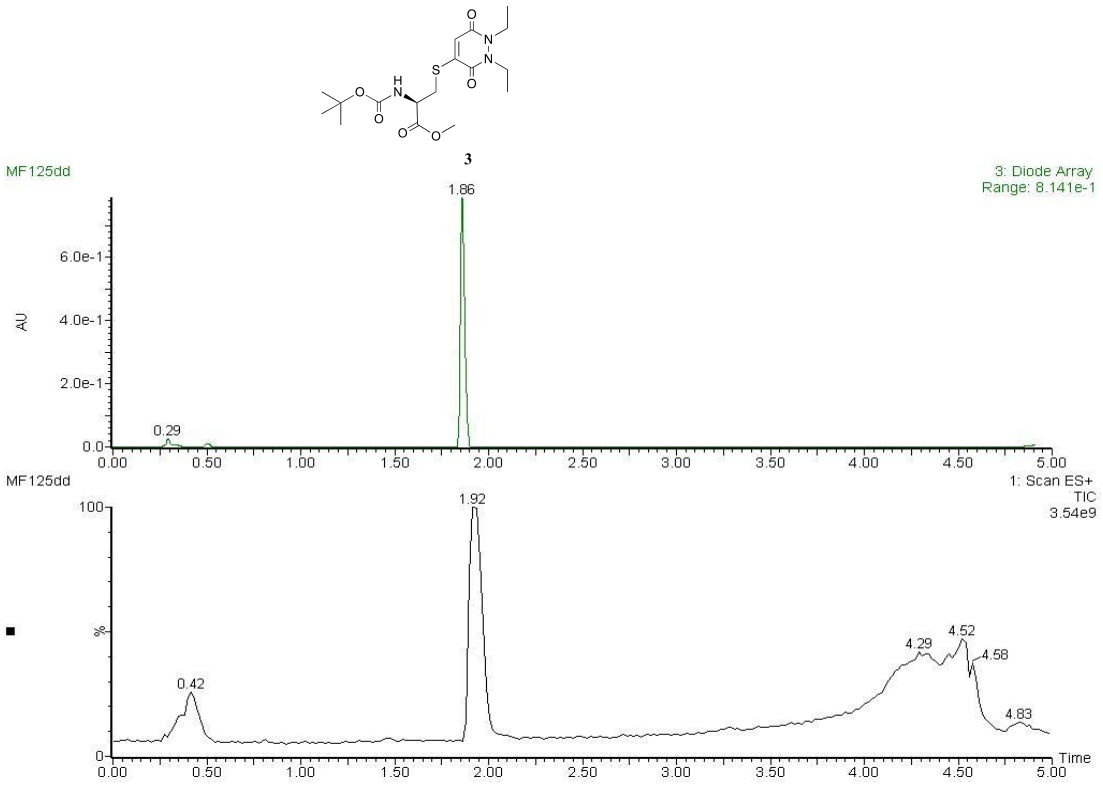

(b)

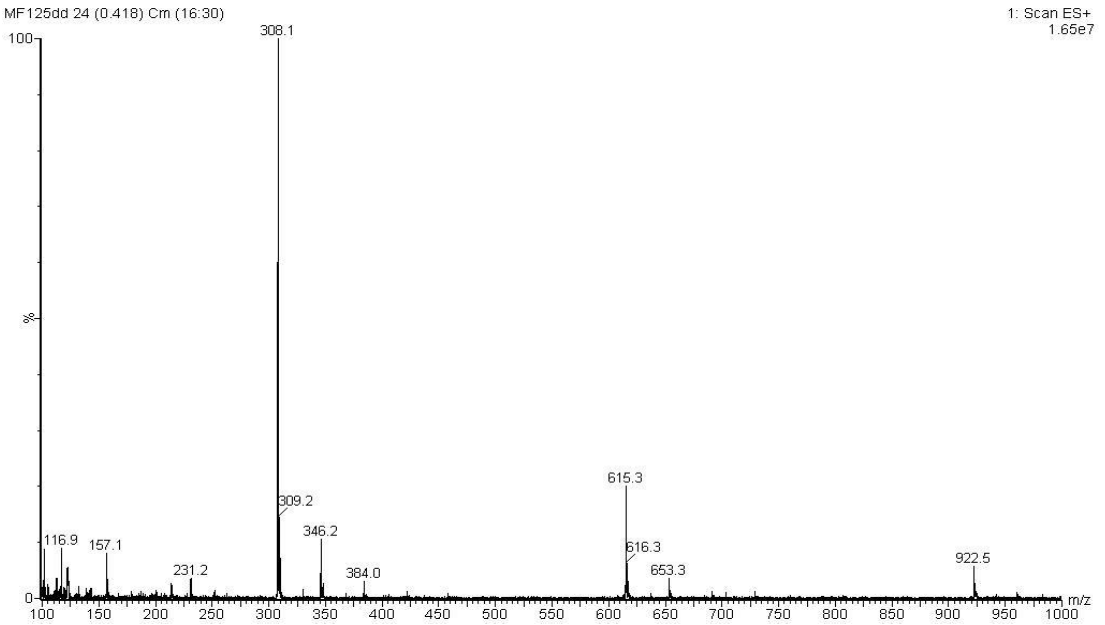

(c)

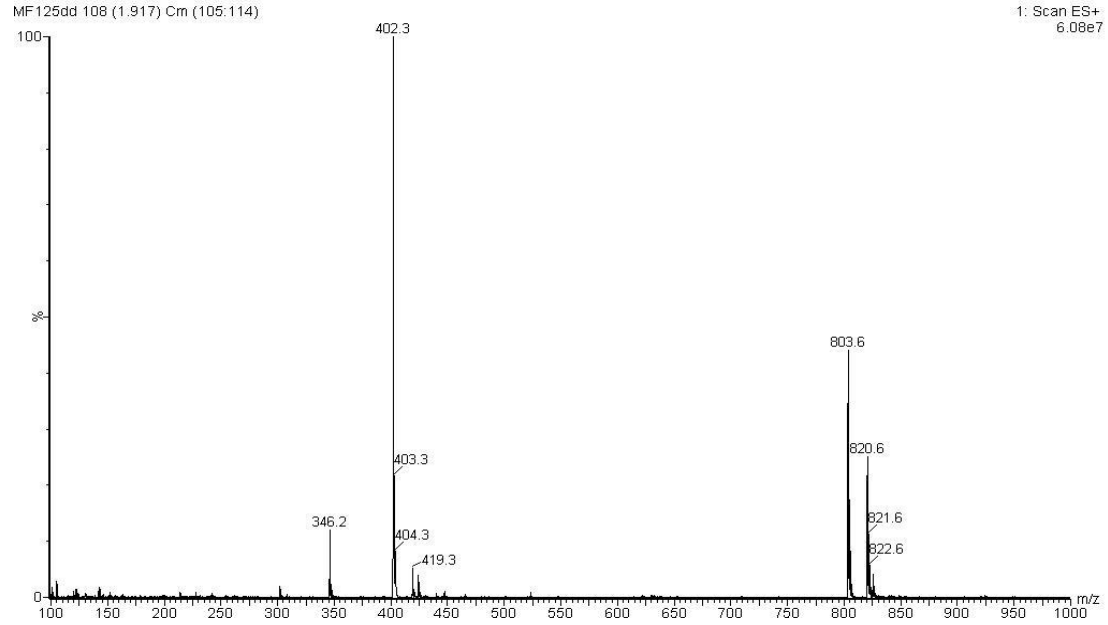

Figure **S65**. (a) TIC and UV trace at t = 4 h, (b) MS data at 0.29–0.42 mins in the UV and (c) MS data at 1.86 mins in the UV for PD **3** incubated with GSH **1** (10 eq.) at pH 5.0.

LC-MS data for t = 24 h

(a)

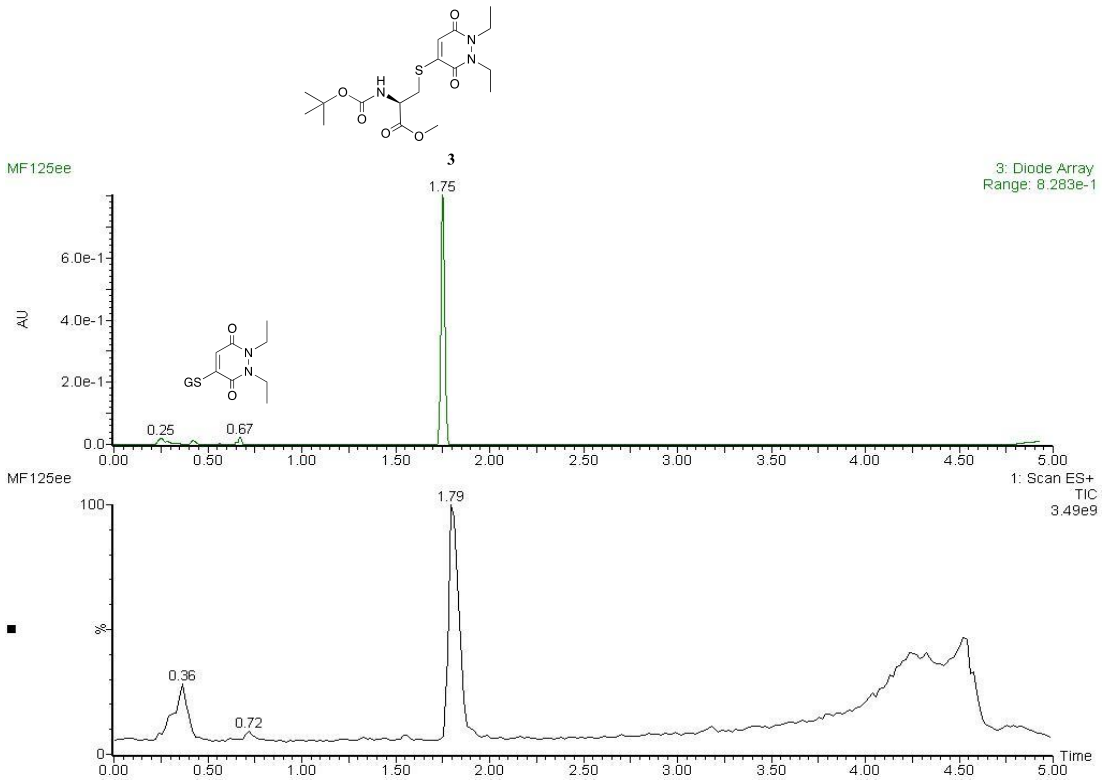
3
MF125ee
3: Diode Array
Range: 8.283e-1
1.75
AU
6.0e-1
4.0e-1
2.0e-1
0.0
GS
0.25
0.67
0.00
0.50
1.00
1.50
2.00
2.50
3.00
3.50
4.00
4.50
5.00
MF125ee
1: Scan ES+
TIC
3.49e9
100
%
1.79
0.36
0.72
0
Time

(b)

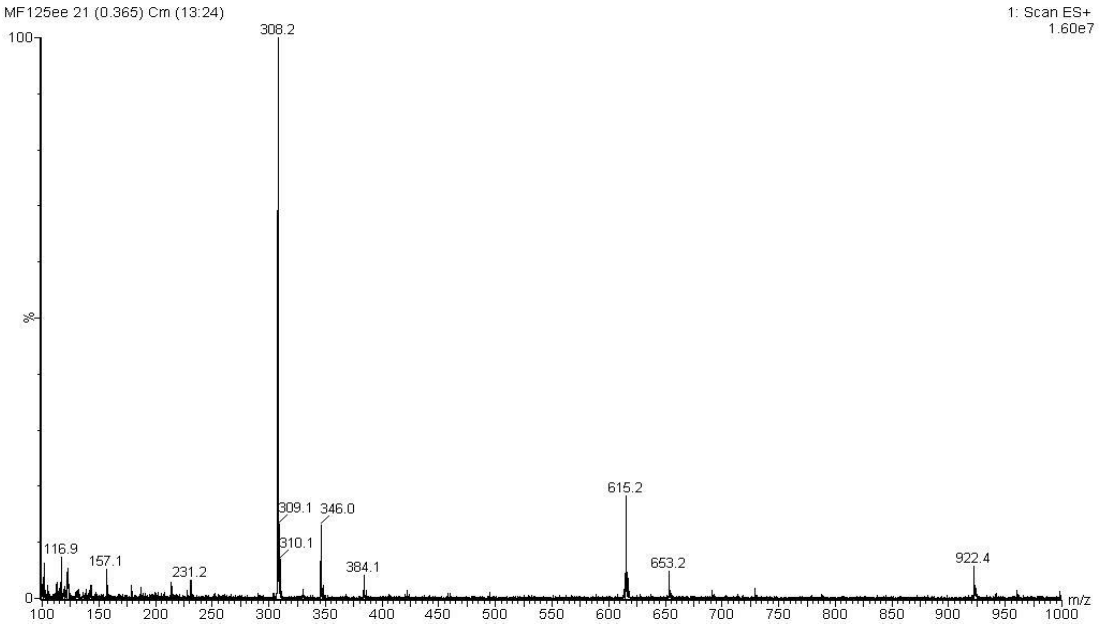
MF125ee 21 (0.365) Cm (13:24)
1: Scan ES+
1.60e7
100
%
308.2
615.2
309.1
346.0
310.1
116.9
157.1
231.2
384.1
653.2
922.4
0
100
150
200
250
300
350
400
450
500
550
600
650
700
750
800
850
900
950
1000
m/z

(c)

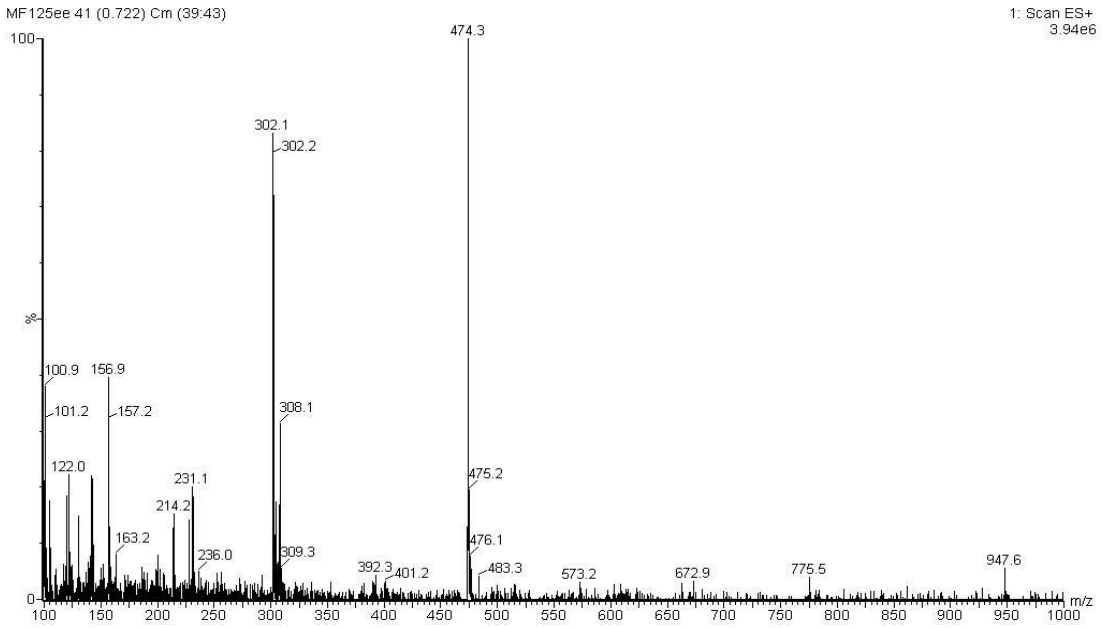

(d)

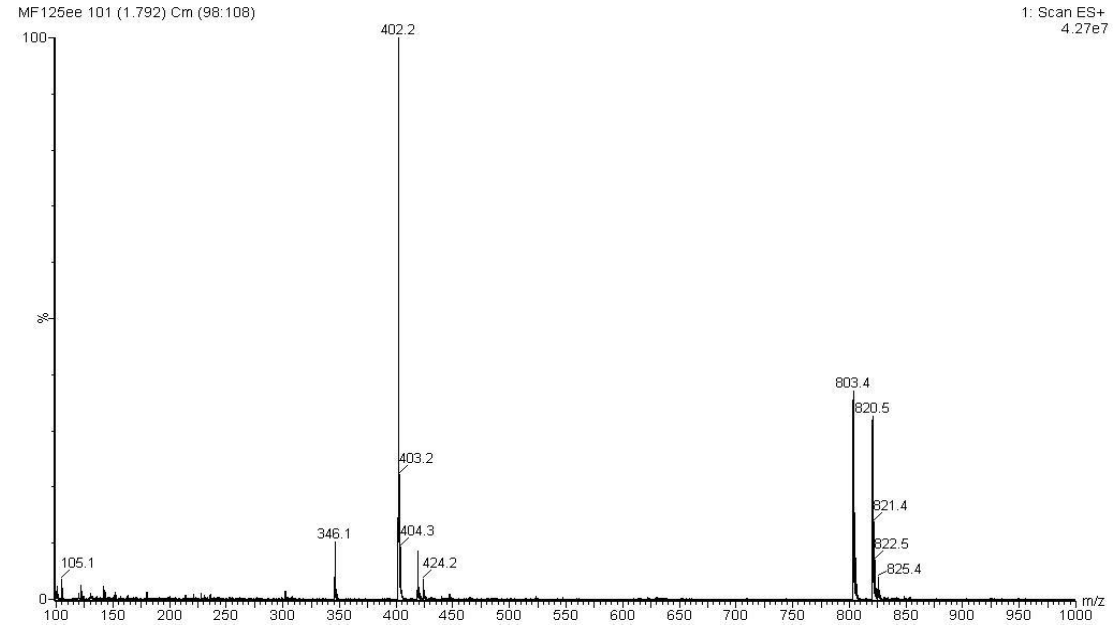

Figure **S66**. (a) TIC and UV trace at t = 24 h, (b) MS data at 0.25–0.42 mins in the UV, (c) MS data at 0.67 mins in the UV and (d) at 1.75 mins in the UV for PD **3** incubated with GSH **1** (10 eq.) at pH 5.0.

Incubation of PD 4 with GSH (10 eq.)

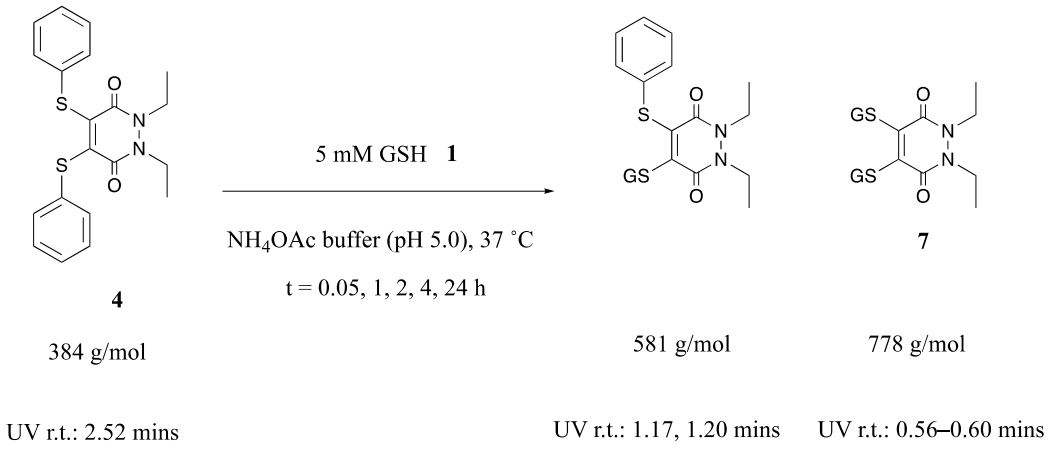

PD **4** (10 µL, 10 mM in MeCN, 1 eq.) was added to GSH **1** (190 µL, 5.3 mM, 10 eq.) in ammonium acetate buffer (50 mM, pH 5.0). The mixture was incubated at 37 ˚C for 24 h. The samples were analysed by LC-MS at t = 0.05, 1, 2, 4 and 24 h.

LC-MS data for t = 0.05 h

(a)

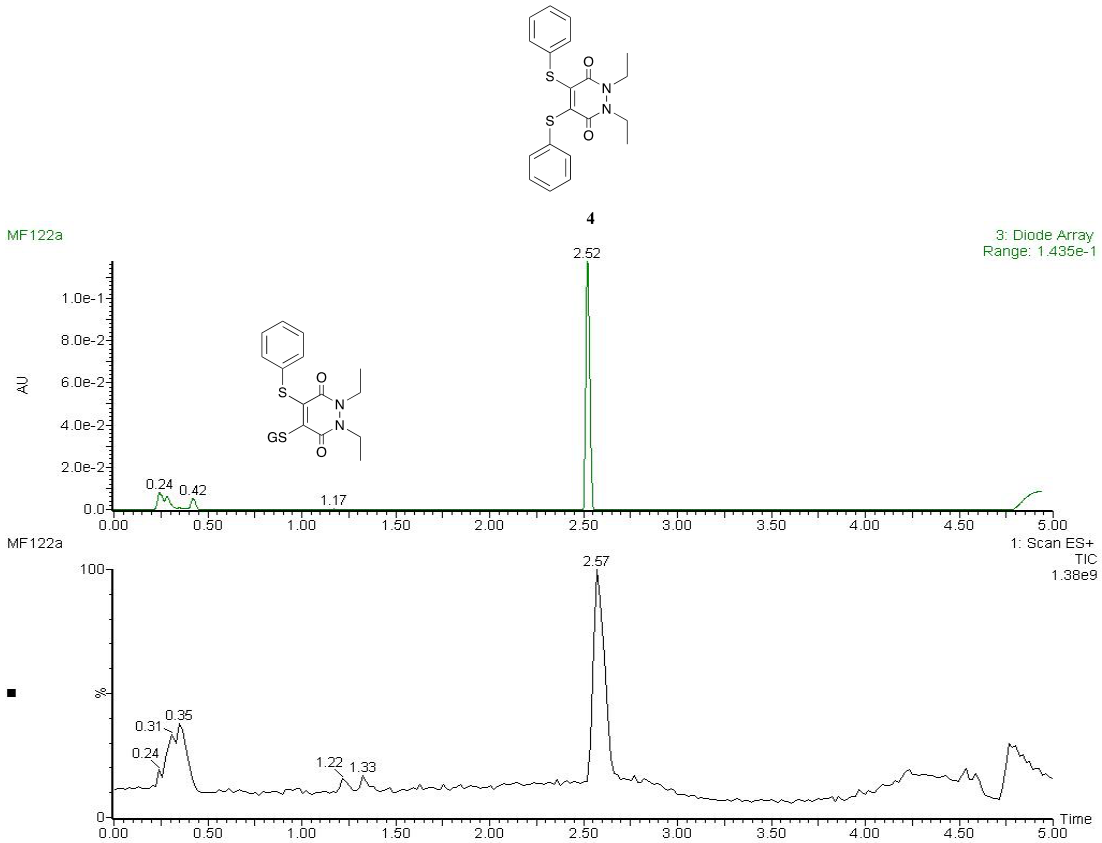

(b)

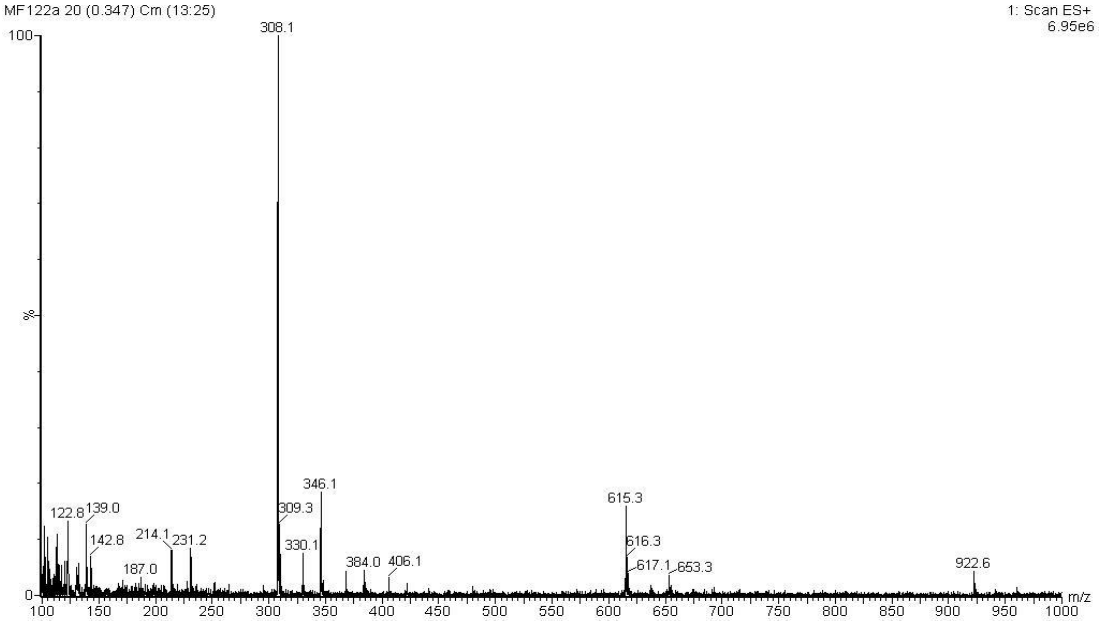
MF122a 20 (0.347) Cm (13:25)
1: Scan ES+
6.95e6
100
%
0
308.1
346.1
309.3
615.3
122.8
139.0
142.8
214.1
231.2
330.1
616.3
617.1
653.3
187.0
384.0
406.1
922.6
m/z
100 150 200 250 300 350 400 450 500 550 600 650 700 750 800 850 900 950 1000

(c)

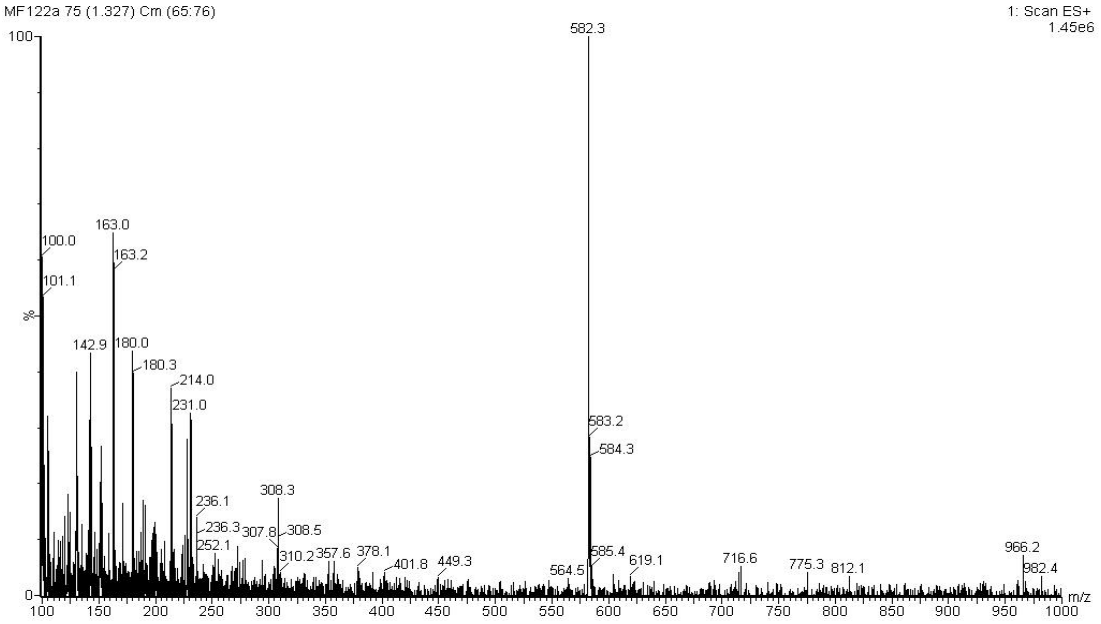
MF122a 75 (1.327) Cm (65:76)
1: Scan ES+
1.45e6
100
%
0
582.3
163.0
100.0
163.2
101.1
142.9
180.0
180.3
214.0
231.0
583.2
584.3
308.3
236.1
236.3
307.8
308.5
252.1
310.2
357.6
378.1
401.8
449.3
564.5
585.4
619.1
716.6
775.3
812.1
966.2
982.4
m/z
100 150 200 250 300 350 400 450 500 550 600 650 700 750 800 850 900 950 1000

(d)

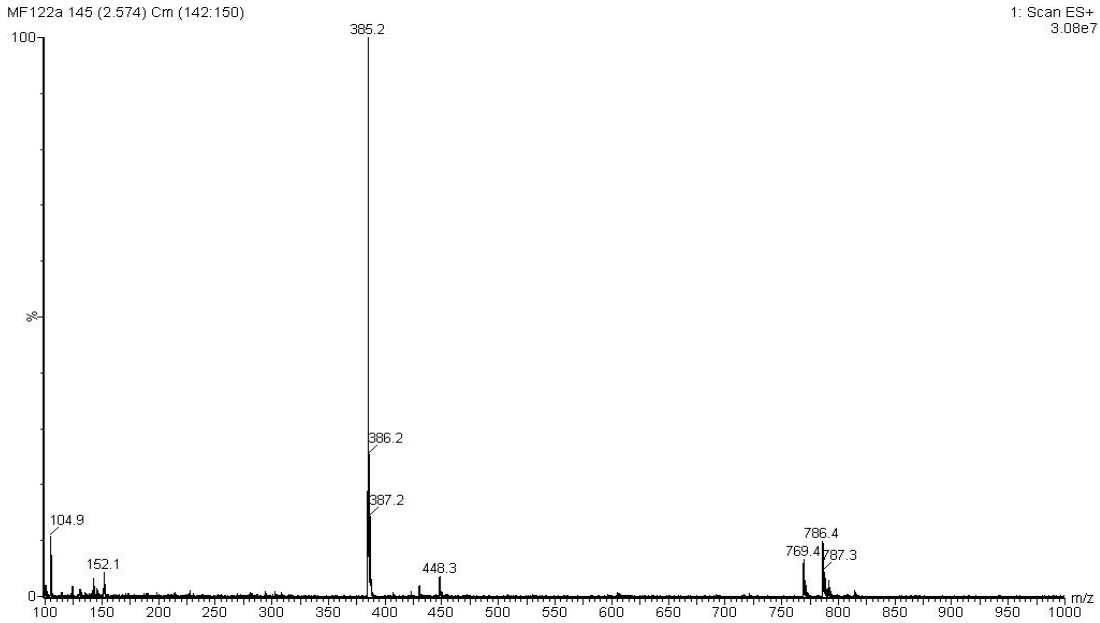

Figure **S67**. (a) TIC and UV trace at t = 0.05 h, (b) MS data at 0.24–0.42 mins in the UV, (c) MS data at 1.17 mins in the UV and (d) at 2.52 mins in the UV for PD **4** incubated with GSH **1** (10 eq.) at pH 5.0.

LC-MS data for t = 1 h

(a)

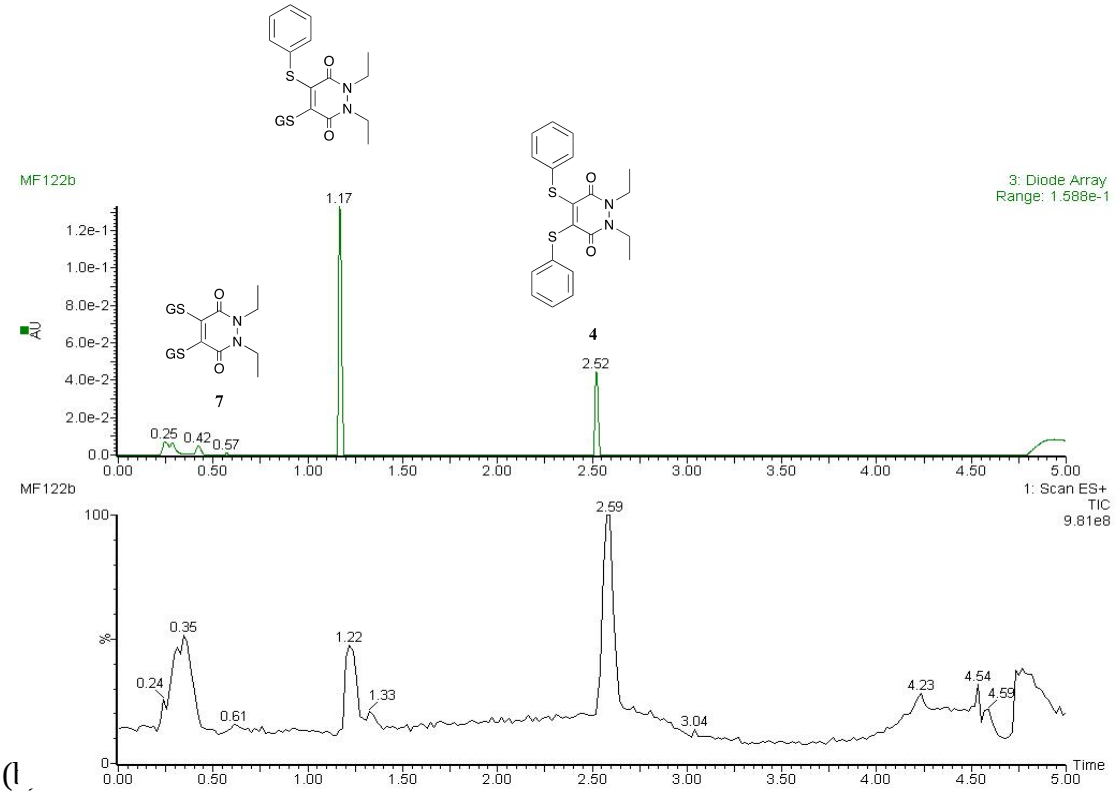

(l

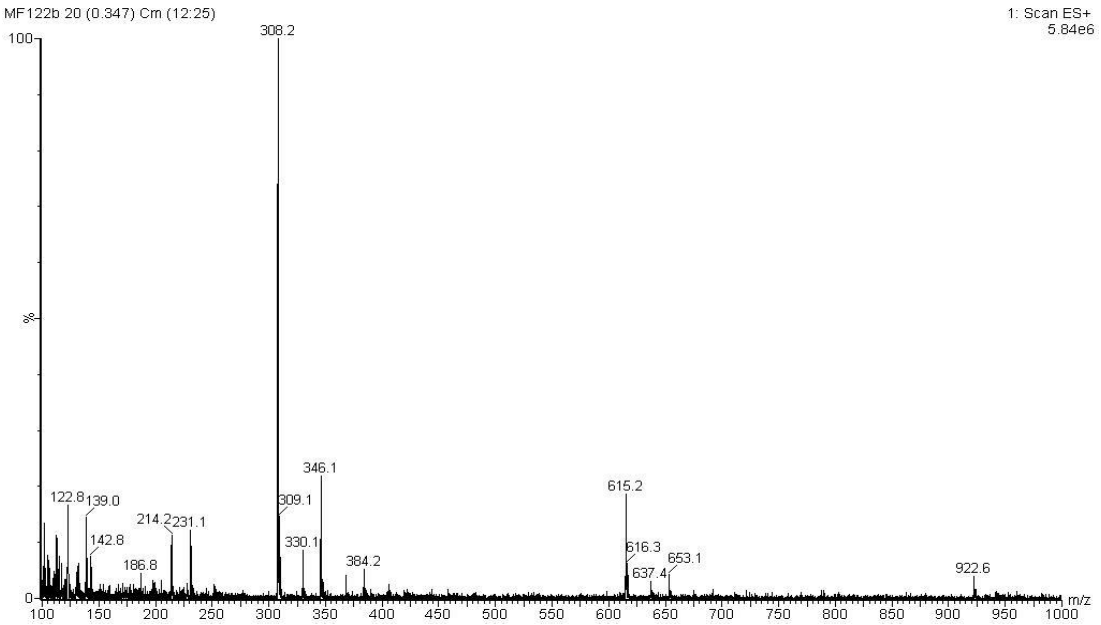
MF122b 20 (0.347) Cm (12:25)
1: Scan ES+
5.84e6
100
%
0
308.2
346.1
615.2
122.8
139.0
214.2
231.1
309.1
142.8
330.1
616.3
653.1
186.8
384.2
637.4
922.6
100 150 200 250 300 350 400 450 500 550 600 650 700 750 800 850 900 950 1000
m/z

(c)

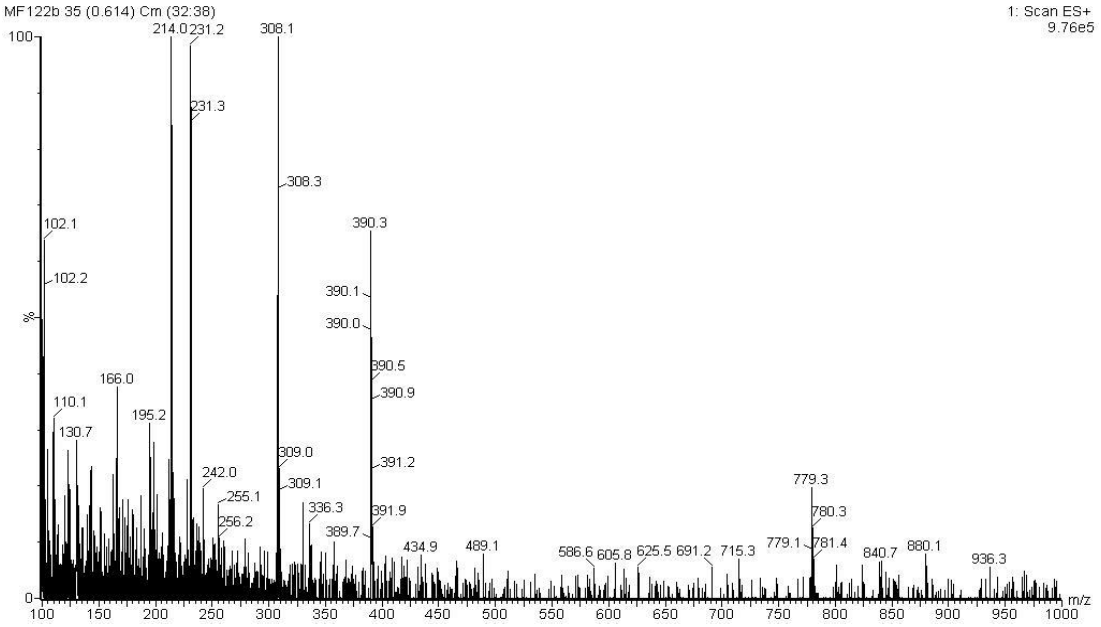
MF122b 35 (0.614) Cm (32:38)
1: Scan ES+
9.76e5
100
%
0
214.0
231.2
308.1
231.3
308.3
102.1
390.3
102.2
390.1
390.0
390.5
166.0
390.9
110.1
195.2
130.7
309.0
391.2
242.0
309.1
779.3
255.1
336.3
780.3
256.2
391.9
389.7
434.9
489.1
586.6
605.8
625.5
691.2
715.3
779.1
781.4
840.7
880.1
936.3
100 150 200 250 300 350 400 450 500 550 600 650 700 750 800 850 900 950 1000
m/z

(d)

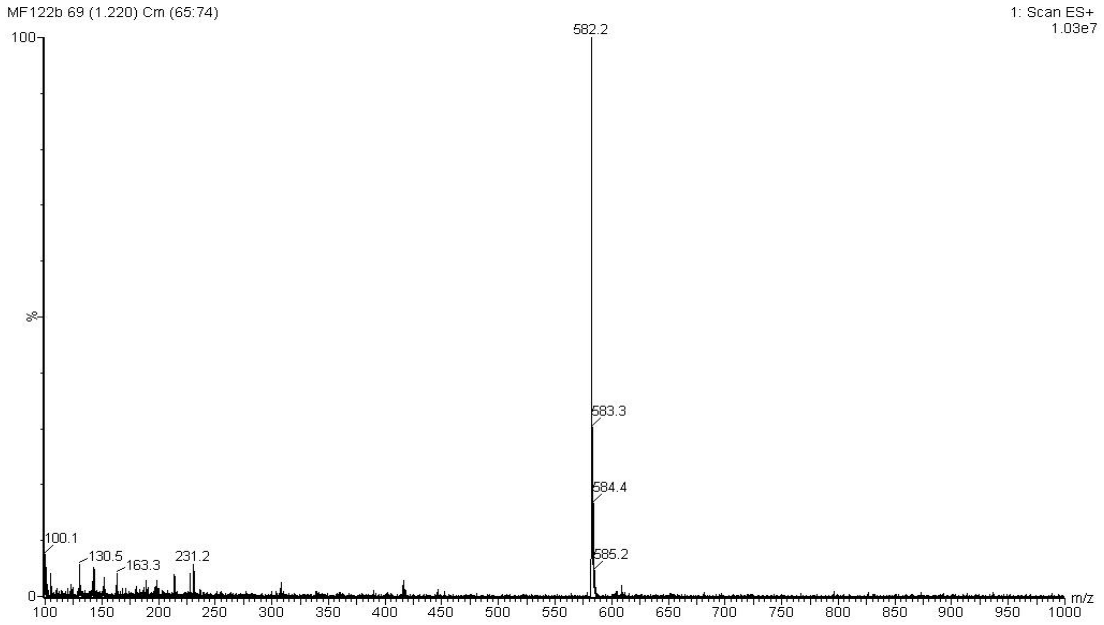

(e)

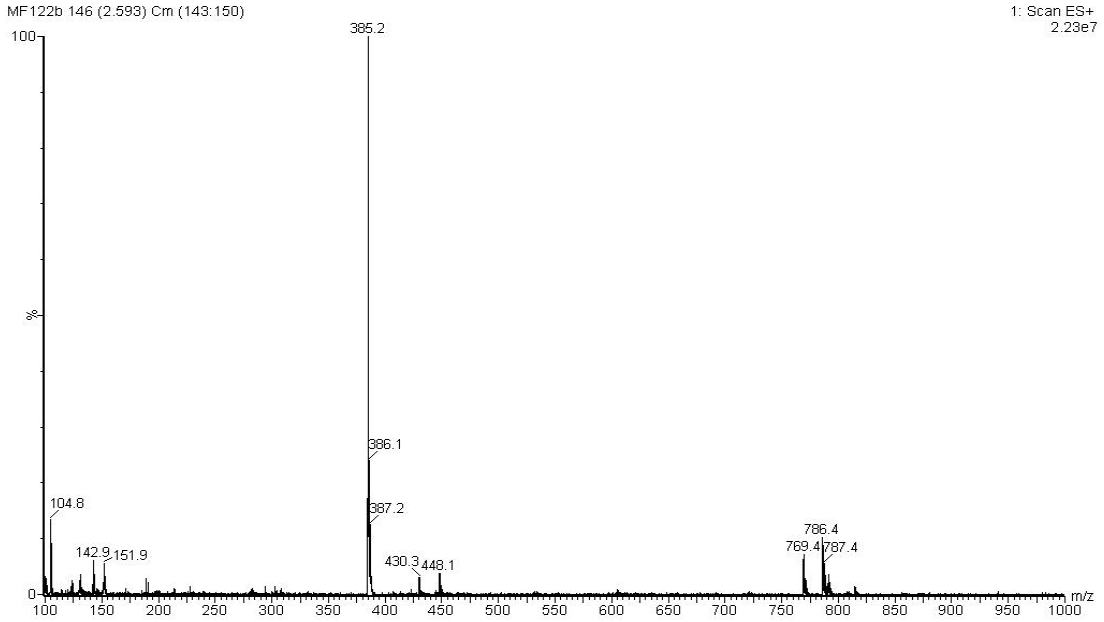

Figure **S68**. (a) TIC and UV trace at t = 1 h, (b) MS data at 0.25–0.42 mins in the UV, (c) MS data at 0.57 mins in the UV, (d) at 1.17 mins in the UV and (e) at 2.52 mins in the UV for PD **4** incubated with GSH **1** (10 eq.) at pH 5.0.

LC-MS data for t = 2 h

(a)

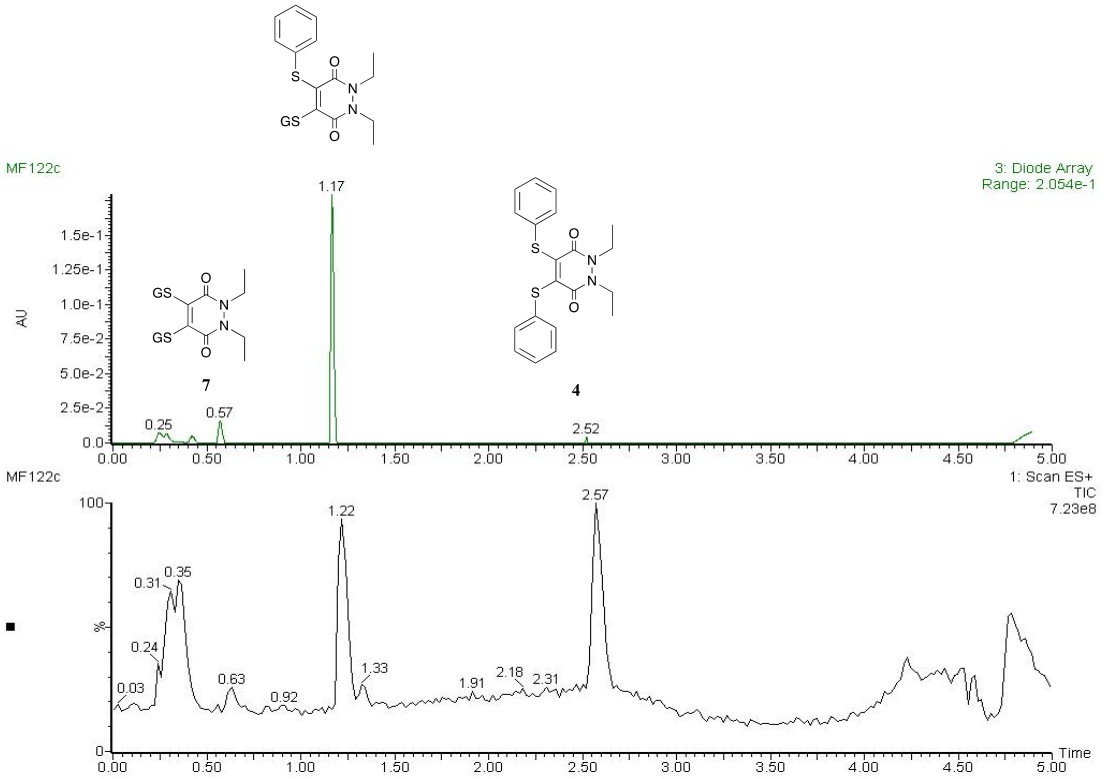
MF122c
3: Diode Array
Range: 2.054e-1
AU
1.17
0.25
0.57
2.52
7
4
MF122c
1: Scan ES+
TIC
7.23e8
%
2.57
1.22
0.31
0.35
0.24
0.03
0.63
0.92
1.33
1.91
2.18
2.31
Time

(b)

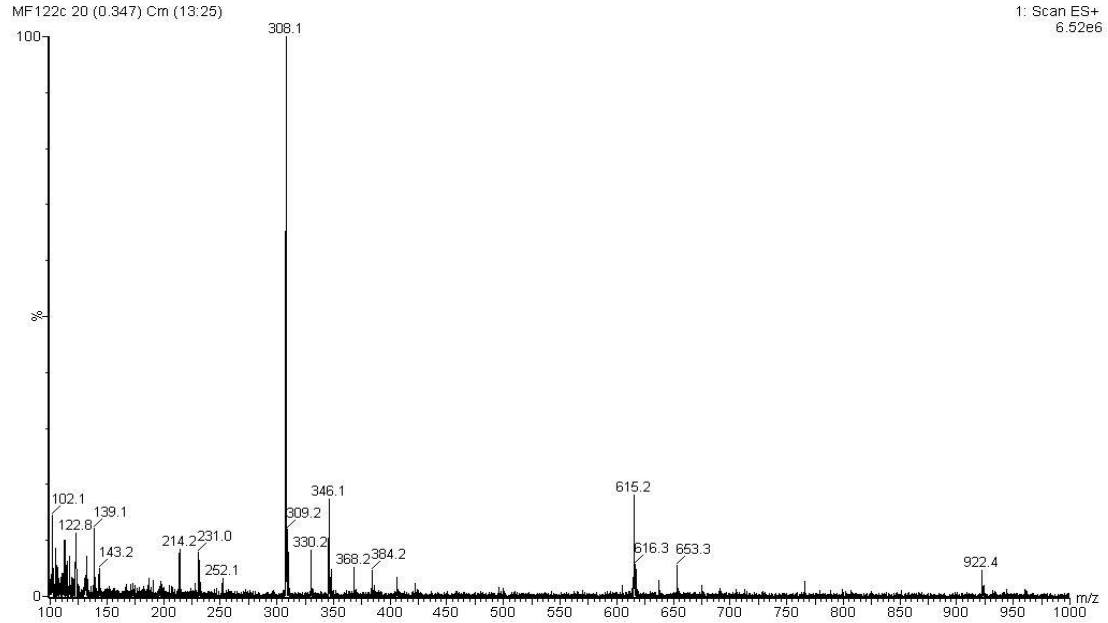
MF122c 20 (0.347) Cm (13:25)
1: Scan ES+
6.52e6
%
308.1
346.1
615.2
102.1
139.1
122.8
143.2
214.2
231.0
252.1
309.2
330.2
368.2
384.2
616.3
653.3
922.4
m/z

(c)

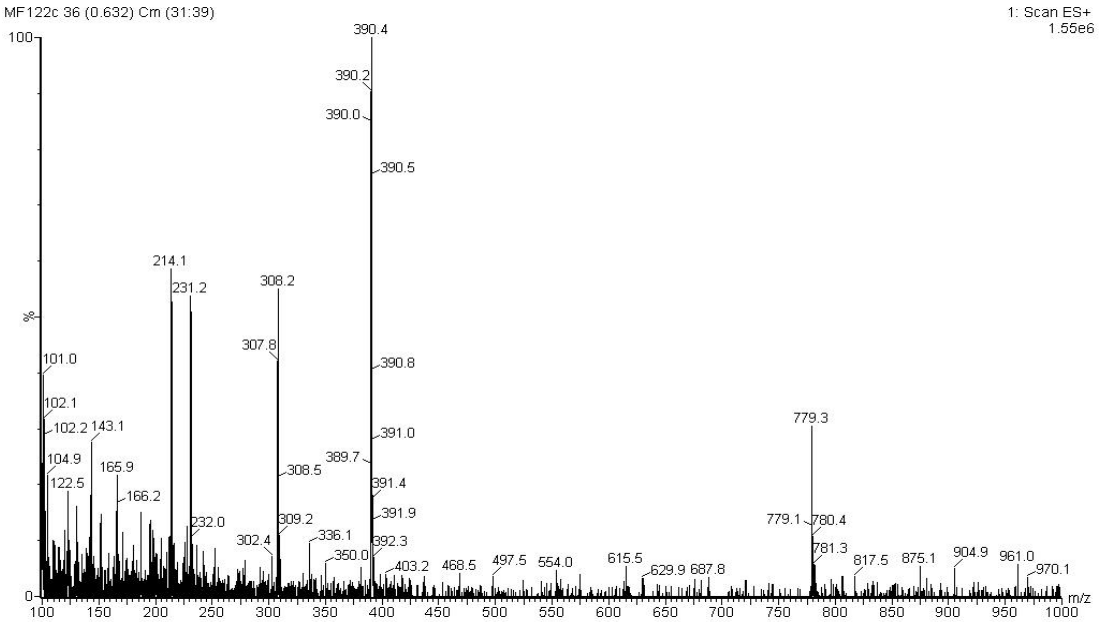
MF122c 36 (0.632) Cm (31:39)
1: Scan ES+
1.55e6
100
%
0
390.4
390.2
390.0
390.5
214.1
231.2
308.2
307.8
390.8
101.0
102.1
102.2
143.1
391.0
389.7
104.9
165.9
308.5
391.4
122.5
166.2
391.9
232.0
309.2
302.4
336.1
392.3
350.0
403.2
468.5
497.5
554.0
615.5
629.9
687.8
779.3
779.1
780.4
781.3
817.5
875.1
904.9
961.0
970.1
m/z
100 150 200 250 300 350 400 450 500 550 600 650 700 750 800 850 900 950 1000

(d)

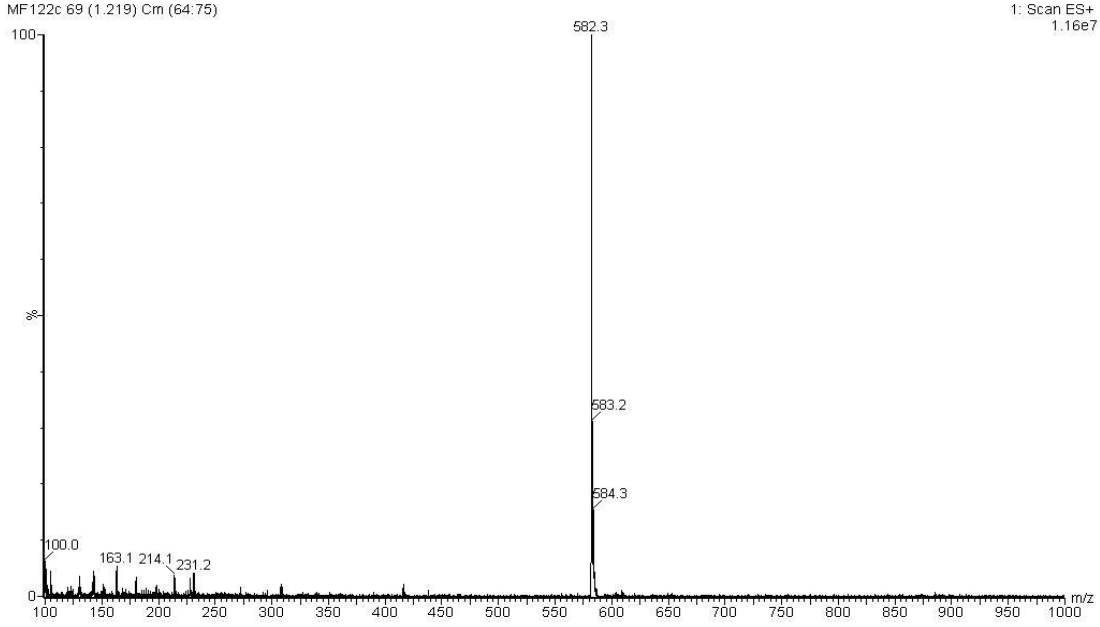
MF122c 69 (1.219) Cm (64:75)
1: Scan ES+
1.16e7
100
%
0
582.3
583.2
584.3
100.0
163.1
214.1
231.2
m/z
100 150 200 250 300 350 400 450 500 550 600 650 700 750 800 850 900 950 1000

(e)

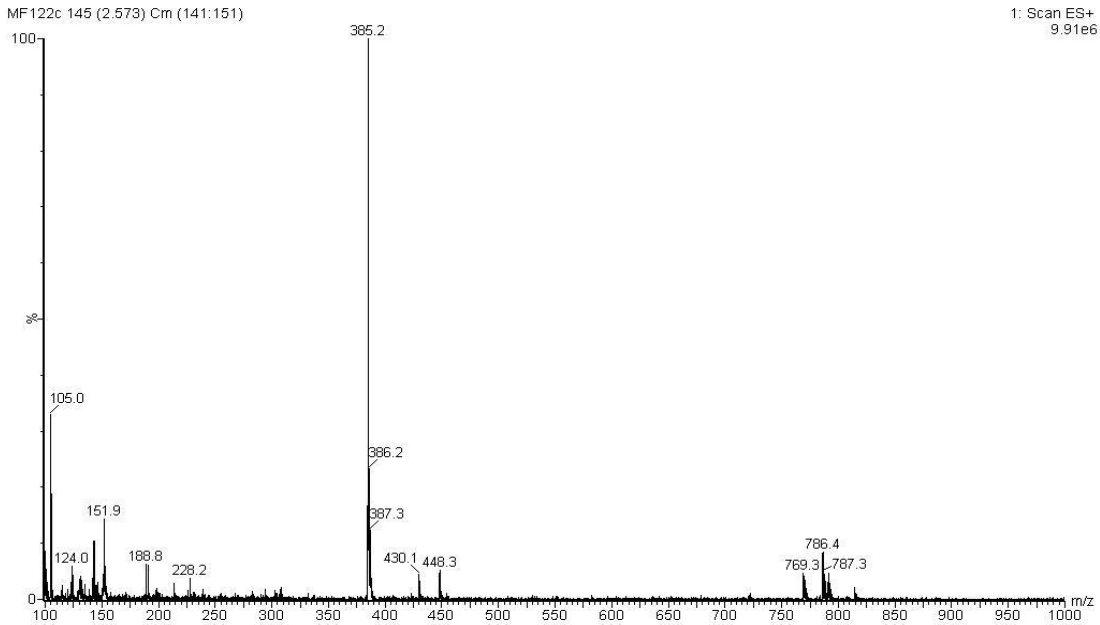

Figure **S69**. (a) TIC and UV trace at t = 2 h, (b) MS data at 0.25–0.42 mins in the UV, (c) MS data at 0.57 mins in the UV, (d) at 1.17 mins in the UV and (e) at 2.52 mins in the UV for PD **4** incubated with GSH **1** (10 eq.) at pH 5.0.

LC-MS data for t = 4 h

(a)

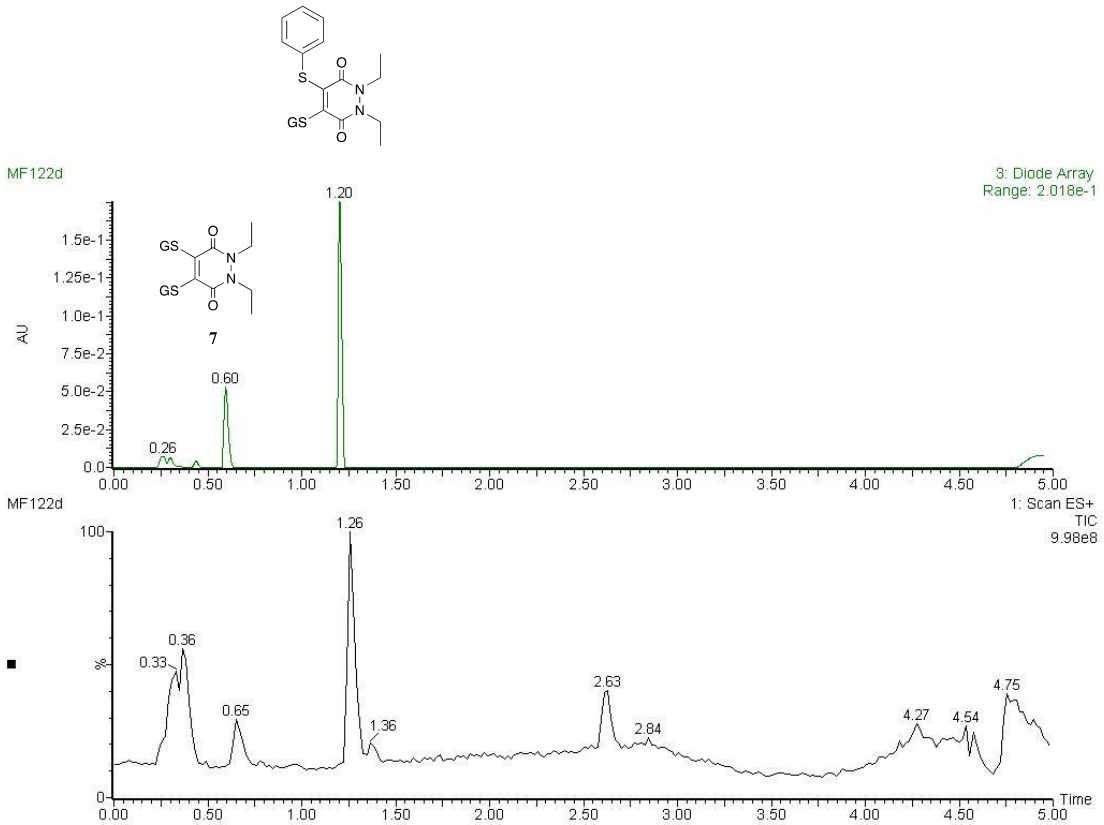
MF122d
3: Diode Array
Range: 2.018e-1
1.20
GS
GS
7
0.60
0.26
AU
1.5e-1
1.25e-1
1.0e-1
7.5e-2
5.0e-2
2.5e-2
0.0
0.00
0.50
1.00
1.50
2.00
2.50
3.00
3.50
4.00
4.50
5.00
MF122d
1: Scan ES+
TIC
9.98e8
1.26
0.36
0.33
0.65
1.36
2.63
2.84
4.27
4.54
4.75
%
100
0
Time

(b)

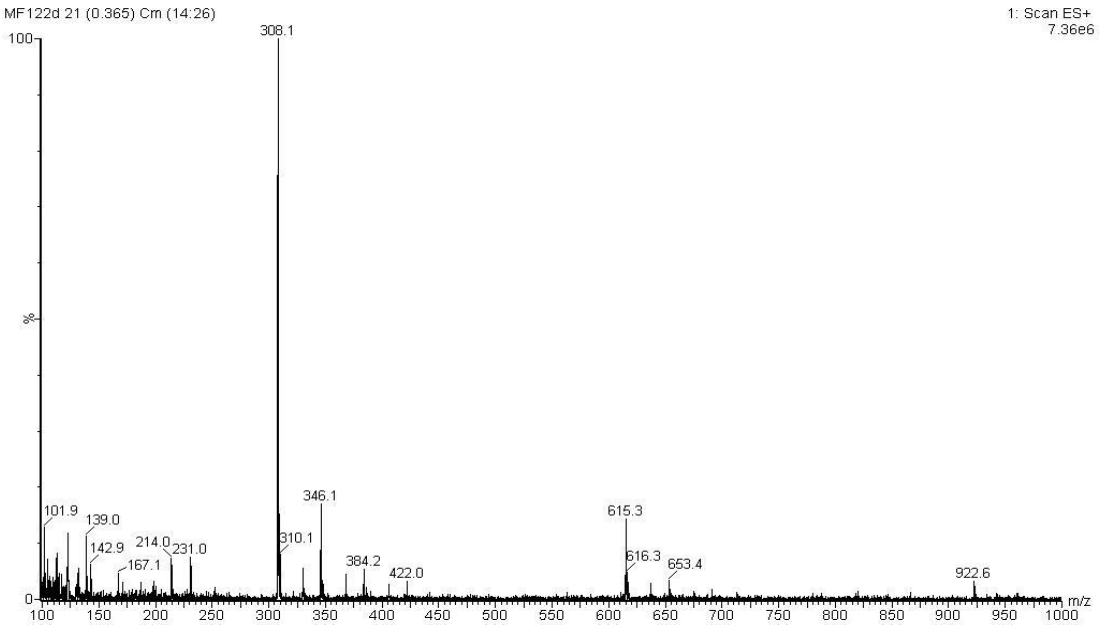
MF122d 21 (0.365) Cm (14:26)
1: Scan ES+
7.36e6
308.1
346.1
615.3
101.9
139.0
142.9
214.0
231.0
167.1
310.1
384.2
422.0
616.3
653.4
922.6
%
100
0
m/z
100
150
200
250
300
350
400
450
500
550
600
650
700
750
800
850
900
950
1000

(c)

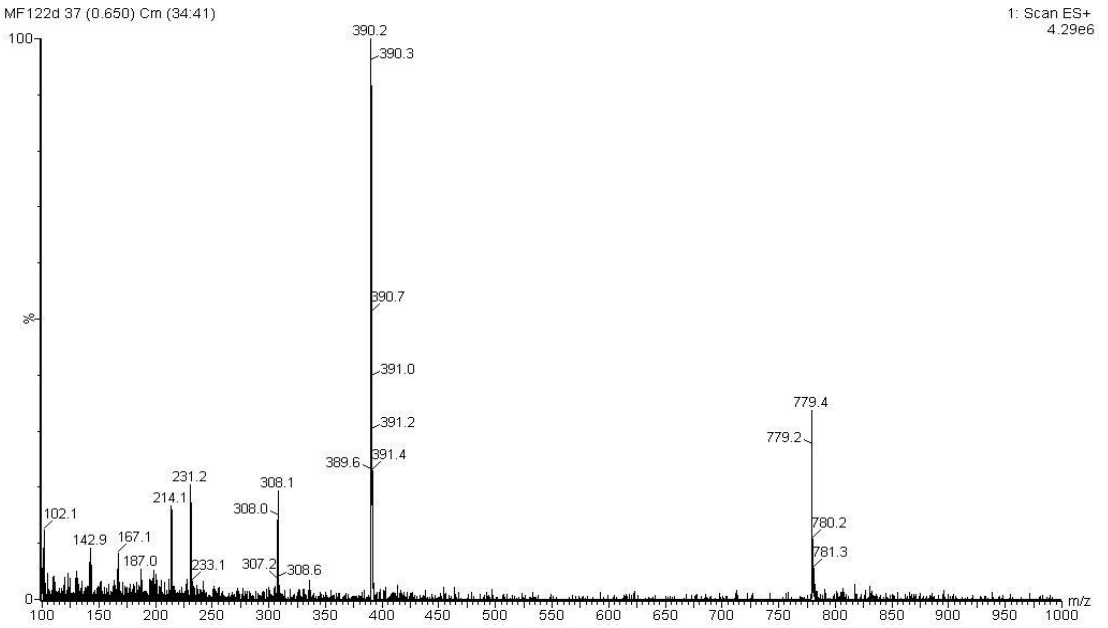

(d)

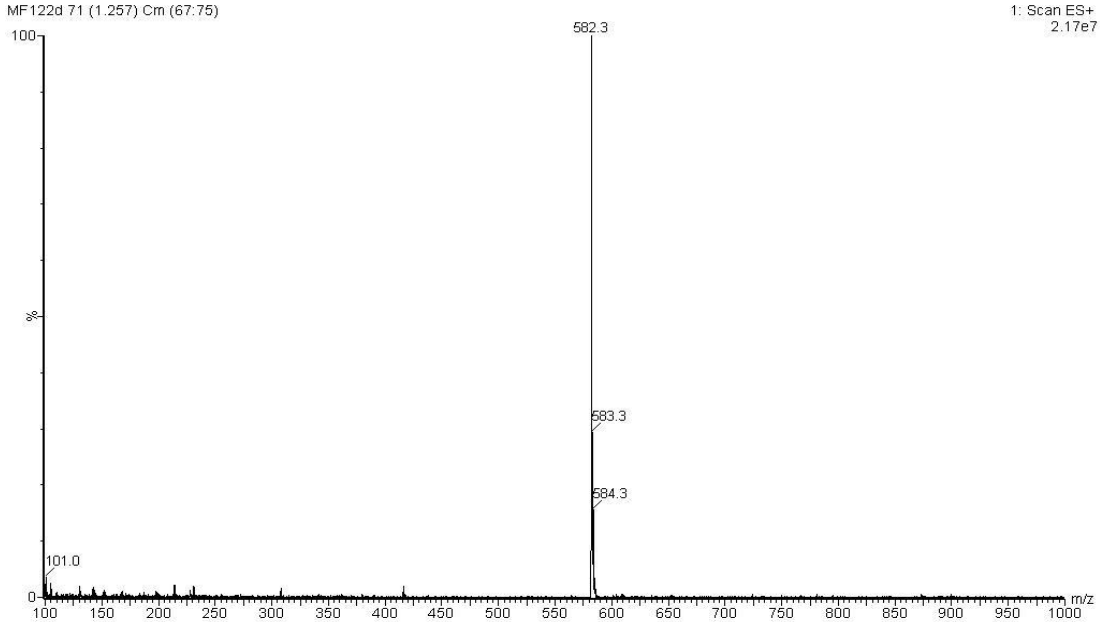

Figure **S70**. (a) TIC and UV trace at t = 4 h, (b) MS data at 0.26–0.42 mins in the UV, (c) MS data at 0.60 mins in the UV and (d) at 1.20 mins in the UV for PD **4** incubated with GSH **1** (10 eq.) at pH 5.0.

LC-MS data for t = 24 h

(a)

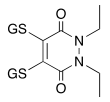
GS
GS
O
N
N
O

7

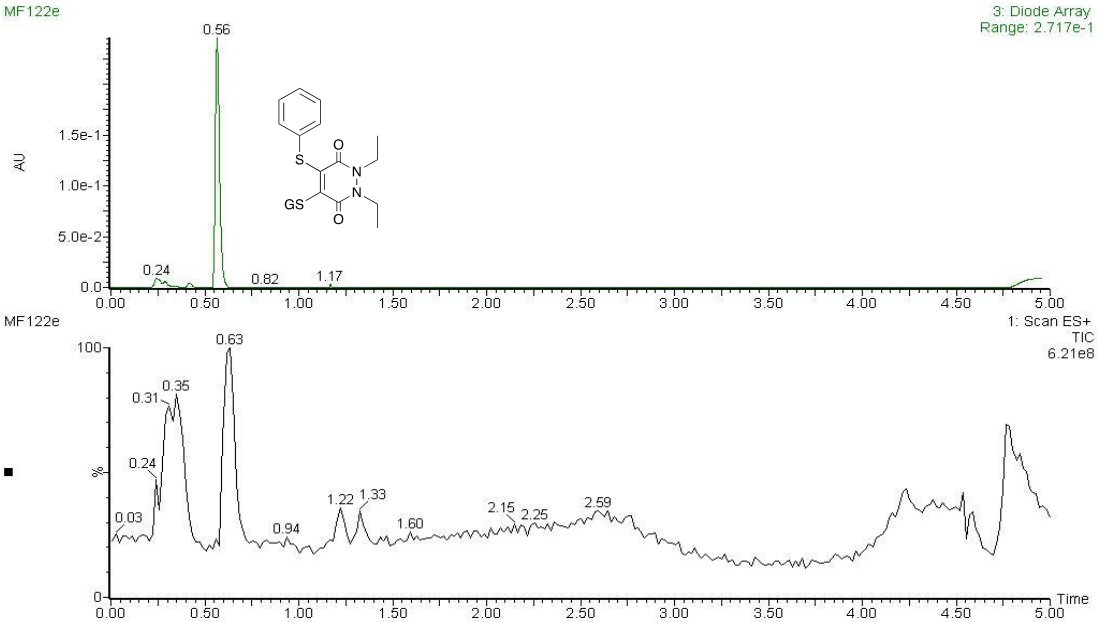
MF122e
3: Diode Array
Range: 2.717e-1
AU
0.56
0.24
0.82
1.17
S
GS
MF122e
1: Scan ES+
TIC
6.21e8
%
0.63
0.35
0.31
0.24
0.03
0.94
1.22
1.33
1.60
2.15
2.25
2.59
Time

(b)

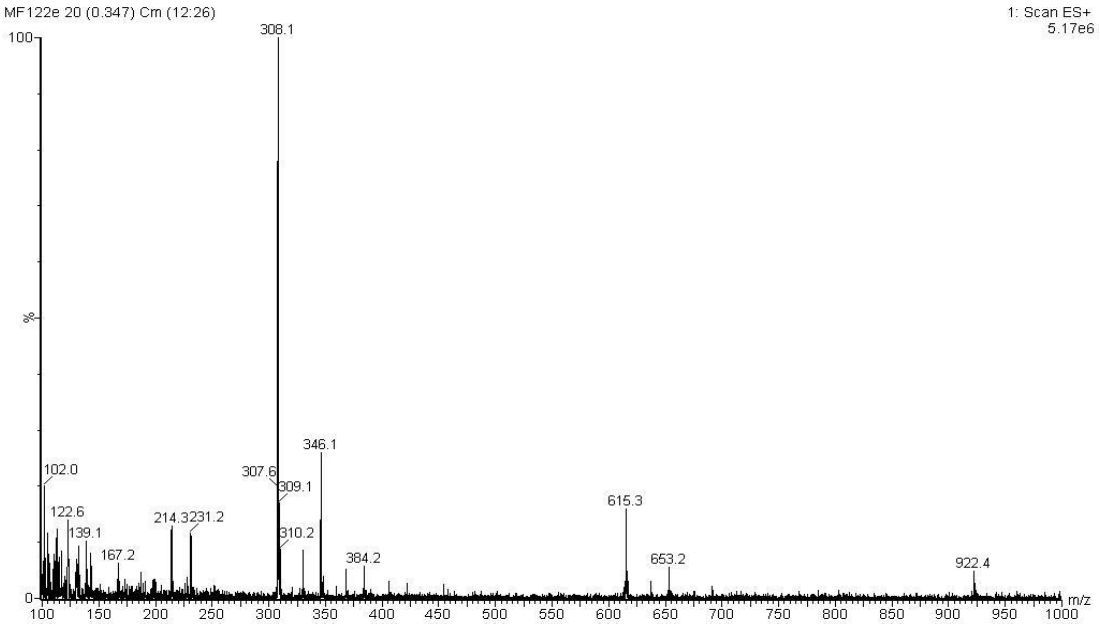
MF122e 20 (0.347) Cm (12:26)
1: Scan ES+
5.17e6
%
308.1
346.1
102.0
307.6
309.1
122.6
139.1
214.3
231.2
310.2
167.2
384.2
615.3
653.2
922.4
m/z

(c)

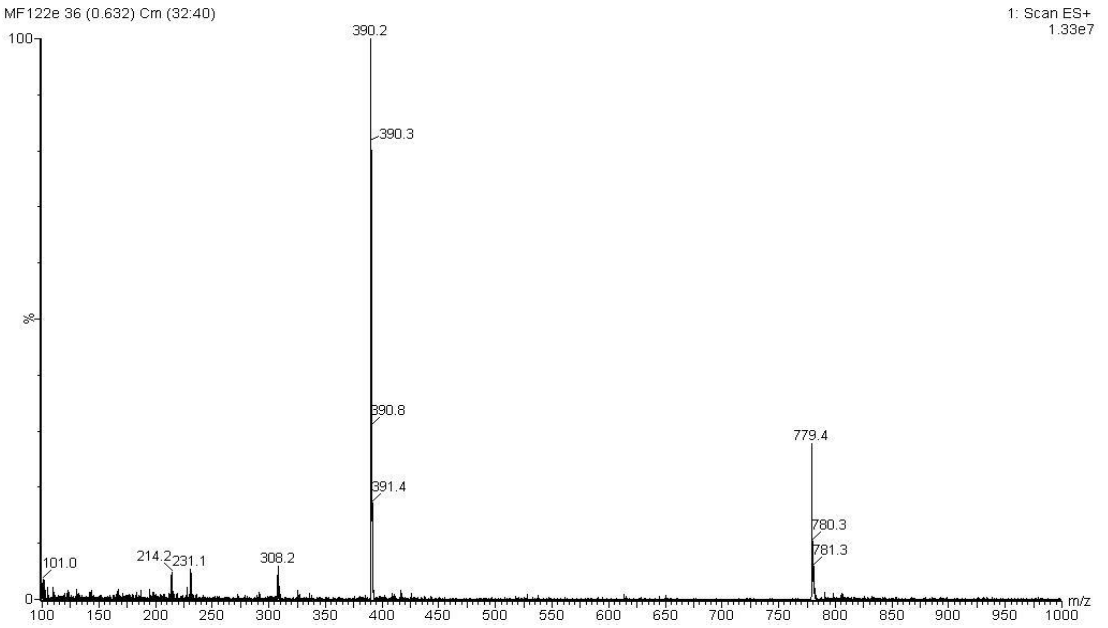

(d)

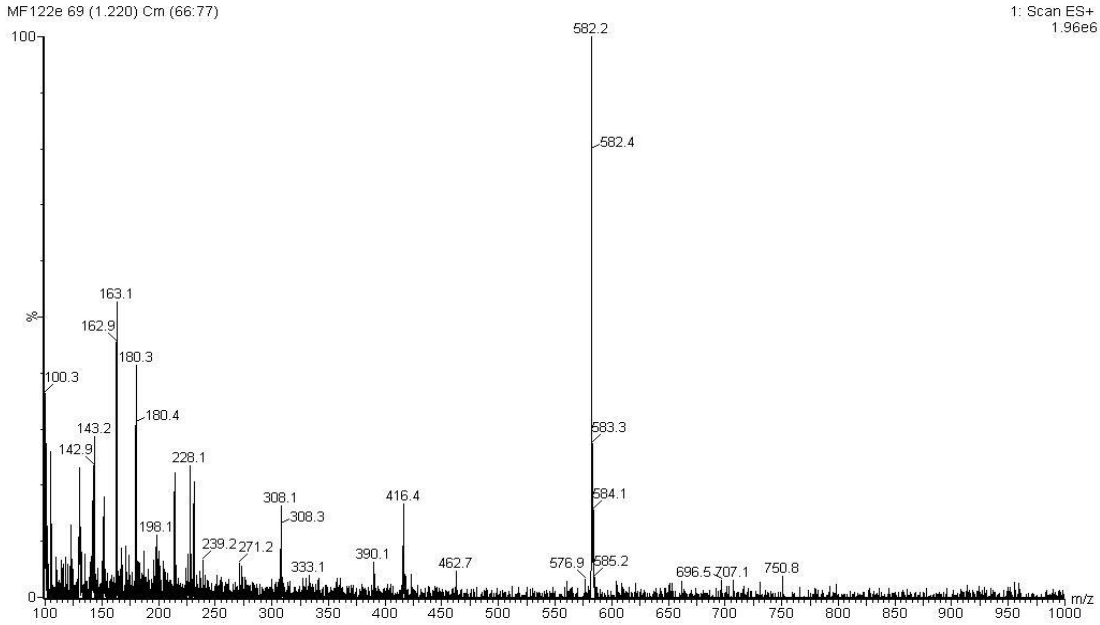

Figure **S71**. (a) TIC and UV trace at t = 24 h, (b) MS data at 0.24–0.42 mins in the UV, (c) MS data at 0.56 mins in the UV and (d) at 1.17 mins in the UV for PD **4** incubated with GSH **1** (10 eq.) at pH 5.0.

Incubation of PD 5 with GSH (10 eq.)

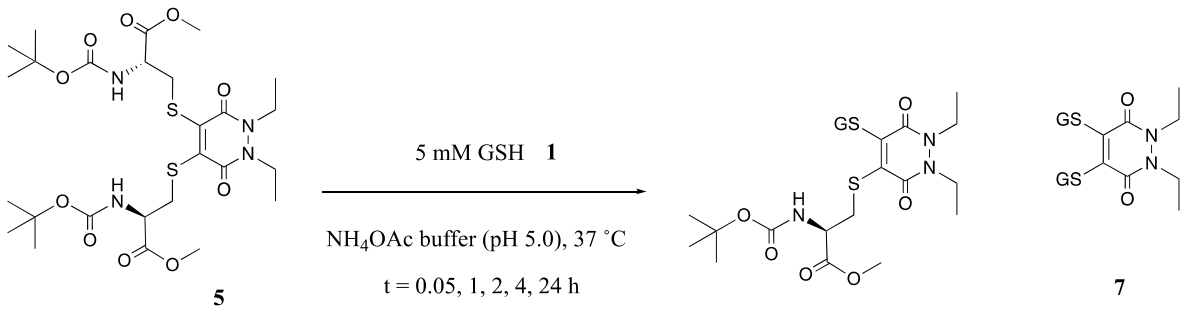

PD **5** (10 µL, 10 mM in MeCN, 1 eq.) was added to GSH **1** (190 µL, 5.3 mM, 10 eq.) in ammonium acetate buffer (50 mM, pH 5.0). The mixture was incubated at 37 ˚C for 24 h. The samples were analysed by LC-MS at t = 0.05, 1, 2, 4 and 24 h.

LC-MS data for t = 0.05 h

(a)

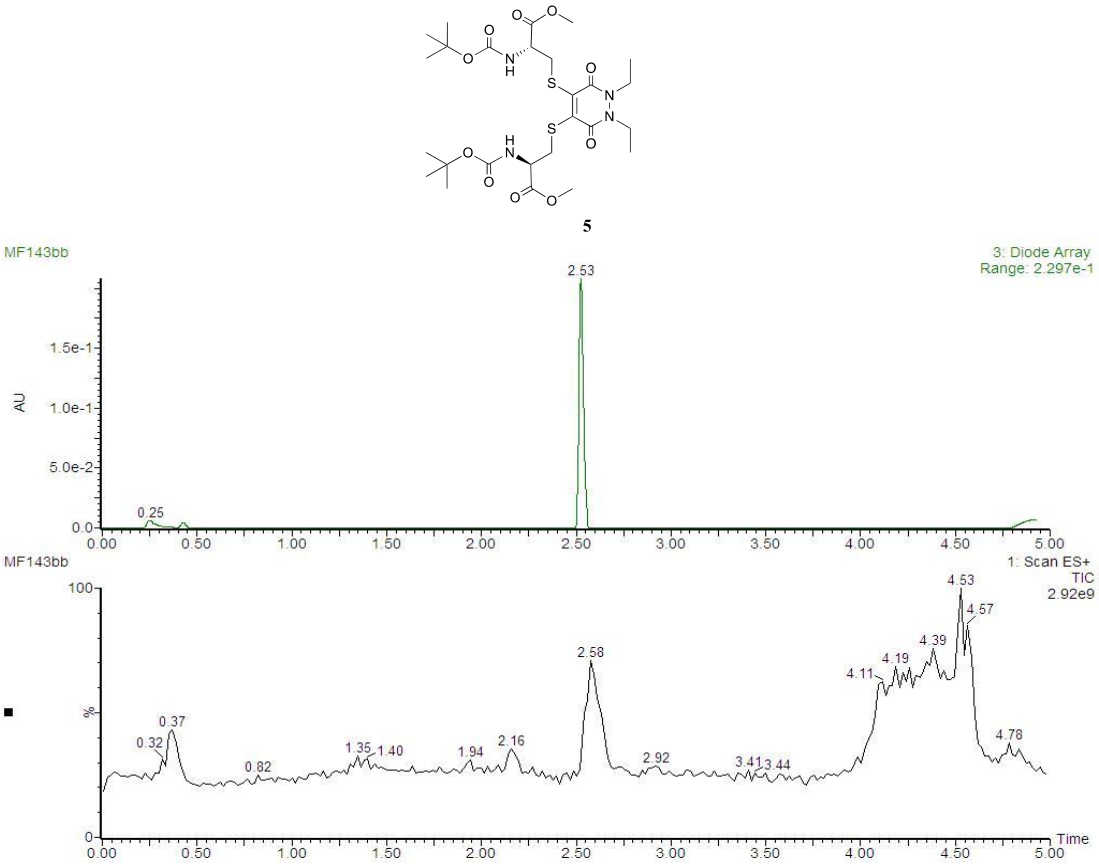

(b)

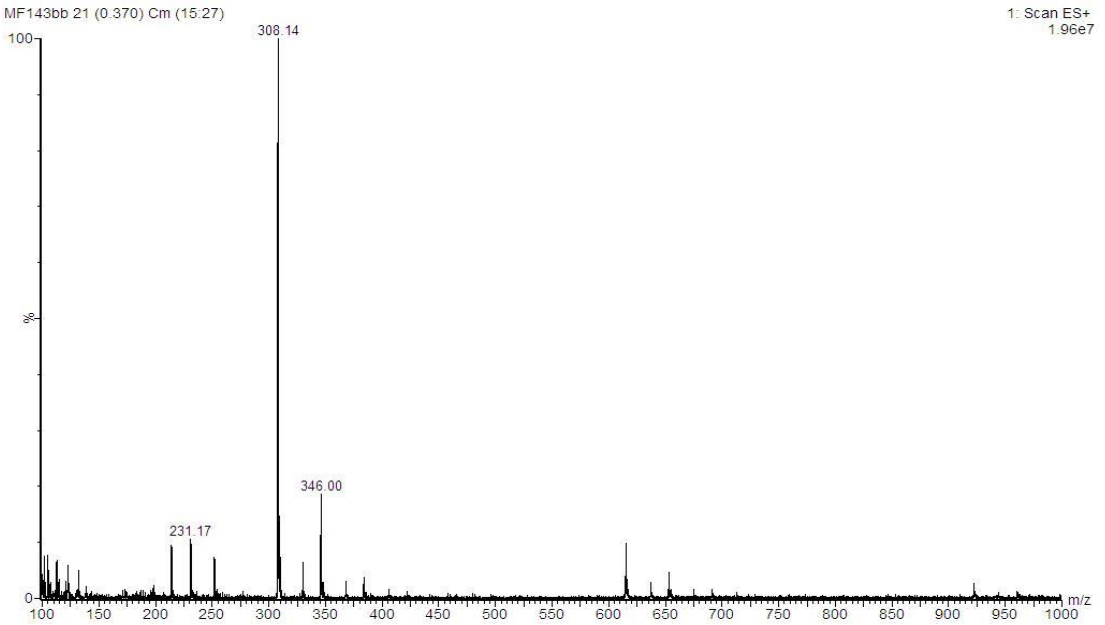

(c)

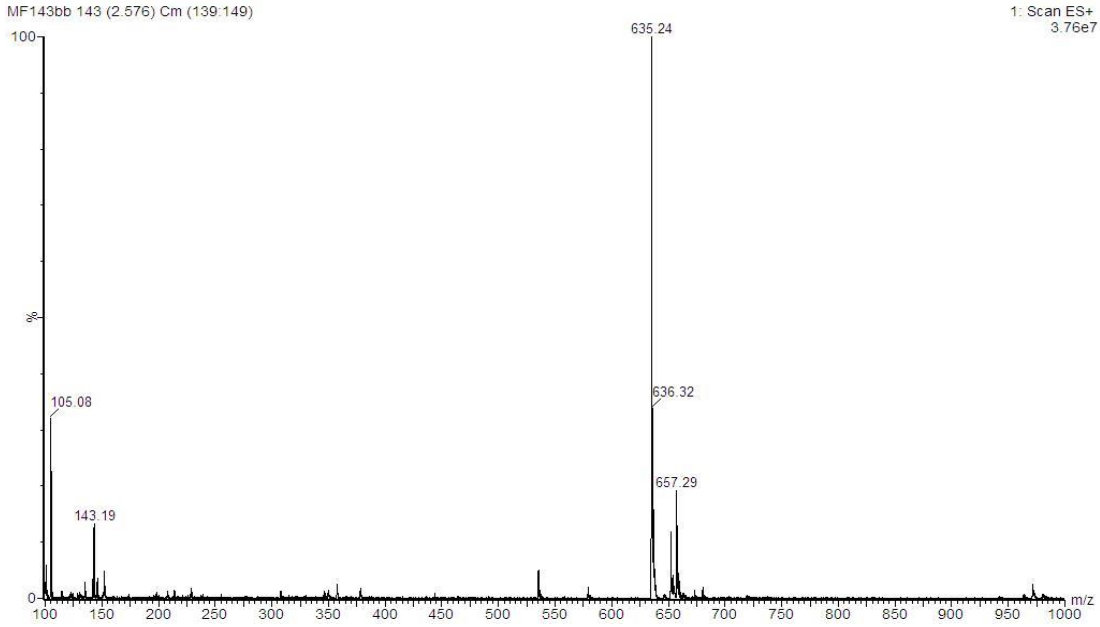

Figure **S72**. (a) TIC and UV trace at t = 0.05 h, (b) MS data at 0.25–0.42 mins in the UV and (c) MS data at 2.53 mins in the UV for PD **5** incubated with GSH **1** (10 eq.) at pH 5.0.

LC-MS data for t = 1 h

(a)

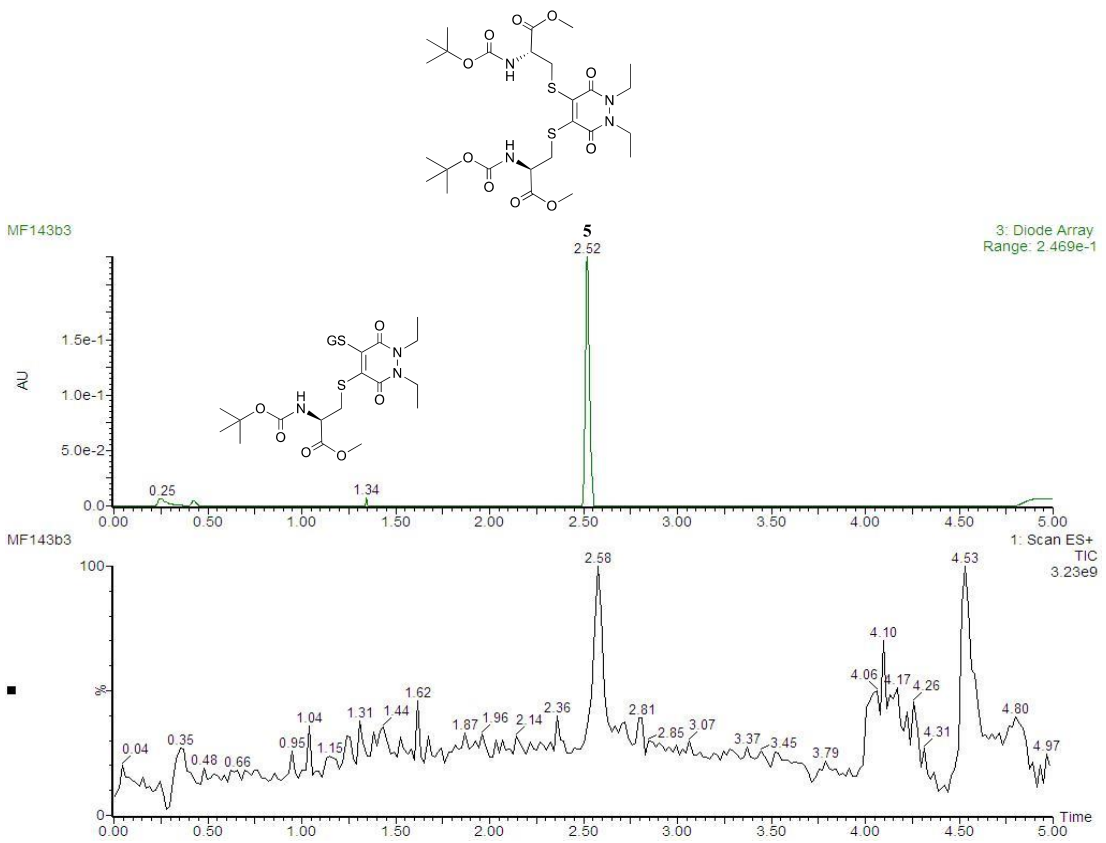
MF143b3
5
2.52
3: Diode Array
Range: 2.469e-1
AU
1.5e-1
1.0e-1
5.0e-2
0.0
0.25
1.34
0.00
0.50
1.00
1.50
2.00
2.50
3.00
3.50
4.00
4.50
5.00
MF143b3
1: Scan ES+
TIC
3.23e9
100
%
0
2.58
4.53
4.10
4.06
4.17
4.26
4.80
4.31
4.97
1.62
1.04
1.31
1.44
1.87
1.96
2.14
2.36
2.81
2.85
3.07
3.37
3.45
3.79
0.04
0.35
0.48
0.66
0.95
1.15
Time

(b)

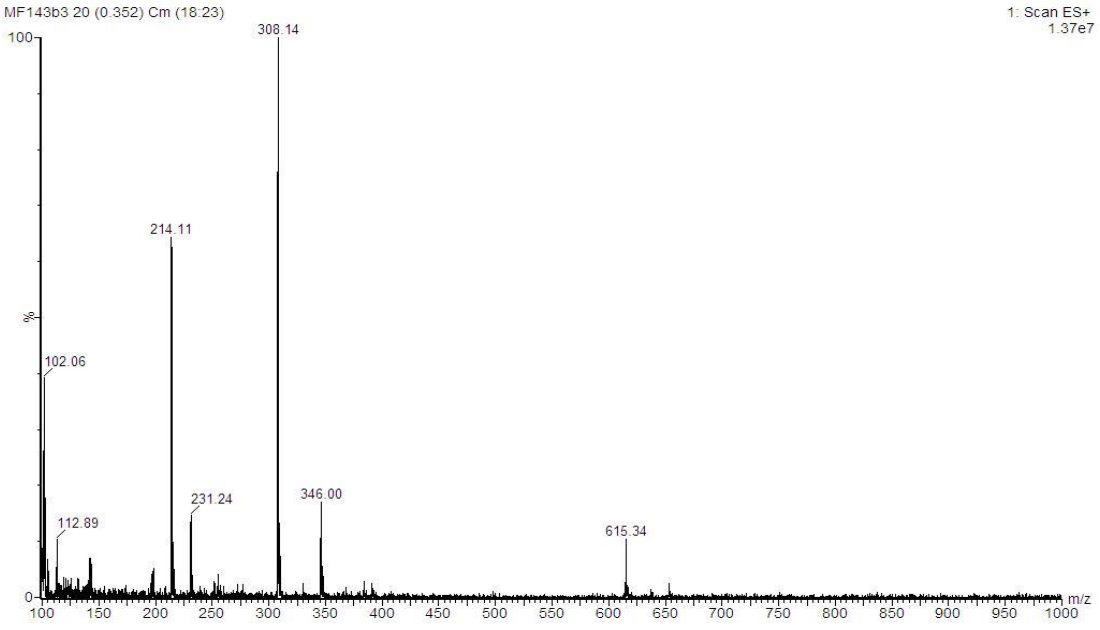
MF143b3 20 (0.352) Cm (18:23)
1: Scan ES+
1.37e7
100
%
0
308.14
214.11
102.06
231.24
346.00
112.89
615.34
100
150
200
250
300
350
400
450
500
550
600
650
700
750
800
850
900
950
1000
m/z

(c)

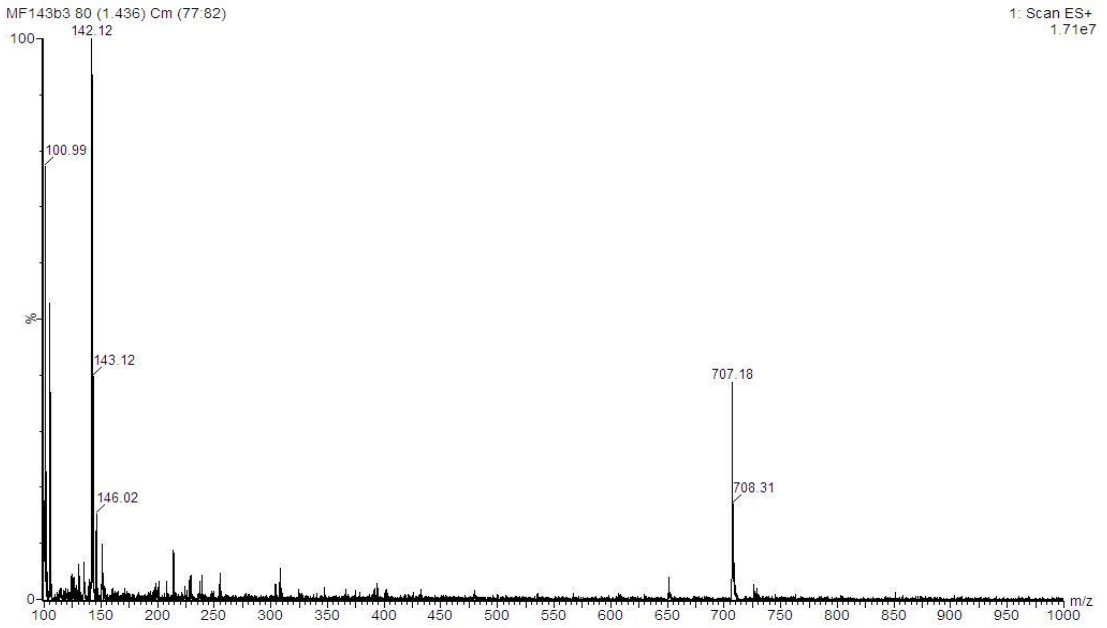

(d)

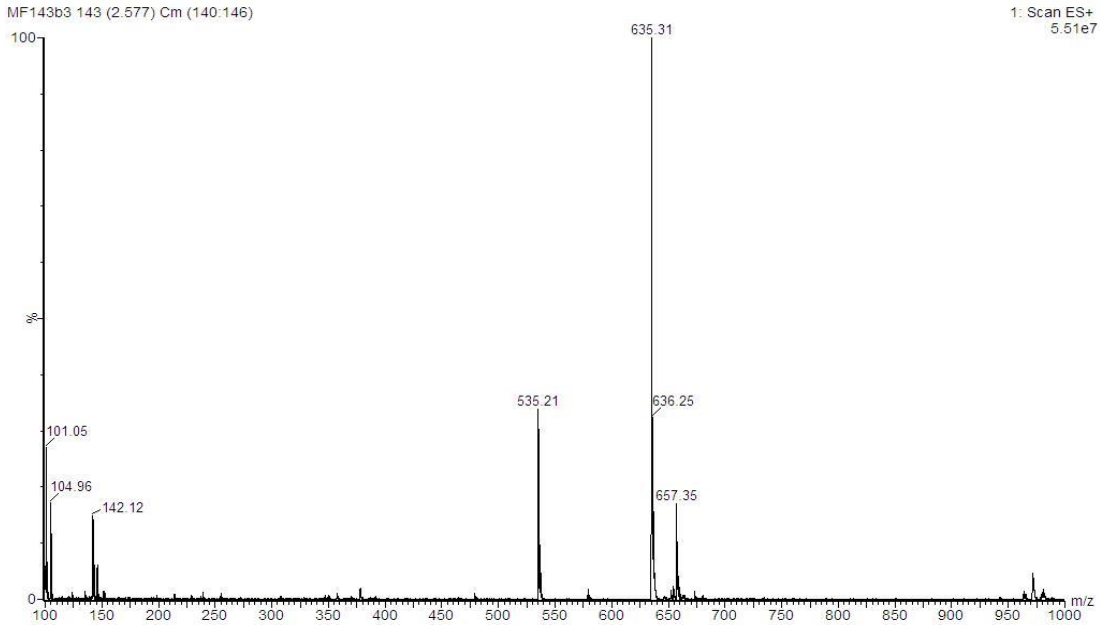

Figure **S73**. (a) TIC and UV trace at t = 1 h, (b) MS data at 0.25–0.42 mins in the UV, (c) MS data at 1.34 mins in the UV and (d) at 2.52 mins in the UV for PD **5** incubated with GSH **1** (10 eq.) at pH 5.0.

LC-MS data for t = 2 h

(a)

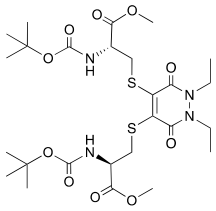

5

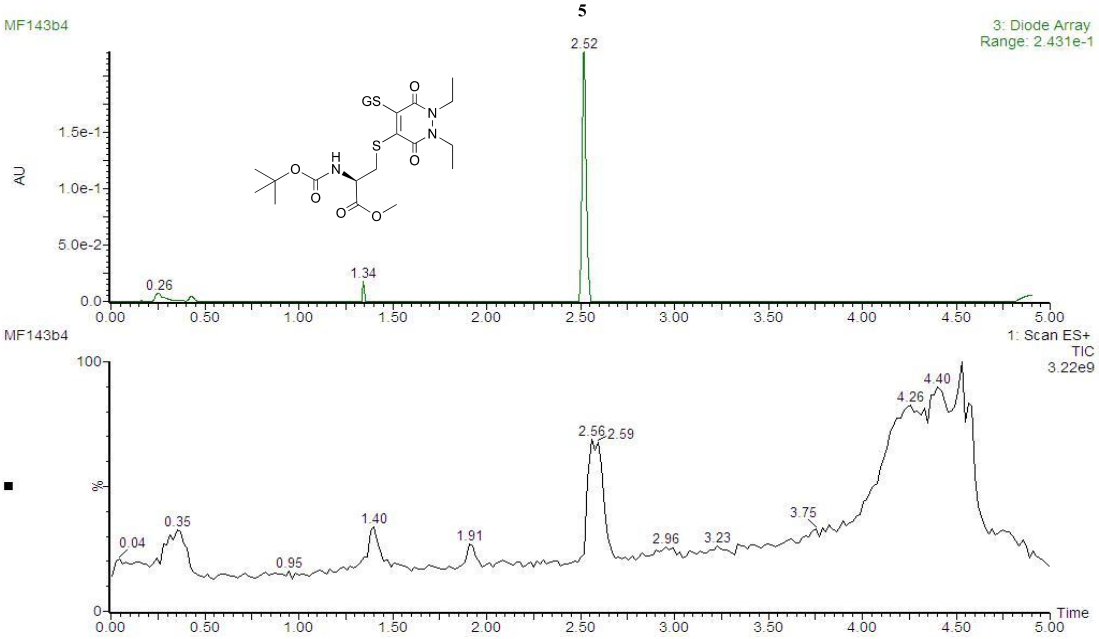
MF143b4
3: Diode Array
Range: 2.431e-1
AU
2.52
1.34
0.26
MF143b4
1: Scan ES+
TIC
3.22e9
%
4.40
4.26
2.56
2.59
0.35
0.04
1.40
1.91
0.95
2.96
3.23
3.75
Time

(b)

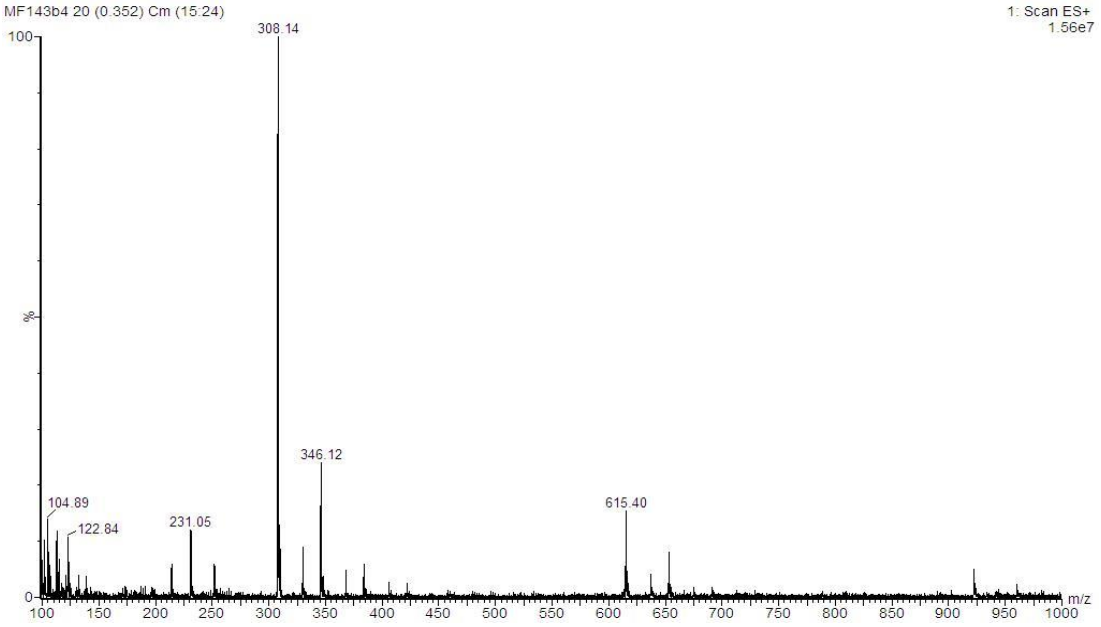
MF143b4 20 (0.352) Cm (15:24)
1: Scan ES+
1.56e7
308.14
%
346.12
104.89
122.84
231.05
615.40
m/z

(c)

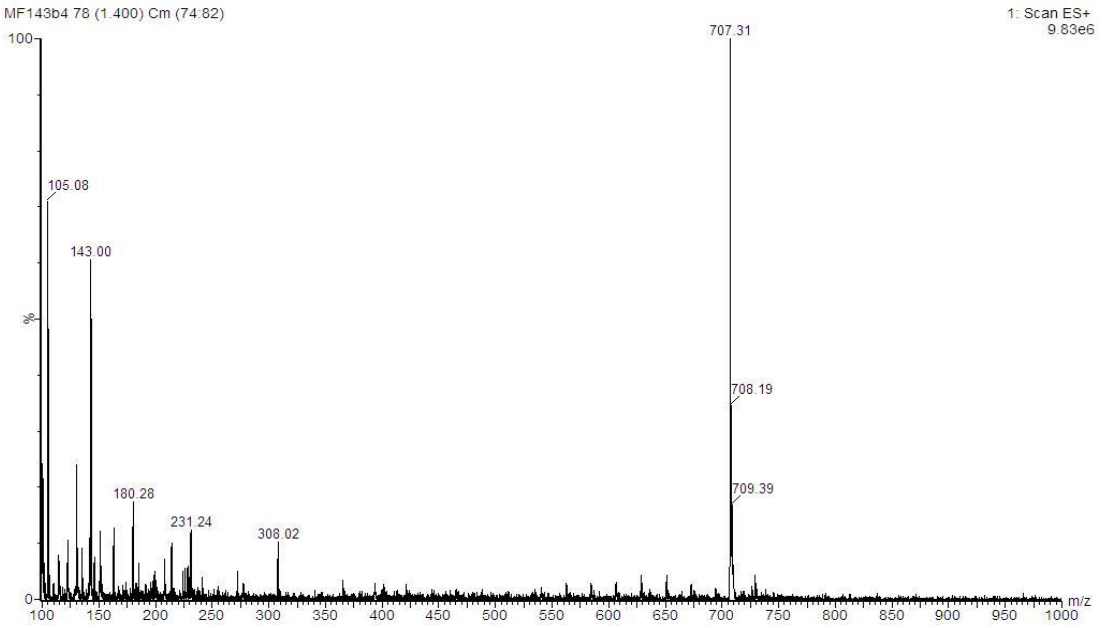

(d)

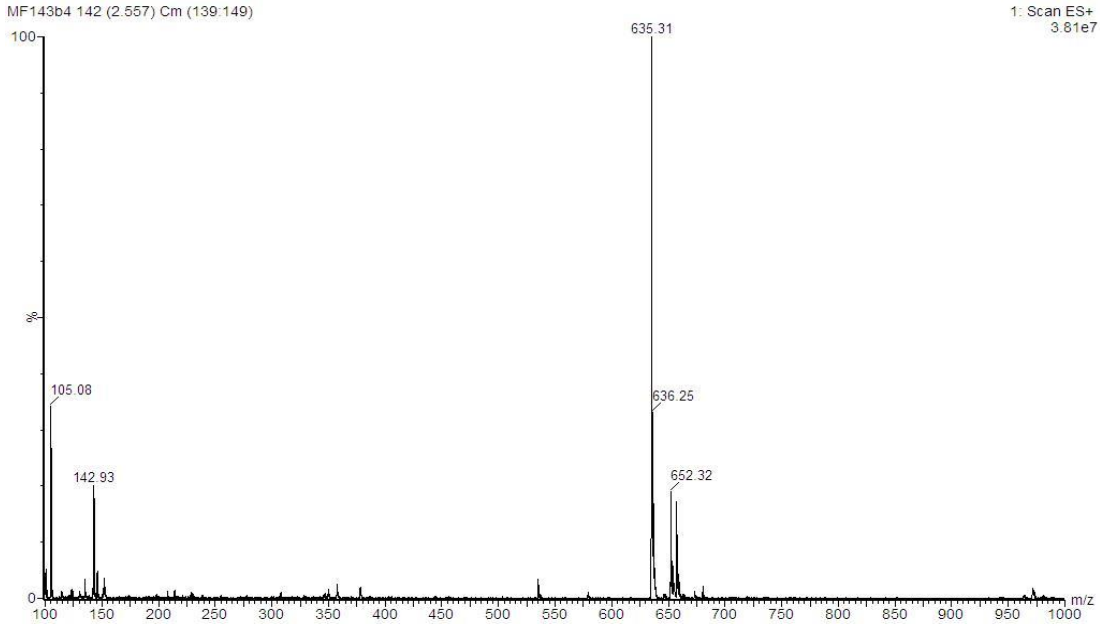

Figure **S74**. (a) TIC and UV trace at t = 2 h, (b) MS data at 0.26–0.42 mins in the UV, (c) MS data at 1.34 mins in the UV and (d) at 2.52 mins in the UV for PD **5** incubated with GSH **1** (10 eq.) at pH 5.0.

LC-MS data for t = 4 h

(a)

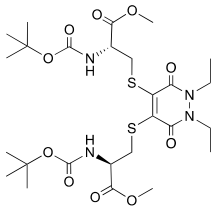

5

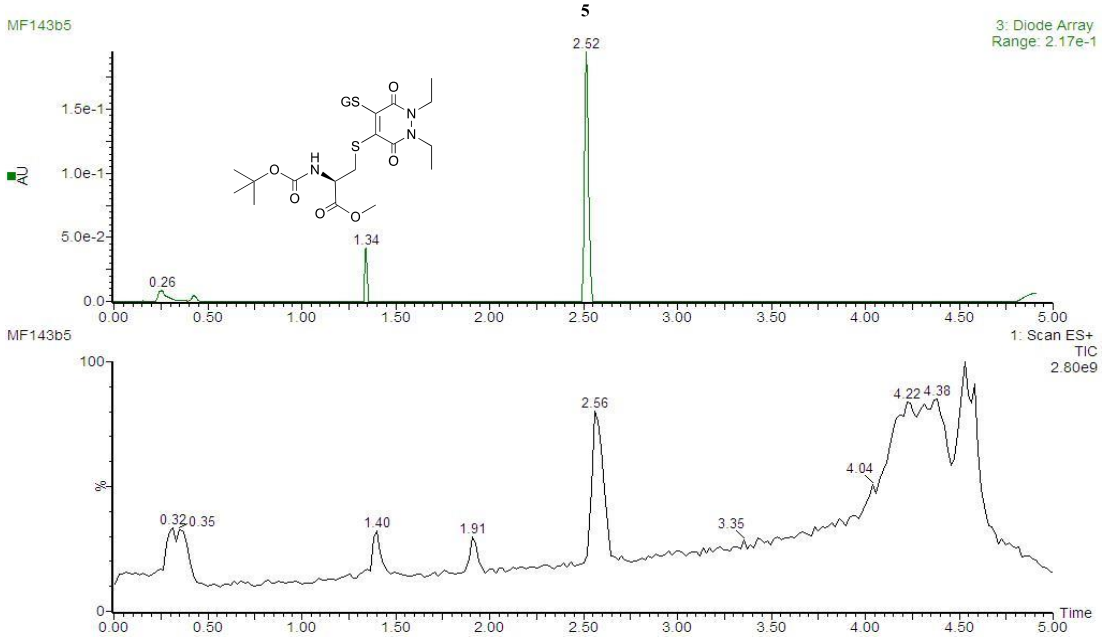
MF143b5
3: Diode Array
Range: 2.17e-1
AU
2.52
1.34
0.26
MF143b5
1: Scan ES+
TIC
2.80e9
%
2.56
4.22
4.38
4.04
0.32
0.35
1.40
1.91
3.35
Time

(b)

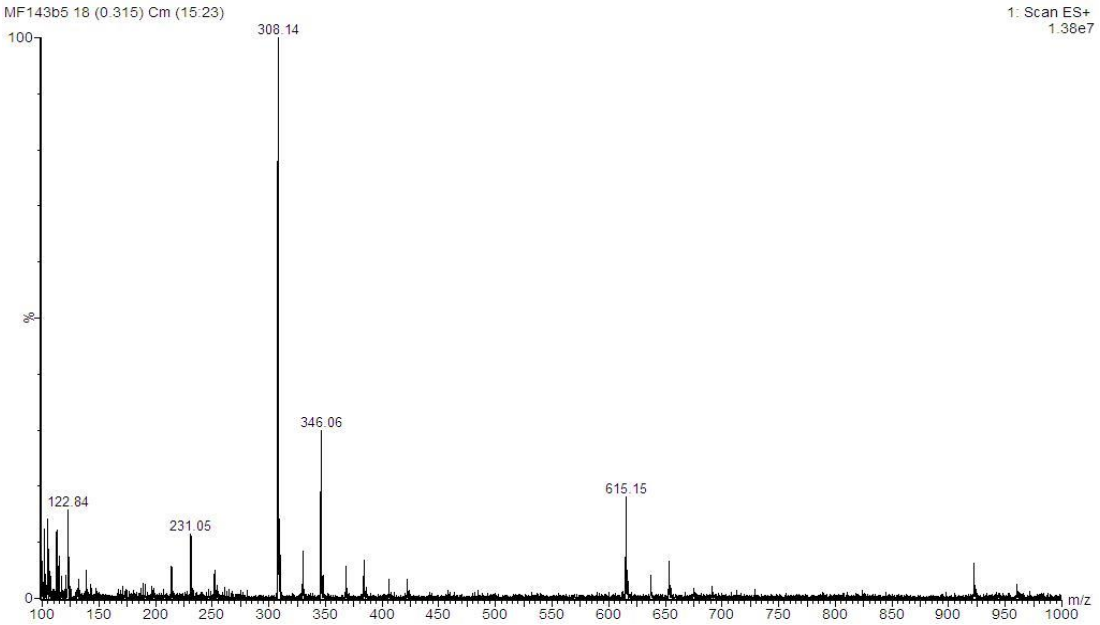
MF143b5 18 (0.315) Cm (15:23)
1: Scan ES+
1.38e7
308.14
346.06
615.15
122.84
231.05
%
m/z

(c)

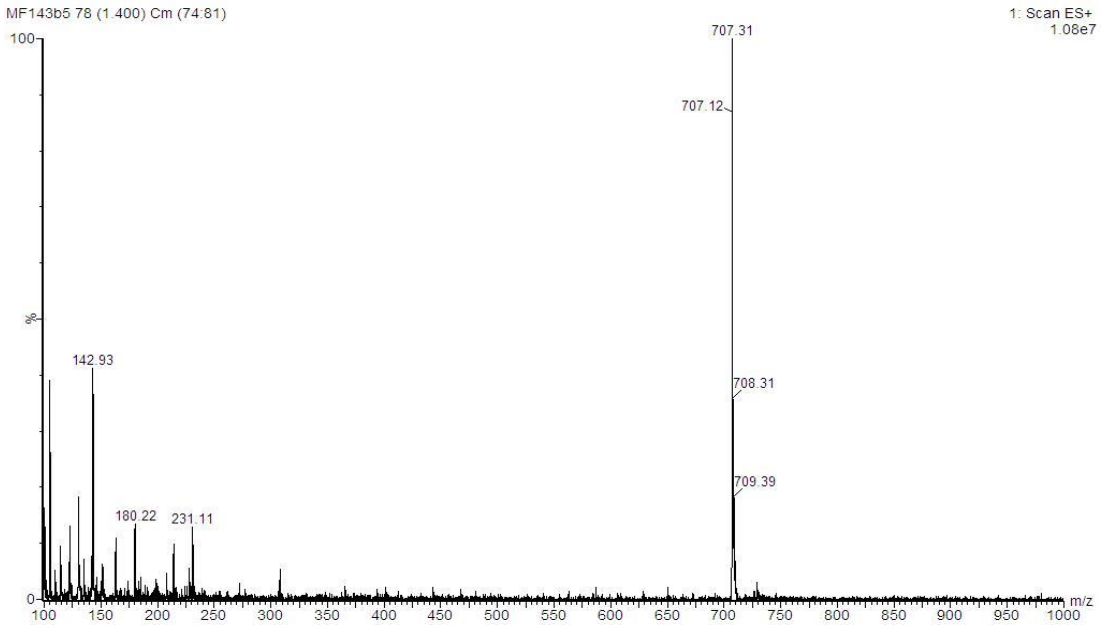

(d)

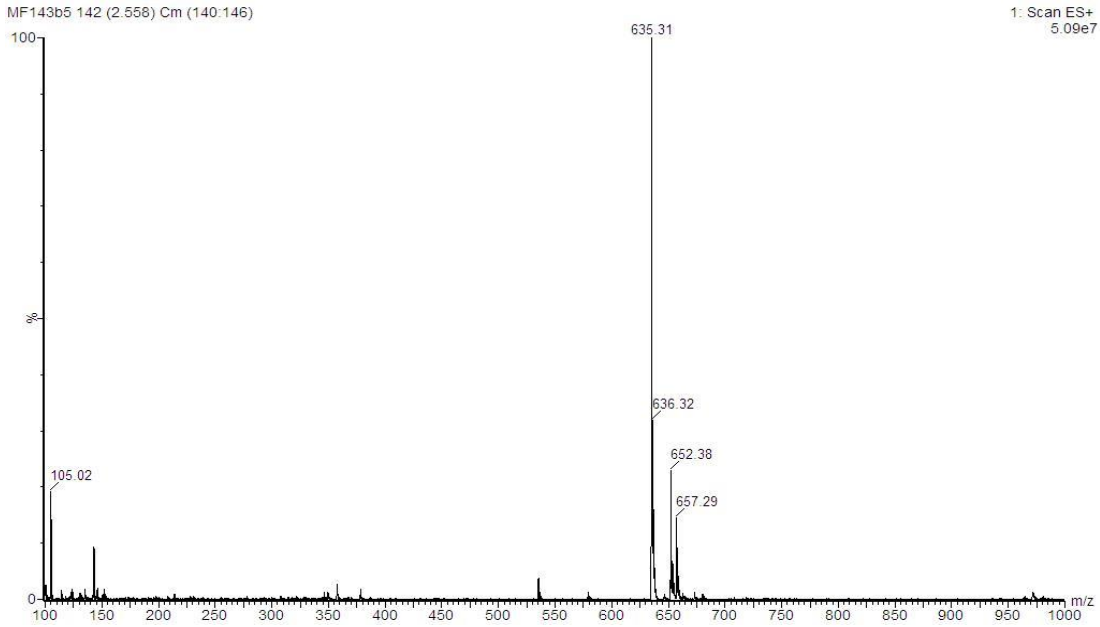

Figure **S75**. (a) TIC and UV trace at t = 4 h, (b) MS data at 0.26–0.42 mins in the UV, (c) MS data at 1.34 mins in the UV and (d) at 2.52 mins in the UV for PD **5** incubated with GSH **1** (10 eq.) at pH 5.0.

LC-MS data for t = 24 h

(a)

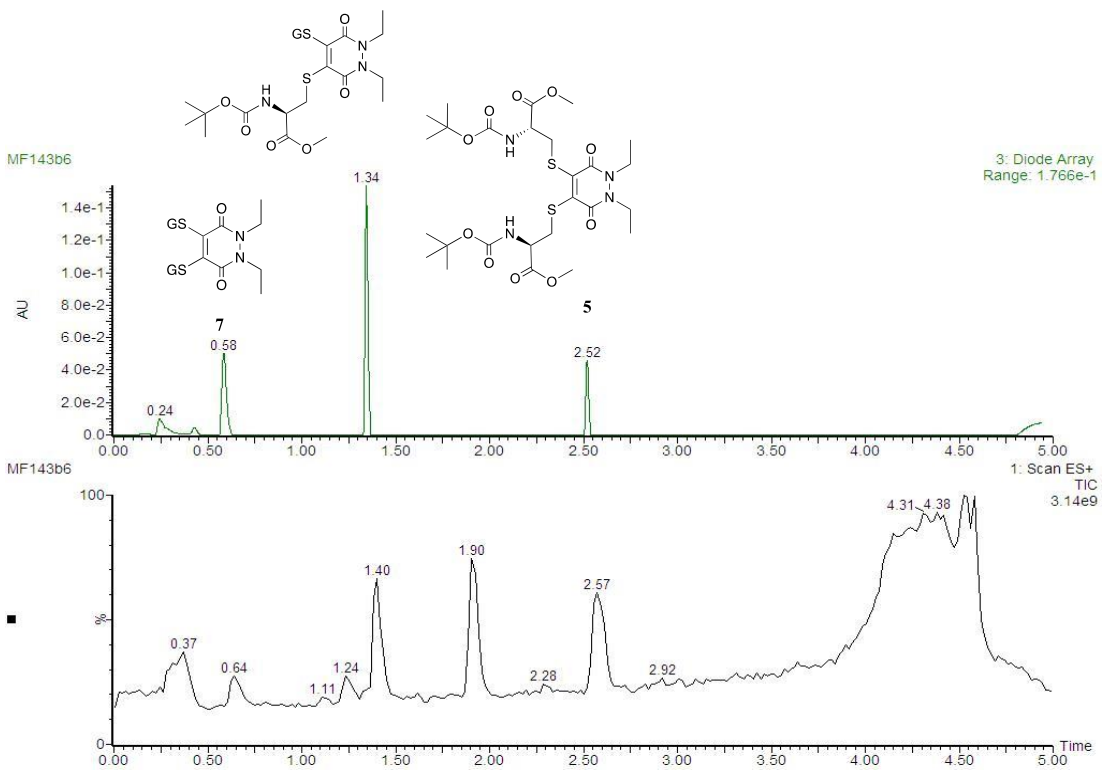
MF143b6
3: Diode Array
Range: 1.766e-1
AU
7
5
0.24
0.58
1.34
2.52
MF143b6
1: Scan ES+
TIC
3.14e9
%
0.37
0.64
1.11
1.24
1.40
1.90
2.28
2.57
2.92
4.31
4.38
Time

(b)

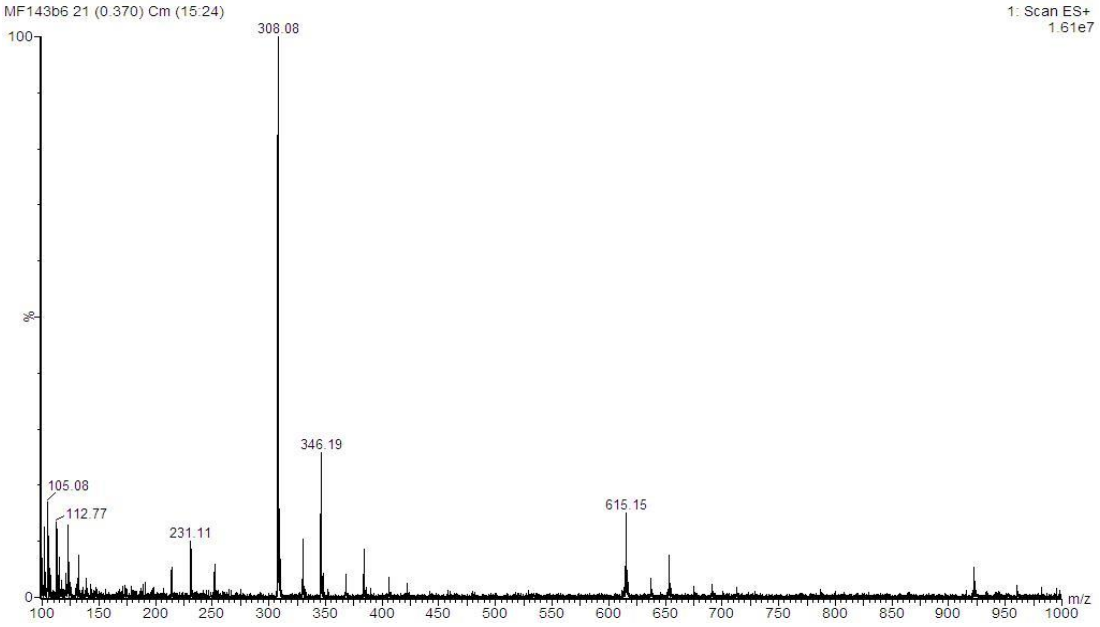
MF143b6 21 (0.370) Cm (15:24)
1: Scan ES+
1.61e7
%
308.08
346.19
105.08
112.77
231.11
615.15
m/z

(c)

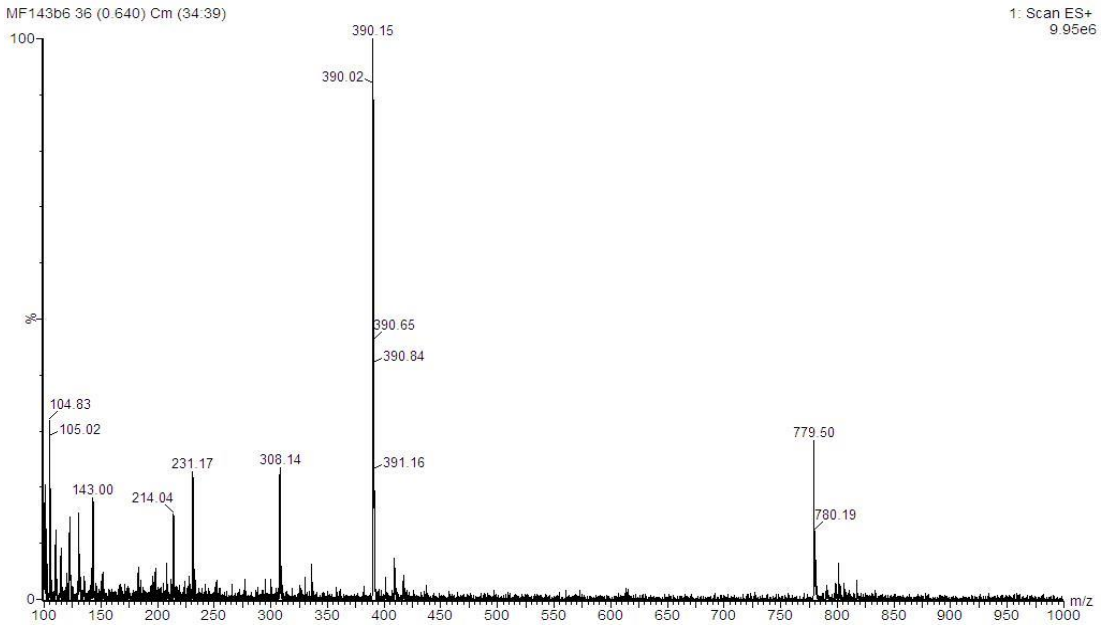
MF143b6 36 (0.640) Cm (34:39)
1: Scan ES+
9.95e6
100
%
0
390.15
390.02
390.65
390.84
104.83
105.02
231.17
308.14
391.16
143.00
214.04
779.50
780.19
m/z
100 150 200 250 300 350 400 450 500 550 600 650 700 750 800 850 900 950 1000

(d)

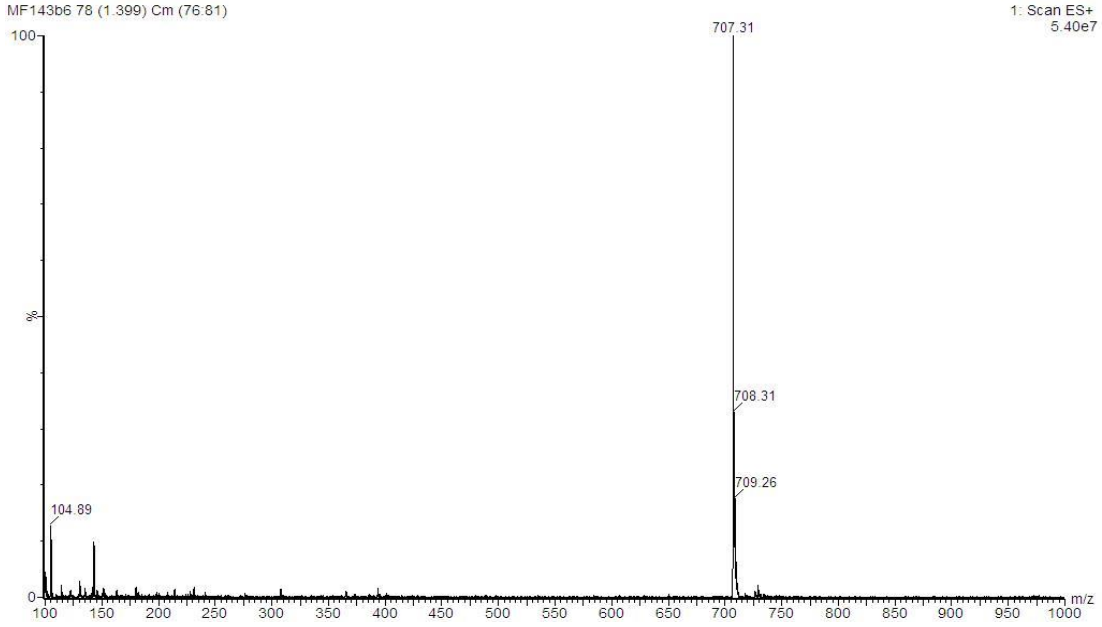
MF143b6 78 (1.399) Cm (76:81)
1: Scan ES+
5.40e7
100
%
0
707.31
708.31
709.26
104.89
m/z
100 150 200 250 300 350 400 450 500 550 600 650 700 750 800 850 900 950 1000

(e)

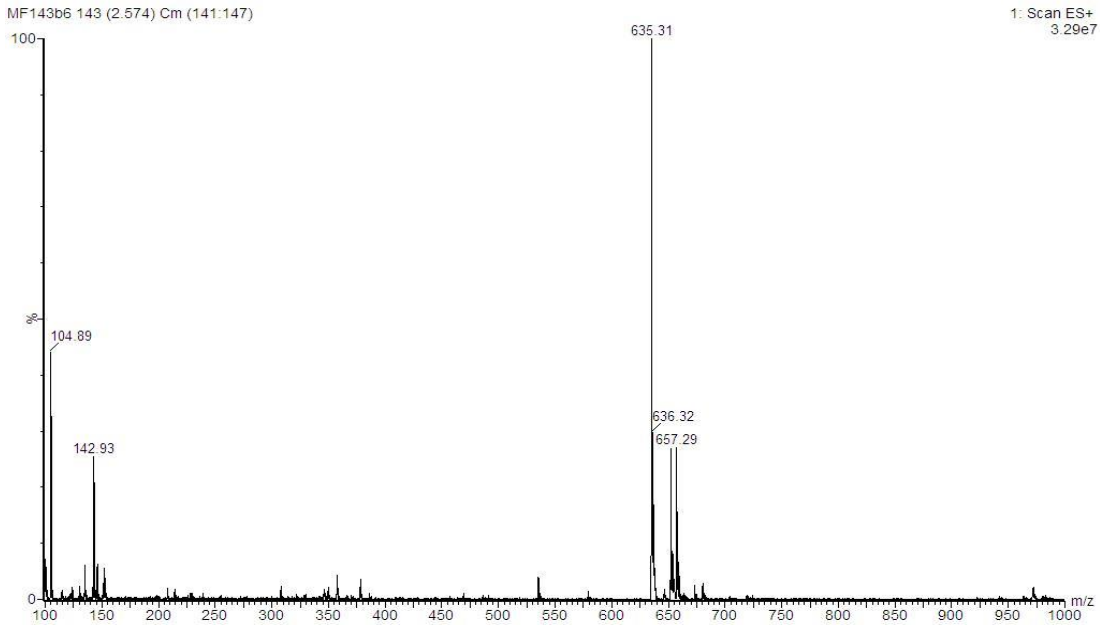

Figure **S76**. (a) TIC and UV trace at t = 24 h, (b) MS data at 0.24–0.42 mins in the UV, (c) MS data at 0.58 mins in the UV, (d) at 1.34 mins in the UV and (e) at 2.52 mins in the UV for PD **5** incubated with GSH **1** (10 eq.) at pH 5.0.

Incubation of PD 6 with GSH (10 eq.)

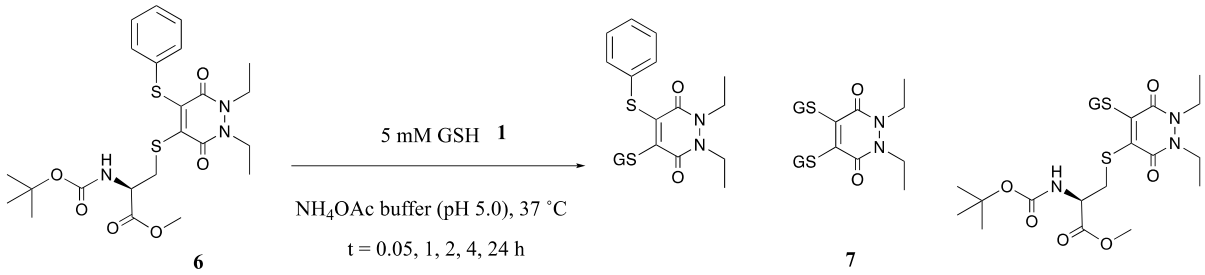

PD **6** (10 µL, 10 mM in MeCN, 1 eq.) was added to GSH **1** (190 µL, 5.3 mM, 10 eq.) in ammonium acetate buffer (50 mM, pH 5.0). The mixture was incubated at 37 ˚C for 24 h. The samples were analysed by LC-MS at t = 0.05, 1, 2, 4 and 24 h.

LC-MS data for t = 0.05 h

(a)

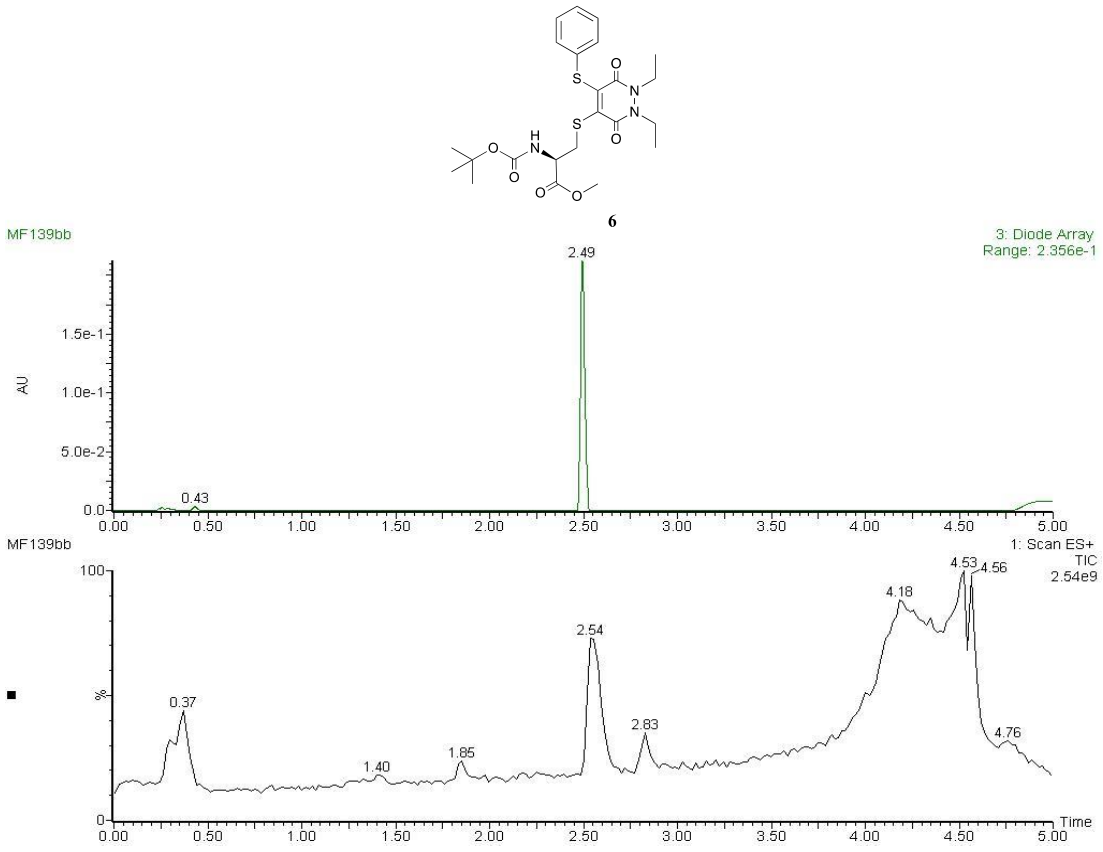

(b)

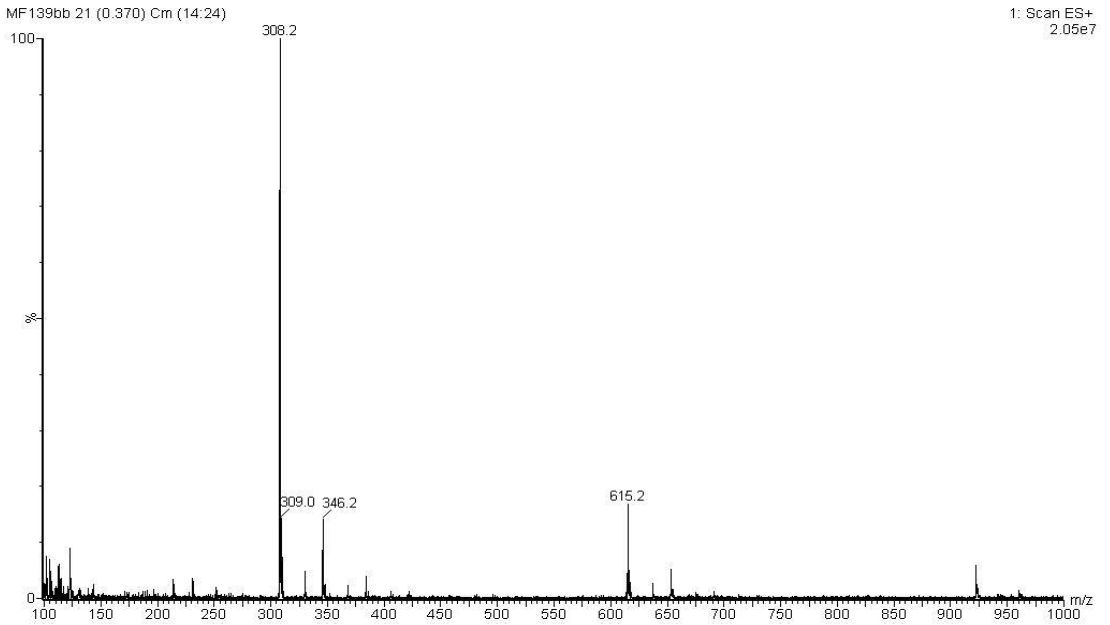

(c)

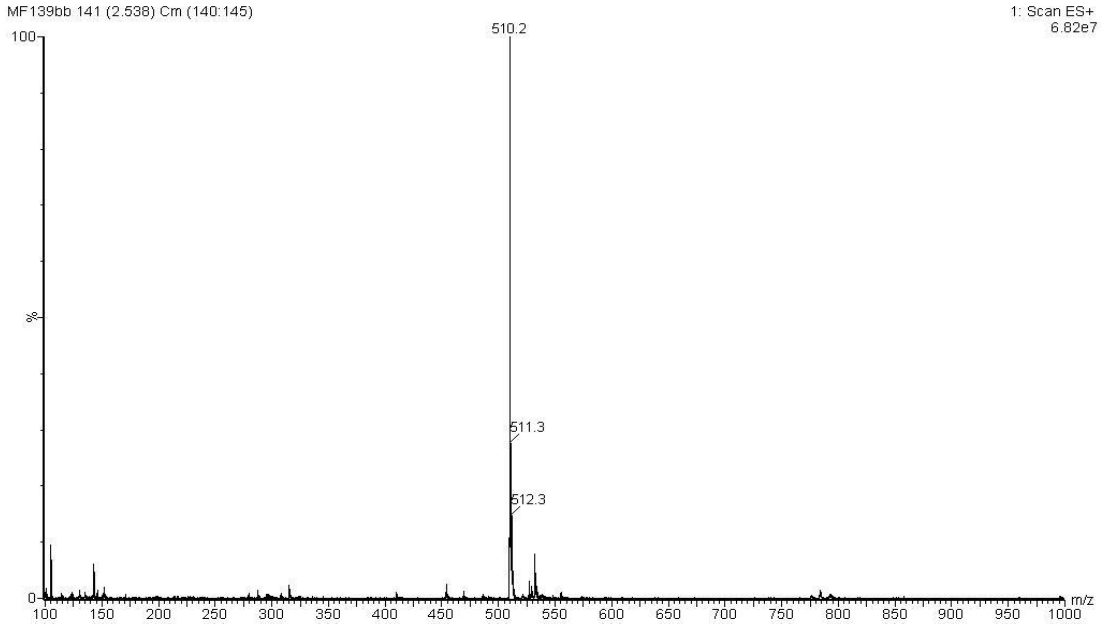

Figure **S77**. (a) TIC and UV trace at t = 0.05 h, (b) MS data at 0.24–0.43 mins in the UV and (c) MS data at 2.49 mins in the UV for PD **6** incubated with GSH **1** (10 eq.) at pH 5.0.

LC-MS data for t = 1 h

(a)

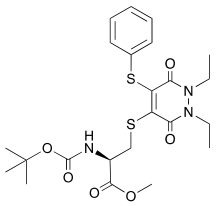

6

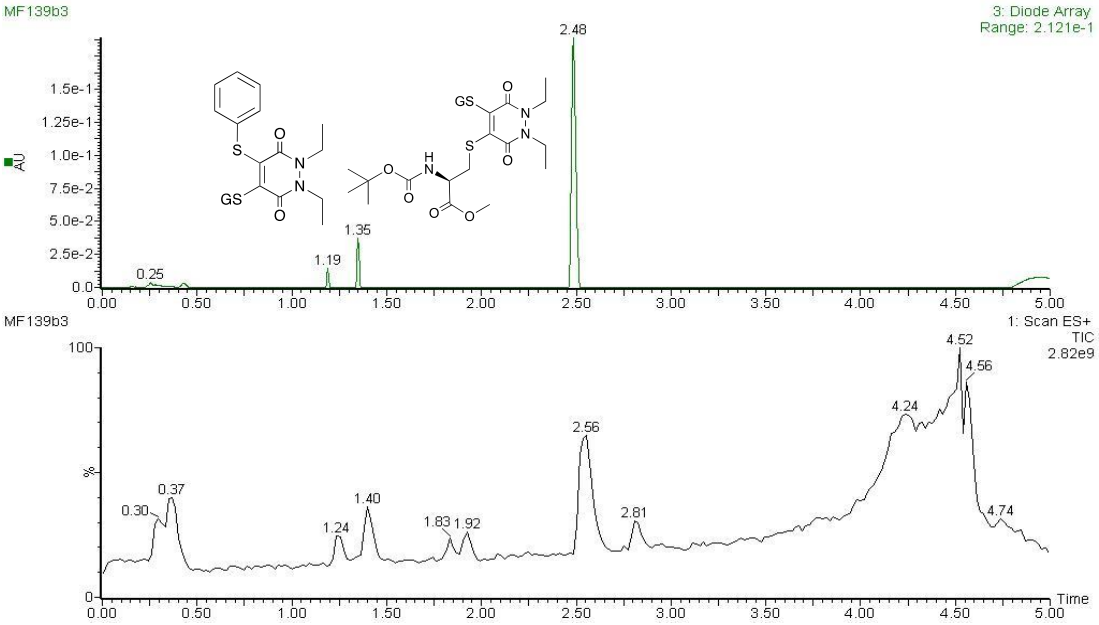
MF139b3
3: Diode Array
Range: 2.121e-1
AU
2.48
1.35
1.19
0.25
MF139b3
1: Scan ES+
TIC
2.82e9
4.52
4.56
4.24
2.56
0.37
0.30
1.40
1.24
1.83
1.92
2.81
4.74
%
Time

(b)

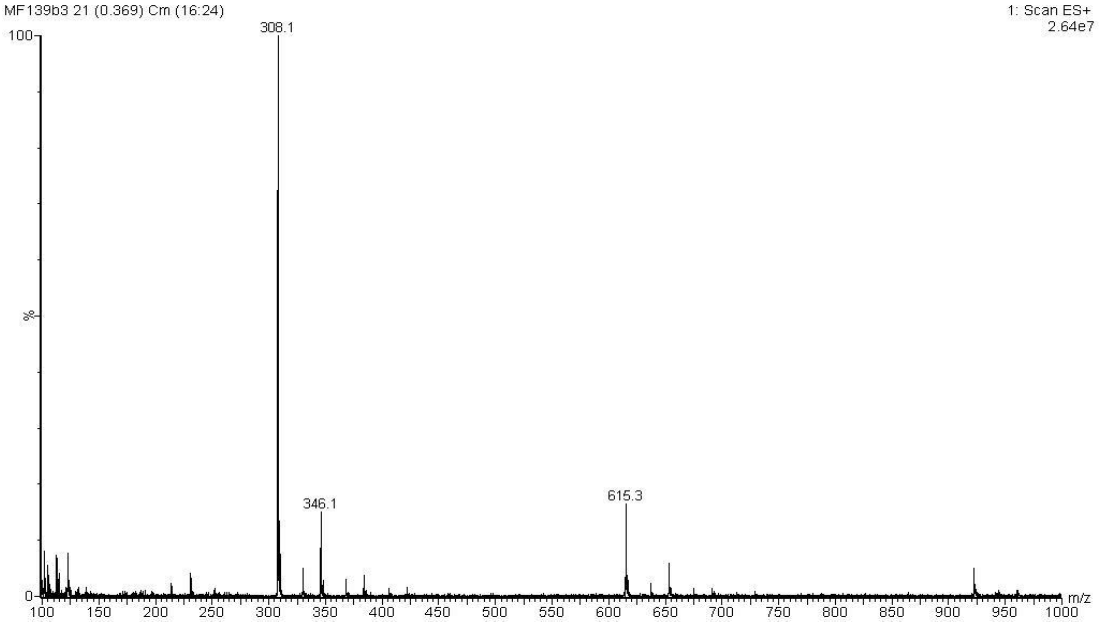
MF139b3 21 (0.369) Cm (16:24)
1: Scan ES+
2.64e7
308.1
346.1
615.3
%
m/z

(c)

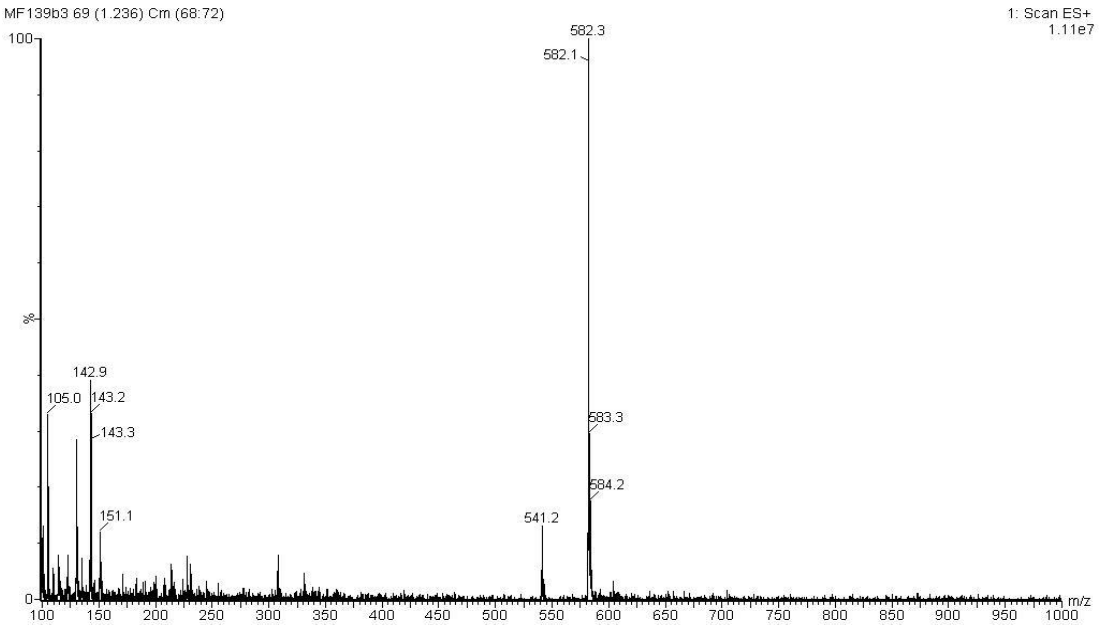
MF139b3 69 (1.236) Cm (68:72)
1: Scan ES+
1.11e7
100
%
0
582.3
582.1
142.9
105.0
143.2
143.3
151.1
541.2
583.3
584.2
100 150 200 250 300 350 400 450 500 550 600 650 700 750 800 850 900 950 1000
m/z

(d)

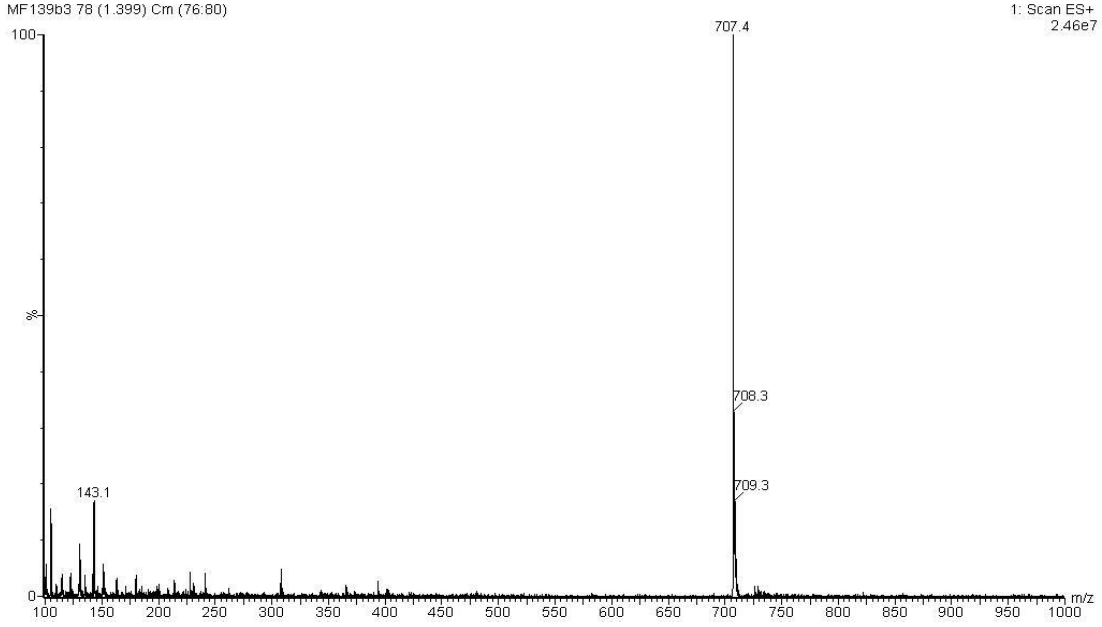
MF139b3 78 (1.399) Cm (76:80)
1: Scan ES+
2.46e7
100
%
0
707.4
708.3
709.3
143.1
100 150 200 250 300 350 400 450 500 550 600 650 700 750 800 850 900 950 1000
m/z

(e)

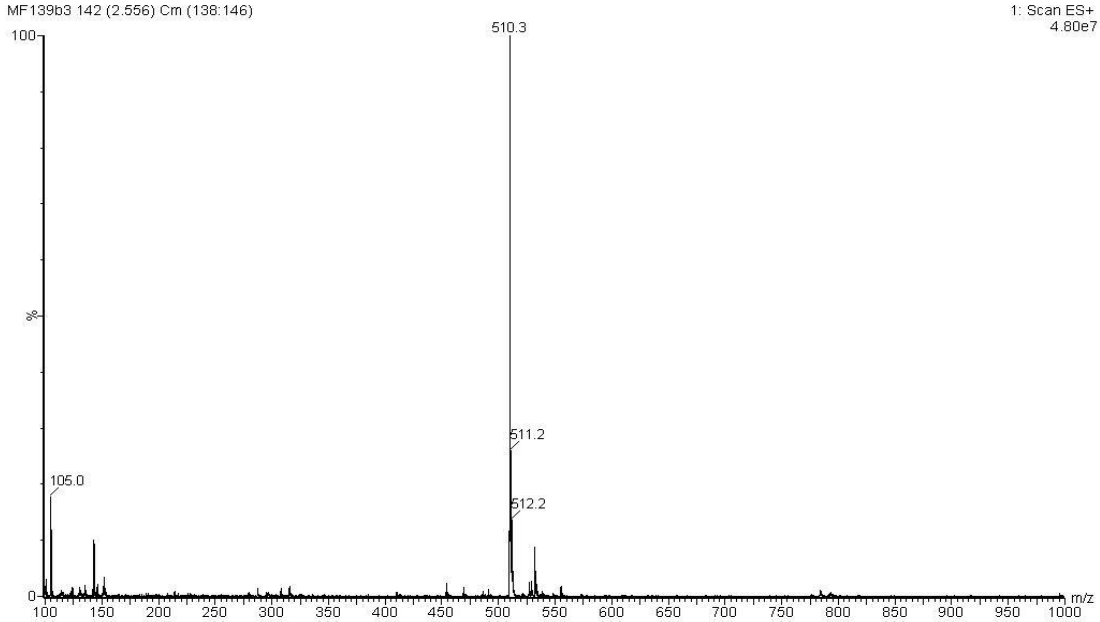

Figure **S78**. (a) TIC and UV trace at t = 1 h, (b) MS data at 0.25–0.43 mins in the UV, (c) MS data at 1.19 mins in the UV, (d) at 1.35 mins in the UV and (e) at 2.48 mins in the UV for PD **6** incubated with GSH **1** (10 eq.) at pH 5.0.

LC-MS data for t = 2 h

(a)

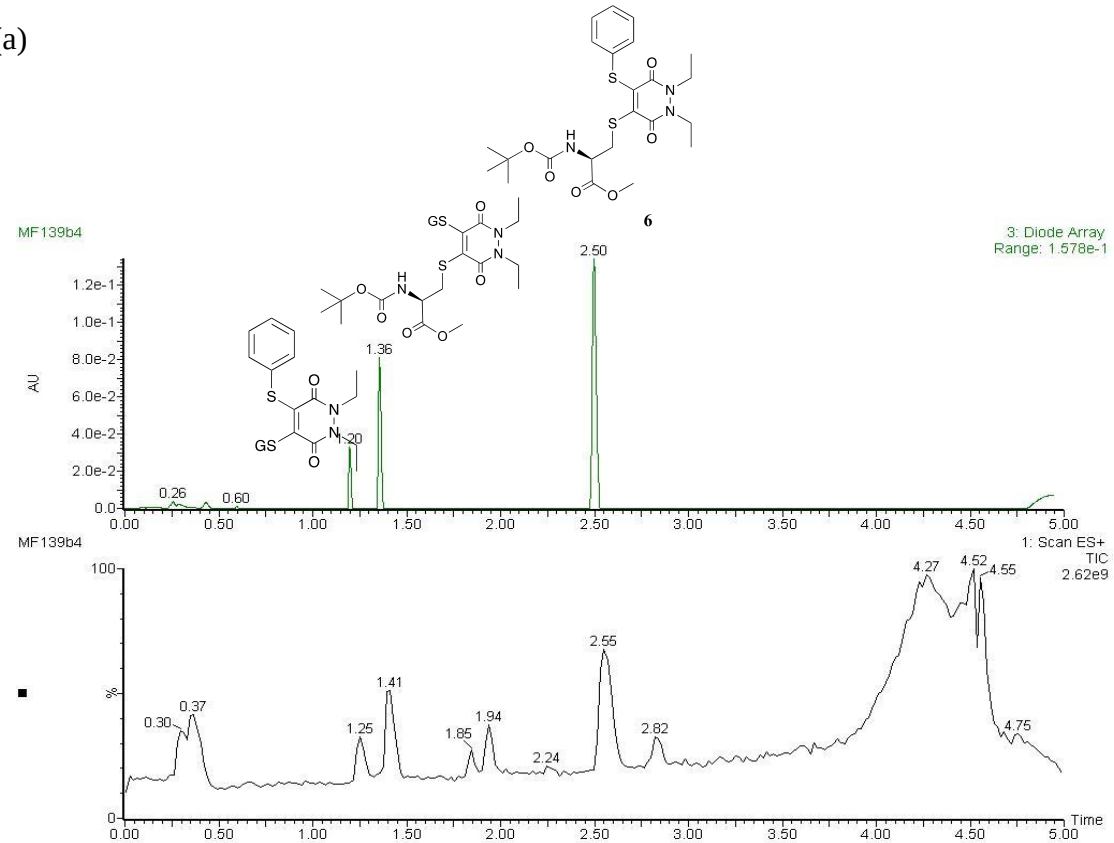

(b)

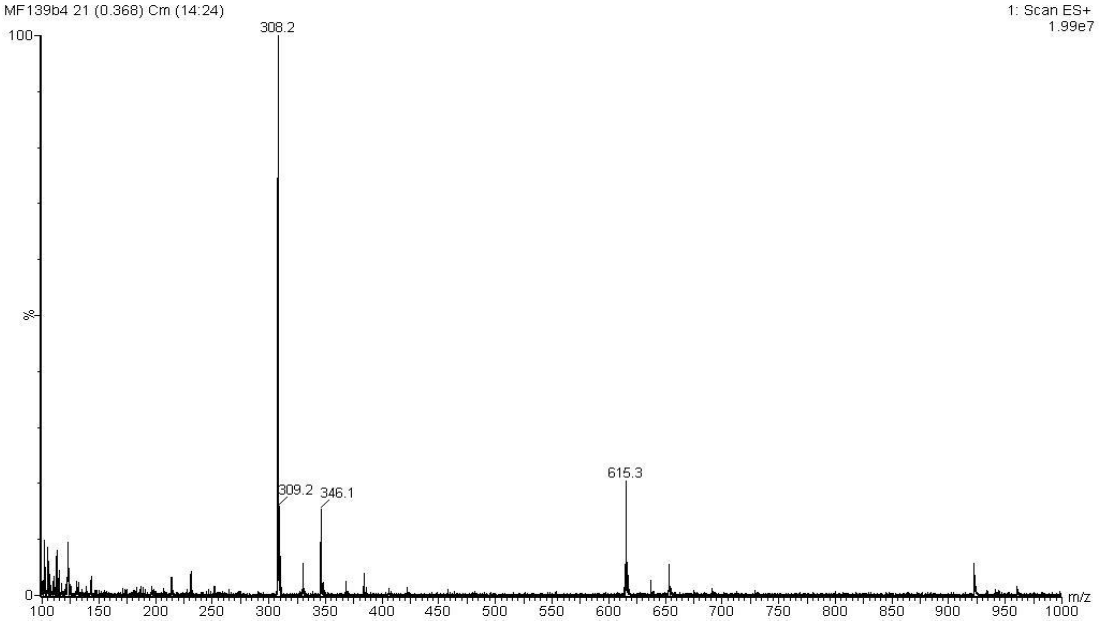
MF139b4 21 (0.368) Cm (14:24)
1: Scan ES+
1.99e7
100
%
0
308.2
309.2
346.1
615.3
100 150 200 250 300 350 400 450 500 550 600 650 700 750 800 850 900 950 1000
m/z

(c)

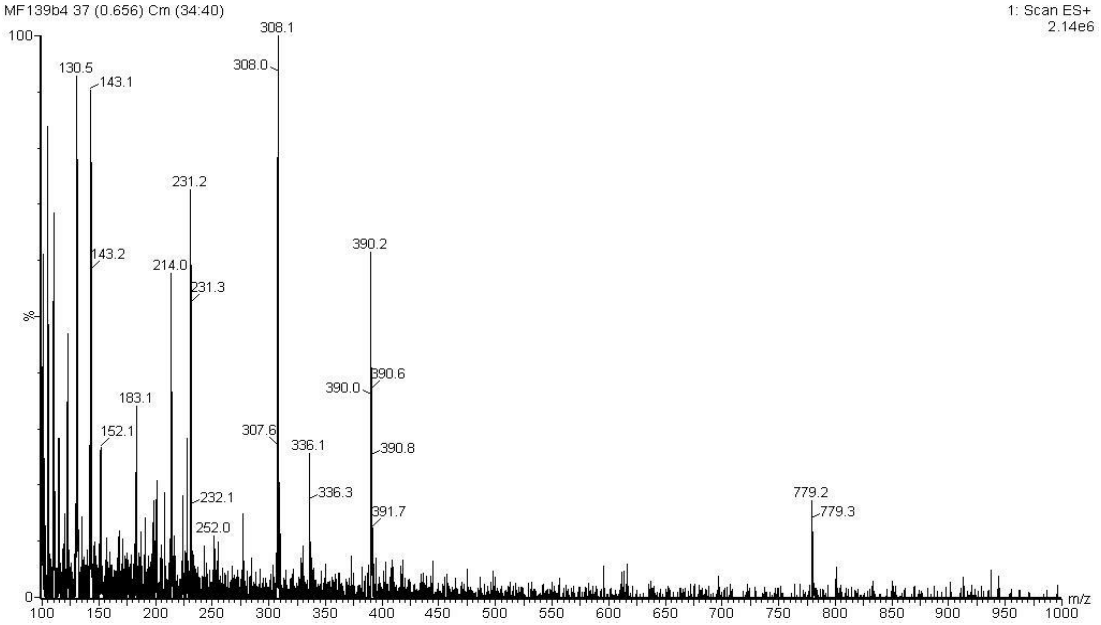
MF139b4 37 (0.656) Cm (34:40)
1: Scan ES+
2.14e6
100
%
0
308.1
308.0
130.5
143.1
231.2
143.2
214.0
231.3
390.2
390.6
390.0
183.1
152.1
307.6
336.1
390.8
336.3
232.1
391.7
252.0
779.2
779.3
100 150 200 250 300 350 400 450 500 550 600 650 700 750 800 850 900 950 1000
m/z

(d)

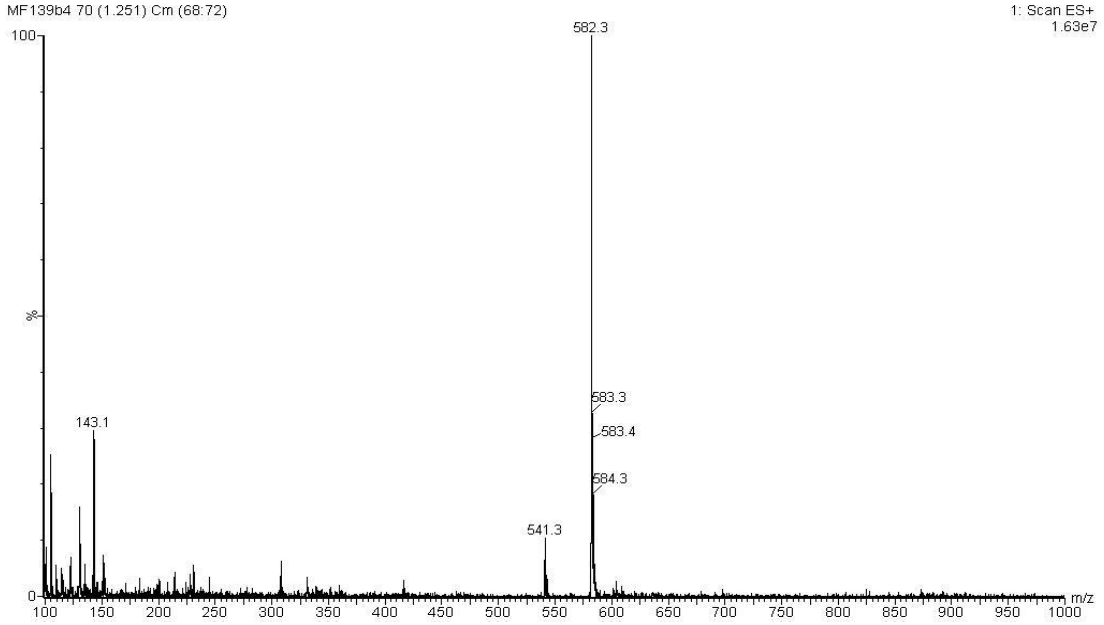
MF139b4 70 (1.251) Cm (68:72)
1: Scan ES+
1.63e7
100
%
0
582.3
583.3
583.4
584.3
143.1
541.3
100 150 200 250 300 350 400 450 500 550 600 650 700 750 800 850 900 950 1000
m/z

(e)

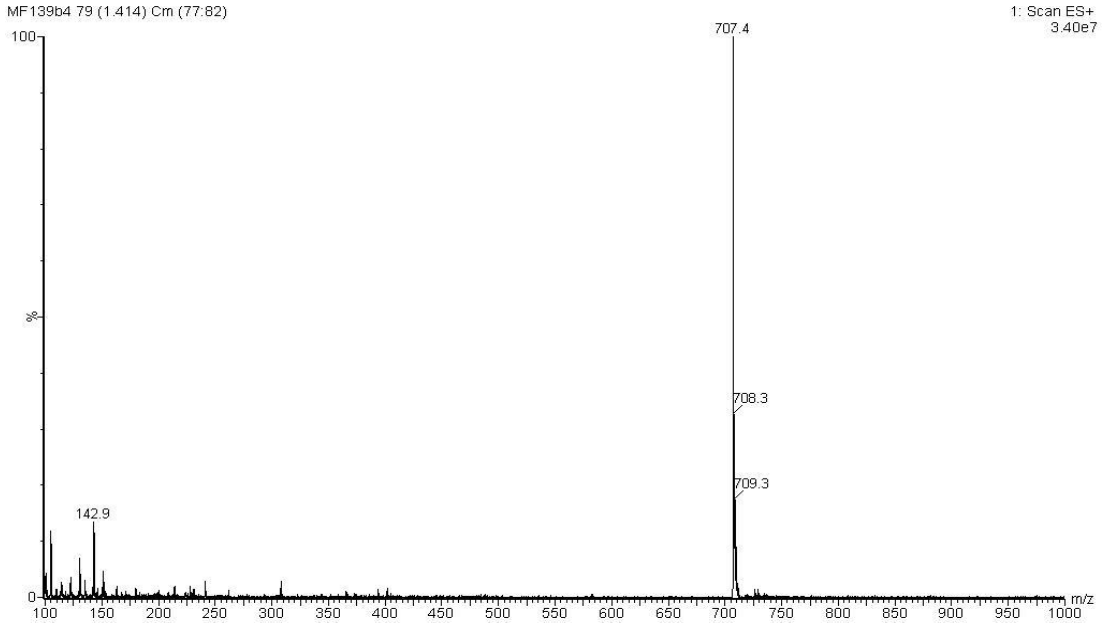
MF139b4 79 (1.414) Cm (77:82)
1: Scan ES+
3.40e7
100
%
0
707.4
708.3
709.3
142.9
100 150 200 250 300 350 400 450 500 550 600 650 700 750 800 850 900 950 1000
m/z

(f)

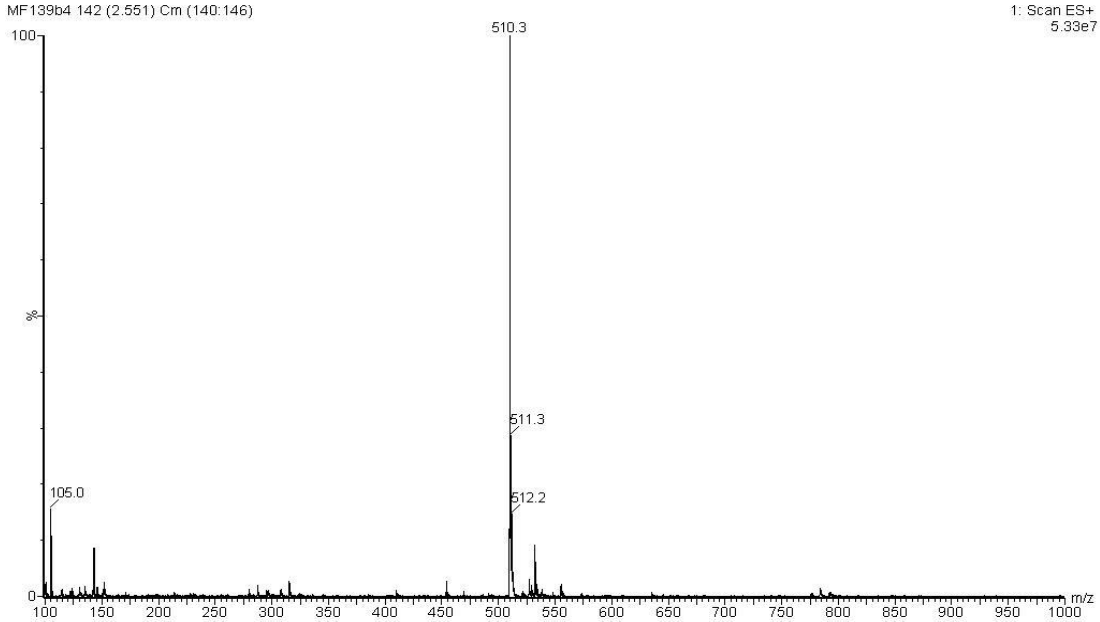

Figure **S79**. (a) TIC and UV trace at t = 2 h, (b) MS data at 0.26–0.43 mins in the UV, (c) MS data at 0.60 mins in the UV, (d) at 1.20 mins in the UV, (e) at 1.36 mins in the UV and (f) at 2.50 mins in the UV for PD **6** incubated with GSH **1** (10 eq.) at pH 5.0.

LC-MS data for t = 4 h

(a)

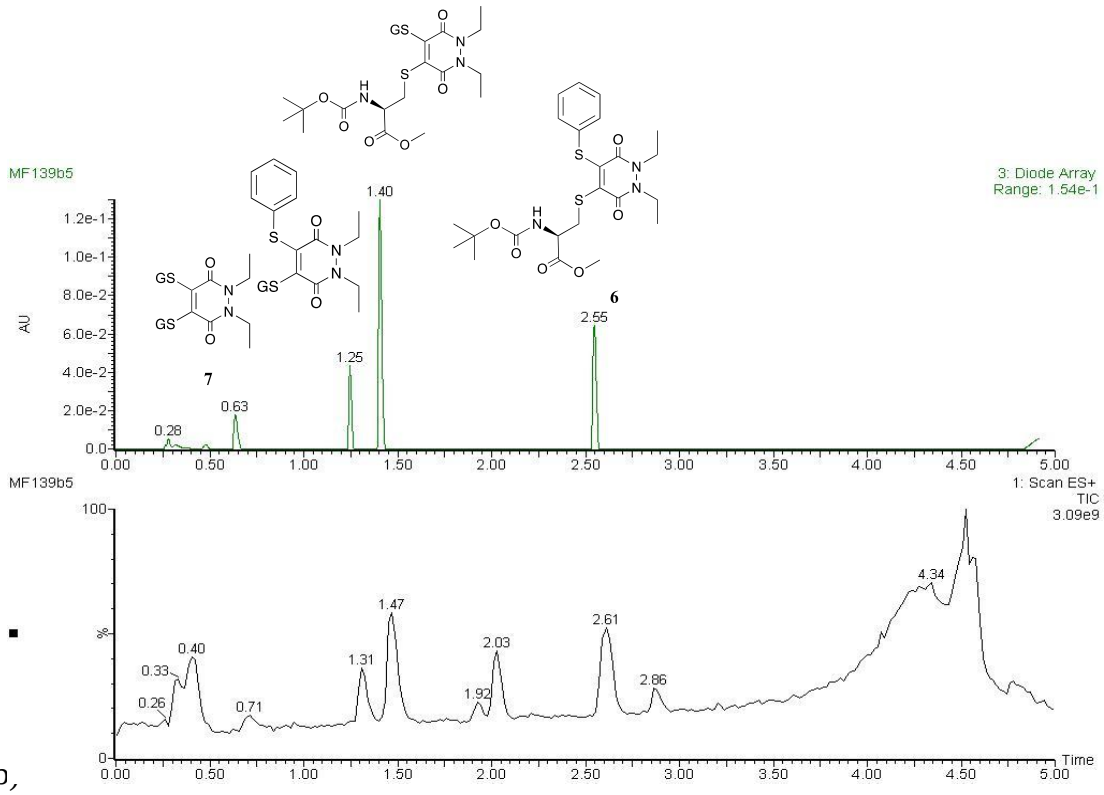

(b)

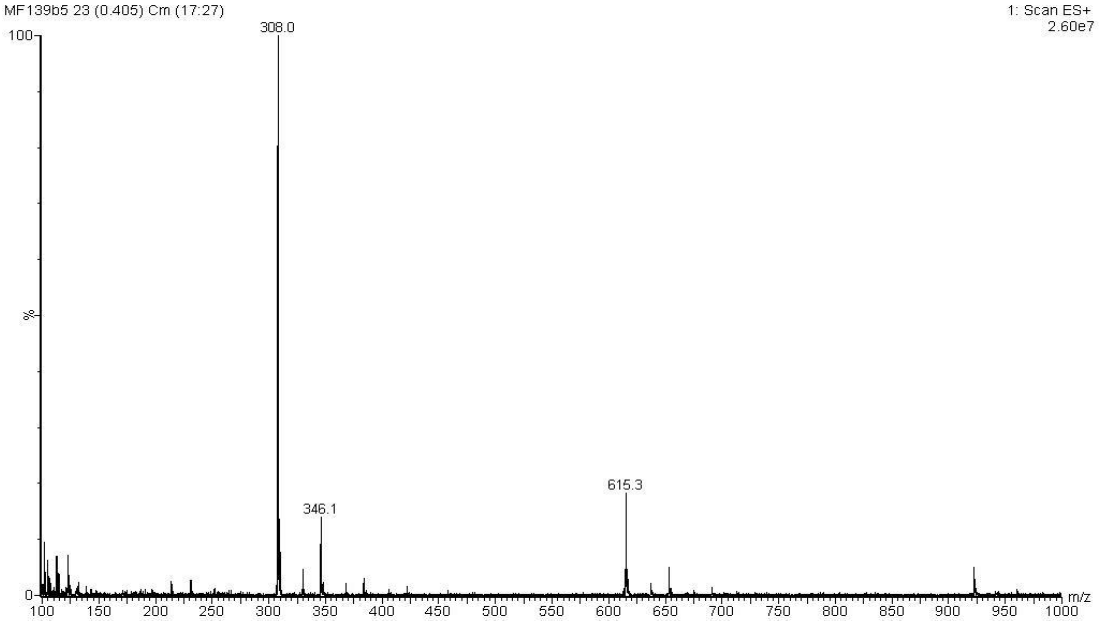
MF139b5 23 (0.405) Cm (17:27)
1: Scan ES+
2.60e7
100
%
0
308.0
346.1
615.3
100 150 200 250 300 350 400 450 500 550 600 650 700 750 800 850 900 950 1000
m/z

(c)

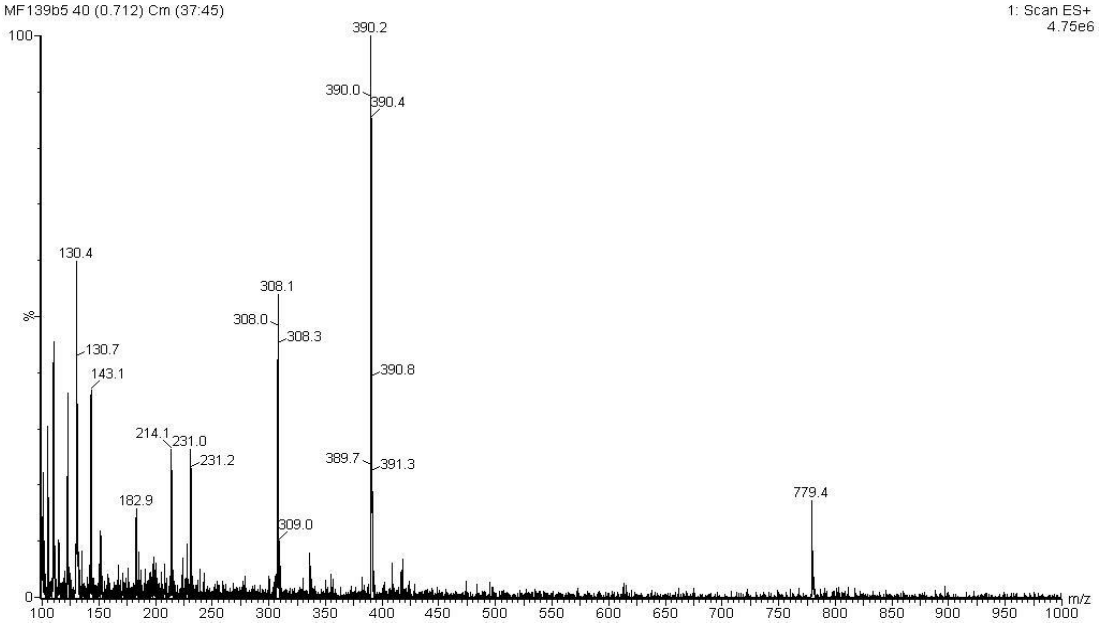
MF139b5 40 (0.712) Cm (37:45)
1: Scan ES+
4.75e6
100
%
0
390.2
390.0
390.4
130.4
308.1
308.0
308.3
130.7
143.1
390.8
214.1
231.0
231.2
389.7
391.3
182.9
309.0
779.4
100 150 200 250 300 350 400 450 500 550 600 650 700 750 800 850 900 950 1000
m/z

(d)

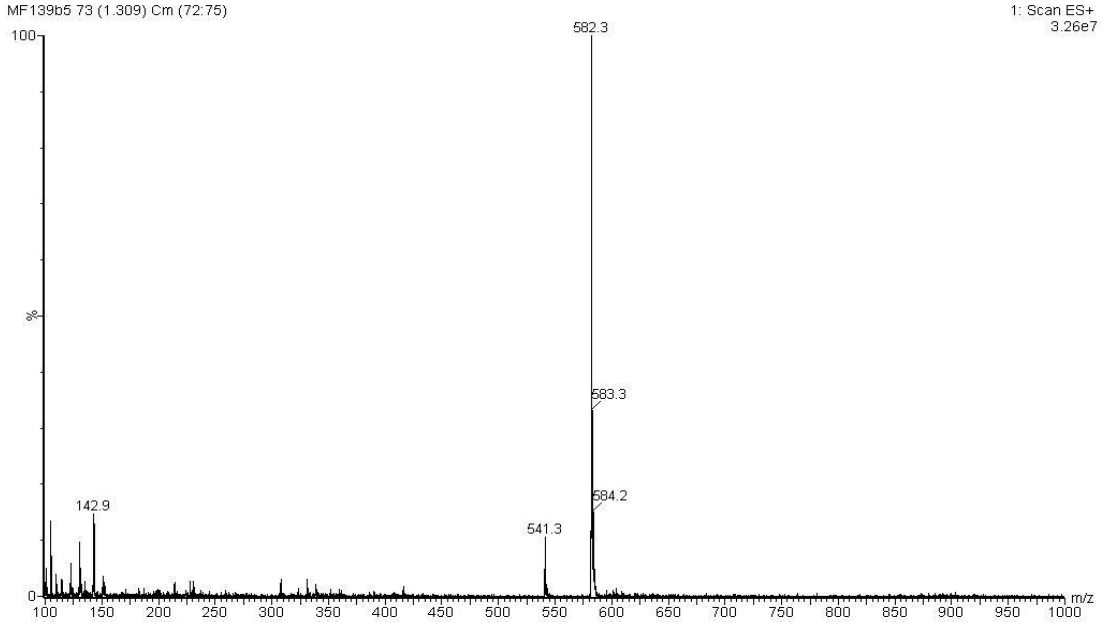
MF139b5 73 (1.309) Cm (72:75)
1: Scan ES+
3.26e7
100
%
0
582.3
583.3
584.2
142.9
541.3
100 150 200 250 300 350 400 450 500 550 600 650 700 750 800 850 900 950 1000
m/z

(e)

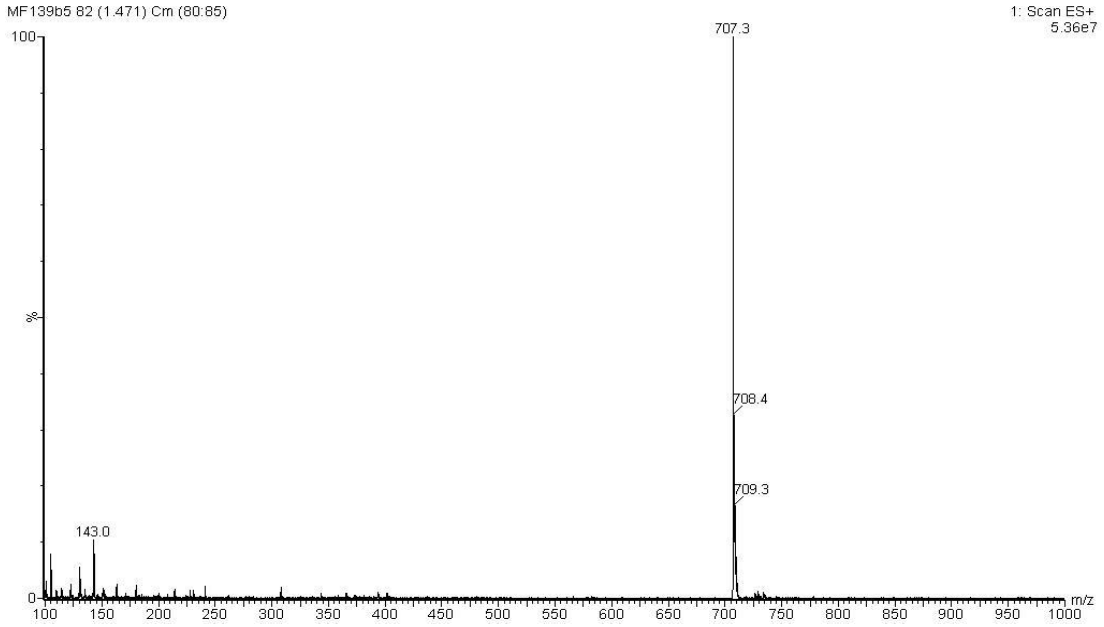
MF139b5 82 (1.471) Cm (80:85)
1: Scan ES+
5.36e7
100
%
0
707.3
708.4
709.3
143.0
100 150 200 250 300 350 400 450 500 550 600 650 700 750 800 850 900 950 1000
m/z

(f)

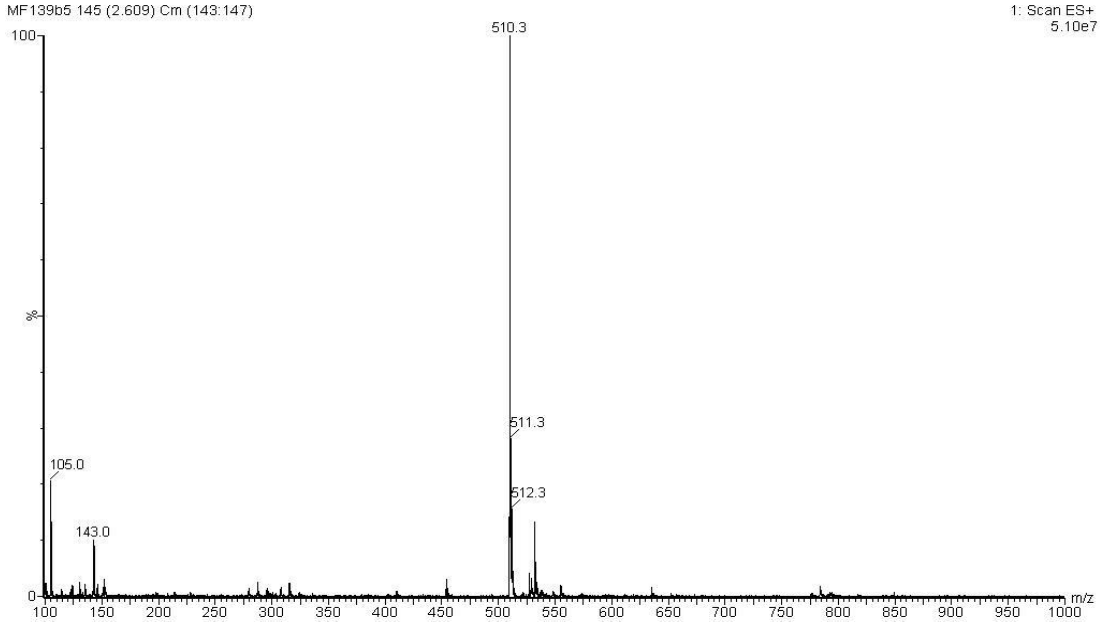

Figure **S80**. (a) TIC and UV trace at t = 4 h, (b) MS data at 0.28–0.43 mins in the UV, (c) MS data at 0.63 mins in the UV, (d) at 1.25 mins in the UV, (e) at 1.40 mins in the UV and (f) at 2.55 mins in the UV for PD **6** incubated with GSH **1** (10 eq.) at pH 5.0.

LC-MS data for t = 24 h

(a)

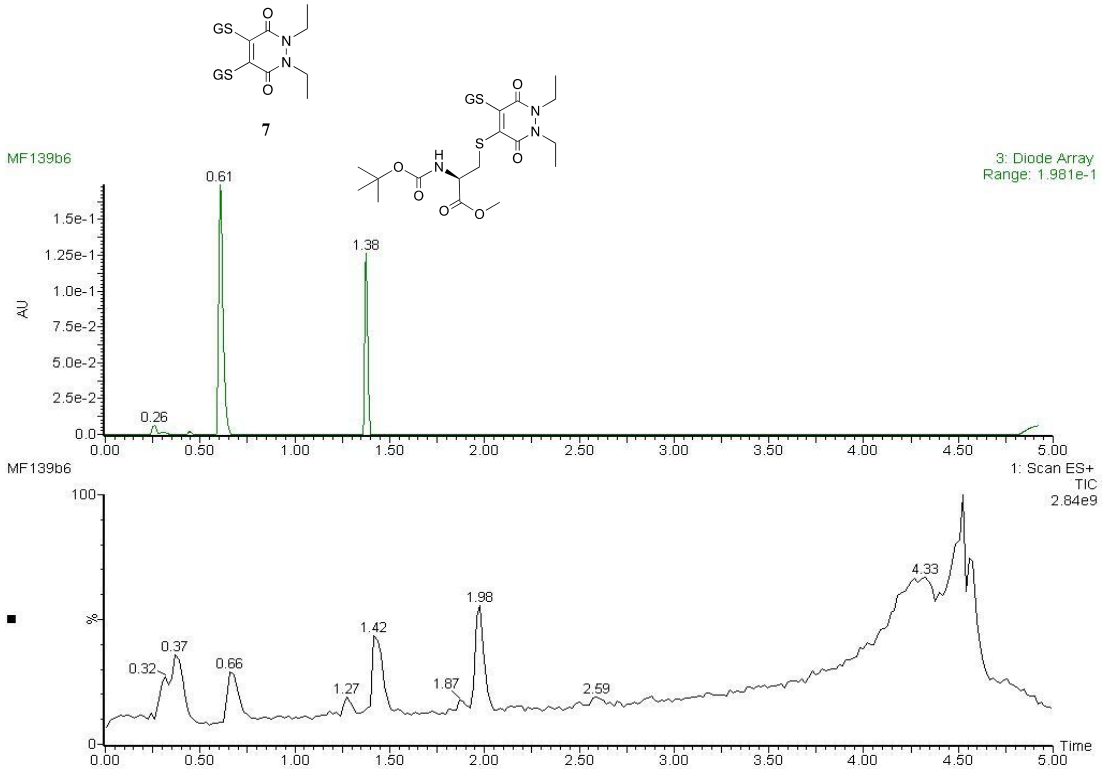

(b)

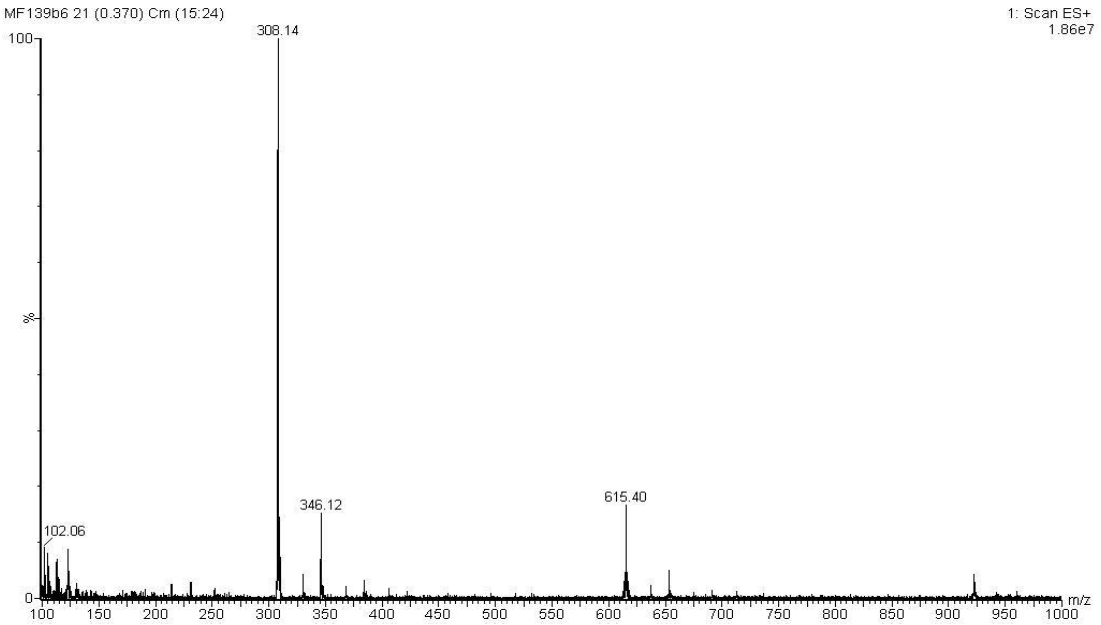
MF139b6 21 (0.370) Cm (15:24)
1: Scan ES+
1.86e7
100
%
0
308.14
346.12
615.40
102.06
100 150 200 250 300 350 400 450 500 550 600 650 700 750 800 850 900 950 1000
m/z

(c)

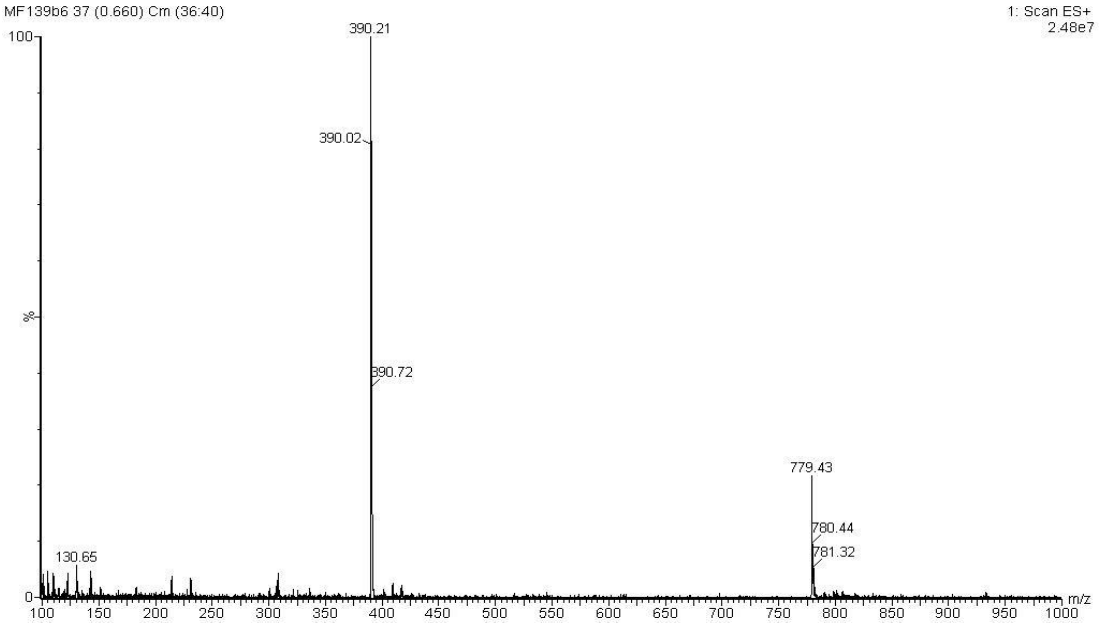
MF139b6 37 (0.660) Cm (36:40)
1: Scan ES+
2.48e7
100
%
0
390.21
390.02
390.72
779.43
780.44
781.32
130.65
100 150 200 250 300 350 400 450 500 550 600 650 700 750 800 850 900 950 1000
m/z

(d)

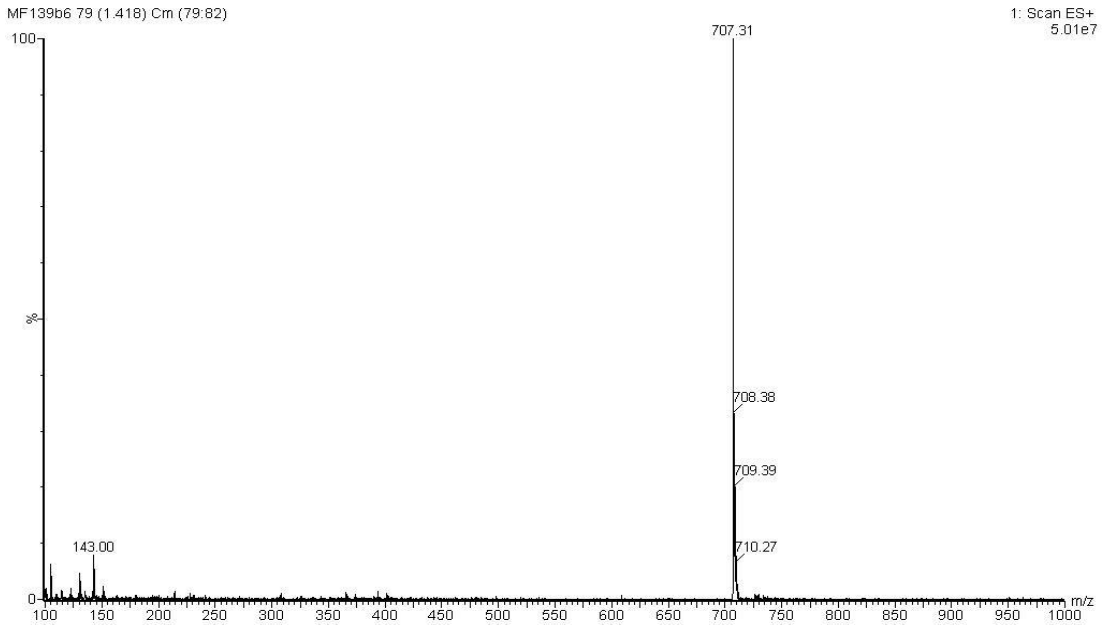

Figure **S81**. (a) TIC and UV trace at t = 24 h, (b) MS data at 0.26–0.43 mins in the UV, (c) MS data at 0.61 mins in the UV and (d) at 1.38 mins in the UV for PD **6** incubated with GSH **1** (10 eq.) at pH 5.0.

Incubation of PD 13 with GSH (10 eq.) at pH 6.5

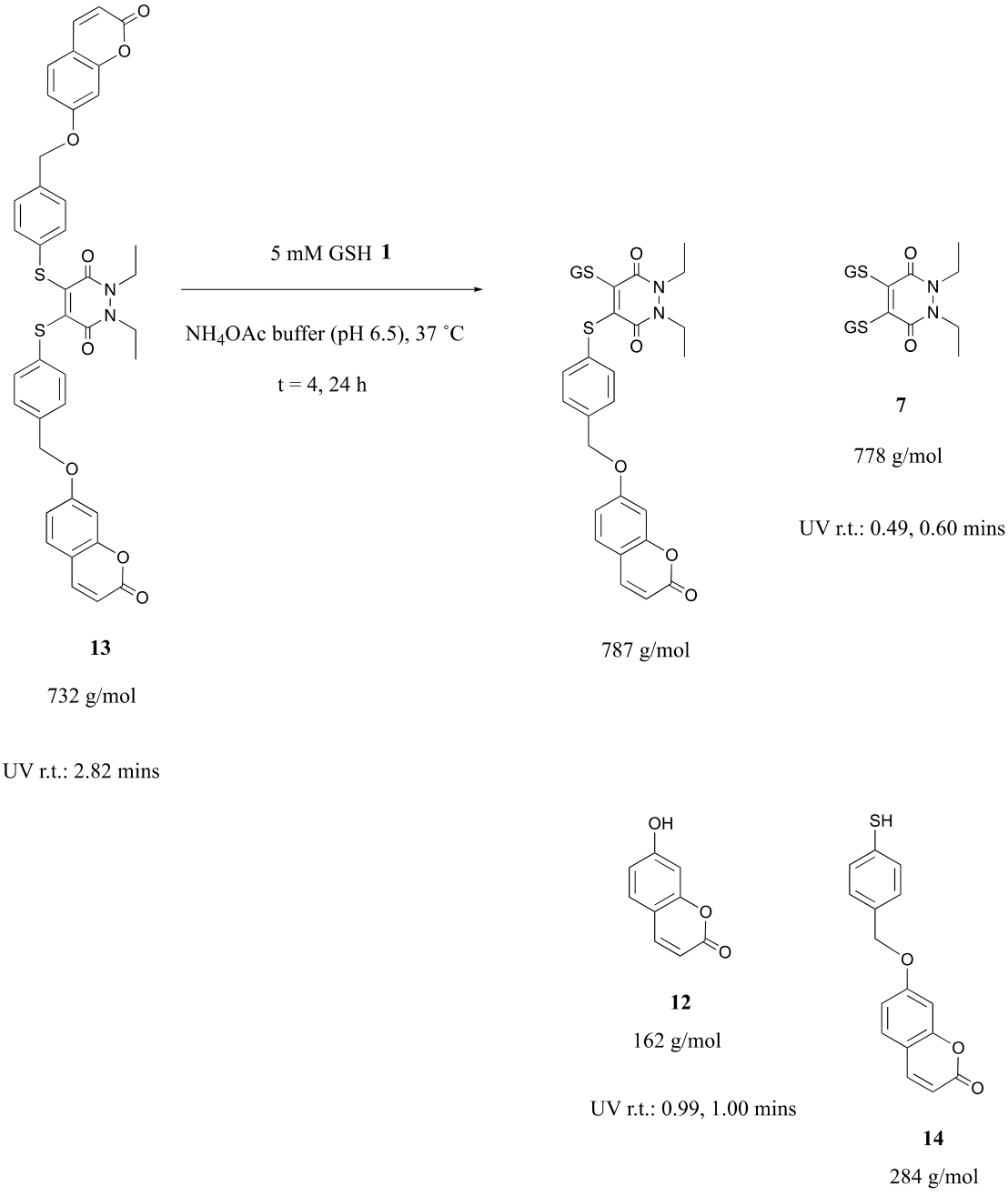

Pyridazinedione **13** (10 µL, 10 mM in THF, 1 eq.) was added to GSH **1** (190 µL, 5 mM, 10 eq.) in ammonium acetate buffer (50 mM, pH 6.5). The mixture was incubated at 37 ˚C for 24 h. The samples were analysed by LCMS at t = 4 and 24 h.

LC-MS data for t = 4 h

(a)

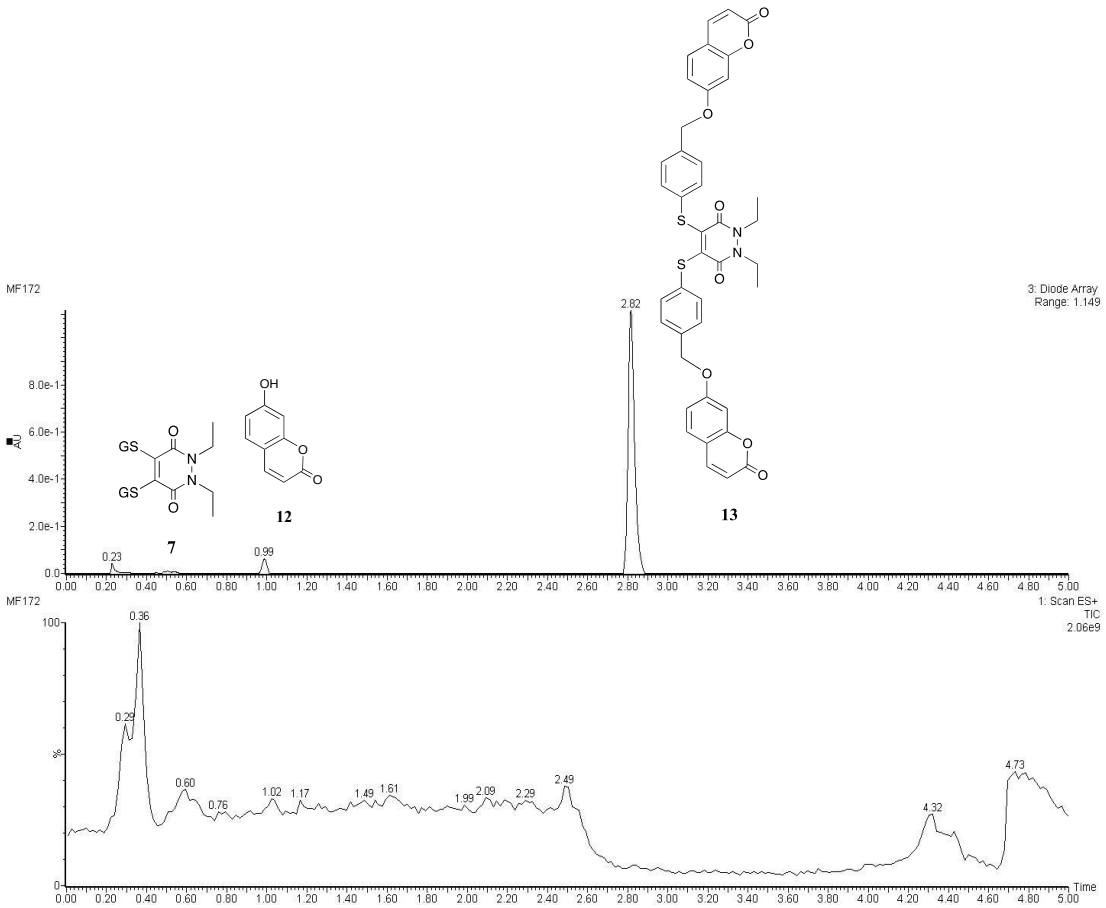
MF172
3: Diode Array
Range: 1.149
AU
2.82
0.23
0.99
7
12
13
MF172
1: Scan ES+
TIC
2.06e9
0.36
0.29
0.60
0.76
1.02
1.17
1.49
1.61
1.99
2.09
2.29
2.49
4.32
4.73
%
Time

(b)

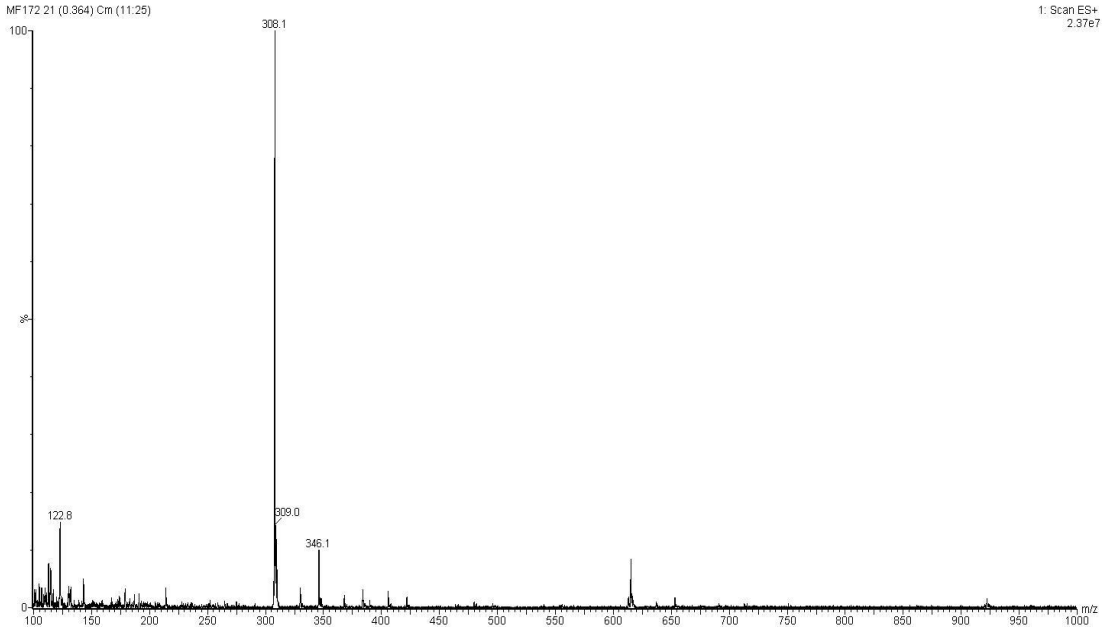
MF172 21 (0.364) Cm (11:25)
1: Scan ES+
2.37e7
308.1
309.0
122.8
346.1
%
m/z

(c)

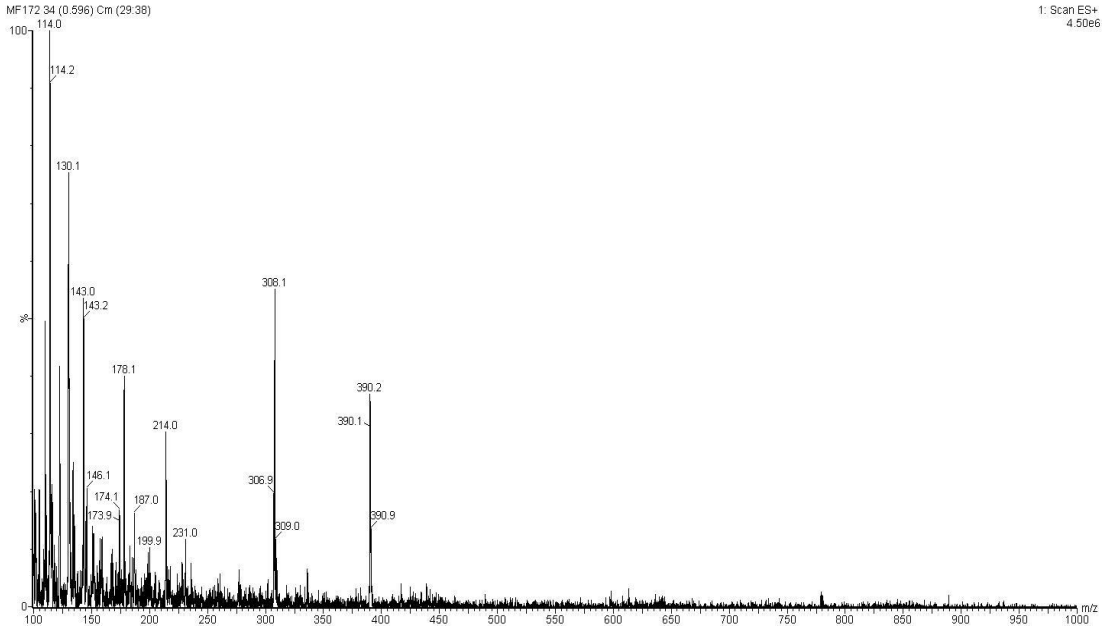
MF172 34 (0.596) Cm (29:38)
1: Scan ES+
4.50e6
100
%
0
114.0
114.2
130.1
143.0
143.2
178.1
214.0
146.1
174.1
173.9
187.0
199.9
231.0
306.9
308.1
309.0
390.2
390.1
390.9
100
150
200
250
300
350
400
450
500
550
600
650
700
750
800
850
900
950
1000
m/z

(d)

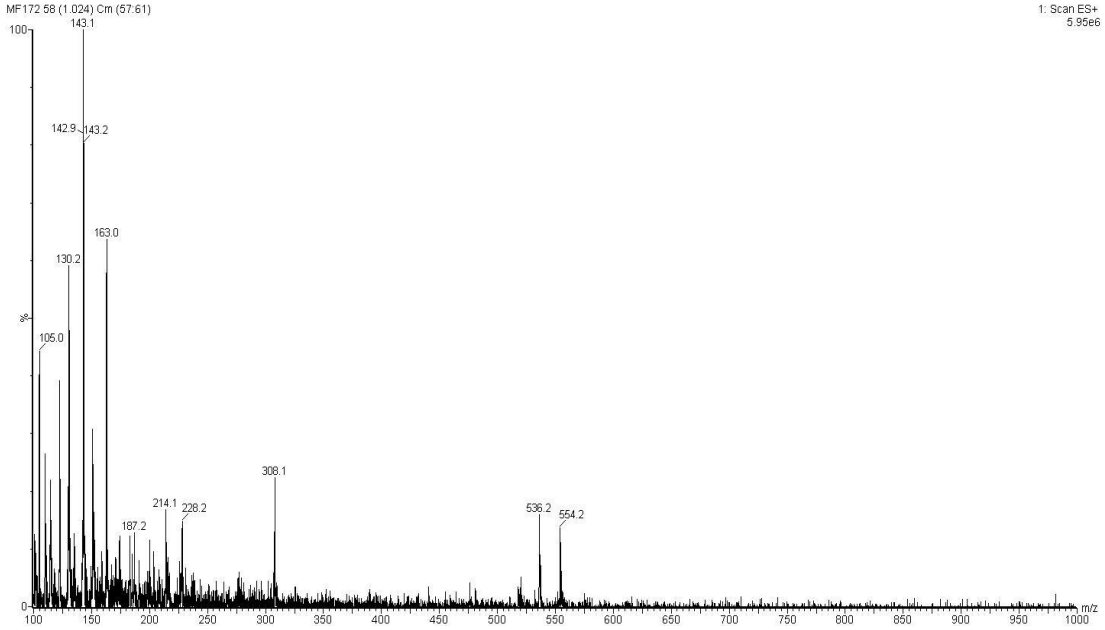
MF172 58 (1.024) Cm (57:61)
1: Scan ES+
5.95e6
100
%
0
143.1
142.9
143.2
163.0
130.2
105.0
308.1
214.1
228.2
187.2
536.2
554.2
100
150
200
250
300
350
400
450
500
550
600
650
700
750
800
850
900
950
1000
m/z

(e)

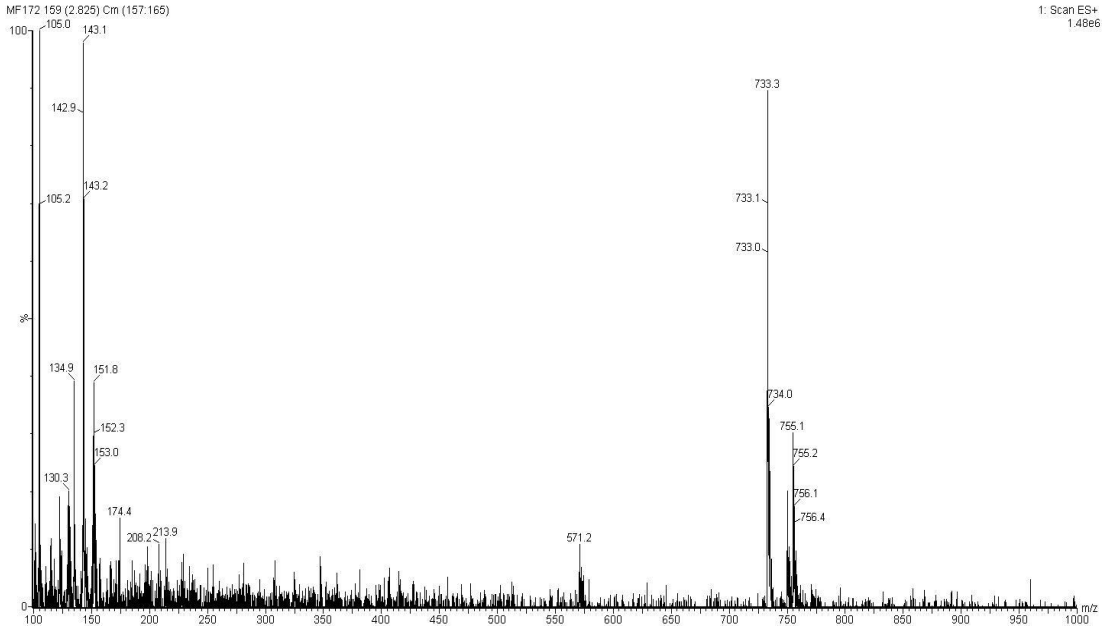

Figure **S82**. (a) TIC and UV trace at t = 4 h, (b) MS data at 0.23 mins in the UV, (c) at 0.50 mins in the UV, (d) at 0.99 mins in the UV and (e) at 2.82 mins in the UV for PD **13** incubated with GSH **1** (10 eq.) at pH 6.5.

LC-MS data for t = 24 h

(a)

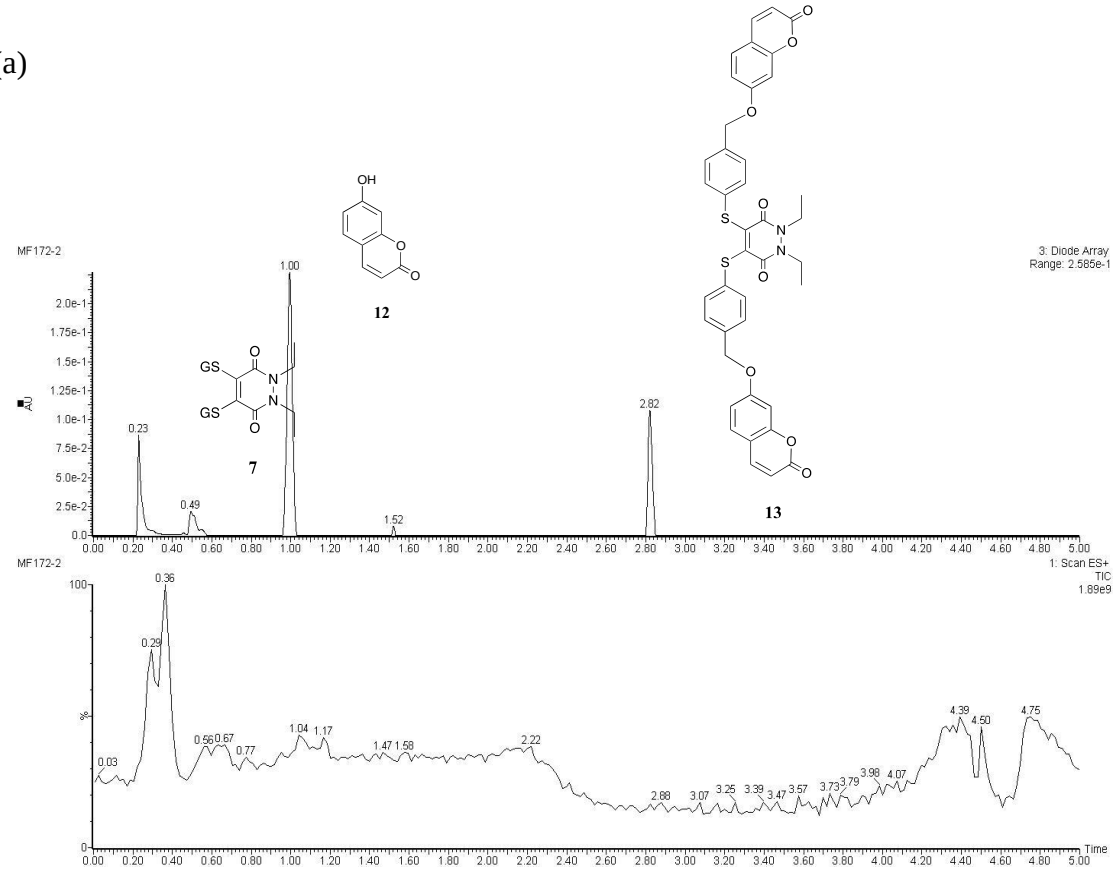

(b)

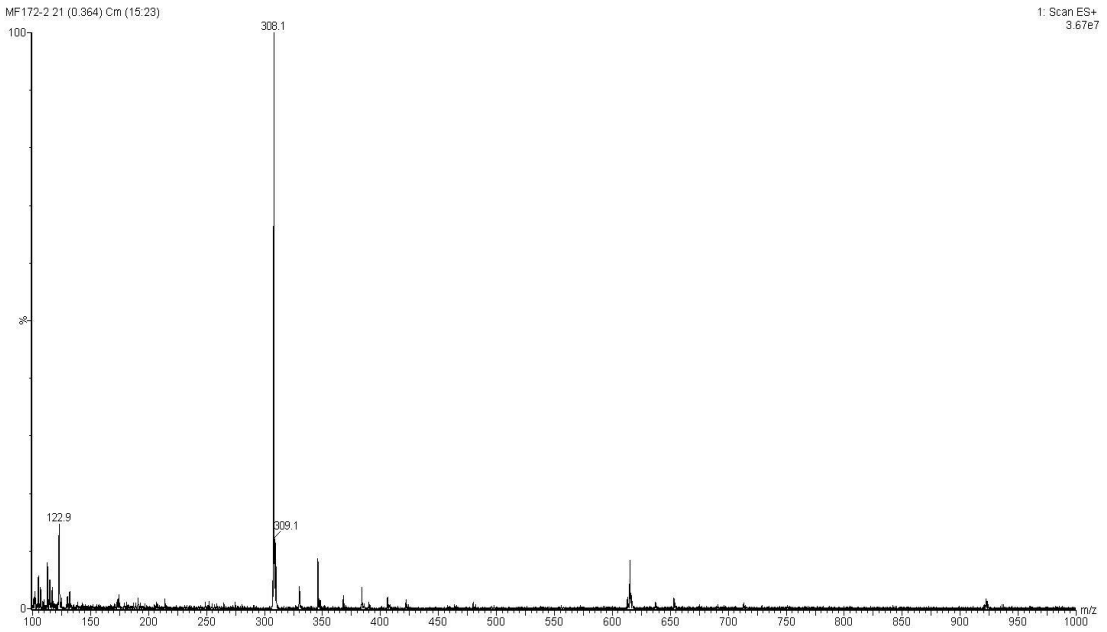
MF172-2 21 (0.364) Cm (15:23)
1: Scan ES+
3.67e7
100
%
0
308.1
309.1
122.9
m/z
100 150 200 250 300 350 400 450 500 550 600 650 700 750 800 850 900 950 1000

(c)

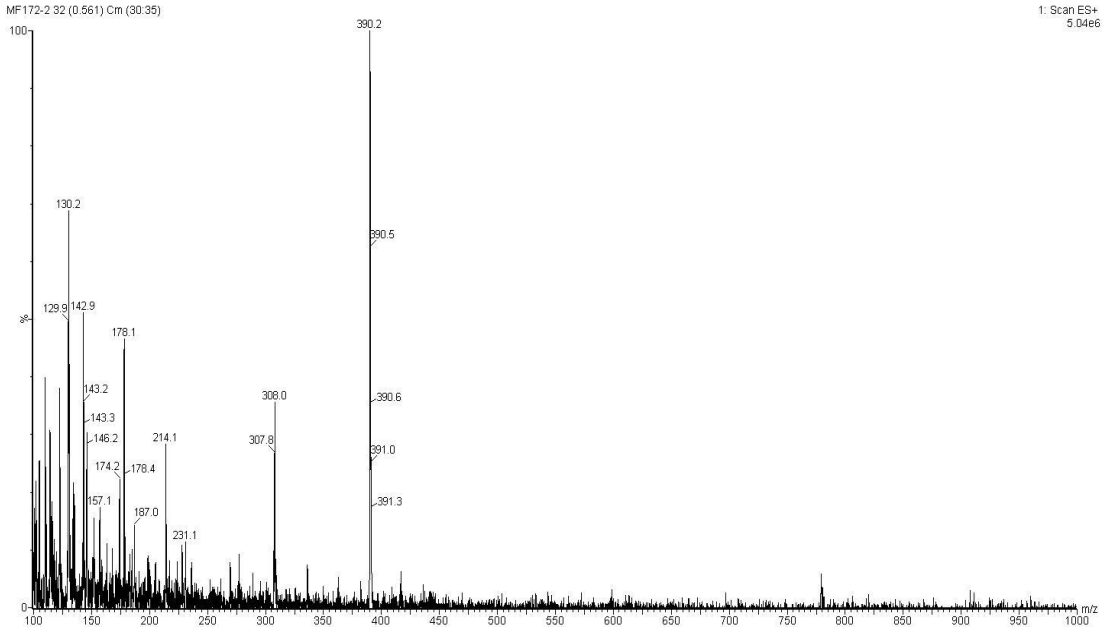
MF172-2 32 (0.561) Cm (30:35)
1: Scan ES+
5.04e6
100
%
0
390.2
390.5
130.2
129.9
142.9
178.1
143.2
143.3
146.2
174.2
178.4
157.1
187.0
214.1
231.1
308.0
307.8
390.6
391.0
391.3
m/z
100 150 200 250 300 350 400 450 500 550 600 650 700 750 800 850 900 950 1000

(d)

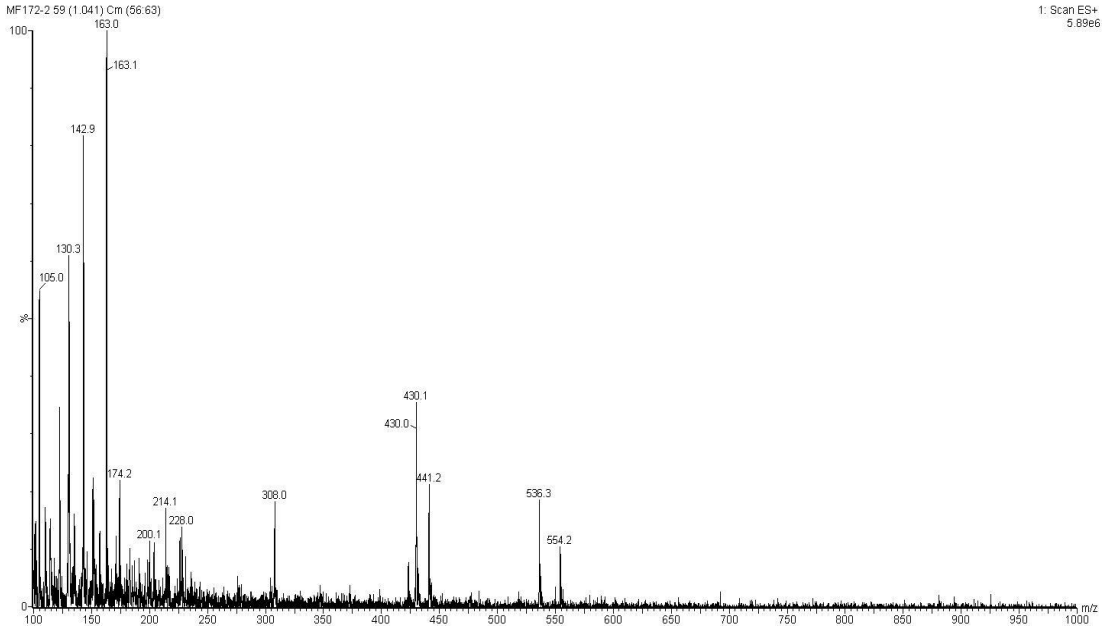

(e)

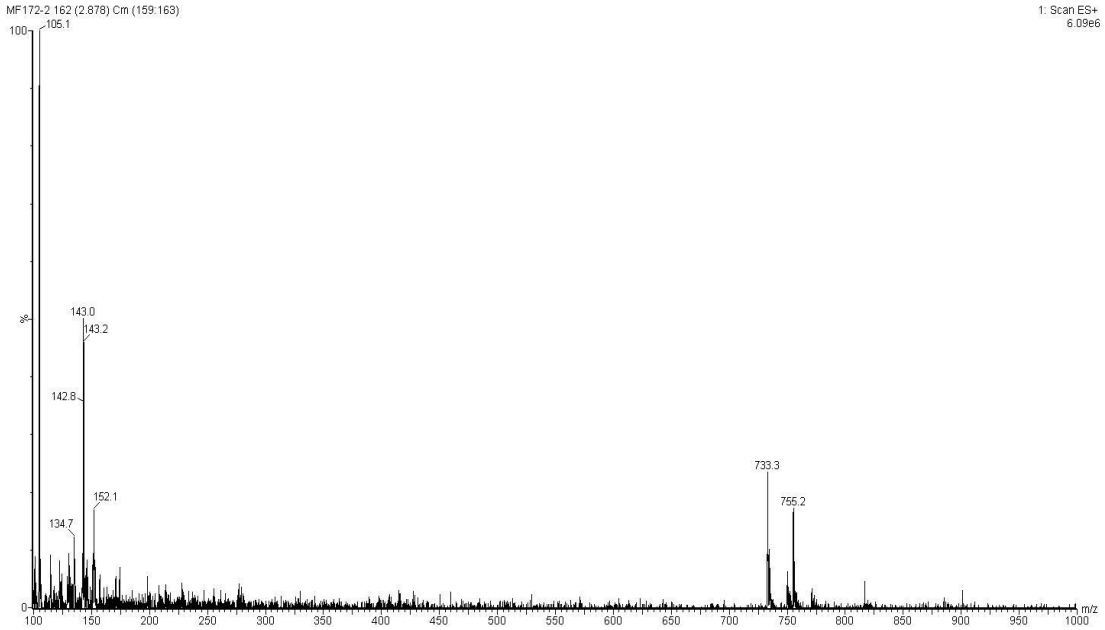

Figure **S83**. (a) TIC and UV trace at t = 24 h, (b) MS data at 0.23 mins in the UV, (c) at 0.50 mins in the UV, (d) at 1.00 mins in the UV and (e) at 2.82 mins in the UV for PD **13** incubated with GSH **1** (10 eq.) at pH 6.5.

Incubation of PD 16 with GSH (10 eq.) at pH 6.5

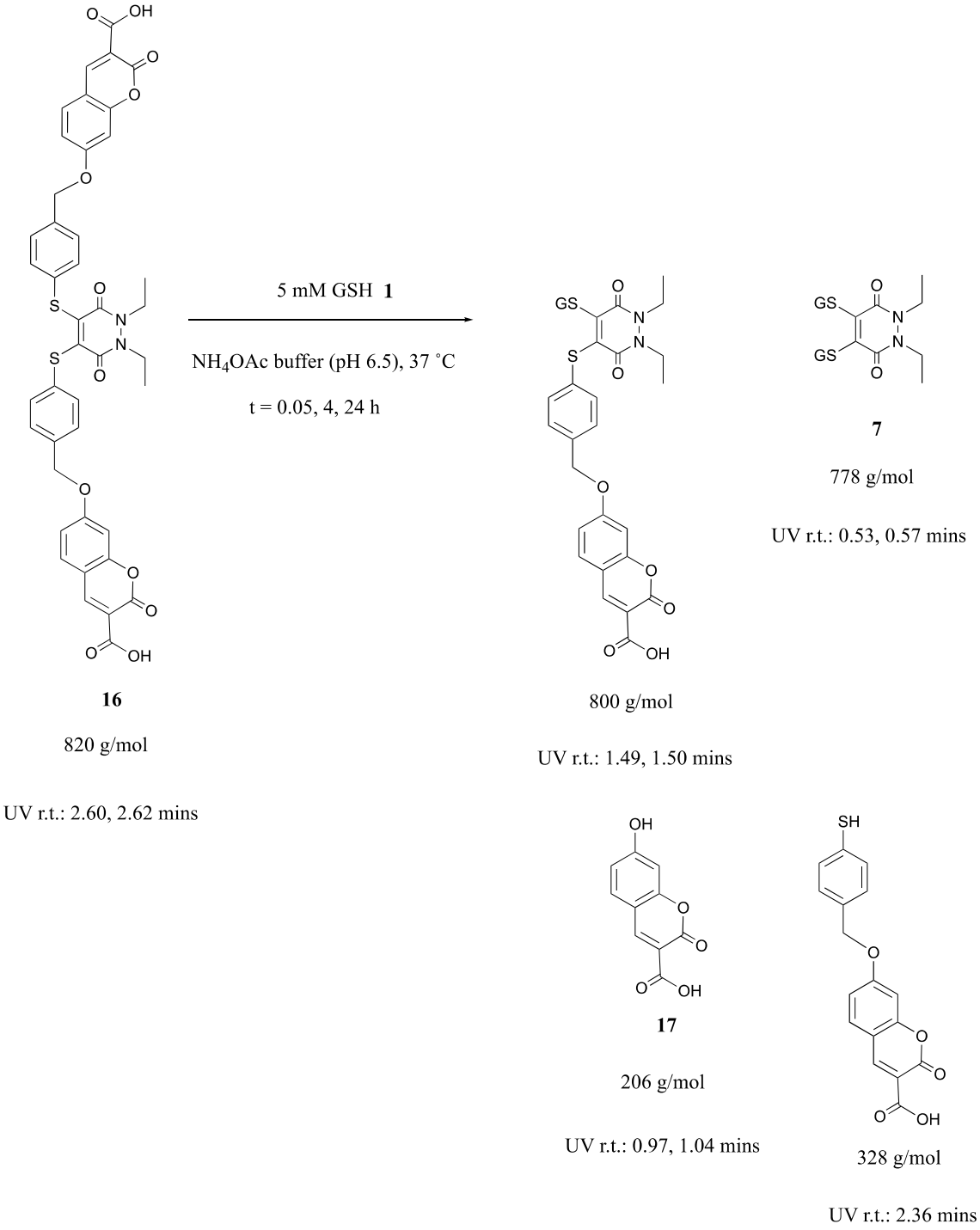

PD **16** (15 µL, 10 mM in DMSO, 1 eq.) was added to GSH **1** (285 µL, 5.3 mM, 10 eq.) in ammonium acetate buffer (50 mM, pH 6.5). The mixture was incubated at 37 ˚C for 24 h. The samples were analysed by LC-MS at t = 0.05, 4 and 24 h.

LC-MS data for t = 0.05 h

(a)

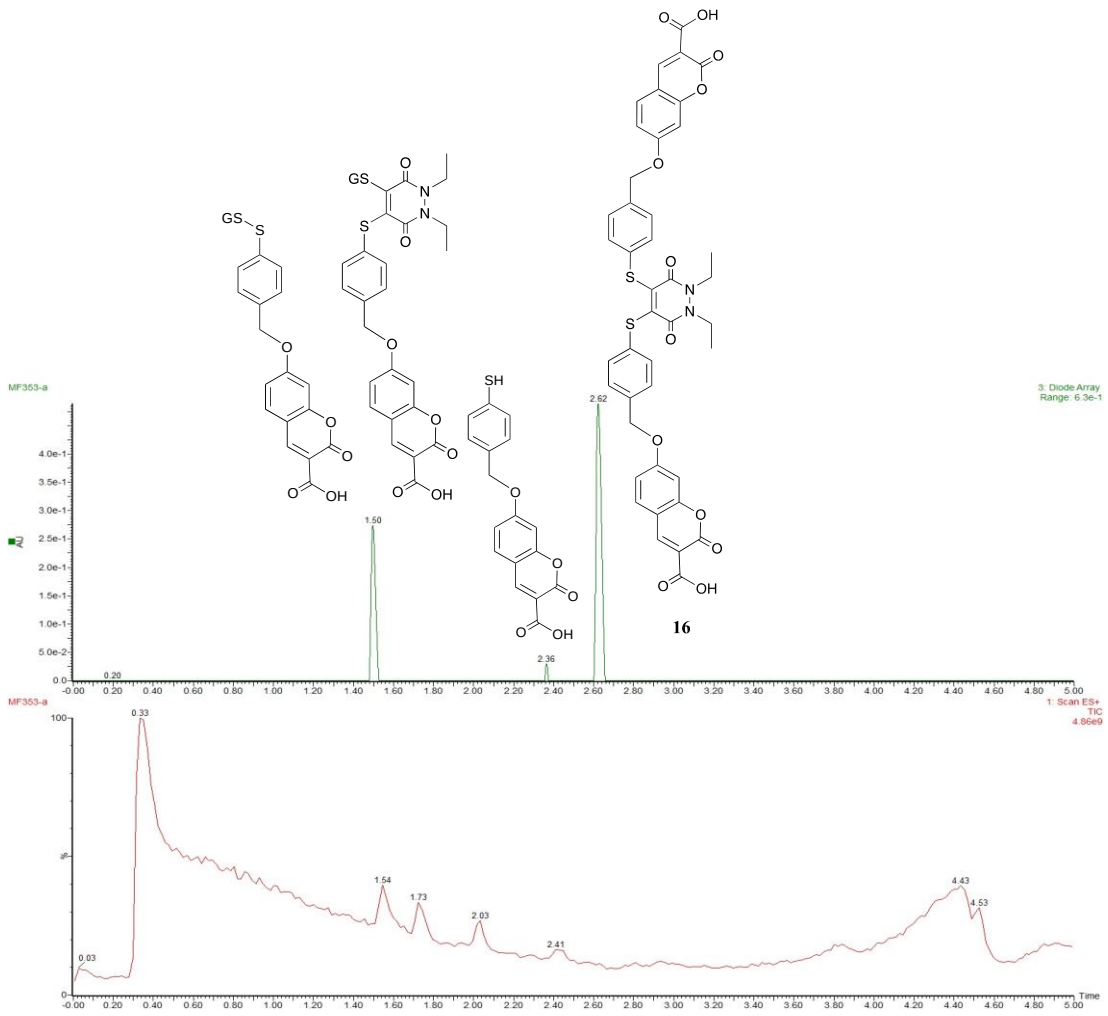
MF353-a
3: Diode Array
Range: 6.3e-1
1.50
2.36
2.62
0.20
MF353-a
1: Scan ES+
TIC
4.86e9
0.03
0.33
1.54
1.73
2.03
2.41
4.43
4.53
Time

16

(b)

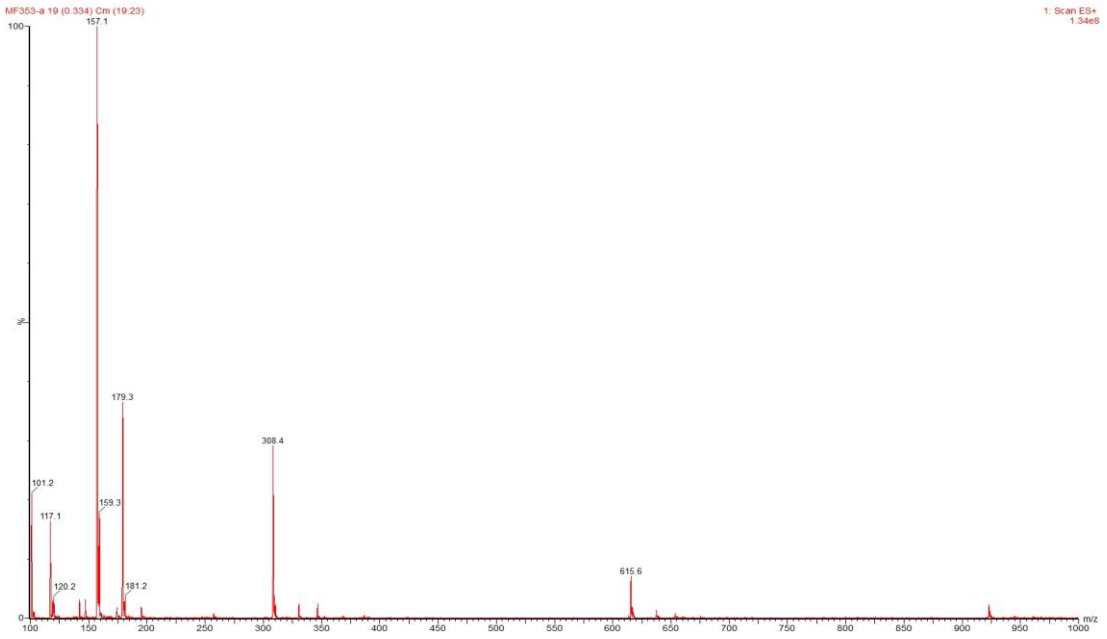
MF353-a 19 (0.334) Cm (19:23)
1: Scan ES+
1.34e8
100
%
0
157.1
179.3
308.4
101.2
159.3
117.1
120.2
181.2
615.6
100
150
200
250
300
350
400
450
500
550
600
650
700
750
800
850
900
950
1000
m/z

(c)

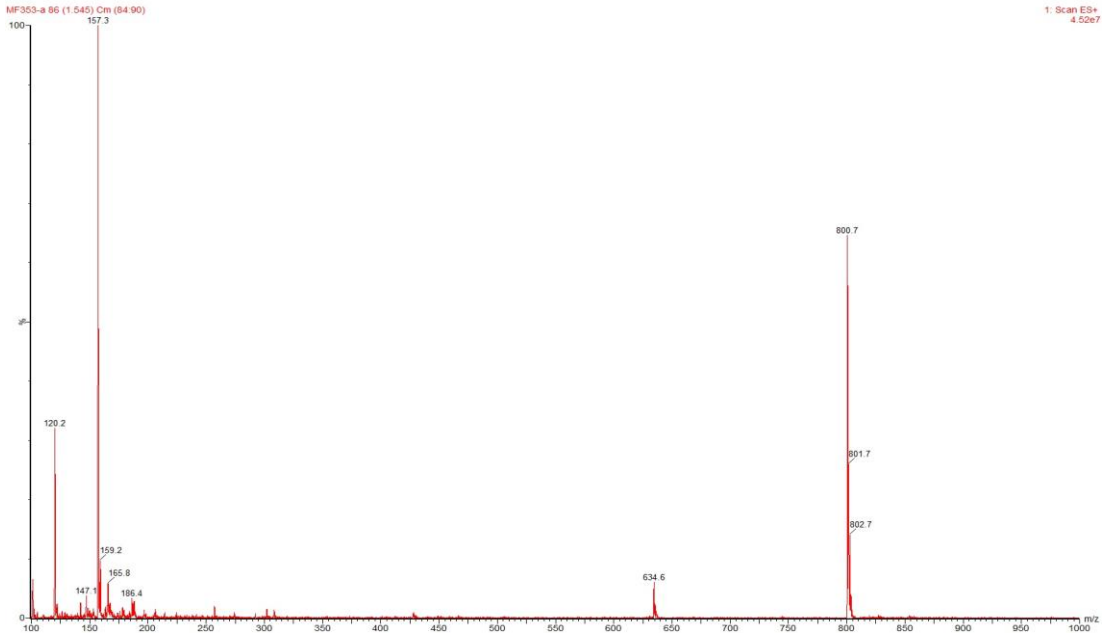
MF353-a 86 (1.545) Cm (84:90)
1: Scan ES+
4.52e7
100
%
0
157.3
800.7
120.2
801.7
802.7
159.2
165.8
147.1
186.4
634.6
100
150
200
250
300
350
400
450
500
550
600
650
700
750
800
850
900
950
1000
m/z

(d)


MF353-a 96 (1.725) Cm (94:98)
1: Scan ES+
3.42e7
100
%
0
157.2
242.6
120.1
120.4
243.5
159.1
165.7
147.1
188.3
800.7
m/z
100 150 200 250 300 350 400 450 500 550 600 650 700 750 800 850 900 950 1000

(e)

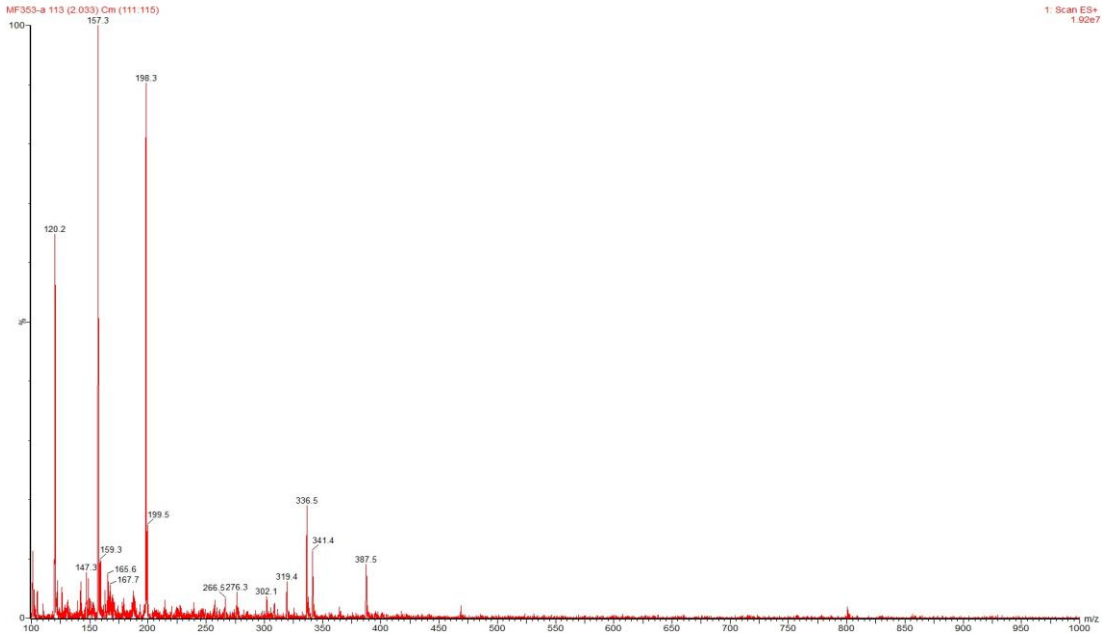
MF353-a 113 (2.033) Cm (111:115)
1: Scan ES+
1.92e7
100
%
0
157.3
198.3
120.2
336.5
199.5
341.4
159.3
387.5
147.3
165.6
167.7
319.4
266.5
276.3
302.1
m/z
100 150 200 250 300 350 400 450 500 550 600 650 700 750 800 850 900 950 1000

(f)

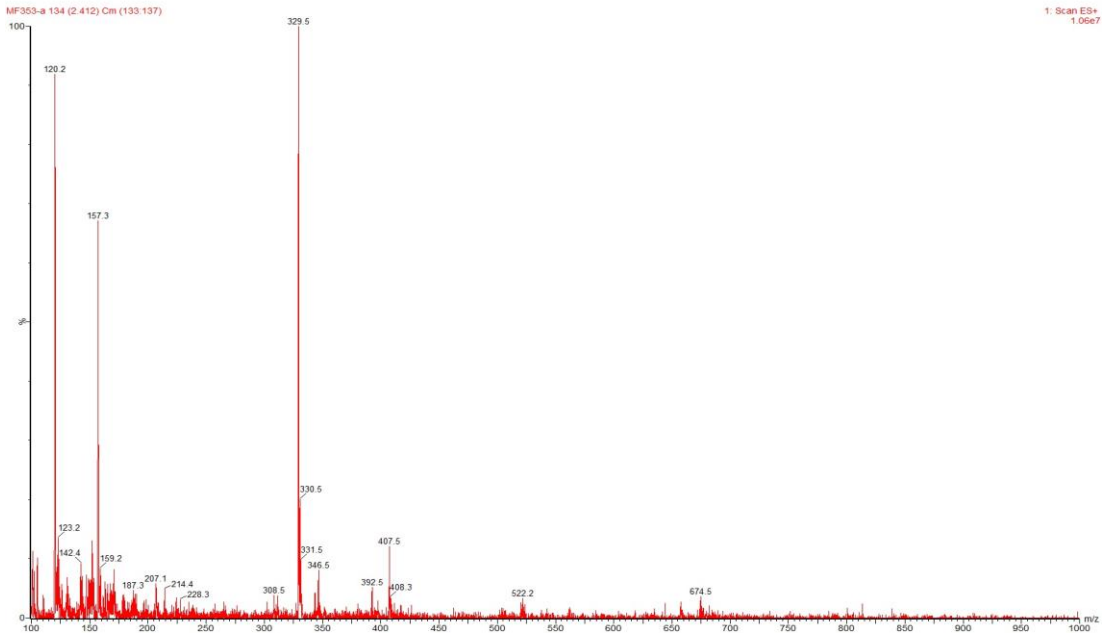

(g)

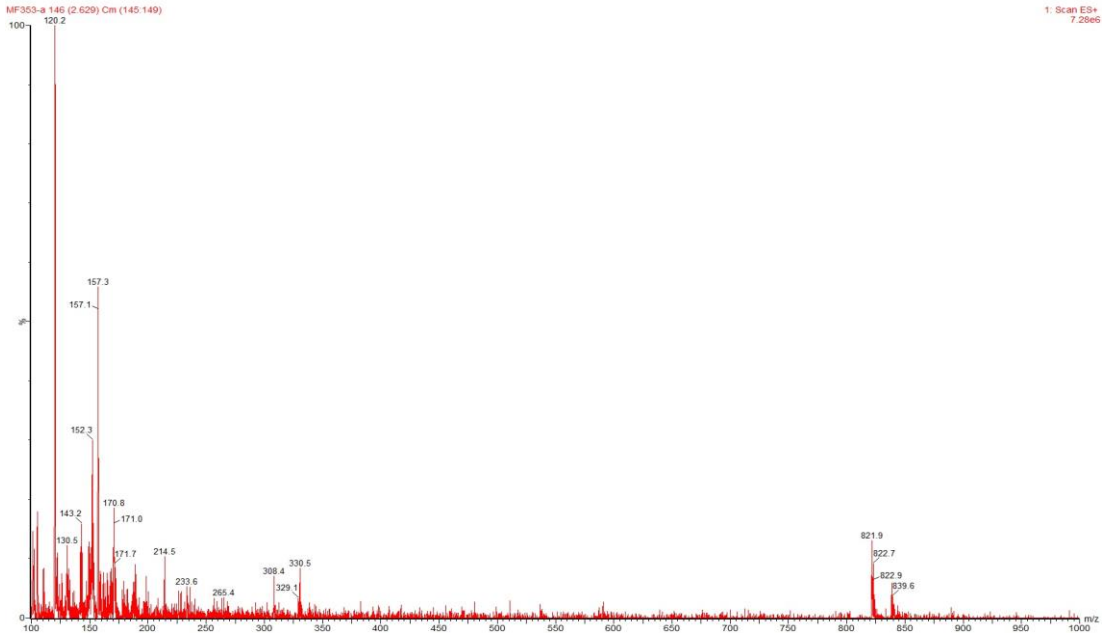

Figure **S84**. (a) TIC and UV trace at t = 0.05 h, (b) MS data at 0.32 mins in the UV, (c) at 1.50 mins in the UV, (d) at 1.73 mins in the TIC, (e) at 2.03 mins in the TIC, (f) at 2.36 mins in the UV and (g) at 2.52 mins in the UV for PD **16** incubated with GSH **1** (10 eq.) at pH 6.5. Please note that peaks at 1.73 and 2.03 mins in the TIC are minor impurities on the column that could be removed; they are consistently present.

LC-MS data for t = 4 h

(a)

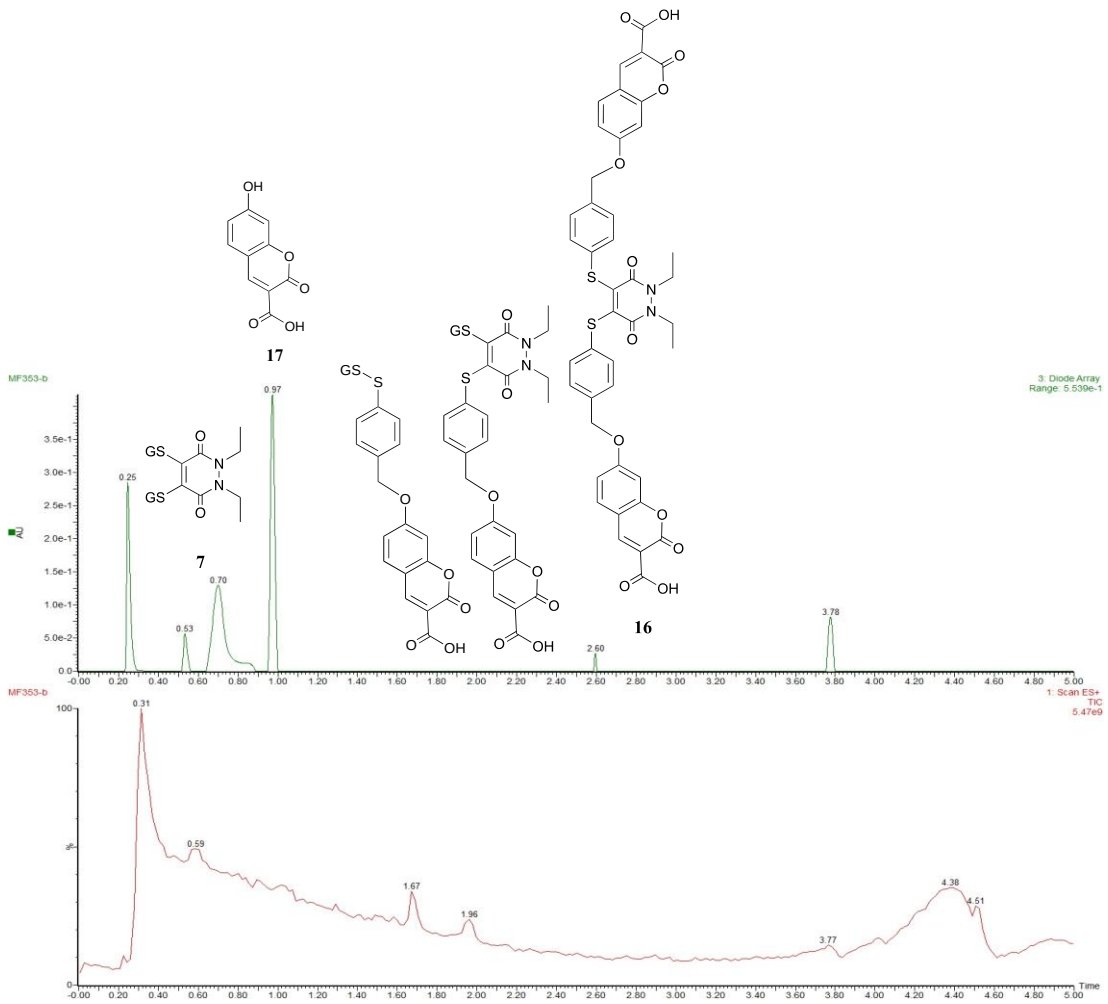
17
7
16
MF353-b
3: Diode Array
Range: 5.539e-1
0.25
0.53
0.70
0.97
2.60
3.78
MF353-b
1: Scan ES+
TIC
5.47e9
0.31
0.59
1.67
1.96
3.77
4.38
4.51
Time

(b)

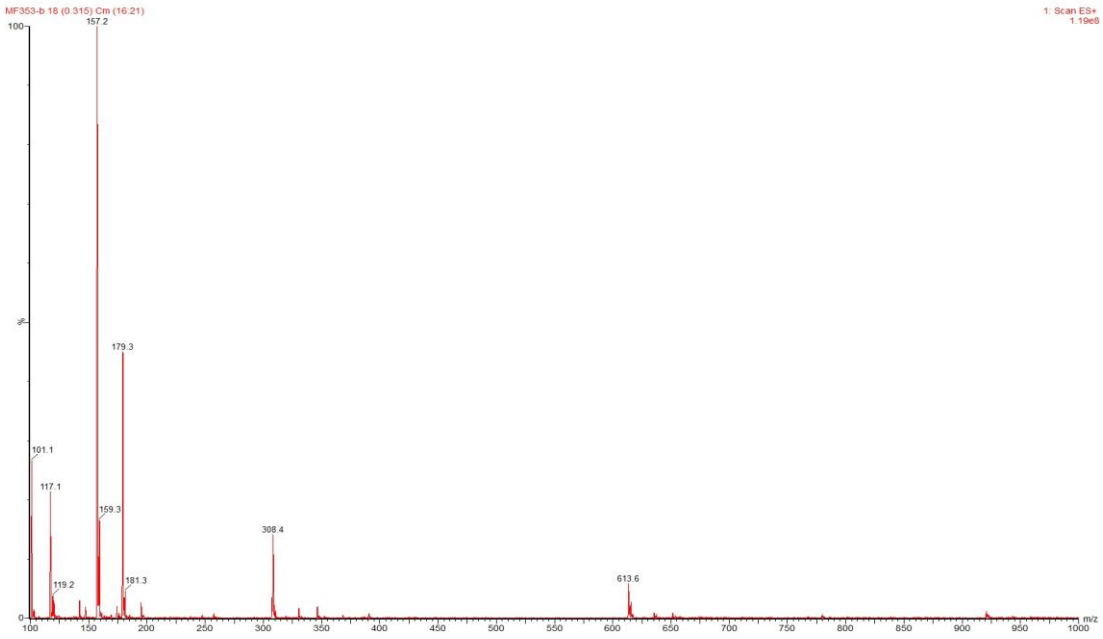
MF353-b 18 (0.315) Cm (16:21)
1: Scan ES+
1.19e8
100
%
0
157.2
179.3
101.1
117.1
159.3
308.4
119.2
181.3
613.6
100
150
200
250
300
350
400
450
500
550
600
650
700
750
800
850
900
950
1000
m/z

(c)

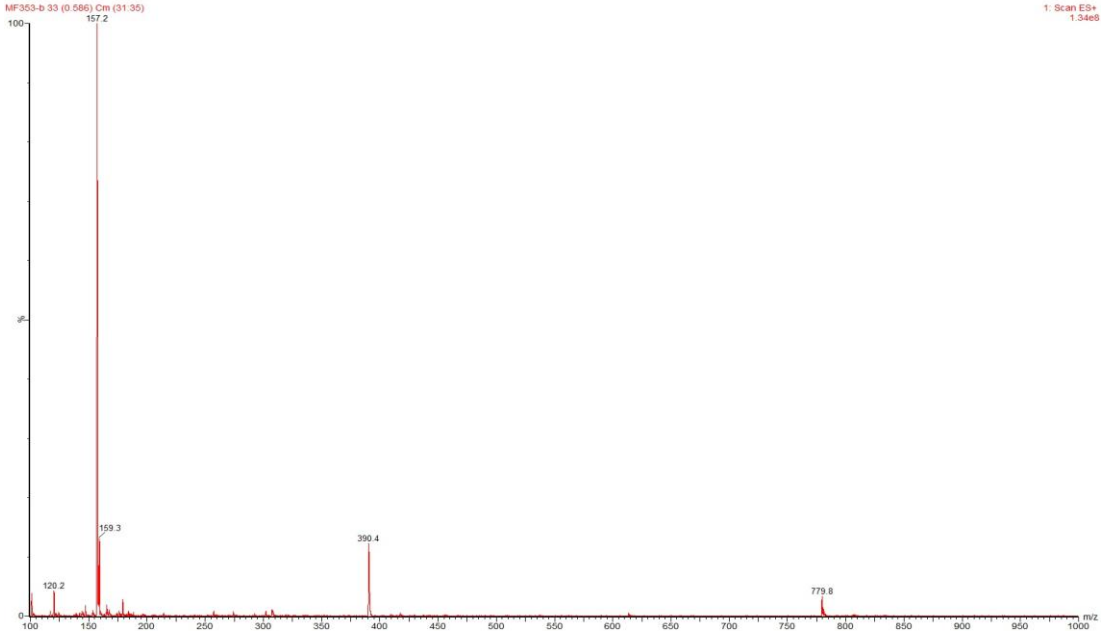
MF353-b 33 (0.586) Cm (31:35)
1: Scan ES+
1.34e8
100
%
0
157.2
159.3
390.4
120.2
779.8
100
150
200
250
300
350
400
450
500
550
600
650
700
750
800
850
900
950
1000
m/z

(d)


MF353-b 38 (0.676) Cm (38:48)
1: Scan ES+
1.32e8
157.3
159.2
120.3
%
m/z

(e)


MF353-b 57 (1.020) Cm (54:57)
1: Scan ES+
1.14e8
157.3
120.2
159.2
207.2
%
m/z

(f)

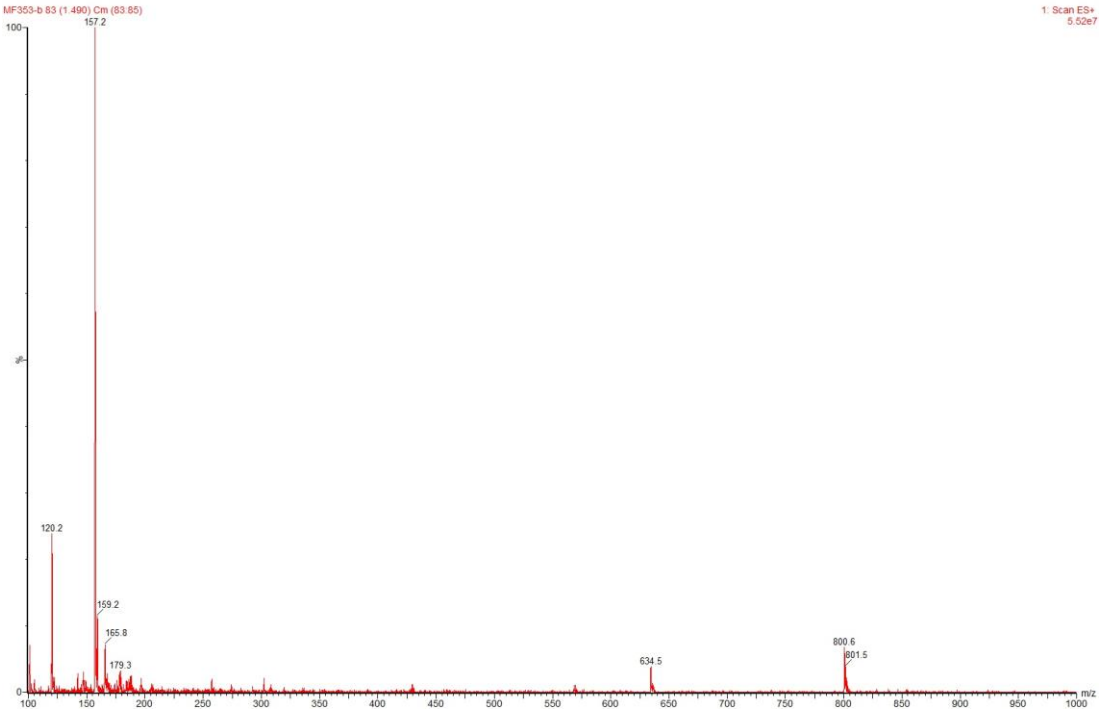
MF353-b 83 (1.490) Cm (83:85)
1: Scan ES+
5.52e7
157.2
120.2
159.2
165.8
179.3
634.5
800.6
801.5
%
m/z

(g)


MF353-b 93 (1.671) Cm (93:95)
1: Scan ES+
5.31e7
242.6
157.3
120.2
243.7
156.8
159.3
165.7
147.3
167.8
188.5
%
m/z

(h)


MF353-b 109 (1.960) Cm (107:110)
1: Scan ES+
2.65e7
100
%
0
157.1
198.4
120.2
120.4
159.3
199.2
142.3
165.8
276.5
302.2
319.5
336.5
341.6
387.4
m/z
100 150 200 250 300 350 400 450 500 550 600 650 700 750 800 850 900 950 1000

(i)

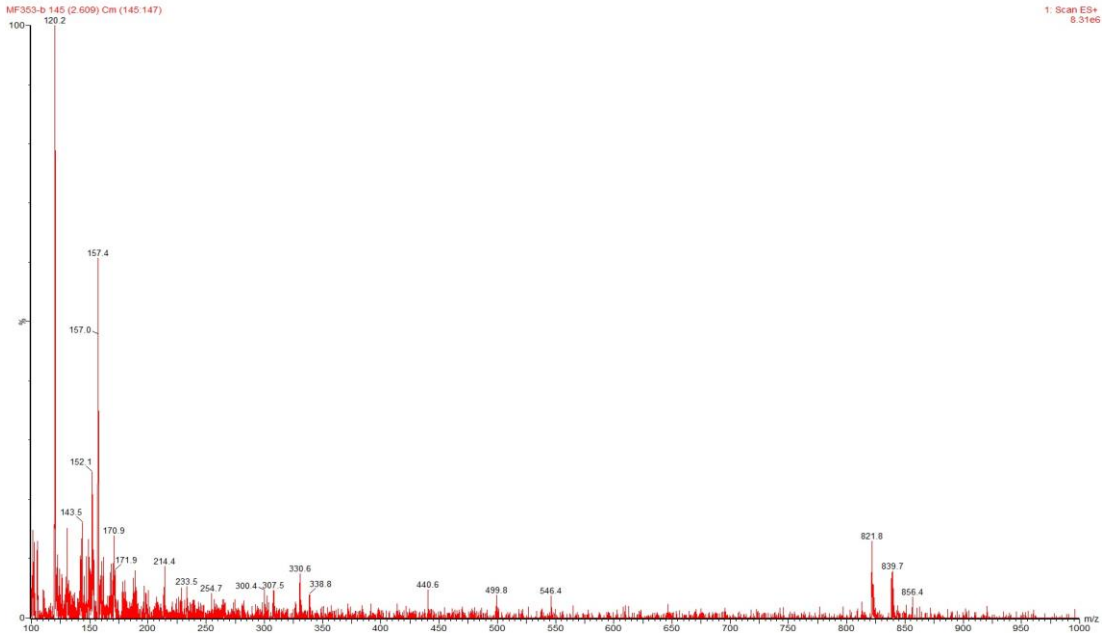
MF353-b 145 (2.609) Cm (145:147)
1: Scan ES+
8.31e6
100
%
0
120.2
157.4
157.0
152.1
143.5
170.9
171.9
214.4
233.5
254.7
300.4
307.5
330.6
338.8
440.6
499.8
546.4
821.8
839.7
856.4
m/z
100 150 200 250 300 350 400 450 500 550 600 650 700 750 800 850 900 950 1000

(j)

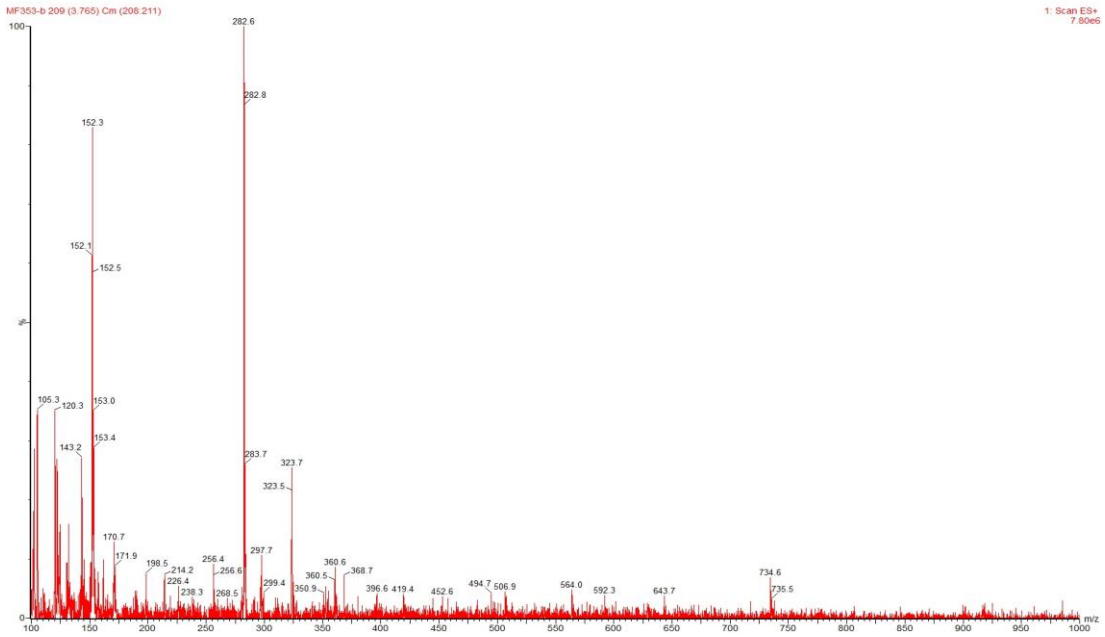

Figure **S85**. (a) TIC and UV trace at t = 4 h, (b) MS data at 0.25 mins in the UV, (c) at 0.53 mins in the UV, (d) at 0.70 mins in the UV, (e) at 0.97 mins in the UV, (f) at 1.49 mins in the TIC, (g) at 1.67 mins in the TIC, (h) at 1.96 mins in the TIC, (i) at 2.60 mins in the UV and (j) at 3.78 mins in the UV for PD **16** incubated with GSH **1** (10 eq.) at pH 6.5. Please note that peaks at 1.67 and 1.96 mins in the TIC, and at 3.78 mins in the UV are minor impurities on the column that could be removed; they are consistently present.

LC-MS data for t = 24 h

(a)

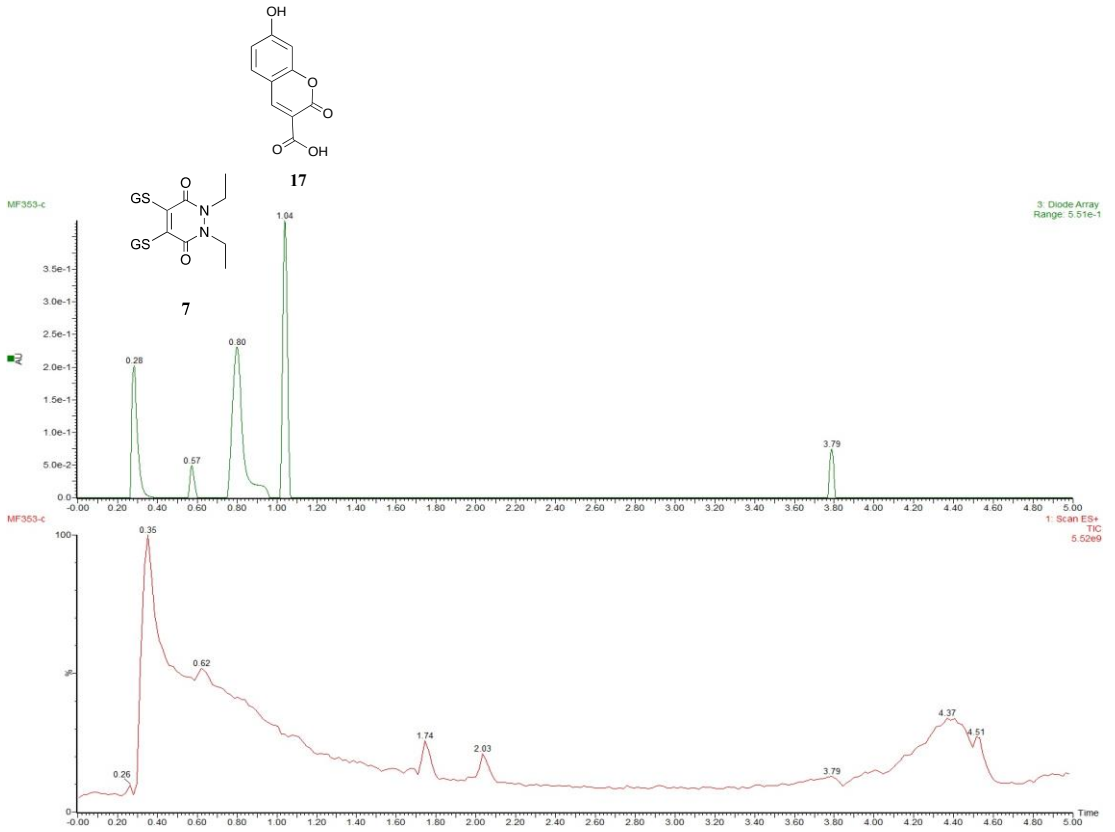
OH
O
O
O
OH
17
GS
GS
O
N
N
O
7
MF353-c
3: Diode Array
Range: 5.51e-1
1.04
0.80
0.28
0.57
3.79
MF353-c
1: Scan ES+
TIC
5.52e9
0.35
0.62
0.26
1.74
2.03
3.79
4.37
4.51
%
Time

(b)

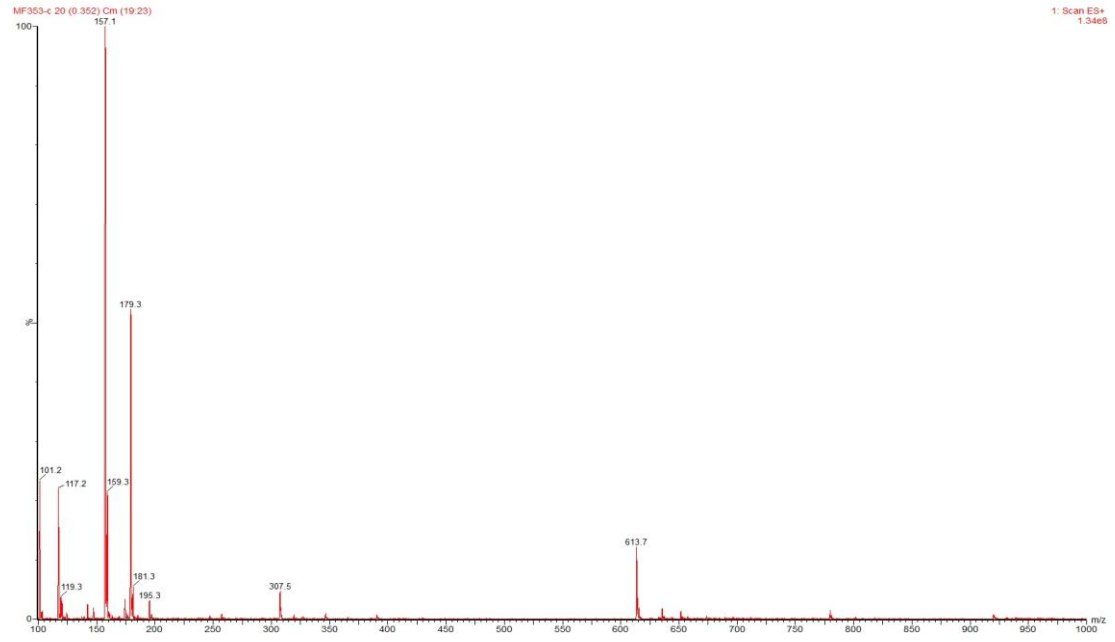
MF353-c 20 (0.352) Cm (19:23)
1: Scan ES+
1.34e8
157.1
179.3
101.2
117.2
159.3
613.7
119.3
181.3
195.3
307.5
%
m/z

(c)

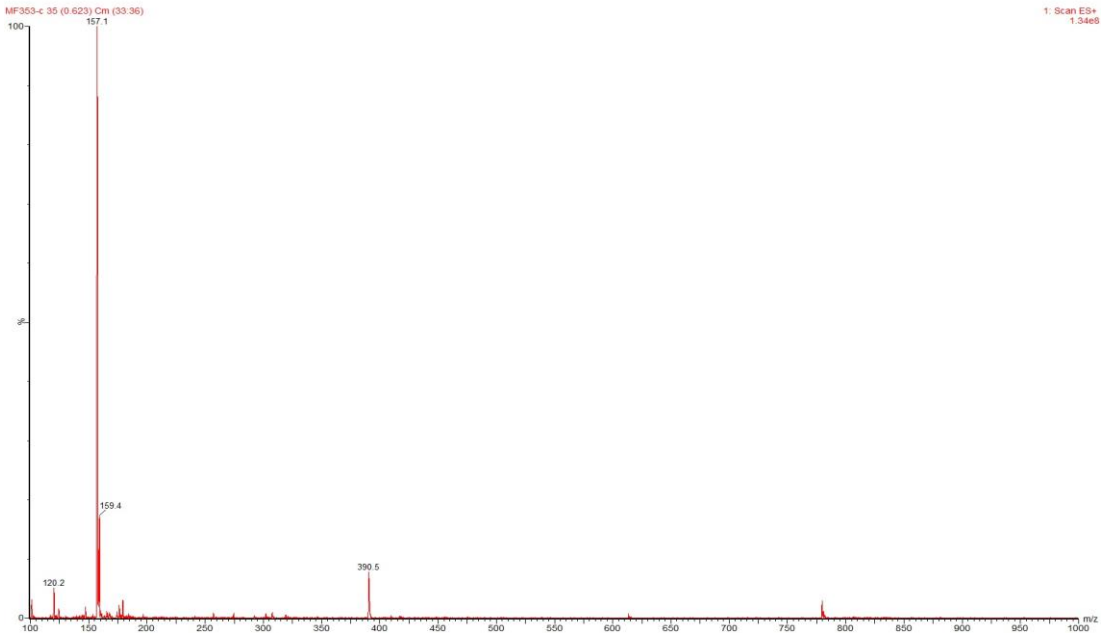
MF353-c 35 (0.623) Cm (33:36)
1: Scan ES+
1.34e8
100
%
0
157.1
159.4
120.2
390.5
m/z
100
150
200
250
300
350
400
450
500
550
600
650
700
750
800
850
900
950
1000

(d)


MF353-c 41 (0.732) Cm (41:51)
1: Scan ES+
1.30e8
100
%
0
157.3
159.3
120.4
m/z
100
150
200
250
300
350
400
450
500
550
600
650
700
750
800
850
900
950
1000

(e)


MF353-c 56 (1.004) Cm (56:59)
1: Scan ES+
8.77e7
100
%
0
157.3
120.2
159.3
207.2
100
150
200
250
300
350
400
450
500
550
600
650
700
750
800
850
900
950
1000
m/z

(f)


MF353-c 97 (1.745) Cm (95:99)
1: Scan ES+
3.51e7
100
%
0
242.6
157.3
120.3
243.8
159.3
147.4
214.4
100
150
200
250
300
350
400
450
500
550
600
650
700
750
800
850
900
950
1000
m/z

(g)

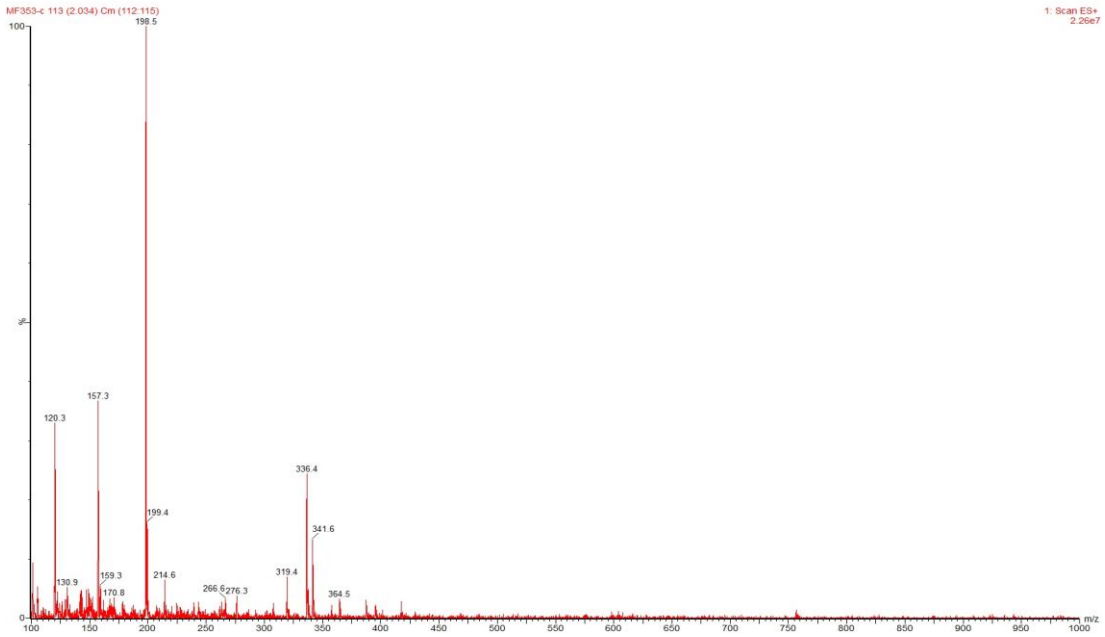

(h)

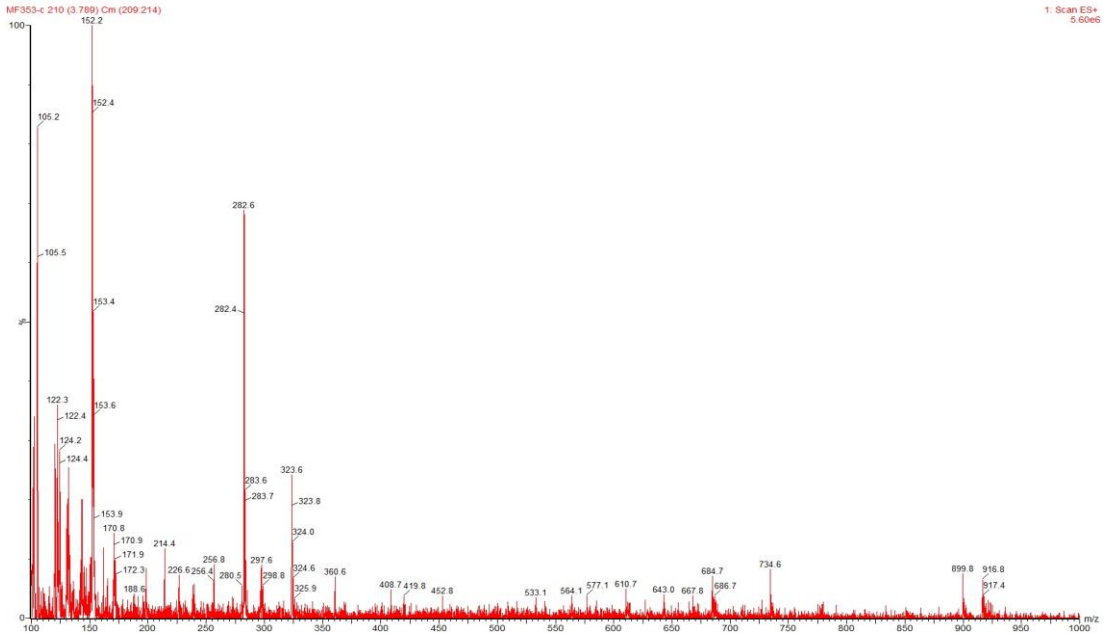

Figure **S86**. (a) TIC and UV trace at t = 24 h, (b) MS data at 0.28 mins in the UV, (c) at 0.57 mins in the UV, (d) at 0.80 mins in the UV, (e) at 1.04 mins in the UV, (f) at 1.74 mins in the TIC, (g) at 2.03 mins in the TIC and (h) at 3.79 mins in the TIC for PD **16** incubated with GSH **1** (10 eq.) at pH 6.5. Please note that peaks at 1.74 and 2.03 mins in the TIC, and at 3.79 mins in the UV are minor impurities on the column that could be removed; they are consistently present.

Fluorescence emission spectroscopy of the reaction between PD 16 and GSH (10 eq.) at pH 6.5

UV absorption of 7-hydroxy-2-oxo-2*H*-chromene-3-carboxylic acid 17

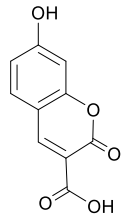

17

7-Hydroxy-2-oxo-2*H*-chromene-3-carboxylic acid **17** (100 µL, 10 mM in DMSO) was added to ammonium acetate buffer (1900 µL, 50 mM, pH 6.5). The solution was then scanned in the 200–800 nm range using a UV–Vis spectrophotometer in order to obtain 7-hydroxy-2-oxo-2*H*-chromene-3-carboxylic acid **17**'s maximum UV absorption in the DMSO/buffer mixture.

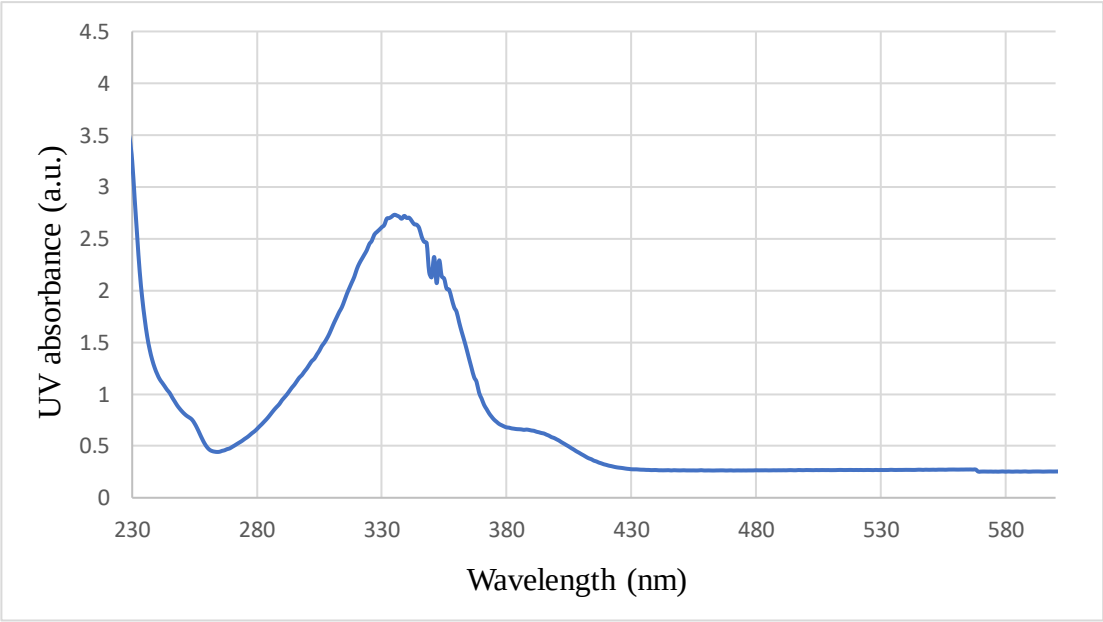

Figure **S87**. UV absorbance spectrum of 7-hydroxy-2-oxo-2*H*-chromene-3-carboxylic acid **17** in a 5:95 mixture of DMSO/NH_4OAc buffer (50 mM, pH 6.5). When scanned in the 200–800 nm range, 7-hydroxy-2-oxo-2*H*-chromene-3-carboxylic acid **17**'s maximum UV absorption occurred at 335 nm and ε_{335} = 5462 $M^{-1}cm^{-1}$.

Fluorescence emission of 7-hydroxy-2-oxo-2*H*-chromene-3-carboxylic acid 17

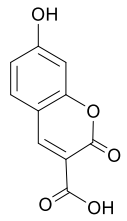

17

7-Hydroxy-2-oxo-2*H*-chromene-3-carboxylic acid **17** (100 µL, 10 mM in DMSO) was added to ammonium acetate buffer (1900 µL, 50 mM, pH 6.5). The solution was then excited at 335 nm using a fluorescence spectrophotometer in order to obtain 7-hydroxy-2-oxo-2*H*-chromene-3-carboxylic acid **17**'s maximum fluorescence intensity in the DMSO/buffer mixture.

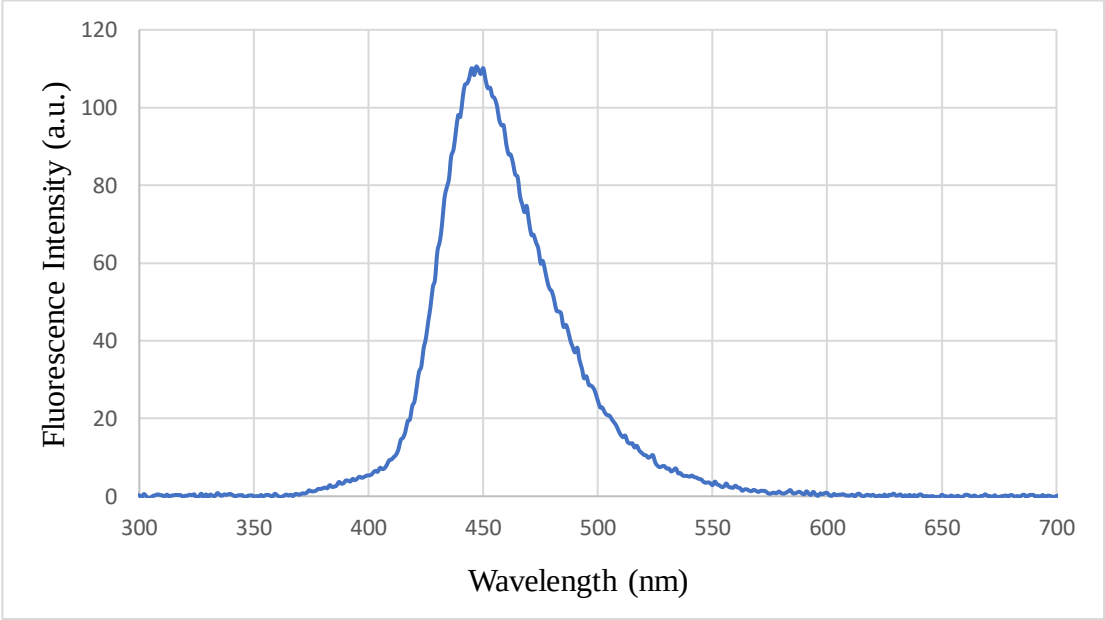

Figure **S88**. Fluorescence emission spectrum of 7-hydroxy-2-oxo-2*H*-chromene-3-carboxylic acid **17** in a 5:95 mixture of DMSO/NH_4OAc buffer (50 mM, pH 6.5). When excited at 335 nm, 7-hydroxy-2-oxo-2*H*-chromene-3-carboxylic acid **17**'s maximum fluorescence emission occurred at 447 nm with a maximum intensity of 110.6 a.u.

Fluorescence emission of PD 16

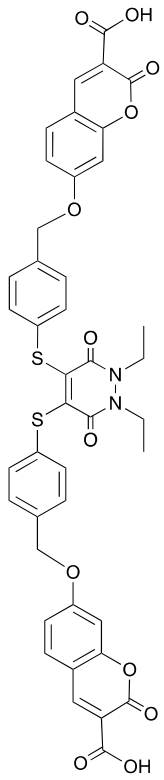

16

PD **16** (100 µL, 10 mM in DMSO) was added to ammonium acetate buffer (1900 µL, 50 mM, pH 6.5). The solution was incubated at 37 ˚C for 48 h. The solution was then excited at 335 nm using a fluorescence spectrophotometer in order to obtain PD **16**'s maximum fluorescence intensity in the DMSO/buffer mixture.

(a)

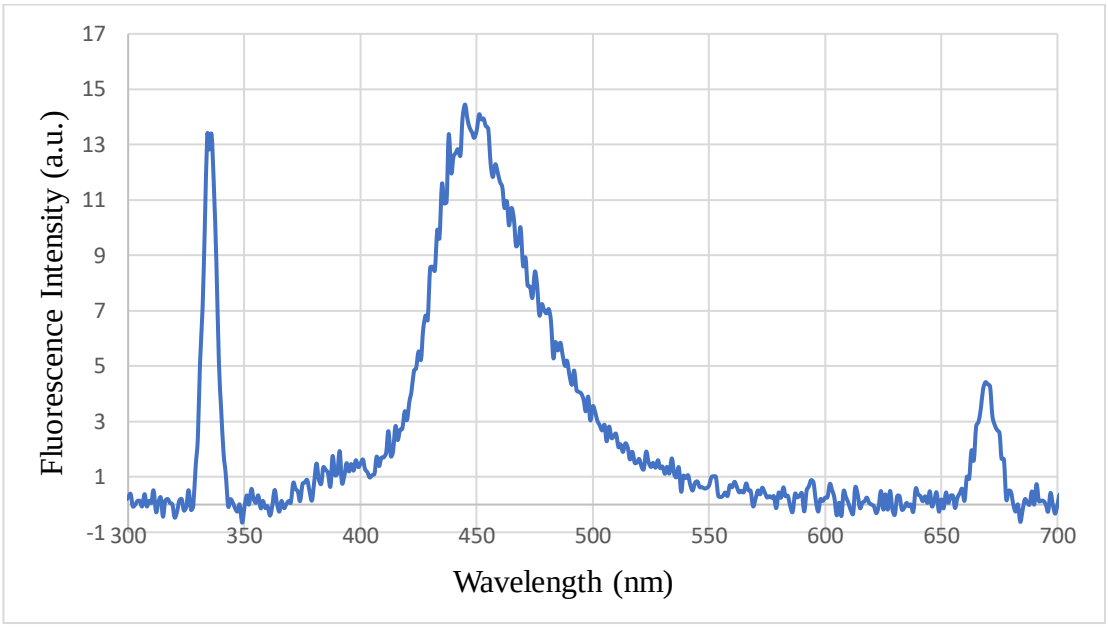
Fluorescence Intensity (a.u.)
17
15
13
11
9
7
5
3
1
-1
300
350
400
450
500
550
600
650
700
Wavelength (nm)

(b)

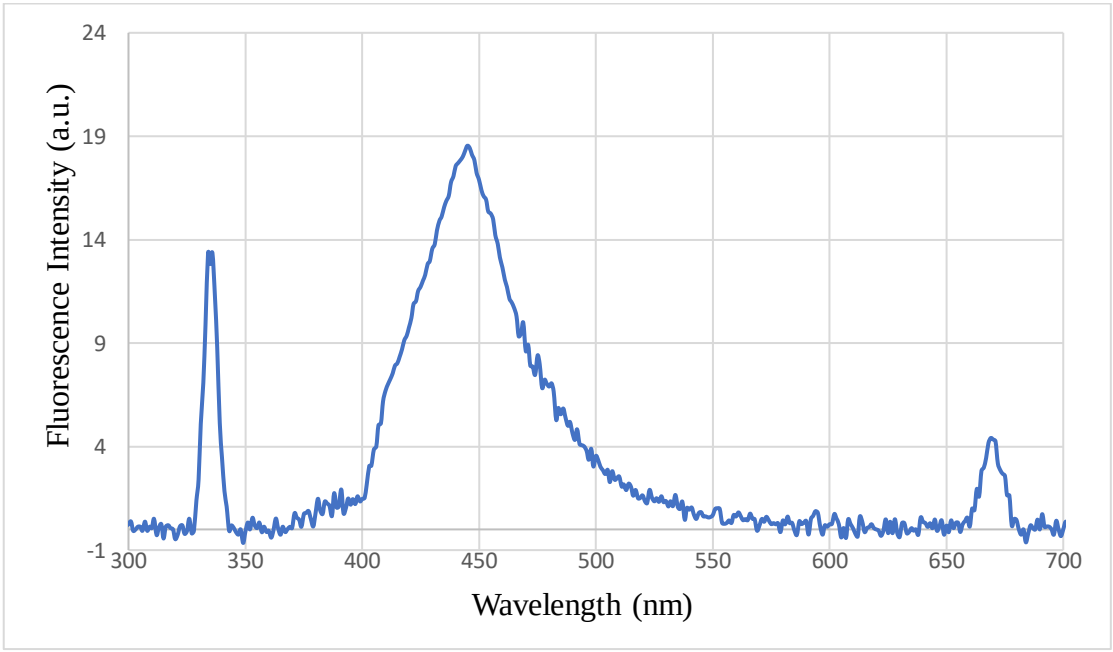
Fluorescence Intensity (a.u.)
24
19
14
9
4
-1
300
350
400
450
500
550
600
650
700
Wavelength (nm)

(c)

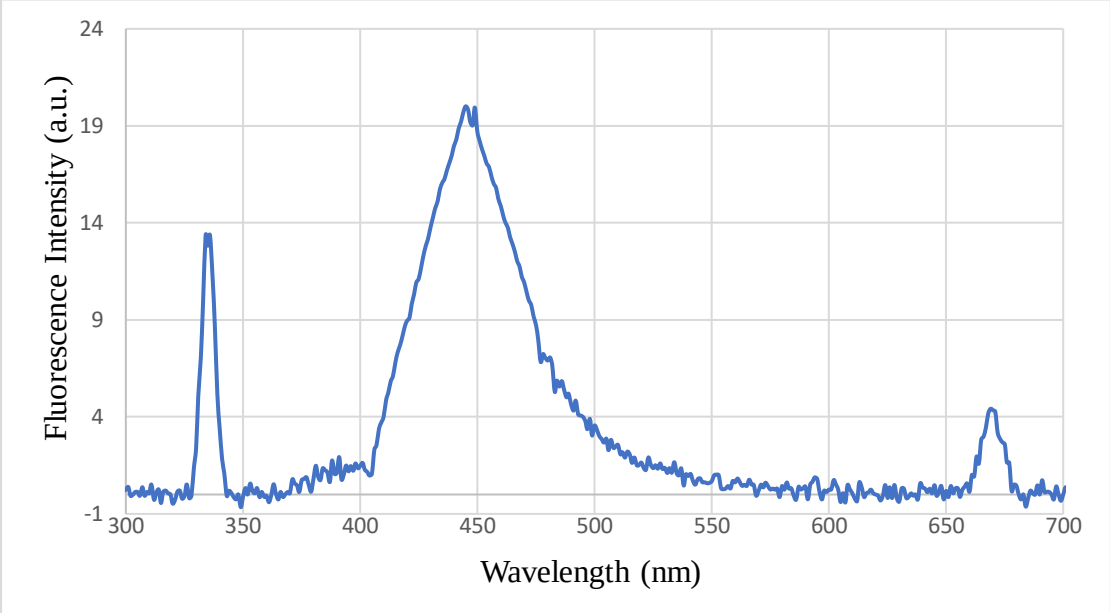

Figure **S89**. Fluorescence emission spectrum of PD **16** in a 5:95 mixture of DMSO/NH_4OAc buffer (50 mM, pH 6.5). When excited at 335 nm (and performed in triplicate), PD **16**'s maximum fluorescence emission occurred at 445 nm with a maximum intensity of (a) 14.4 a.u., (b) 18.5 a.u. and (c) 20.0 a.u.

Fluorescence emission spectroscopy of the reaction between PD 16 and GSH (10 eq.) at pH 6.5

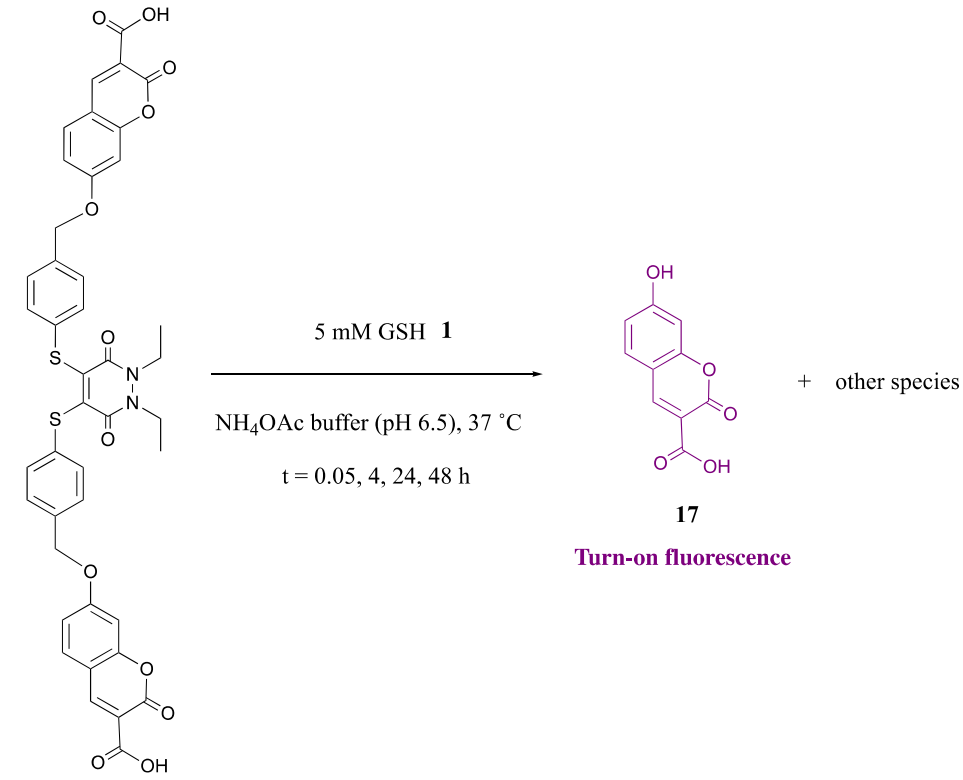

16

Quenched fluorescence

17

Turn-on fluorescence

PD **16** (40 µL, 10 mM in DMSO, 1 eq.) was added to GSH **1** (760 µL, 5.3 mM, 10 eq.) in ammonium acetate buffer (50 mM, pH 6.5). The mixture was incubated at 37 ˚C for 48 h. The reaction was excited at 335 nm at t = 0.05, 4, 24 and 48 h and the maximum fluorescence absorption was recorded at each time point.

Fluorescence emission at t = 0.05 h

(a)

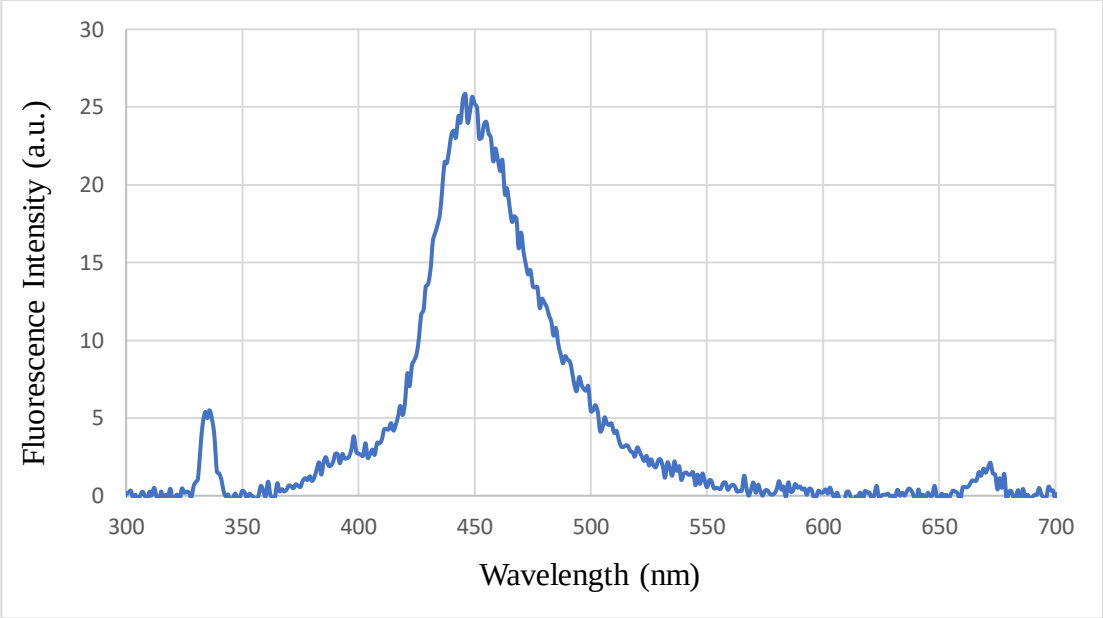

(b)

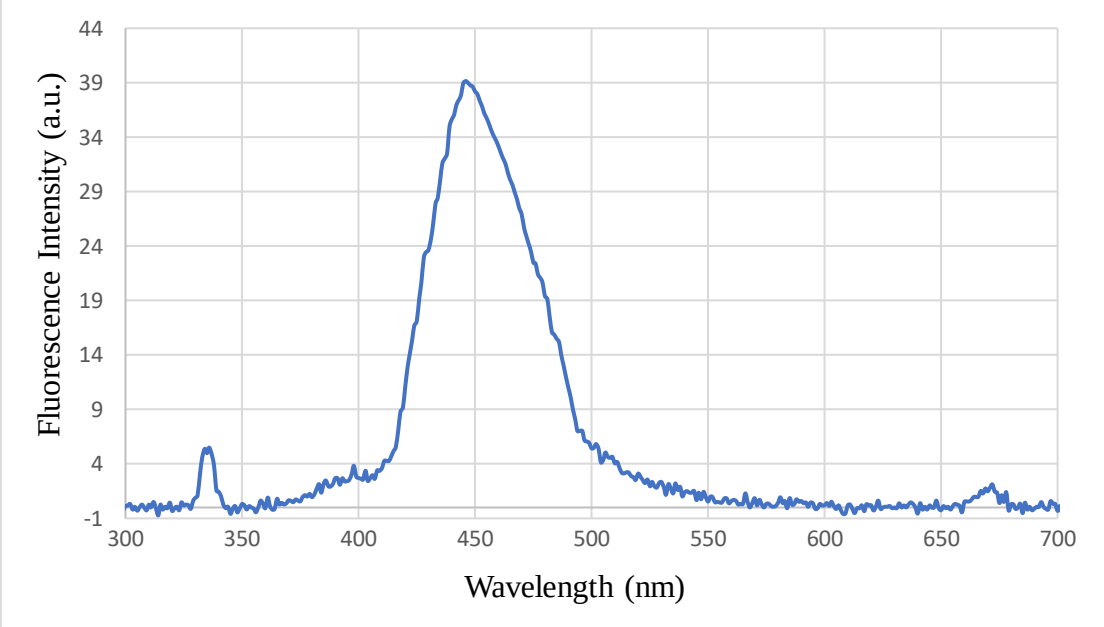

(c)

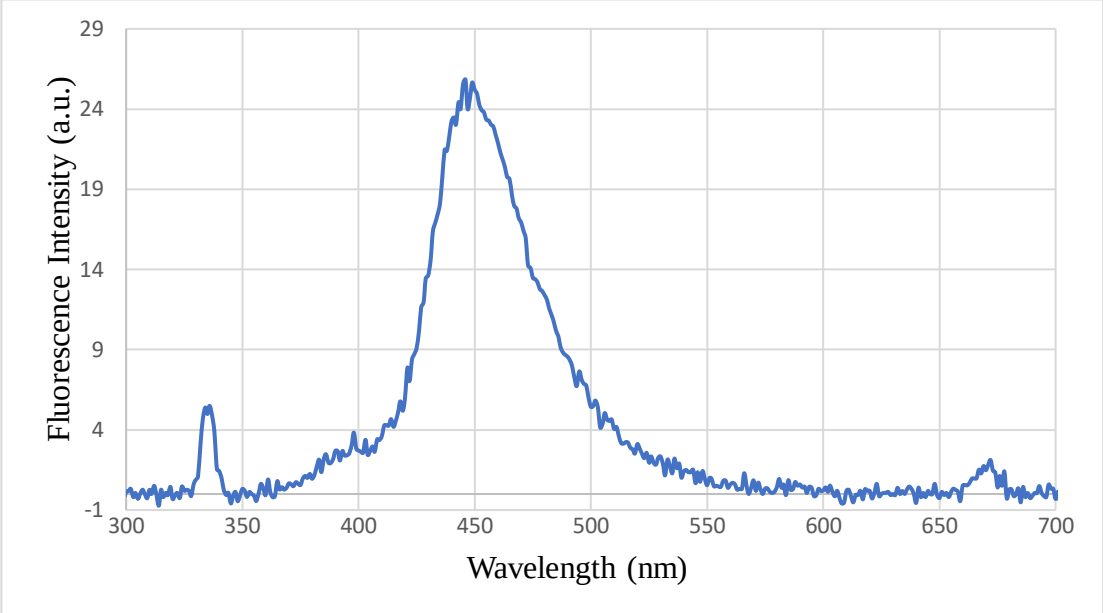

Figure **S90**. Fluorescence emission spectrum of the reaction between PD **16** and GSH **1** to release 7-hydroxy-2-oxo-2*H*-chromene-3-carboxylic acid **17** at t = 0.05 h. When excited at 335 nm (and performed in triplicate), maximum fluorescence emission occurred at 446 nm with a maximum intensity of (a) 25.8 a.u., (b) 39.1 a.u. and (c) 31.1 a.u.

Fluorescence emission at t = 4 h

(a)

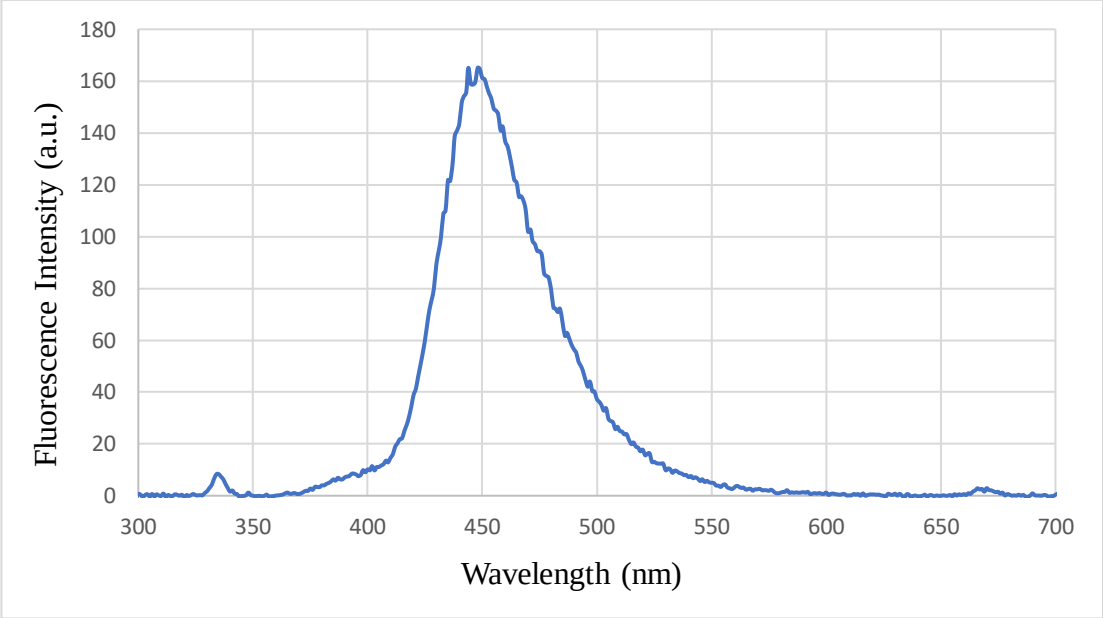

(b)

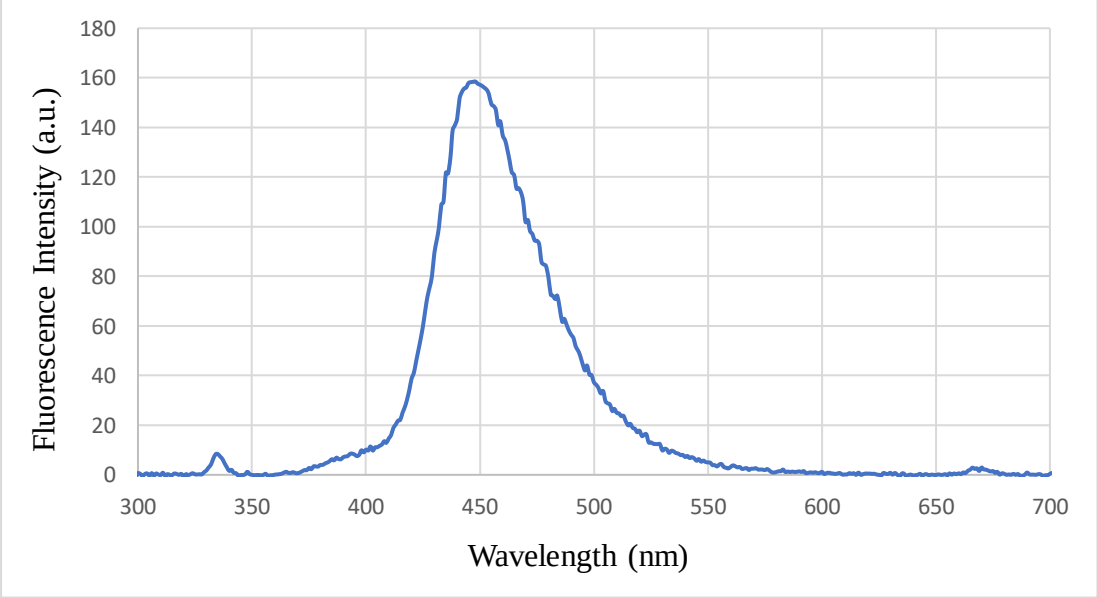

(c)

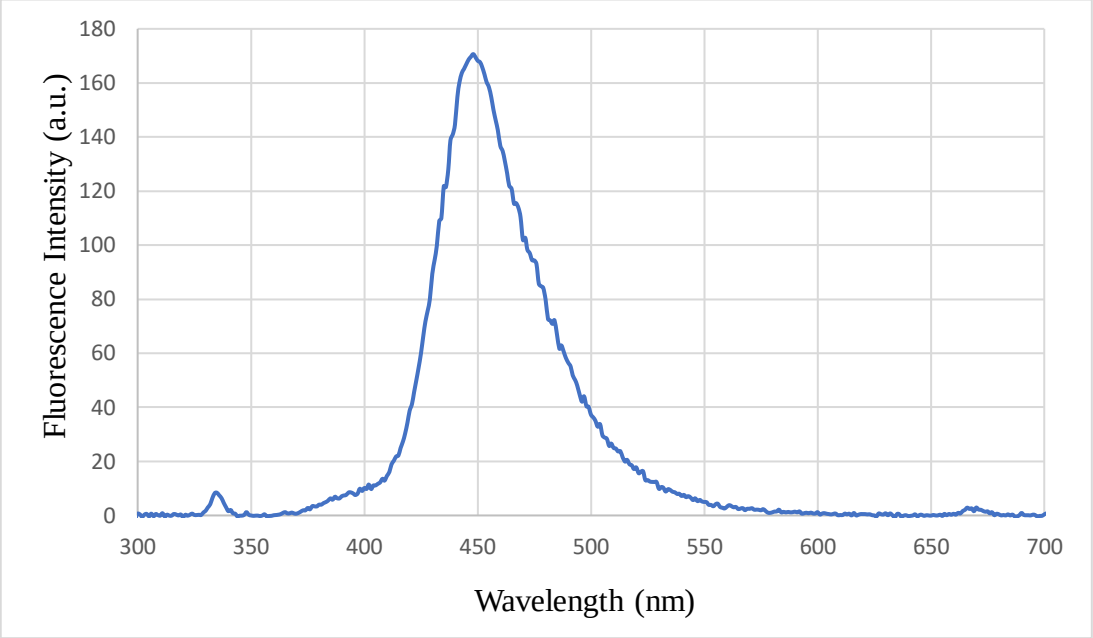

Figure **S91**. Fluorescence emission spectrum of the reaction between PD **16** and GSH **1** to release 7-hydroxy-2-oxo-2*H*-chromene-3-carboxylic acid **17** at t = 4 h. When excited at 335 nm (and performed in triplicate), maximum fluorescence emission occurred at 448 nm with a maximum intensity of (a) 165.1 a.u., (b) 158.5 a.u. and (c) 170.7 a.u.

Fluorescence emission at t = 24 h

(a)

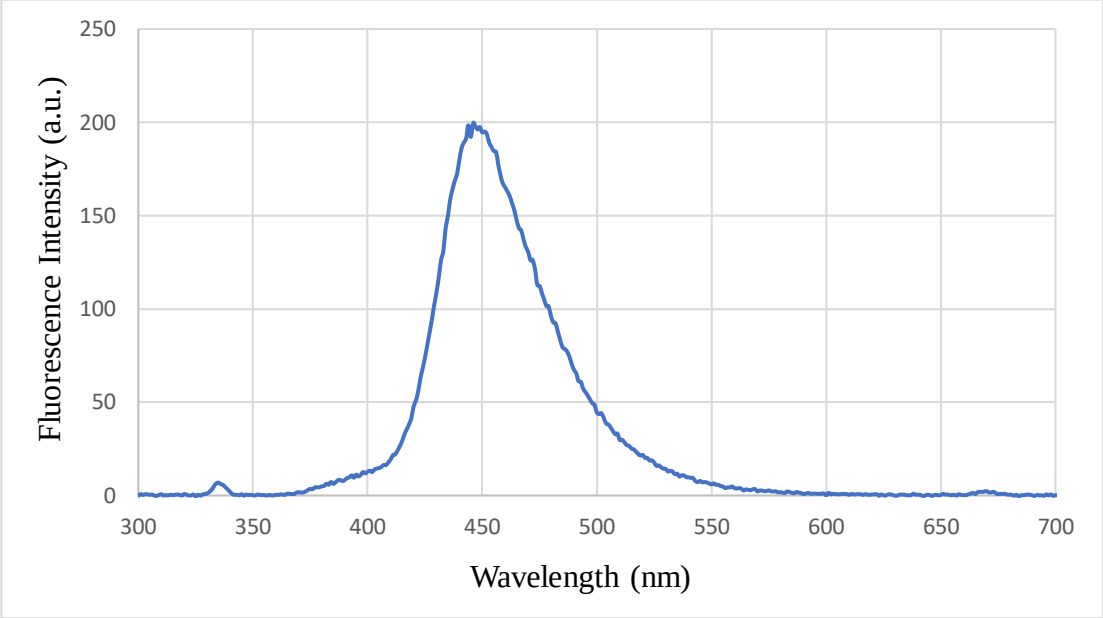
Fluorescence Intensity (a.u.)
250
200
150
100
50
0
300
350
400
450
500
550
600
650
700
Wavelength (nm)

(b)

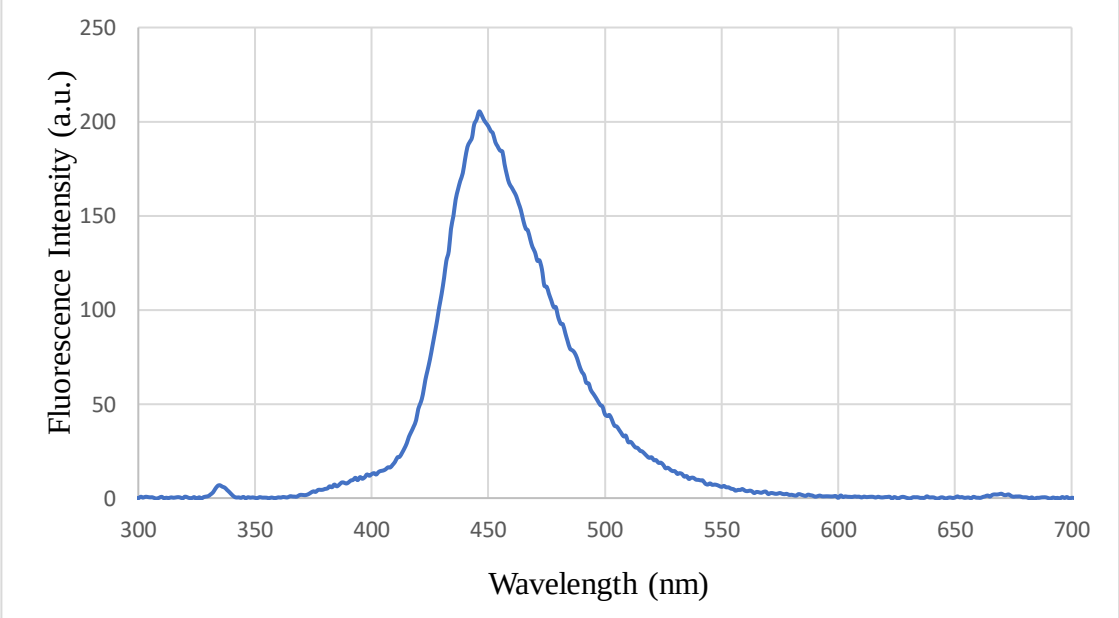
Fluorescence Intensity (a.u.)
250
200
150
100
50
0
300
350
400
450
500
550
600
650
700
Wavelength (nm)

(c)

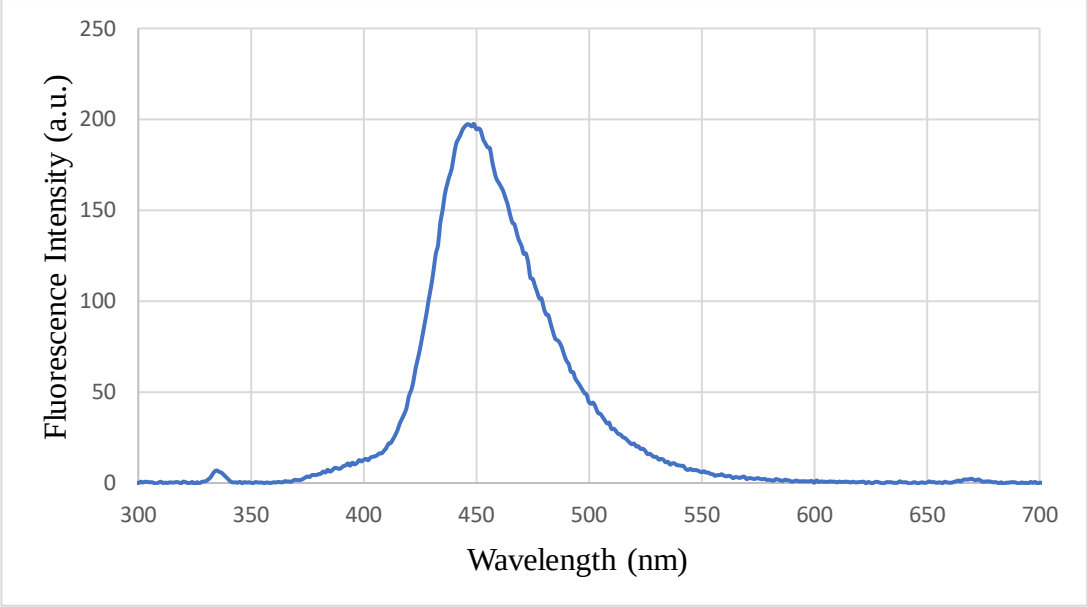

Figure **S92**. Fluorescence emission spectrum of the reaction between PD **16** and GSH **1** to release 7-hydroxy-2-oxo-2*H*-chromene-3-carboxylic acid **17** at t = 24 h. When excited at 335 nm (and performed in triplicate), maximum fluorescence emission occurred at 446 nm with a maximum intensity of (a) 199.6 a.u., (b) 205.3 a.u. and (c) 197.8 a.u.

Fluorescence emission at t = 48 h

(a)

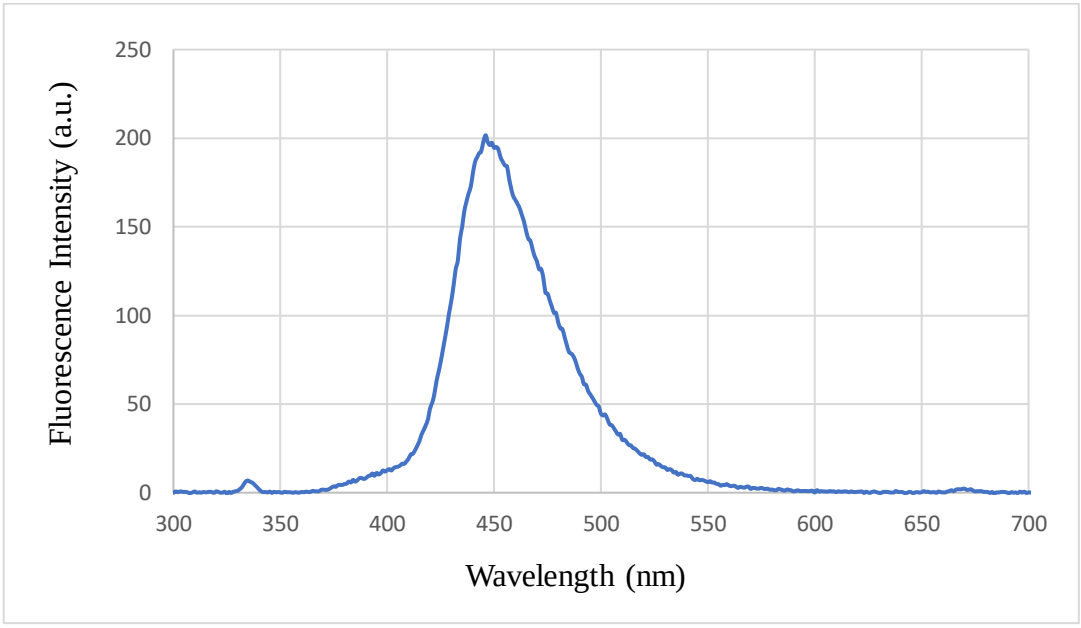

(b)

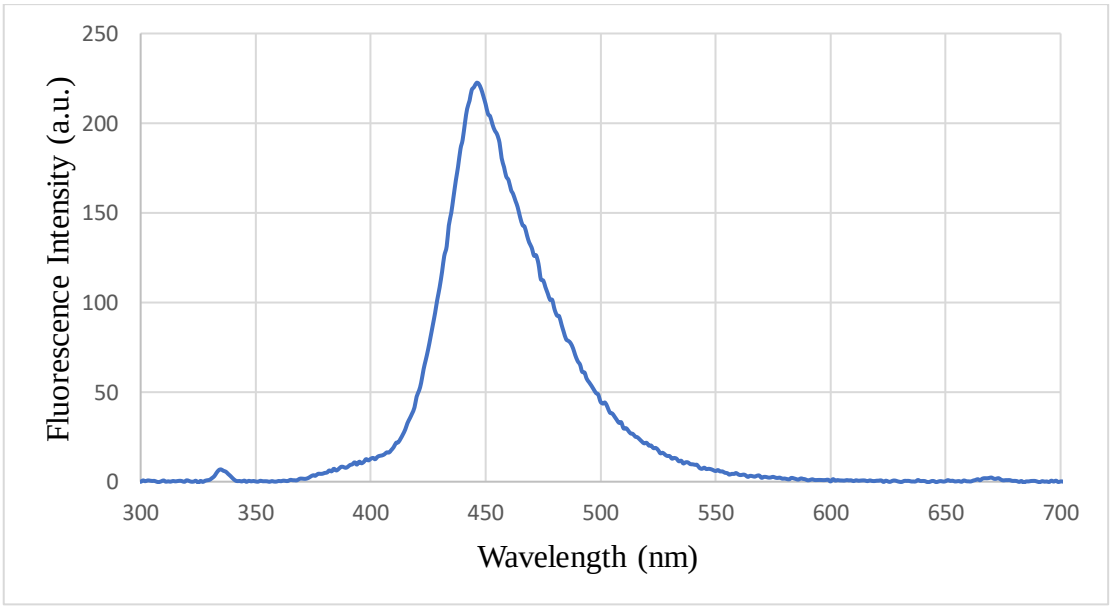

(c)

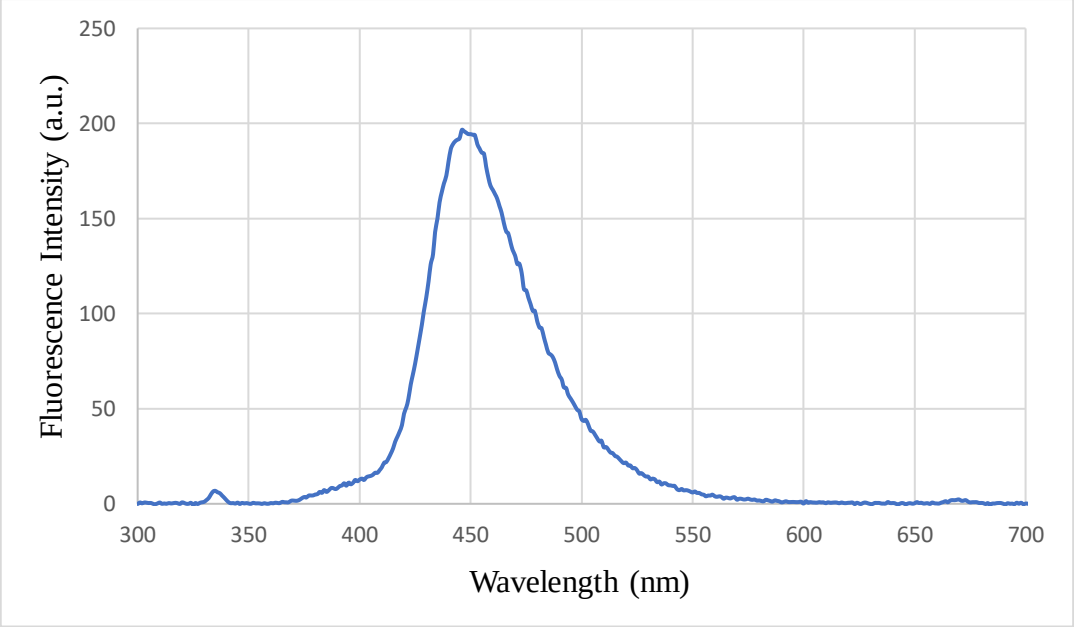

Figure **S93**. Fluorescence emission spectrum of the reaction between PD **16** and GSH **1** to release 7-hydroxy-2-oxo-2*H*-chromene-3-carboxylic acid **17** at t = 48 h. When excited at 335 nm (and performed in triplicate), maximum fluorescence emission occurred at 446 nm with a maximum intensity of (a) 201.7 a.u., (b) 222.1 a.u. and (c) 196.6 a.u.

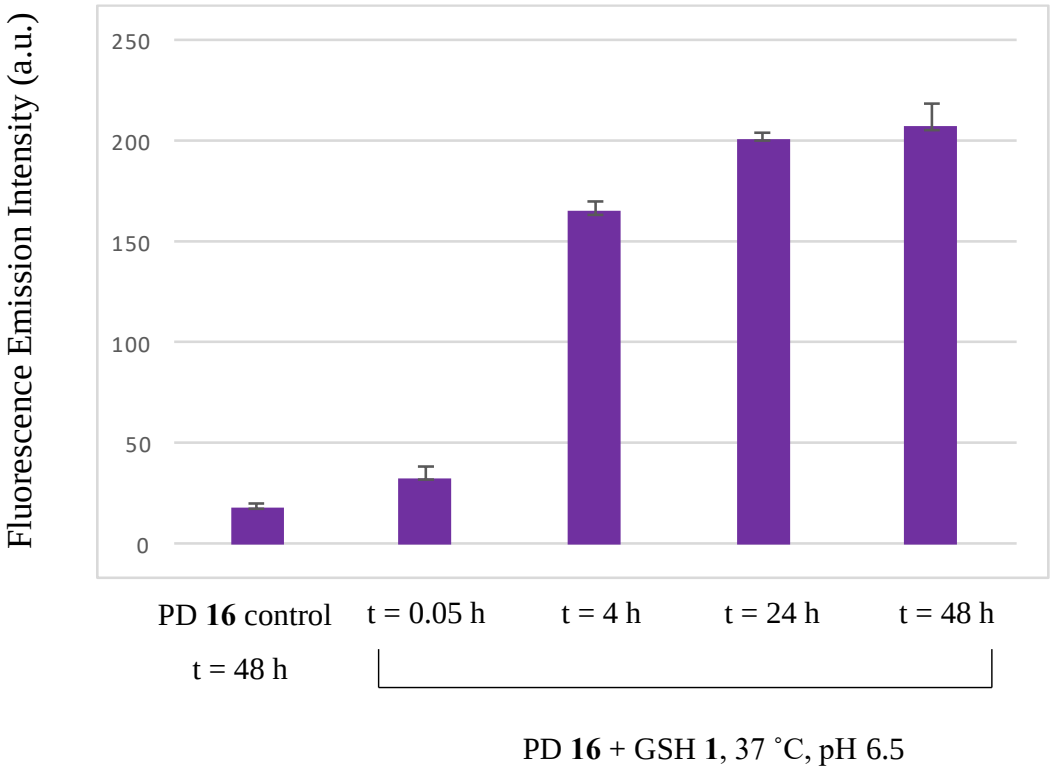

Figure **S94**. Summary of fluorescence emission data for the reaction between PD **16** and GSH **1** at 37 ˚C and pH 6.5.

References

1 M. T. Lee, A. Maruani, J. R. Baker and S. Caddick, *Chem. Sci.*, 2016, **7**, 799–802.

2 V. Chudasama, M. E. B. Smith, F. F. Schumacher, D. Papaioannou, G. Waksman, J. R. Baker and S. Caddick, *Chem. Commun.*, 2011, **47**, 8781–8783.

3 US Pat., 7 456 205, 2008.

4 S. Kohmoto, E. Mori and K. Kishikawa, *J. Am. Chem. Soc.*, 2007, **129**, 13364–13365.